H24/3263

MONASH UNIVERSITY
THESIS ACCEPTED IN SATISFACTION OF THE
REQUIREMENTS FOR THE DEGREE OF
DOCTOR OF PHILOSOPHY
ON..... 5 July 2002 .....
.....[redacted].....
Sec. Research Graduate School Committee

Tissue Distribution and Regulation of the Granzyme B Inhibitor, Proteinase Inhibitor 9

Claire Elizabeth Hirst

Monash University

Department of Biochemistry and Molecular Biology

Submitted in total fulfilment

of the requirements of the degree of

Doctor of Philosophy

February, 2002

Table of Contents

Abstract

Granzyme B (graB) is a pro-apoptotic proteinase present in cytotoxic T lymphocytes (CTL) and NK cells, which is involved in the lymphocyte mediated clearance of virally infected and tumourigenic cells. Proteinase inhibitor 9 (PI-9), an intracellular serpin, efficiently inhibits graB in a dose-dependent manner. The abundant expression of PI-9 in cytotoxic lymphocytes (CL) suggests that it protects these cells from ectopic graB. Limited RNA analyses of PI-9 expression indicates a restricted distribution in immune tissues and immune privileged sites. This thesis expands upon these studies by examining the tissue distribution and regulation of PI-9.

Several monoclonal and polyclonal antibodies specific for PI-9 were produced and characterised, allowing examination of PI-9 distribution by immunohistochemistry, immunofluorescence and immunoblotting. Another monoclonal antibody was produced that recognises a conserved epitope and therefore interacts with many serpins by immunoblotting. Studies with this antibody demonstrated that it recognises unfolded serpin and can inhibit serpin polymerisation, possibly because the epitope is only exposed in a polymerogenic intermediate.

Tissue distribution studies demonstrated that in addition to expression in immune cells and tissues, PI-9 is present in epithelial cells and in immune privileged sites such as the testis and placenta. Specifically, PI-9 is present in the Sertoli cells of the seminiferous tubules, possibly to protect against autoreactive CTL. Unexpectedly, graB was also detected within the testis, predominantly in germ cells. This suggests that graB may have novel functions in the testis, to hydrolyse extracellular matrix components to facilitate the migration of developing germ cells.

Finally, examination of leukocyte subsets indicated that PI-9 is expressed in $CD4^+$ and $CD8^+$ T cells, NK cells and at lower levels in B cells and myeloid cells. Further studies showed that PI-9 is upregulated in response to CTL degranulation and co-localises with graB-containing granules in CTL and NK cells, consistent with a role in protecting CL from leakage of endogenous graB. High levels of PI-9 were also detected in dendritic cells (DC) within the thymic medulla and tonsillar germinal centres. Analysis of DC subsets purified from peripheral blood indicated that PI-9 is also expressed in $CD123^+$ plasmacytoid DC, $CD16^+$ monocyte DC precursors and monocyte derived DC (MDDC), and is upregulated upon TNFα induced maturation of MDDC. The regulated expression of PI-9 in these leukocyte subsets supports the hypothesis that it protects effector, accessory and bystander cells from ectopic graB.

Declaration of Authenticity

This thesis contains no material which has been accepted for the award of any other degree or diploma in any University or other institution and is less than 100,000 words in length. To the best of my knowledge and belief, this thesis contains no material previously published or written by any person, except where due reference has been made.

[redacted]

Claire Hirst

WITH COMPLIMENTS

SIGNATURE:

Originals Sighted By: [redacted] Date: 23/10/02

MONASH RESEARCH GRADUATE SCHOOL
Research Services

MONASH
UNIVERSITY

Research Services

MONASH RESEARCH GRADUATE SCHOOL
PO Box 3A
Monash University
Victoria 3800, Australia
Telephone: +61 3 9905 3009
Facsimile: +61 3 9905 5042
Email: mrgs@adm.monash.edu.au
www.monash.edu.au/phdschol

Publications Arising from this Thesis

Data presented in this thesis is described in the following papers;

* **Hirst CE**, Buzza MS, Sutton VR, Trapani JA, Loveland KA, Bird PI. (2001) Perforin-independent expression of granzyme B and proteinase inhibitor 9 in testis and placenta suggests a role for granzyme B-mediated proteolysis in reproduction. *Mol. Hum. Reprod.* 7(12):1133-1142.

Hirst CE, Buzza MS, Warren H, Cameron PU and Bird PI. PI-9 is upregulated in activated cytotoxic lymphocytes and antigen presenting cells to inactivate ectopic granzyme B. (submitted).

* Buzza MS, **Hirst CE**, Bird CH, Hosking P, McKendrick J and Bird PI. (2001) The granzyme B inhibitor is present in endothelial and mesothelial cells, suggesting it protects bystander cells during immune responses. *Cell. Immunol.* 210(1):21-29.

* Bird CH, Blink EJ, **Hirst CE**, Buzza MS, Steele PM, Sun J, Jans DA, Bird PI. (2001) Nucleocytoplasmic distribution of the ovalbumin serpin PI-9 requires a nonconventional nuclear import pathway and the export factor crm1. *Mol. Cell. Biol.* 21(16):5396-5407

The production and characterisation of antibodies to PI-9 directly contributed to the following papers;

Bird CH, Sutton VR, Sun J, **Hirst CE**, Novak A, Kumar S, Trapani JA, Bird PI. (1998) Selective regulation of apoptosis: the cytotoxic lymphocyte serpin proteinase inhibitor 9 protects against granzyme B-mediated apoptosis without perturbing the Fas cell death pathway. *Mol. Cell. Biol.* 18(11):6387-6398.

* Reprints of these manuscripts are located at the rear of this thesis.

Acknowledgements

Firstly, I'd like to thank my supervisor Dr Phillip Bird for his support, guidance and continued interest throughout my PhD. His advice during the good and bad times, have helped turned adversity into accomplishment.

I'd also like to thank my fellow Bird lab members past and present – Marguerite Buzza, Dion Kaiserman, Cathy Bird, Kate Scarff, Anneliese Gillard, Fiona Scott, Juiru Sun and Qi (George) Zhou for providing reagents, technical assistance and advice, but more importantly for providing a challenging but entertaining environment to work in.

Some of this work would not have been possible without the assistance of people from other labs. Thanks to Kate Loveland and the members of her lab - Terri Meehan, Marilyn Bakker and Liz Christy, to members of the Serpin-Protease Group - Steve Bottomley, Rob Pike, James Whisstock, James Irving and Mary Pearce, and also to Joe Trapani, Viv Sutton, Hillary Warren and Paul Cameron who provided reagents or technical assistance, and have been acknowledged where appropriate.

Thank you also to Professors Hatem Salem and Chris Mitchell for giving me the opportunity to start and complete my PhD in their departments, initially at the Department of Medicine, Box Hill Hospital and then at the Department of Biochemistry and Molecular Biology.

I would also like to thank my family and friends. Thank you to Mum and Dad, for all their generosity and assistance, especially over the last two years. To my brother Alastair and his girlfriend Gen, fellow PhD students, for interesting discussions regarding the highs and lows of doing a PhD. To Dion's family for not minding an extra mouth to feed and to Darren, for putting up with me never having any time and forgetting to return his calls.

And last but certainly not least, thank you Dion for all your assistance and support in keeping me together in body and soul, particularly in these last few months.

Abbreviations

α_1-AC	α_1-antichymotrypsin
α_1-AT	α_1-antitrypsin
AT	antithrombin
bp	base pair
BSA	bovine serum albumin
°C	degrees celsius
catG	cathepsin G
cDNA	complementary DNA
CL	cytotoxic lymphocytes
ConA	concanavalin A
CTL	cytotoxic T lymphocytes
d	day/s
dATP	deoxyadenosine triphosphate
DC	dendritic cells
dH_2O	distilled water
ddH_2O	double distilled water
DMEM	Dulbecco's modified Eagle's medium
DNA	deoxyribonucleic acid
ELISA	enzyme-linked immunosorption assay
FCS	foetal calf serum
FITC	fluorescein isothiocyanate
graB	granzyme B
h	hour/s
HRP	horseradish peroxidase
Ig	immunoglobulin
IL	interleukin
kDa	kiloDalton
MDDC	monocyte derived dendritic cells
min	minute/s
M/NEI	monocyte/neutrophil elastase inhibitor

mRNA	messenger ribonucleic acid
NK	natural killer
nt	nucleotide
ov-serpin	ovalbumin-type serpin
PAGE	polyacrylamide gel electrophoresis
PAI-1	plasminogen activator inhibitor-1
PAI-2	plasminogen activator inhibitor-2
PBL	peripheral blood leukocytes
PBS	phosphate buffered saline
PCR	polymerase chain reaction
PE	phycoerythrin
PI	propidium iodide
PI-6	proteinase inhibitor 6
PI-8	proteinase inhibitor 8
PI-9	proteinase inhibitor 9
PMA	phorbol 12-myristate 13-acetate
RCL	reactive centre loop
RITC	rhodamine isothiocyanate
RNA	ribonucleic acid
RT	reverse transcriptase
s	second/s
SCCA-1	squamous cell carcinoma antigen-1
SCCA-2	squamous cell carcinoma antigen-2
SPI-3	serine proteinase inhibitor 3
SPI-6	serine proteinase inhibitor 6
TNFα	tumour necrosis factor alpha
UTR	untranslated region
v/v	volume per volume
w/v	weight per volume

Chapter 1

Literature Review

1.1 Apoptosis in the immune system

Regulation of cell number is one of the most critical mechanisms of homeostasis in multicellular organisms. The fine balance between cell proliferation and cell death must be carefully maintained to ensure the correct physiological development and to prevent pathogenesis. Recently there has been much research into cell death and the mechanisms by which it is mediated. It was noted as early as 1972 that two morphologically distinct mechanisms of cell death occur; the controlled self-destruction of cells and cellular degeneration caused by injury. The term apoptosis was introduced to separate the process of programmed cell death from necrosis (Kerr *et al.*, 1972).

The characteristic morphological changes associated with apoptosis include chromatin and cytoplasmic condensation, plasma membrane blebbing and loss of cell volume, with the eventual formation of membrane enclosed apoptotic bodies. These bodies are rapidly phagocytosed by adjacent cells, thus preventing potentially harmful intracellular contents leaking into the extracellular space. Apoptotic cell death has been observed in many tissues under a variety of circumstances. Apart from induction of apoptosis by a variety of toxicological signals, programmed cell death is also apparent during embryogenesis, hormone induced atrophy, tumour regression and in normal cell turnover in tissues.

Apoptosis also plays important roles in the generation and maintenance of the immune response. During the development of the T and B cell repertoire, cells that undergo receptor rearrangements resulting in non-productive or auto-reactive receptors are deleted via apoptosis. Furthermore, cell mediated immunity by cytotoxic T lymphocytes or NK cells, utilises apoptosis to remove tumourigenic, virally infected and foreign cells. Following the immune response, the clonally expanded, antigen-specific T and B cells are removed by activation induced cell death.

1.2 The apoptotic pathway

Apoptosis is often referred to as programmed cell death, as it represents a mechanism of cellular suicide that can be activated in every nucleated cell. It is a process that occurs in all metazoans and thus represents a common pathway of cell death conserved through evolution. There are several steps involved in the apoptotic pathway; initially the cell receives a signal to undergo apoptosis, which results in the activation of pre-existing proteins (often zymogens) within the cell. These proteins are involved in many separate and overlapping pathways within the cell which lead to the biochemical and morphological changes associated with apoptosis.

1.2.1 Initiation of apoptosis

Apoptosis can be induced by a myriad of extracellular or intracellular signals that can be divided into a number of categories including cellular neglect, cellular disruption and killer cell mediated apoptosis. Cells that are lacking in growth factors, hormones or essential nutrients undergo apoptosis; this cause of apoptosis is particularly evident in embryonic development and tumour atrophy. Disruption to intracellular components, such as radiation induced DNA damage or perturbation of biochemical pathways by chemicals, often leads to apoptosis and is the cause of the many effects of radiotherapy and chemotherapy. Cytotoxic lymphocyte mediated apoptosis of target cells occurs via ligand dependent death receptor oligomerisation and/or the granule mediated release of cytotoxic molecules into the target cytoplasm.

1.2.2 Effectors of apoptosis

Our understanding of the effector stage of apoptosis has profited from studies of the nematode *Caenorhabditis elegans*. During normal development, 131 of the 1090 somatic cells die by apoptosis. Genetic analysis has identified that the *ced*-3 and *ced*-4 genes must be functional for apoptosis and that their overexpression results in premature apoptosis (Ellis and Horvitz, 1986). Conversely, the overexpression of *ced*-9 can prevent apoptosis, while loss of this gene results in cell death (Hengartner *et al.*, 1992). Mammalian homologues have been identified for these three genes. *ced*-3 and *ced*-9 are represented in the mammalian genome by the caspase and Bcl-2 families respectively, however only one mammalian homologue, Apaf-1, has been identified for *ced-4*.

1.2.2.1 Caspases

The caspases (cysteine aspartic acid proteinase) represent a distinct family of cysteine proteinases, with all members sharing specificity for cleavage after aspartic acid residues. There are 10 human caspases (caspase-1 to -10) with two additional caspases described in mice that have no human counterparts (caspase-11 and -12), however not all of these proteins are directly involved in apoptosis. The caspases are synthesised as inactive pro-enzymes with a variably sized N-terminal pro-domain. Activation involves the removal of the pro-domain and the cleavage of the C-terminal portion into a large and a small subunit. The processed caspase then forms a homodimer comprising two large and two small subunits. The processing of procaspases into their active form involves cleavage following aspartic acid residues and therefore, active caspases are able to process and activate other procaspases. Some procaspases can also undergo auto-processing to the final active conformation. This mechanism of cis- and trans-activation results in an amplified cascade of caspase activation, rapidly expanding the original signal into the biochemical changes associated with apoptosis.

The caspases can be divided into three groups based on their proteolytic actions (summarised in Table 1.1). The substrate specificity of group III caspases resembles the cleavage sites found in group II procaspases, suggesting that group III caspases act as upstream activators of group II caspases. The optimal cleavage site for group II caspases is DEXD, a sequence similar to sites found in several downstream substrates that are cleaved during apoptosis, suggesting that members of this group act as downstream effectors of apoptosis. Group I caspases (caspase-1, -4 and -5) are not thought to be actively involved in apoptosis but are instead restricted to pathways of cytokine processing. The pro-apoptotic caspases (groups II and III) can also be grouped according to their primary structure. Procaspase-3, -6, and -7 contain short pro-domains while procaspase-2, -8, -9, and -10 contain large pro-domains. These large pro-domains contain motifs that allow protein-protein interactions with similar motifs found in adaptor molecules.

Apical caspases

The apical caspases contain protein-protein interaction domains that allow them to bind to homologous domains in adaptor molecules that are associated with death receptors (illustrated in Figure 1.1). These interactions can induce auto-activation of the pro-caspases which then process and activate the effector caspases.

Apical caspases			
Caspase	Alternative name	Group[a]	Prodomain motifs
2	ICH-1 Nedd2	II	CARD
8	MACH, ICE-LAP5, FLICE, Mch5	III	DED
9	ICE-LAP6, Mch6, Apaf-3	III	CARD
10	Mch4, ICE-LAP4, FLICE2	III	DED
Effector caspases			
3	CPP32, Yama, apopain	II	-
6	Mch2	III	-
7	Mch3, ICE-LAP3, CMH-1	II	-
Cytokine processing caspases			
1	ICE	I	-
4	TX, ICH-2, ICErel-II	I	-
5	ICErel-III, TY, ICH-3	I	-

Table 1.1 The caspases. The caspases can be divided into three groups based on their role in apoptosis; caspases that initiate the cascade (apical) those that mediate cleavage of death substrates (effector) and those that predominantly have a cytokine processing role. [a]Caspase grouping by cleavage specificity (Thornberry *et al.*, 1997).

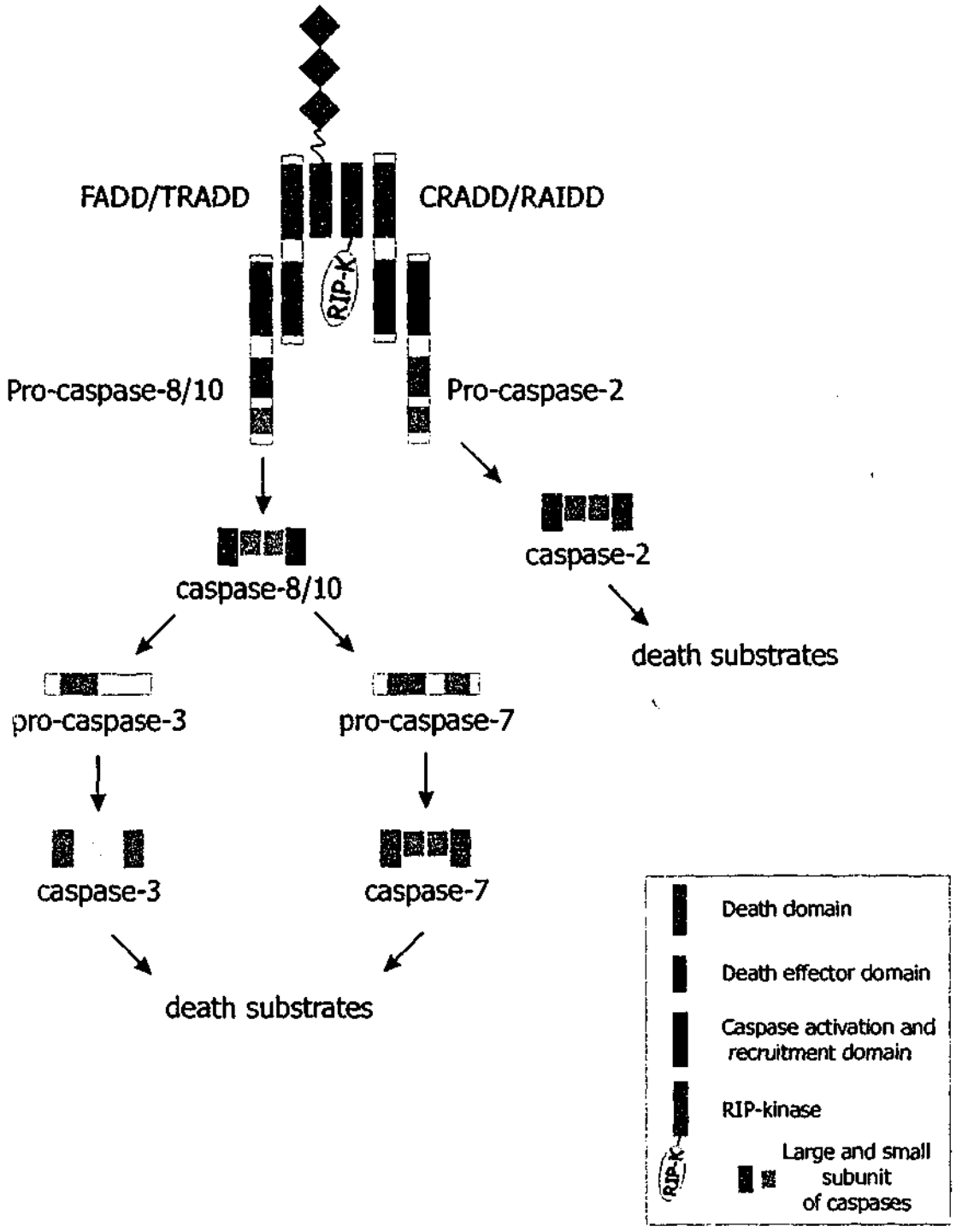

Figure 1.1 Activation of the apical caspases. The pro-domains of procaspase-8 and -10 contain a death effector domain (DED) (Muzio *et al.*, 1996; Vincenz and Dixit, 1997), which allows them to interact with the DED found in the adaptor molecules FADD and TRADD (Chinnaiyan *et al.*, 1995; Hsu *et al.*, 1995). Binding of an extracellular ligand such as FasL or TNFα induces trimerisation of members of the TNFα receptor family. The receptor associated FADD or TRADD then recruit and bring procaspase-8 or -10 into close association, allowing auto-processing of the procaspases into their active form. In an analogous manner, the pro-domain of procaspase-2 contains a domain that allows the protein-protein interaction with the caspase recruitment domain (CARD) found in a variety of adaptor molecules. The interaction of the CARD in procaspase-2 with CRADD/RAIDD and RIP-kinase mediates the recruitment, oligomerisation and activation of procaspase-2 (Ahmad *et al.*, 1997; Duan and Dixit, 1997).

Activated caspase-8 can process all procaspases *in vitro* (Srinivasula *et al.*, 1996a; Muzio *et al.*, 1997) however under physiological conditions this is probably restricted to procaspase-3 (Stennicke *et al.*, 1998). Caspase-9 and -10 can cleave procaspase-3 and -7 *in vitro* (Fernandes-Alnemri *et al.*, 1996) although caspase-9 in complex with Apaf-1 predominantly acts on procaspase-3 (Li. *et al.*, 1997). Although procaspase-2 possesses a large CARD containing pro-domain and therefore is considered an apical caspase, it has cleavage specificity more homologous to that of the effector caspases (Thornberry *et al.*, 1997). To date, caspase-2 has not been shown to activate any procaspases.

Effector caspases

The effector caspases are directly involved in the cleavage of "death substrates"- cellular proteins whose cleavage results in the biochemical processes that are the hallmark of apoptosis. The effector caspases (caspase-3, -6 and -7) are predominantly activated by the apical caspases, however they can also be activated by other proteinases. Granzyme B, a serine proteinase that shares the caspases' specificity for cleavage after aspartic acid residues, has been shown to activate many procaspases *in vitro*, however *in vivo* this is probably restricted to procaspase-3 and -7 (Yang *et al.*, 1998). Another serine proteinase, cathepsin G, has also been shown to cleave and activate procaspase-7 (Zhou and Salvesen, 1997).

The effector caspases mediate the cleavage of a wide variety of cytoplasmic and nuclear proteins. These substrates include structural proteins found in the nucleus and cytoplasm, as well as proteins involved in DNA repair, signal transduction, cell cycle control, and proteins directly involved in the apoptotic process. The rapidly expanding list of proteins cleaved by caspases has been recently reviewed (Earnshaw *et al.*, 1999).

Cytokine processing caspases

The third group of caspases includes caspase-1, -4 and -5. Although caspase-1 (ICE) was the first caspase identified to induce apoptosis in cells (Miura *et al.*, 1993), caspase-1 null mice have no defect in the apoptotic pathway (Kuida *et al.*, 1995; Li *et al.*, 1995). These mice are essentially normal except for a defect in the processing of interleukin-1β and -1α, which is severely affected. Caspase-4 and -5 share a high degree of homology to caspase-1 yet have different substrate specificities (Thornberry *et al.*, 2000) and therefore are unable to directly process pro-interleukin 1-β (Munday *et al.*,

1995). Caspase-4 has been shown to activate procaspase-1 (Faucheu *et al.*, 1995), and therefore caspase-4 and -5 are thought to be upstream activators of caspase-1.

1.2.2.3 Apaf-1 and the mitochondria

The only known mammalian homologue of *ced*-4 is Apaf-1 (apoptotic protease activating factor 1). Apaf-1 consists of a N-terminal caspase recruitment domain (CARD), a central CED-4 homology domain and a number of WD-40 domains at the C-terminus (Zou *et al.*, 1997). Apaf-1 recruits and activates procaspase-9 by homologous CARD, found in both Apaf-1 and procaspase-9, following release of cytochrome *c* and ATP from the mitochondria, forming the multimeric complex known as the apoptosome (Li *et al.*, 1997; illustrated in Figure 1.2).

Release of cytochrome *c* from the mitochondria is initiated by many apoptotic signals, however the exact mechanism by which this release is mediated is not known. The mitochondria undergo a number of dramatic changes early in the apoptotic process, including breakdown of the inner mitochondrial transmembrane potential ($\Delta\Psi_m$) and opening of permeability transition pores. It is not currently known whether these changes result in the release of cytochrome *c* or whether it is released due to loss of membrane integrity following mitochondrial disruption. Alternatively several members of the pro-apoptotic Bcl-2 family, described in section 1.2.3.1, are thought to be involved in the release of cytochrome *c* via formation of membrane channels.

Cytochrome *c* is not the only apoptogenic protein released from mitochondria during apoptosis. Apoptosis inducing factor (AIF) (Susin *et al.*, 1996) and Smac/DIABLO (second mitochondria-derived activator of caspase/direct IAP binding protein with low pI (Du *et al.*, 2000; Verhagen *et al.*, 2000)) are also released from the intermembrane space. Smac/DIABLO is a pro-apoptotic protein that promotes apoptosis by displacement of XIAP from caspase-9 (Ekert *et al.*, 2001; Srinivasula *et al.*, 2001) thus neutralising the inhibition of apoptosis by XIAP.

Release of AIF into the cytoplasm results in apoptosis, however its release can be prevented by overexpression of Bcl-2 (Susin *et al.*, 1996). Further analysis of the apoptogenic activity of AIF has demonstrated that it acts independently of the caspases (Susin *et al.*, 1999), however analysis of AIF null embryonic fibroblasts suggests AIF acts upstream of cytochrome *c* release and formation of the apoptosome (Joza *et al.*, 2001) and thus the downstream apoptotic changes are dependent on caspase-9.

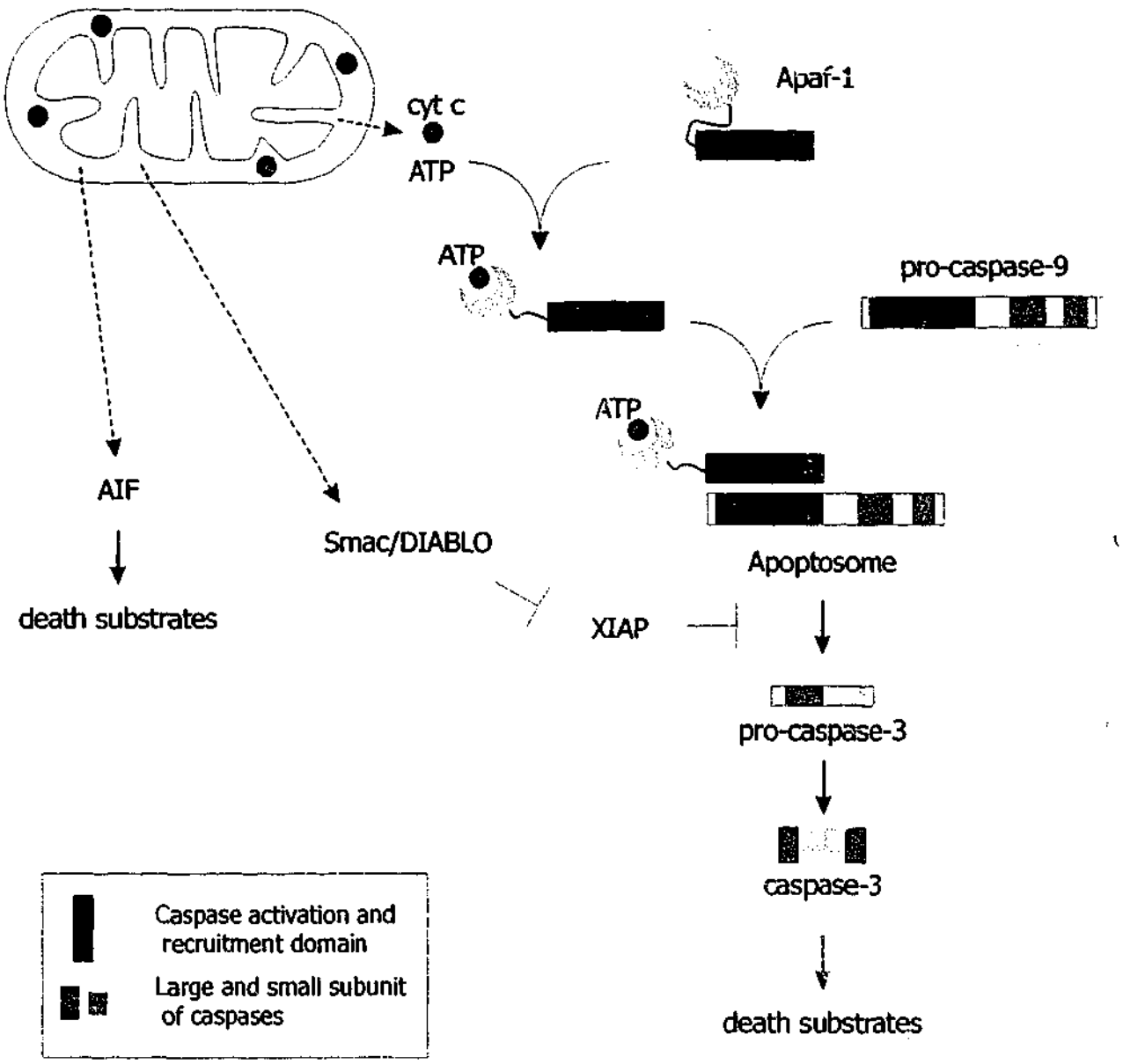

Figure 1.2 Mitochondrial pathways of cell death. Procaspase-9 is activated following release of cytochrome *c* (cyt *c*) and ATP from the intermembrane space of the mitochondria. Cyt *c* and ATP bind to cytosolic Apaf-1 inducing an allosteric change which allows the association of the CARD in Apaf-1 with the CARD in the prodomain of procaspase-9 and forming the apoptosome. The apoptosome can then process and activate procaspase-3. This activity can be regulated by XIAP, which itself can be regulated by the pro-apoptotic protein Smac/DIABLO. AIF released from mitochondria can act upon death substrates independently of the caspases.

1.2.3 Regulation of apoptosis

1.2.3.1 Bcl-2 family

The Bcl-2 superfamily consists of 19 mammalian and at least seven viral homologues of the *C.elegans* protein CED-9 (reviewed in Gross *et al.*, 1999a) that contain characteristic Bcl-2 homology (BH) domains. The mammalian family can be divided into two subfamilies based on their role in promoting or inhibiting apoptosis. The anti-apoptotic members contain BH domains 1 to 4, except for A1 and Boo, which lack the BH3 domain, while the pro-apoptotic members have either BH domains 1-3 or only the BH3 domain (illustrated in Figure 1.3A). The BH3 domain allows hetero-dimerisation of Bcl-2 family members and furthermore, the BH3 domain of the pro-apoptotic members can bind to a groove formed by the BH domains 1-3 of the anti-apoptotic members.

Most of the Bcl-2 superfamily also possess a hydrophobic C-terminal domain, which facilitates their association with the outer mitochondrial membrane, a localisation central to their role in promoting or preventing apoptosis. The anti-apoptotic members prevent apoptosis by binding to and blocking the pro-apoptotic members from releasing apoptogenic mitochondrial proteins from the intermembrane space. The exact mechanism by which the pro-apoptotic members facilitate this release is not yet known, however research is currently focusing on the ability of some of the BH3 only members to form membrane permeable pores. BH3 only members may also perturb the existing permeability transition pore by disrupting either the outer membrane voltage-dependent anion channel (VDAC) or the inner membrane adenine nucleotide translocator (ANT) or both. Opening of these channels dissipates the H^+ gradient, uncouples the electron transport chain and can also result in the release of apoptogenic proteins from the intermembrane space (reviewed in Gross *et al.*, 1999a; Adams and Cory, 2001; Shi, 2001).

The Bcl-2 family are differentially expressed and regulated. Several members of the anti-apoptotic family are induced by cytokines and therefore appear in a stage specific manner during development. This is particularly apparent in the testis where the level and pattern of expression of the anti-apoptotic Bcl-2 family members varies in different cell types, which is thought to regulate germ cell apoptosis during juvenile and adult spermatogenesis (Meehan *et al.*, 2001). The BH3 only members are under the strictest control due to their potent pro-apoptotic properties and as such are regulated by a number of mechanism including sequestration, phosphorylation status and a need for proteolytic activation (as illustrated in Figure 1.3B)

Figure 1.3 The Bcl-2 superfamily. (A) The Bcl-2 superfamily is composed of anti-apoptotic (blue) and pro-apoptotic (orange) proteins. Members contain a number of Bcl-2 homology (BH) domains which allow homo- and hetero-dimerisation. Some members also contain a C-terminal membrane anchor. Modified from Adams and Cory, 1998. (B) Bcl-2 family members are regulated via a number of mechanisms. Bim is sequestered to the microtubule-associated dynein motor complex. Disruption of the interaction between the light chain and the dynein motor complex frees Bim to bind Bcl-2 and neutralise its anti-apoptotic activity (Puthalakath *et al.*, 1999). Phosphorylation of Bad by Akt results in its sequestration in the cytosol by 14-3-3 preventing neutralisation of Bcl-$_{XL}$ or Bcl-2 (Zha *et al.*, 1996). Conversely, Bik requires phosphorylation, by casein kinase II, to be active and bind Bcl-2 (Verma et al., 2001). Bid is inert until an N-terminal fragment is cleaved by caspase-8 (Li *et al.*, 1998; Luo *et al.*, 1998) or graB (Barry *et al.*, 2000; Heibein *et al.*, 2000; Sutton *et al.*, 2000; Alimonti *et al.*, 2001) which cleave at aspartic acid^{59} or aspartic acid^{75} respectively (Li *et al.*, 1998). Truncated Bid (tBid) then translocates to the mitochondria (Gross *et al.*, 1999b) due to post-translational myristoylation at the N-terminal glycine residue exposed by caspase-8 cleavage (Zha *et al.*, 2000). Once there it can associate with Bak or Bax to form membrane pores (Wei *et al.*, 2000; Wei *et al.*, 2001). Active tBid can be inhibited by Bcl-$_{XL}$, while phosphorylation of Bid by casein kinase I or II can prevent its activation by caspase-8 (Desagher *et al.*, 2001). Modified from Adams and Cory, 2001.

A

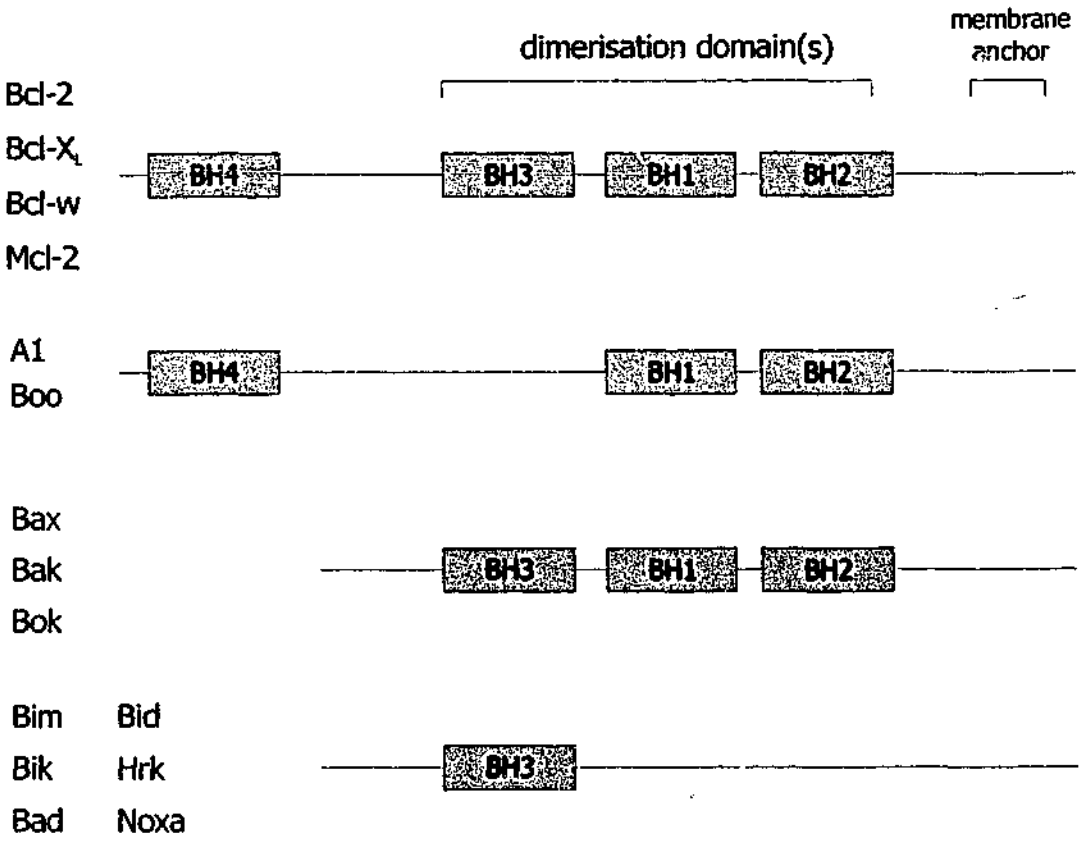
dimerisation domain(s)
membrane anchor
Bcl-2
Bcl-X$_L$
Bcl-w
Mcl-2
A1
Boo
Bax
Bak
Bok
Bim
Bid
Bik
Hrk
Bad
Noxa
BH4
BH3
BH1
BH2

B

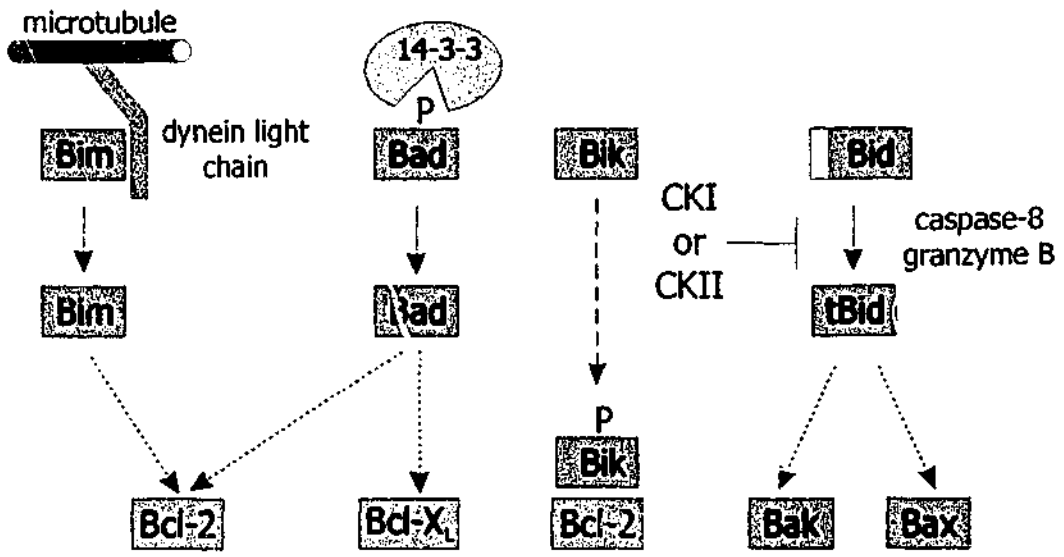
microtubule
dynein light chain
14-3-3
P
Bim
Bad
Bik
Bid
CKI
or
CKII
caspase-8
granzyme B
tBid
P
Bcl-2
Bcl-X$_L$
Bcl-2
Bak
Bax

1.2.3.2 FLIP

Viruses have evolved many mechanisms to evade the host's immune response. The human Herpes viruses and Molluscipox virus express a protein, v-FLIP (viral-Flice inhibitory protein), which blocks signalling through death receptors. v-FLIP contains two death-effector domains (DED) which interact with the adaptor protein FADD, thereby blocking the recruitment and activation of procaspase-8 and -10 induced by ligation of Fas or members of the TNFα receptor family (Thome *et al.*, 1997). The mammalian homologue of v-FLIP is c-FLIP (Irmler *et al.*, 1997) and two splice variants have been described; c-FLIP$_S$, a short isoform, contains two DED while c-FLIP$_L$, the longer form, contains a catalytically inert caspase domain in addition to the two DED (Hu *et al.*, 1997; Irmler *et al.*, 1997).

Examination of c-FLIP expression indicates highest levels are found in melanoma cell lines (Irmler *et al.*, 1997) and this expression correlates with resistance to TRAIL mediated apoptosis (Griffith *et al.*, 1998). This suggests that c-FLIP constitutes a mechanism by which tumour cells can evade the immune response. *In vivo* analysis of c-FLIP overexpressing tumours demonstrates that these cells are resistant to clearance by CTL (Medema *et al.*, 1999). The importance of c-FLIP in modulating signalling through the death receptors is revealed by analysis of c-FLIP null mice (Yeh *et al.*, 2000). c-FLIP is required for embryonic survival and embryonic fibroblasts derived from the null mice are extremely sensitive to low doses of TNFα, suggesting that c-FLIP can modulate signalling through the death receptors.

1.2.3.3 Inhibitors of caspases

p35

Several viruses have evolved apoptotic inhibitors that act on the caspases directly. The Baculovirus protein, p35, can block the apoptotic response induced by viral infection (Clem *et al.*, 1991), and subsequent transfection studies have indicated that p35 can prevent apoptosis mediated by a number of pathways including Fas, TNFα and growth factor withdrawal (Rabizadeh *et al.*, 1993; Beidler *et al.*, 1995; Martinou *et al.*, 1995). p35 exhibits a broad inhibitory profile as it can inhibit most caspases in a number of organisms. Inhibition is dependent upon caspase cleavage of p35 and the formation of a stable p35- caspase complex (Bump *et al.*, 1995; Xue and Horvitz, 1995).

IAPs

The inhibitor of apoptosis proteins (IAPs) were first identified in Baculovirus as factors that could prevent apoptosis of virally infected insect cells in the absence of p35 (Crook *et al.*, 1993). Subsequently many homologues have been identified (eight human IAPs have been identified to date) with a common structure consisting of an N-terminal domain, which contains one to three Baculovirus IAP repeat (BIR) motifs. The majority of IAPs also contain a C-terminal RING finger domain (reviewed in Stennicke *et al.*, 2002). In mammals, XIAP, cIAP-1 and cIAP-2 have been shown to specifically inhibit caspase-3 and -7 (Deveraux *et al.*, 1997; Roy *et al.*, 1997) and the Apaf-1 induced activation of procaspase-9 (Deveraux *et al.*, 1998). There is also evidence that the other human IAPs can act as caspase inhibitors (reviewed in Stennicke *et al.*, 2002).

The mechanism of caspase inhibition by IAPs has been elucidated by the use of BIR deletion mutants of XIAP and the crystallisation of XIAP with caspase-3 (Riedl *et al.*, 2001) and -7 (Chai *et al.*, 2001; Huang *et al.*, 2001). The inhibition of caspase-3 by XIAP is mediated by contact with BIR domains 1 and 2 (Deveraux *et al.*, 1999; Riedl *et al.*, 2001) while caspase-9 is inhibited by the third BIR domain (Srinivasula *et al.*, 2001). However, the inhibition of caspase-7 by XIAP is mediated by the linker region between BIR domains 1 and 2, with the BIR domains primarily acting to maintain the conformation of this linker region (Chai *et al.*, 2001; Huang *et al.*, 2001).

CrmA

Another viral inhibitor of apoptosis is the Cowpox virus protein, cytokine response modifier A (crmA), which attenuates the anti-viral inflammatory response by inhibition of caspase-1 processing of IL1-β (Ray *et al.*, 1992). CrmA is a member of a superfamily of serine proteinase inhibitors (serpins), which were previously thought to only inhibit serine proteinases (see section 1.6). Thus the inhibition of caspase-1 was the first report of cross-class inhibition of cysteine proteinases by a serpin (Komiyama *et al.*, 1994). Subsequently, crmA has been shown to be an efficient inhibitor of caspase-8 (Srinivasula *et al.*, 1996a) and to a lesser extent caspase-3, -6 and -7 (Zhou *et al.*, 1997) and the serine proteinase granzyme B (Quan *et al.*, 1995).

1.3 Lymphocyte mediated apoptosis

Cytotoxic lymphocytes (CL) induce apoptosis of virally infected or aberrant cells following recognition of the target cells via specific cell surface receptors. Cytotoxic T lymphocytes (CTL) express antigen-specific T cell receptors that recognise peptide in the context of MHC Class I presented on target cells (reviewed in Mescher, 1995). Natural Killer (NK) cells express a number of inhibitory and activating receptors that belong to either the immunoglobulin superfamily or the C-type lectin family (reviewed in Brooks *et al.*, 2000). The inhibitory NK receptors sense the presence of MHC class I as "self", and hence the absence of MHC class I (which is often down regulated in virally infected and tumourigenic cells) is sensed as a foreign or aberrant cell and is targeted for removal.

Cytotoxic lymphocytes induce apoptosis of target cells via two major pathways ligation of death receptors on the surface of the target cell or the release of cytotoxic granular proteins into the cytoplasm of the target cell (reviewed in Trapani and Jans, 1999; Smyth *et al.*, 2001). Both of these pathways then act on the endogenous apoptotic proteins described above.

1.3.1 Death receptor mediated apoptosis

The death receptors are a subset of the tumour necrosis factor receptor (TNF-R) family. The 6 members and their ligands, which are currently known to have a role in apoptosis, are illustrated in Figure 1.4A. A number of decoy receptors also exist to regulate the activity of the death receptors. These receptors lack the cytoplasmic death domain necessary for transducing the apoptotic signal, and therefore regulate apoptosis by competing for ligand binding (reviewed in Schmitz *et al.*, 2000).

Fas is the most studied member of the TNF-R family, although the mechanism of activation is thought to be conserved between the family members. Ligation of the death receptor by its cognate ligand induces trimerisation of the receptor and initiation of the apoptotic signal which is mediated by interaction of homologous protein-protein domains found in adaptor molecules and caspases (as illustrated in Figure 1.4B).

Fas mediated activation of procaspase-8 can initiate two major apoptotic pathways in the cell: Via activation of caspase-3 and other effector caspases, or via amplification through the mitochondria by the cleavage of Bid, resulting in release of cytochrome *c* and Apaf-1 and the subsequent formation of the apoptosome.

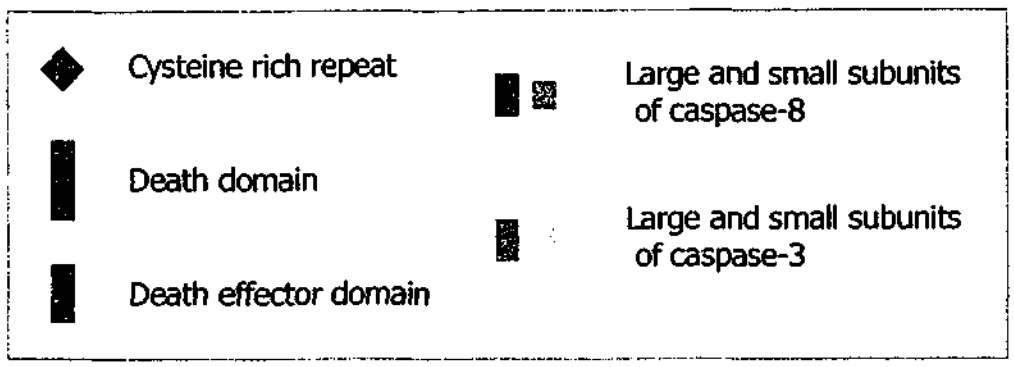

Figure 1.4 Death receptor induced apoptosis. (A) The 6 members of the TNF-R family and their natural ligands currently known to have a role in apoptosis. These receptors contain between 2-5 cysteine-rich repeats in their extracellular domain and a death domain (DD) in their cytoplasmic tail. The cytoplasmic DD is required for transduction of the apoptotic signal. (B) Fas-mediated pathways of apoptosis. Trimerisation of Fas induces the formation of the death inducing signalling complex (DISC). The DD of Fas binds to the DD of FADD and FADD then recruits procaspase-8 by their homologous DED. The proximity induced autoactivation of procaspase-8 then initiates two major apoptotic pathways in the cell. Caspase-8 cleaves and activates procaspase-3 or the apoptotic signal is amplified through the mitochondria by the caspase-8 mediated cleavage of Bid.

A

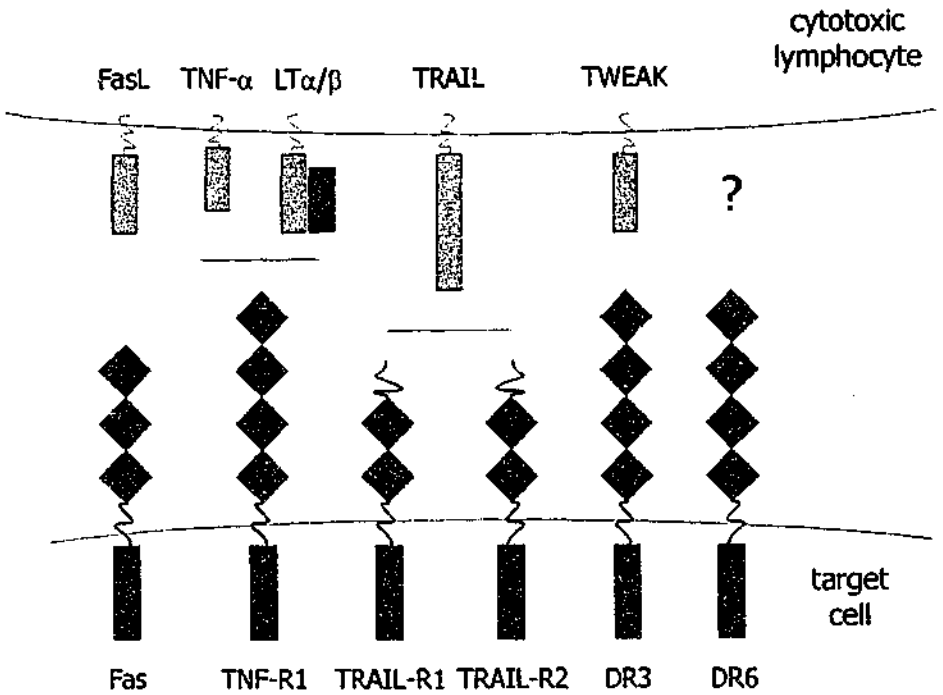
cytotoxic lymphocyte
FasL
TNF-α
LTα/β
TRAIL
TWEAK
?
target cell
Fas
TNF-R1
TRAIL-R1
TRAIL-R2
DR3
DR6

B

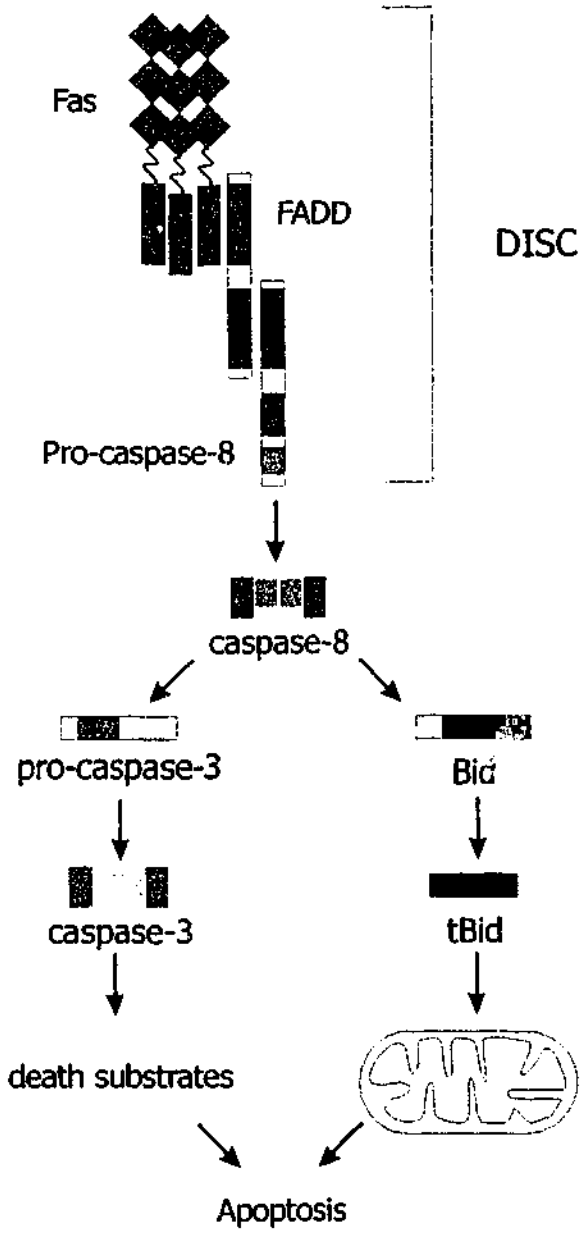
Fas
FADD
DISC
Pro-caspase-8
caspase-8
pro-caspase-3
Bid
caspase-3
tBid
death substrates
Apoptosis

1.3.2 Granule mediated apoptosis

Henkart and co-workers first established the granule exocytosis pathway for lymphocyte cytotoxicity by demonstrating that granules purified from large granular lymphocytes (LGL) induce cytolysis of a number of different cell types. They therefore hypothesised that LGL mediated cytotoxicity was due to release of cytotoxic material from cytoplasmic granules after triggering of a surface receptor (Henkart *et al.*, 1984; Henkart *et al.*, 1985). Subsequent analysis of the contents of granules has identified a number of cytotoxic proteins including the pore forming protein, perforin, and a group of serine proteinases referred to as granzymes (granule associated enzymes).

1.3.2.1 Granule exocytosis

Once a target cell is identified the cytotoxic lymphocyte conjugates with it. This interaction induces a reorganisation of the effector machinery in the cytotoxic lymphocyte towards the target cell, along with a marked redistribution of molecules in the membrane at the site of contact. Membrane reorganisation at the site of contact results in the formation of two concentric rings. The c-SMAC (central-supramolecular activation complex) which contains signalling molecules (TCR, CD2 and CD28) is in turn surrounded by the p-SMAC (peripheral supramolecular activation complex) containing the adhesion molecules, LFA-1 and talin (Monks *et al.*, 1998). This arrangement of proteins at the CTL/target synapse resembles that seen between $CD4^+$ T helper cells and antigen presenting cells (reviewed in Delon, 2000). However, there is a space between the c-SMAC and the surrounding p-SMAC, which allows the exocytosis of granule contents towards the target cell (Stinchcombe *et al.*, 2001; Figure 1.5A).

The signalling cascade initiated by ligation of the TCR also brings about changes in cell architecture. Lck mediated phosphorylation of the TCR recruits and activates ZAP-70, which in turn leads to the recruitment of phospholipase C-γ, PI-3 kinase, Ikt and Ras to the TCR complex. The subsequent generation of diacylglycerol, activated protein kinase C, inositol phosphates and intracellular calcium fluxes, results in cytoskeletal rearrangements that align the secretory apparatus to the immunological synapse (reviewed in Bromley *et al.*, 2001). The reorientation of microtubule organising centre (MTOC) and the Golgi complex toward the target cell (Geiger *et al.*, 1982; Kupfer and Dennert, 1984) is followed by polarisation of the granules to align with the point of membrane contact (Yannelli *et al.*, 1986; Figure 1.5B and C).

The interactions between an effector cells and its target are transitory, as the CL are "serial killers" that can detach and re-engage multiple targets (Sanderson, 1976;

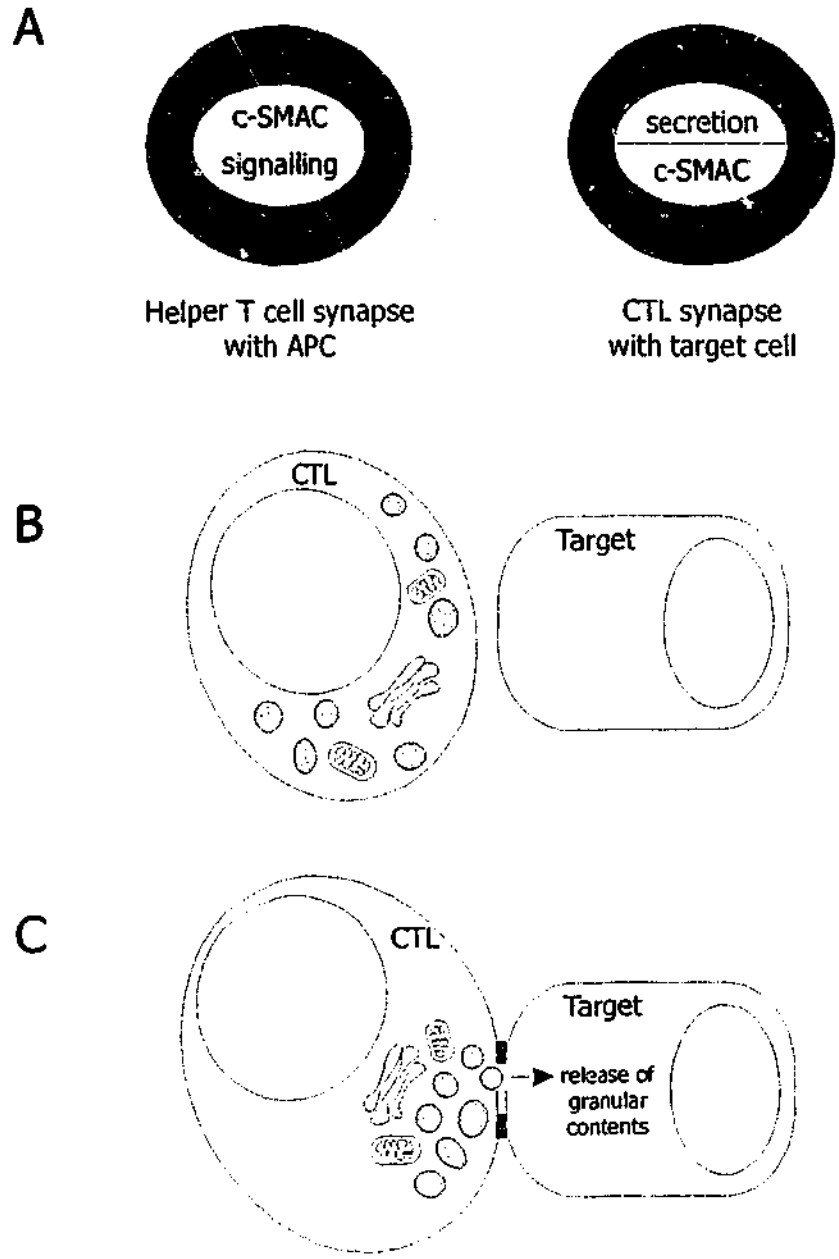

Figure 1.5 Granule exocytosis. (A) The immunological synapse observed between CD4' T helper cells and antigen presenting cells (APC) is also found at the CTL/target interface, however there is a space between the c-SMAC and the surrounding p-SMAC which allows the exocytosis of granule contents towards the target cell (modified from Stinchcombe *et al.*, 2001). (B) Prior to target cell engagement the secretory apparatus of the CTL is randomly distributed. (C) Following signalling through the TCR the MTOC, Golgi apparatus and granules polarise at the point of membrane contact. The granules can then be exocytosed through the immunological synapse.

Rothstein *et al.*, 1978). This serial killing is possible as TCR signalling and granule exocytosis induce the synthesis of cytotoxic proteins to refill the granules (Isaaz *et al.*, 1995), and effector cells release only a portion of granules per target cell engaged (Stinchcombe *et al.*, 2001).

1.3.2.2 Granule contents

Granules contain a number of proteins, although not all of them have a defined role in apoptosis. TIA-1 is a 15 kDa protein located in the granules of NK cells and $CD8^+$ T cells (Anderson *et al.*, 1990) with four predicted transmembrane domains, indicating it is a granular membrane protein. Upon degranulation, TIA-1 translocates to the plasma membrane, which suggests a possible role in the regulation of effector functions (Medley *et al.*, 1996). Granulysin and NK lysin possess antibacterial activity as well as lytic activity against mammalian cell lines (Andersson *et al.*, 1995; Pena and Krensky, 1997). FasL is also stored within cytotoxic granules, and can also be released during granule exocytosis, to initiate the death receptor pathway and augment the granule pathways of apoptosis (Bossi and Griffiths, 1999). Perforin and the granzymes are the most abundant proteins of granules and most research has investigated the role of the granzymes in inducing apoptosis.

1.3.2.3 Perforin mediated uptake of granular contents

Perforin is synthesised as a 70 kDa inactive precursor which is cleaved by a cysteine proteinase in an acidic compartment to yield a 60 kDa active form (Uellner *et al.*, 1997). Perforin polymerises in the presence of Ca^{2+} and inserts into phospholipid bilayers in a manner analogous to the complement C5-C9 complex (Zalman *et al.*, 1985; Young *et al.*, 1986a). These perforin pores can induce membrane damage and cause the release of intracellular contents (as measured by ^{51}Cr release). The size of the perforin pore is dependent upon the number of aggregated perforin monomers and can range from 5 to 15 nm in diameter, allowing diffusion of molecules up to 17 kDa (Criado *et al.*, 1985; Young *et al.*, 1986b).

Perforin alone can induce membrane damage severe enough to cause lysis of the target cell and death via necrosis. However, the apoptotic changes that are the hallmark of CL mediated apoptosis are only evident upon entry of the granule contents into the target cell cytoplasm. If sublytic doses of perforin are applied to cells, plasma membrane integrity can be maintained by the endocytosis of the perforated membrane (Carney *et al.*, 1986) which can also result in the pinocytosis of granular contents from the

extracellular fluid (Podack *et al.*, 1988). Recently, granzyme B has been shown to be taken up into cells by receptor mediated endocytosis, suggesting that perforin does not function at the cell surface but is involved in the release of granzyme B from the endosome (Froelich *et al.*, 1996b; Motyka *et al.*, 2000). This is supported by the use of other endosomolytic agents that can substitute for perforin, in releasing granzyme B from the endosome (Froelich *et al.*, 1996b; Pinkoski *et al.*, 1998; Browne *et al.*, 1999).

1.4 Granzymes

The granzymes comprise a subfamily of the chymotrypsin-like family of neutral serine proteinases. Serine proteinases constitute the largest class of mammalian proteinases and are named for the presence of a catalytically essential serine in the active site. The catalytic site also contains a histidine and aspartic acid residue which, although widely separated in the primary sequence, are brought together in the tertiary structure of the proteinase.

The granzymes are synthesised as pre-pro-enzymes. The N-terminal hydrophobic signal peptide directs translocation into the rough endoplasmic reticulum and is then removed leaving a pro-dipeptide at the N-terminus of the enzyme. Pro-granzyme A and B are targeted to granules by the mannose 6-phosphate receptor pathway (Griffiths and Isaaz, 1993) via modification of their N-linked oligosaccharides with mannose 6-phosphate. It is not currently known how the other granzymes are translocated to the granule, however it is thought that a similar mechanism exists. The removal of the pro-peptide occurs in granules, and the proteinase responsible for the activation of granzyme A and B has been identified as dipeptidyl peptidase I (DPPI; also known as Cathepsin C (Pham and Ley, 1999)). The other granzymes are also presumed to be activated by DPPI although this has yet to be confirmed (Pham and Ley, 1999; Wilharm *et al.*, 1999). Therefore, the granzymes are stored in an active form within granules.

Cytotoxic granules are not conventional secretory granules but are modified lysosomes, containing both the normal complement of lysosomal hydrolases in addition to cytotoxic proteins (reviewed in Page *et al.*, 1998). These modified granules are maintained at an acidic pH (Henkart *et al.*, 1987; Burkhardt *et al.*, 1990) which renders the granzymes inactive while the lysosomal cathepsins are active. The granzymes are highly cationic and are compartmentalised within the granule on a scaffold of the anionic chondroitin A sulfate proteoglycan, serglycin (Masson *et al.*, 1990). Serglycin

ensures the correct packaging of granule contents and acts as a carrier for many of the granule contents after release (Spaeny-Dekking *et al.*, 2000; Metkar *et al.*, 2002)

Cytotoxic granules have been studied in many cytotoxic cells and appear to be heterogeneous in structure, consisting of an electron dense core, a multivesiculated region or both (Burkhardt *et al.*, 1990). Immunogold studies indicate that the granzymes, perforin and proteoglycan are located in the electron dense core (Burkhardt *et al.*, 1990; Peters *et al.*, 1991) while the cathepsins are stored in the multivesiculated regions (Peters *et al.*, 1989). Also there is some conjecture as to whether or not a double membrane surrounds these structures, as in some studies no such delimiting membranes could be detected (Burkhardt *et al.*, 1990) whereas in others they were (Peters *et al.*, 1991; Baranov *et al.*, 2000).

1.4.1 Cytotoxicity of the granzymes

Five granzymes have been identified in humans: granzyme A, B, H, K and M (their attributes are described in Table 1.2). In rodents there has been an expansion in the number of granule proteinases; in mice, at least 10 granzymes have been described while in the rat, at least 7 granular proteinases have been cloned. Rodent homologues have been identified for human granzyme A, B, K and M but not for granzyme H. Of the human granzymes only granzyme A and B have been shown to induce apoptosis and the majority of the work on granzymes has focused on these two proteinases.

Granzyme A

Granzyme A (graA) is expressed in CTL and LAK (Hameed *et al.*, 1988; Krahenbuhl *et al.*, 1988) and can cause apoptosis when introduced into the cytoplasm of target cells (Hayes *et al.*, 1989; Shiver *et al.*, 1992; Beresford *et al.*, 1999). The perforin mediated introduction of graA into target cells causes the characteristic apoptotic changes of nuclear condensation and membrane blebbing, however the rate at which graA and perforin initiate apoptosis is much slower then that seen for CL, suggesting graA is not the major proteinase involved in apoptosis. In addition, graA does not cause the oligonucleosomal DNA laddering which is indicative of apoptosis, although single stranded DNA breaks can be detected following longer incubations. This process is not prevented by inhibition of caspases or overexpression of Bcl-2, and is dependent on the cleavage of PHAP-II, a HLA-associated protein (Beresford *et al.*, 1999). PHAP-II/SET is part of a multimeric complex located at the endoplasmic reticulum which, when cleaved by graA, releases a nuclease responsible for the single stranded DNA breaks

Table 1.2 The human granzymes

Granzyme	Other names	Predicted cleavage	Size (kDa)	Chromosomal location	Cellular expression	Proapoptotic function
A	Granzyme A (Krahenbuhl *et al.*, 1988) HuTSP (Fruth *et al.*, 1987) Hanukah factor (Gershenfeld *et al.*, 1988) Q31 tryptase (Poe *et al.*, 1988) Granzyme 1 (Hameed *et al.*, 1988)	Arg/Lys	60 (dimer)	5q11-q12 (Baker *et al.*, 1994a)	CTL and LAK (Hameed *et al.*, 1988; Krahenbuhl *et al.*, 1988)	Only when injected into the cytoplasm of target cells (Hayes *et al.*, 1989; Shiver *et al.*, 1992; Beresford *et al.*, 1999)
B	Granzyme B (Krahenbuhl *et al.*, 1988) HSE 26.1 (Trapani *et al.*, 1988) SECT (Caputo *et al.*, 1988) Granzyme 2 (Hameed *et al.*, 1988)	Asp/Glu	29-33	14q11-q12 (Lin *et al.*, 1990)	CTL and LAK (Hameed *et al.*, 1988; Krahenbuhl *et al.*, 1988, Trapani *et al.*, 1988)	Can induce apoptosis (Shi *et al.*, 1992); can cleave caspases (Darmon *et al.*, 1995) or Bid
H	Granzyme H (Haddad *et al.*, 1991) CGL-2 (Hanson *et al.*, 1990) CSP-C (Klein *et al.*, 1990)	Phe/Tyr (Met) (Edwards *et al.*, 1999)	30	14q11-q12 (Lin *et al.*, 1990)	LAK but not resting NK or T cells (MacIvor *et al.*, 1999)	Can be endocytosed but no induction of apoptosis (Edwards et al., 1999)
K	Granzyme 3 (Hameed *et al.*, 1988) HNK-Tryp-2 (Sayers *et al.*, 1996)	Arg/Leu (Babe *et al.*, 1998)	30	5q11-q12 (Baker *et al.*, 1994a)	NK and T cells (Hameed *et al.*, 1988; Sayers *et al.*, 1996)	Can induce apoptosis after prolonged incubation (Shi *et al.*, 1992)
M	Met-ase (Smyth, 1993)	Met/Leu (Smyth *et al.*, 1995b; Smyth *et al.*, 1996)	30	19p13.3 (Baker *et al.*, 1994b)	NK cells (Smyth *et al.*, 1995a), NK T cells and γδ TCR T cells (Sayers *et al.*, 2001)	None shown

(Beresford *et al.*, 2001). GraA also directly cleaves lamins A, B, and C to disrupt the nuclear lamina (Zhang *et al.*, 2001a), degrades histone H1 (Zhang *et al.*, 2001b) and cleaves nucleolin (Pasternack *et al.*, 1991).

To further understand the role of graA in apoptosis, GraA null mice have been generated. These mice are healthy, have normal haematopoietic development and their CL exhibit normal kinetics of apoptosis induction. The graA null mice are not susceptible to Lymphocytic Choriomeningitis virus or *Listeria* infections, and can eradicate syngeneic tumours as efficiently as normal mice (Ebnet *et al.*, 1995a). These results suggest that graA does not play a major role in granule mediated apoptosis. However, these mice are much more susceptible to Ectromelia infection, although the exact mechanism of this susceptibility is not known (Mullbacher *et al.*, 1996).

GraA can cleave a number of other proteins. It can directly process IL-1β (suggesting CL can contribute to the inflammatory response (Irmler *et al.*, 1995)) and can also induce the secretion of IL-6 and IL-8 from epithelial cells (Sower *et al.*, 1996b) and IL-6, IL-8 and TNFα from monocytes, via cleavage of a cell surface receptor (Sower *et al.*, 1996a). GraA can also cause neurite retraction on astrocytes and neuronal cells due to cleavage of the thrombin receptor (Suidan *et al.*, 1994), however graA cleavage of the thrombin receptor cannot cause platelet aggregation (Suidan *et al.*, 1996). It is apparent that graA can modulate the immune response by acting on a number of cell types, therefore the immune deficiencies detected in the graA null mice infected with Ectromelia virus may be due to a loss of immunomodulatory function rather than a lack in cytotoxic ability.

1.5 Granzyme B

Granzyme B (graB) is the most studied of the granzymes and is unique among serine proteinases in its ability to cleave after acidic residues, particularly aspartic acid (Poe *et al.*, 1991). It is this 'Asp-ase' activity that allows graB to cleave and activate caspases as well as other intracellular components during the induction of apoptosis. Classically, the entry of graB into target cells was thought to be dependent on the ability of perforin to form pores in the plasma membrane. However the size of the poly-perforin pore (160 Å (Young *et al.*, 1986b)) is not consistent with this being a route for graB uptake. Also very high levels of perforin (>4000 U/ml) are required to allow the entry of macromolecules the size of graB (Browne *et al.*, 1999). It has since been proposed that graB is taken up into cells by receptor mediated endocytosis, via the

ubiquitously expressed 300 kDa mannose 6-phoshate receptor (Motyka *et al.*, 2000), and that perforin (Shi *et al.*, 1997) or other endosomolytic agents (Froelich *et al.*, 1996b; Browne *et al.*, 1999) cause the rupture of endosomes and release of graB into the cell.

1.5.1 Importance of granzyme B in granule mediated apoptosis

The importance of graB in granule mediated apoptosis is illustrated by a number of studies. The natural killer-like cell line, YT-INDY, expresses a limited range of cytotoxic molecules (graB, graH and perforin) but can induce DNA fragmentation in target cells by granule mediated apoptosis (Su *et al.*, 1994). Stable transfection of an antisense graB construct into YT cells decreases graB expression by 80% and decreases DNA fragmentation by >95% (Bochan *et al.*, 1995).

Additionally, graB null mice have been generated and are unable to induce the rapid DNA fragmentation that is a hallmark of CL killing (Heusel *et al.*, 1994). However, subsequent analysis of these mice has indicated that, in addition to graB, other granzyme genes at the same locus (granzymes C, D, F and G) were downregulated due to downstream effects of the pGKneo cassette introduced during homologous recombination (Pham *et al.*, 1996). Null mice in which graB alone is removed have yet to be generated.

1.5.2 Granzyme B substrates

GraB has been reported to activate a wide variety of substrates including various components in the nucleus, many of the caspases and most recently Bid, a pro-apoptotic member of the Bcl-2 family. Therefore, graB participates in a number of apoptotic pathways either by directly cleaving death substrates or by activating the caspase cascade, again either directly through cleavage of the caspases or indirectly via the mitochondria.

The list of proteins cleaved by graB is rapidly growing (Andrade *et al.*, 1998; Casciola-Rosen *et al.*, 1999; Stennicke and Salvesen, 1999; Kam *et al.*, 2000) with analysis of the substrate specificity of human graB identifying IEPD as the optimal P_4-P_1 cleavage sequence (Thornberry *et al.*, 1997). However, residues on the P' side of the cleavage event are also important in determining the efficiency of the interaction between the substrate and graB. Optimal binding of graB to substrates is facilitated by an acidic residue at the P_4' site of the substrate which forms a salt bridge with lysine^{27} of graB (Sun *et al.*, 2001).

Granzyme B and the nucleus

The DNA fragmentation that is characteristic of CTL and NK cell attack occurs rapidly after target cell engagement. As such much effort has been invested in determining the mechanism(s) through which DNA cleavage is mediated. Early workers observed that upon graB entering the cytoplasm, it rapidly accumulates in the nucleus (Trapani *et al.*, 1994) and binds to nuclear substrates (Pinkoski *et al.*, 1996). Analysis of the kinetics of the nuclear uptake indicates that graB diffuses to the nucleus and is retained there due to interaction with nuclear proteins (Jans *et al.*, 1996). The translocation of graB into the nucleus precedes DNA fragmentation (Trapani *et al.*, 1998b), is caspase dependent (Trapani *et al.*, 1998a; Pinkoski *et al.*, 2000) and can be blocked by Bcl-2 overexpression (Jans *et al.*, 1999).

Several nuclear substrates of graB have been identified including poly (ADP-ribose) polymerase (PARP) (Froelich *et al.*, 1996a), lamin B (Zhang *et al.*, 2001a), the catalytic subunit of DNA-dependent protein kinase (DNA-PK) and nuclear mitotic apparatus protein (NuMA) (Andrade *et al.*, 1998). However, it is not clear whether graB cleaves these substrates directly, as the cleavage of PARP and lamin B in some studies, is dependent upon the activation of caspases (Darmon *et al.*, 1995; Talanian *et al.*, 1997). These observations must be tempered with consideration that these studies were performed using the caspase inhibitors z-DEVD-fmk and/or z-VAD-fmk, which may inhibit the Asp-ase activity of graB as well as the caspases, depending on the concentration used.

The nuclease responsible for DNA fragmentation has been identified as caspase-activated DNase (CAD, or DFF40). CAD forms a heterodimer with ICAD (inhibitor of CAD, also known as DFF45) in the nucleus, where CAD is retained in its inactive form (Liu *et al.*, 1997; Enari *et al.*, 1998; Liu *et al.*, 1998; Sakahira *et al.*, 1998). As the name suggests CAD activation is dependent upon cleavage of ICAD by caspases, predominantly caspase-3 (Wolf *et al.*, 1999), however graB can directly cleave DFF45/ICAD to active DFF40/CAD in the absence of caspase-3 (Thomas *et al.*, 2000; Sharif-Askari *et al.*, 2001).

Granzyme B activation of the caspases

GraB can activate most of the procaspases *in vitro* (Table 1.3) however under physiological conditions this is probably more restricted. Analysis of the substrate specificity of human and rat graB has identified IE(P/T)D as the optimal cleavage sequence (Thornberry *et al.*, 1997; Harris *et al.*, 1998), which suggests graB can cleave and activate procaspase-3 and -7 and probably procaspase-8 and -10 (see Table 1.3). However, when the optimal substrate sequence is considered with an acidic residue at P_4' (Sun *et al.*, 2001), then procaspase-3 is the favoured graB substrate (see Table 1.3). The analysis of graB substrates is made more difficult due to the use of several sources of graB with mouse, rat and human graB used interchangeably by most groups. Although a direct comparison of human and mouse graB has not been performed, it has been reported that murine graB has a more restricted capacity to activate murine caspases *in vitro* (Van de Craen *et al.*, 1997) than does human graB with the human caspases.

The direct cleavage of a subset of the caspases by graB is supported by *in vivo* analysis which indicates that graB can cleave procaspase-3 (Darmon *et al.*, 1995; Darmon *et al.*, 1996; Shi *et al.*, 1996), procaspase-7 (Chinnaiyan *et al.*, 1996) and procaspase-8 during apoptosis (Medema *et al.*, 1997). Attempts to order the process of caspase activation in cells have been confusing as one study concluded that graB initiates apoptosis through cleavage of procaspase-10 (Talanian *et al.*, 1997) while other studies indicated that it was via cleavage of procaspase-3 (Atkinson *et al.*, 1998; Yang *et al.*, 1998).

Granzyme B and the mitochondria

Analysis of the events induced during graB mediated apoptosis indicates that mitochondrial disruption (release of cytochrome *c* and loss of $\Delta\Psi_m$) occurs at the same time as caspase-3 processing, and precedes other apoptotic changes. There is some controversy as to what mediates mitochondrial disruption, as one study determined graB mediated apoptosis results in the caspase dependent release of cytochrome *c* while loss of $\Delta\Psi_m$ can occur independently of the caspases (MacDonald *et al.*, 1999), whereas another indicated that release of cytochrome *c* and loss of $\Delta\Psi_m$ are both caspase independent (Heibein *et al.*, 1999). These contradictory results may have arisen due to differences in experimental design, the first study used a mixture of human (HeLa and U937) and rat (Rat-1) cell lines with rat or murine graB, while the second study used a human (Jurkat) cell line with human graB. This mixing of reagents from various species

Procaspase	Activation site	Reference(s)
2	DQQD-GKNH	(Harvey *et al.*, 1996)
3	IETD-SGVD*#	(Darmon *et al.*, 1995; Martin *et al.*, 1996; Quan *et al.*, 1996)
5	LEAD-SVCK	(Wang *et al.*, 1996)
6	TEVD-AASV	(Orth *et al.*, 1996)
7	IQAD-SGPI*	(Chinnaiyan *et al.*, 1996; Gu *et al.*, 1996)
8	VETD-SEEQ*	(Muzio *et al.*, 1996; Medema *et al.*, 1997)
9	DQLD-AISS	(Duan *et al.*, 1996; Srinivasula *et al.*, 1996b)
10	IEAD-ALNP*	(Fernandes-Alnemri *et al.*, 1996)

Table 1.3 Cleavage of procaspases by granzyme B. The majority of the caspases have been shown to be cleaved by graB *in vitro*, however whether this occurs *in vivo* is not yet clear. The initial cleavage of the caspases occurs at the C-terminus of the large subunit, which is referred to as the activation site of the caspases.*Indicates the caspase activation site that matches the P_4-P_1 substrate specificity of graB (Thornberry *et al.*, 1997), while #indicates the activation site that matches the P_4-P_1 and P_4' substrate specificity of graB (Sun *et al.*, 2001).

may reveal subtle differences in the cleavage specificity of graB and the activation sequences of the target molecules between species.

Subsequent analysis of mitochondrial pathways to apoptosis has demonstrated that the pro-apoptotic Bcl-2 family member, Bid, can be directly cleaved by graB leading to disruption of the mitochondria (Barry *et al.*, 2000; Heibein *et al.*, 2000; Sutton *et al.*, 2000; Alimonti *et al.*, 2001). Again there is some conjecture as to how graB mediates these effects, as cleavage of Bid by graB is at aspartic acid[75] rather than aspartic acid[59] (the cleavage site of caspase-8) (Li *et al.*, 1998). Therefore, cleavage by graB results in a shorter form of tBid, which lacks the myristoylation site required for efficient localisation to the mitochondria (Zha *et al.*, 2000). As yet the translocation to, and effect upon, the mitochondria of graB matured tBid has not been well characterised.

Conclusions from the above studies should be tempered by the fact that graB was derived from a variety of species and often graB from one species was used to cleave substrates derived from another species. Human graB-matured tBid recruits Bax to the mitochondria and induces cytochrome *c* release (Heibein *et al.*, 2000) and mitochondrial membrane depolarisation (loss of $\Delta\Psi_m$) (Sutton *et al.*, 2000). Mouse/rat graB induces cytochrome *c* release in a Bid-dependent manner but membrane depolarisation is a result of graB directly affecting the permeability transition (PT) pore independent of Bid or other cytosolic factors (Alimonti *et al.*, 2001). This again is in contradiction to a recent study which shows that murine graB causes membrane depolarisation without inducing PT pore opening, dependent upon a cytosolic factor (Thomas *et al.*, 2001).

Pathways to granzyme B mediated apoptosis

While it is clear that graB can cleave many substrates *in vitro*, the analysis of the actual substrates cleaved *in vivo* is not yet clear. Recent studies have focused on the mitochondria in graB mediated apoptosis, however graB has been shown to activate other apoptotic pathways (illustrated in Figure 1.6). Does graB act only upon the mtiochondrial pathway and not cleave the caspases or substrates in the nucleus? The latest studies on graB mediated apoptosis would suggest that the mitochondria is the major pathway, as over expression of Bcl-2 can block apoptosis (Davis *et al.*, 2000; Pinkoski *et al.*, 2001). However, both studies relied upon purified graB and perforin to induce apoptosis. As yet, the amount of graB that is exocytosed by CL is not known and therefore these studies may not accurately reflect apoptosis induced by CL. This is particularly apparent as following prolonged incubation times or using increasing

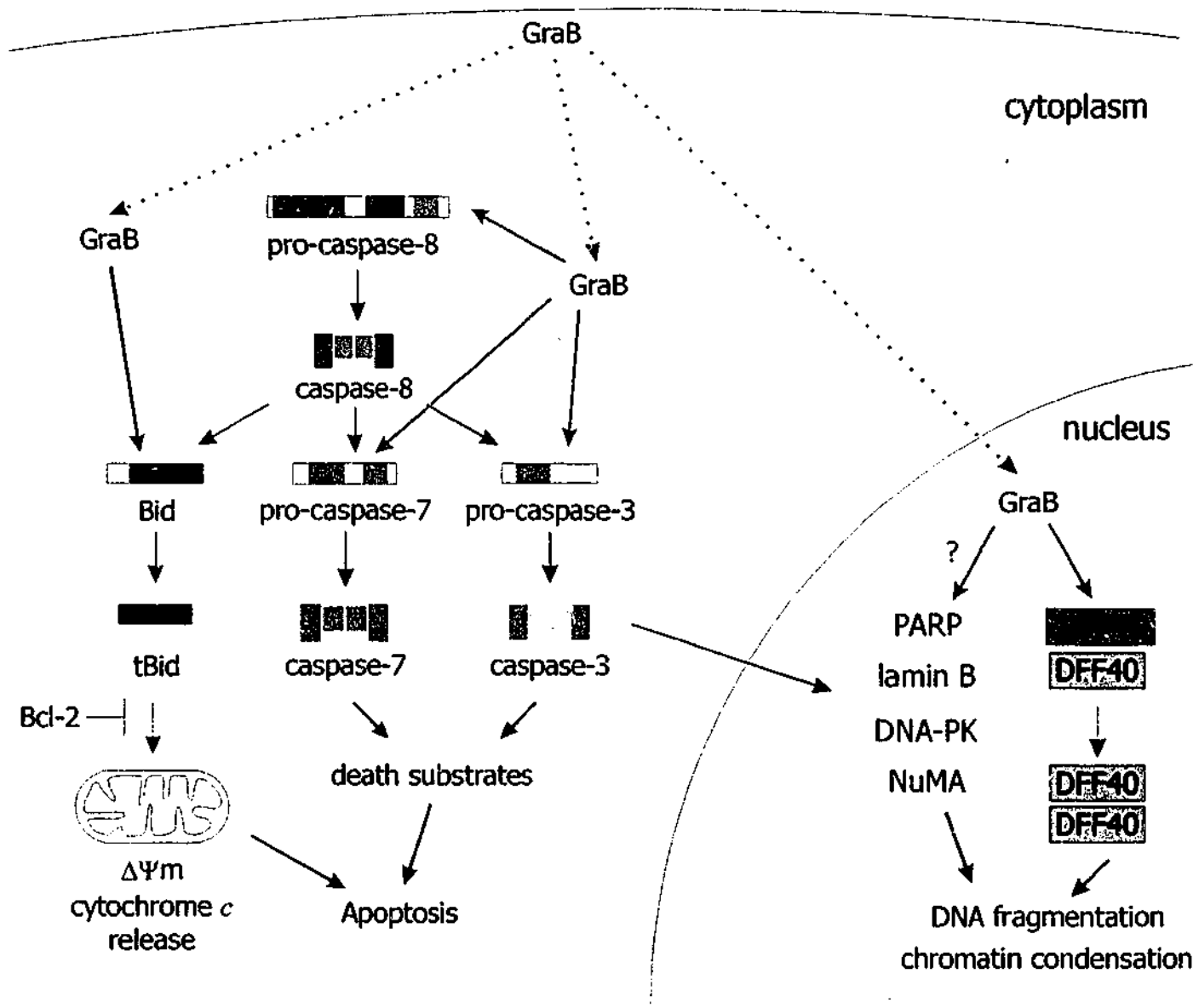

Figure 1.6 Pathways of granzyme B mediated apoptosis. Entry of graB into the cytoplasm of the target cells allows access to a number of potential substrates. GraB can activate mitochondrial pathways of apoptosis by directly cleaving Bid. Alternatively, graB can process a number of the procaspases, the active caspases can then activate pathways of apoptosis via the mitochondria or the nucleus. GraB can also directly process nuclear substrates, although cleavage of some of these nuclear substrates may be caspase-dependent.

amounts of graB, apoptosis can be detected in Bcl-2 overexpressing cells (Pinkoski *et al.*, 2001), suggesting graB can bypass Bcl-2. Furthermore, earlier studies indicated that Bcl-2 could affect the translocation of graB to the nucleus (Jans *et al.*, 1999). This suggests that overexpression of Bcl-2 may affect pathways distal to the mitochondria and hence analysis of graB pathways becomes increasingly difficult.

1.5.3 Other roles for granzyme B

A role for graB in cleavage of autoantigens has been suggested by several recent studies, which have demonstrated a number of autoantigens of systemic autoimmune diseases are efficiently cleaved by graB (Andrade *et al.*, 1998; Casciola-Rosen *et al.*, 1999; Gahring *et al.*, 2001; Hansen *et al.*, 2001; Nagaraju *et al.*, 2001). Further analysis of autoantigen cleavage indicates that they are only cleaved by graB and not caspase-8 even though these proteinases share similar substrate specificities (IEPD for graB and IETD for caspase-8). Furthermore, these autoantigens can be cleaved during granule mediated apoptosis, illustrating the role of CL in the initiation of autoimmune disease (Casciola-Rosen *et al.*, 1999).

An extracellular role for graB has also been suggested by several studies as graB can cleave aggrecan proteoglycan synthesised by chondrocytes (Froelich *et al.*, 1993) and cartilage proteoglycans at the synovium in rheumatoid arthritis (Ronday *et al.*, 2001)). GraB has also been implicated in the passage of $CD34^+$ peripheral blood progenitor cells from bone marrow following chemotherapy (Berthou *et al.*, 1995), with the authors suggesting cleavage of extracellular matrix proteins by graB could be involved in the detachment of cells and their migration across the endothelial cell barrier.

1.5.4 Protection from granzyme B

The potent apoptotic properties of graB suggest that this protein needs to be tightly regulated, as uncontrolled release would be detrimental to cells. The question of why CL are not killed by their own cytotoxins is posed frequently and several protective mechanisms to CL have been described. These mechanisms fall into two main categories i) protection from fratricide – that is protection from other CTL and ii) protection from suicide – that is protection from their own cytotoxic molecules.

CTL fratricide

Analysis of heteroclonal lysis – whether one CTL clone (effector CTL) can kill another CTL clone (target CTL), has suggested that CTL are resistant to cytolysis (Luciani *et al.*, 1986; Blakely *et al.*, 1987). Other studies have suggested CTL susceptibility is related to lytic activity, with the most efficient CTL being the least susceptible to lysis (Kranz and Eisen, 1987; Skinner and Marbrook, 1987), however Zanovello and co-workers suggested the resistance to CTL killing is an artefact of *in vitro* culture of CTL clones (Zanovello *et al.*, 1989).

Analysis of this earlier work is difficult, as the various pathways of cell death were not yet understood and as such it was not known whether this susceptibility was due to pathways mediated by death receptors or granule contents. Therefore, expression of factors such as c-FLIP or Bcl-2 that could modulate the death receptor pathway were not determined in these studies. However, studies performed with purified granules from CTL (Blakely *et al.*, 1987; Verret *et al.*, 1987) suggest that CTL are resistant to the granzyme/perforin pathway of apoptosis.

It has been suggested that the resistance of CTL to perforin is due to differences between the plasma membrane of CTL and other cells. Perforin binds poorly to tightly spaced phospholipid membranes (Antia *et al.*, 1992) suggesting CTL resistance may be partially explained by phospholipid spacing. However other studies contradict this (Ojcius *et al.*, 1990), while some have suggested that CTL membranes differ in total lipid content from other membranes (Takai *et al.*, 1997). Another possibility is that CTL membranes contain a protein that impedes binding of perforin to membrane (Jiang *et al.*, 1990a; Ojcius *et al.*, 1991). Studies have shown that CTL resistance to perforin can be decreased after treatment with trypsin and tunicamycin, suggesting that the molecule responsible for perforin resistance is a glycosylated membrane protein (Jiang *et al.*, 1990b).

Subsequently, the calcium binding protein calreticulin (Dupuis *et al.*, 1993) has been shown to bind perforin (Andrin *et al.*, 1998). Calreticulin is upregulated following T cell activation (Burns *et al.*, 1992) and can regulate perforin mediated lysis of erythrocytes, suggesting that the presence of calreticulin at the CTL cell surface can prevent perforin insertion and polymerisation (Fraser *et al.*, 2000).

CTL suicide

CL also contain mechanisms to protect them from their own cytotoxic molecules. As described above calreticulin can prevent the formation of perforin pores at the plasma membrane. However, calreticulin in granules can also prevent perforin activity during storage either by chelation of calcium (Dupuis *et al.*, 1993), required for perforin polymerisation, or via binding to perforin directly (Andrin *et al.*, 1998). Perforin does not polymerise in the ER or Golgi because it is only activated following cleavage at the C-terminus in an acidic compartment (Uellner *et al.*, 1997), and therefore is only active once it reaches the granule.

Whether CL need to be protected directly from perforin, depends on the ability of perforin to cause death. High concentrations of perforin are required to cause cell lysis whereas relatively small amounts are needed to allow the perforin mediated release of the granzymes into the cytoplasm (Browne *et al.*, 1999). The granzymes are stored as active proteinases following cleavage by DPP-I in the granule (Pham and Ley, 1999), while the acidic pH of the granule reduces granzyme activity (Henkart *et al.*, 1987) Release into a neutral compartment allows the granzymes to regain full activity. The granzymes are packaged in the granules with proteoglycans (Kamada *et al.*, 1989; Masson *et al.*, 1990) and secreted with them (Galvin *et al.*, 1999). The packaging of granzymes with proteoglycans has been suggested to either protect CTL from inappropriate granzyme activity or conversely to protect granzymes from proteolytic inactivation following degranulation (Spaeny-Dekking *et al.*, 2000).

Following granule exocytosis the CTL may be susceptible to graB via receptor mediated uptake by the mannose 6-phosphate receptor (M6PR) (Motyka *et al.*, 2000). This receptor is ubiquitously expressed and can be detected at the plasma membrane in most cell types (Willingham *et al.*, 1983; Geuze *et al.*, 1984; Geuze *et al.*, 1985; Braulke *et al.*, 1987; Griffiths *et al.*, 1990). Therefore, T cells have the potential to internalise exocytosed graB via the M6PR and furthermore, as the M6PR is upregulated on activated T cells (Hindmarsh *et al.*, 2001) this would increase the potential to reinternalise graB following degranulation.

A number of anti-apoptotic factors are upregulated during T cell activation including FLIP (Kirchhoff *et al.*, 2000) and anti-apoptotic members of the Bcl-2 family (Boise *et al.*, 1995; Broome *et al.*, 1995; Cohen *et al.*, 1997) which decrease the susceptibility of CL to apoptosis induced by FasL and growth factor withdrawal.

Ectopic granzyme B

The presence of extracellular graB has been demonstrated in the plasma of normal individuals (Spaeny-Dekking *et al.*, 1998), suggesting graB may escape from the immunological synapse. Increased plasma levels of graB are also detected in the sera of patients with elevated CTL responses (Spaeny-Dekking *et al.*, 1998) and in those with severe Gram negative bacterial infections (Lauw *et al.*, 2000). Additionally, graB is present in bronchoalveolar lavage fluids from hypersensitivity pneumonitis (Tremblay *et al.*, 2000) and the synovial joints of patients with rheumatoid arthritis (Tak *et al.*, 1999). The presence of graB at these sites suggests that graB may play a role in the progression of these diseases.

Extracellular graB can be inhibited to a small degree by α_2-macroglobulin and α_1-antitrypsin (Poe *et al.*, 1991) although this occurs at a level below physiological significance (P. Bird and J. Sun, personal communication). The effect of other extracellular proteinase inhibitors such as elafin and secretory leukocyte protease inhibitor have also been examined (Tremblay *et al.*, 2000), but to date no effective extracellular inhibitors of graB have been described, and it is not known whether extracellular graB is regulated.

As graB can be endocytosed by the ubiquitously expressed M6PR (Motyka *et al.*, 2000), cells in the vicinity of an immune response may also be exposed to high concentrations of graB and inappropriately targeted for removal. Activated perforin has a very short half-life (Podack, 1992) and therefore is rapidly inactivated once released from the effector cell, however other endosomolytic agents can deliver graB into the cytoplasm (Froelich *et al.*, 1996b; Browne *et al.*, 1999). GraB could also enter the cytoplasm of the cytotoxic cell if there is leakage from cytotoxic granules.

The entry of mis-directed graB into the cytoplasm of effector cells or bystander cells could cause apoptosis, which would be detrimental to the effectiveness of the immune response. As such the expression of an intracellular inhibitor of graB would protect these cells from ectopic graB. Work performed in this laboratory has demonstrated that Proteinase Inhibitor 9 (PI-9), a member of the intracellular ov-serpin family, is a potent inhibitor of graB. The expression of PI-9 in cytotoxic lymphocytes and other immune tissues supports its role in inhibiting the pro-apoptotic affects of graB (Sun *et al.*, 1996).

1.6 The serpin superfamily

The serpins (serine proteinase inhibitors) are a superfamily of homologous proteins that share a conserved structure, and function primarily to inhibit the proteolytic activity of serine proteinases. Analysis of genome databases has identified over 400 potential serpin sequences from metazoa, plantae and some viruses (Irving *et al.*, 2000), and recently serpins have been identified in bacteria and yeast (Dr' J. Whisstock, personal communication). Phylogenetic analysis divides these serpins into 16 distinct clades and a number of orphan serpins (Irving *et al.*, 2000).

Serpins regulate serine proteinases in a number of physiological processes including blood coagulation, fibrinolysis, complement activation and tissue remodelling (Potempa *et al.*, 1994), however not all serpins are proteinase inhibitors. A minority of serpins have evolved different roles in hormone transport, blood pressure regulation, protein folding, tumourigenesis and angiogenesis (Pemberton *et al.*, 1988, Doolittle, 1983, Hirayoshi *et al.*, 1991, Zou *et al.*, 1994, Zhang *et al.*, 2000).

The importance of serpins in regulating physiological processes is revealed by mutations in serpins that lead to deficiency or dysfunction (reviewed in Stein and Carrell, 1995). This is exemplified by the Pittsburgh mutant of α_1-antitrypsin (α_1-AT) which results in a severe bleeding disorder. In this mutant a single point mutation substitutes methionine^{358} with arginine, thereby converting α_1-AT from an efficient elastase inhibitor into a thrombin inhibitor (Owen *et al.*, 1983).

1.6.1 Serpin structure

Structure function analysis of serpins has profited from the numerous natural mutations that have been identified and characterised, allowing definition of the functionally important regions (reviewed by Stein and Carrell, 1995). This, in combination with the 14 serpin crystal structures (reviewed in Whisstock *et al.*, 1998), has demonstrated that all inhibitory serpins share a common tertiary structure consisting of three β-pleated sheets (A-C) and nine α-helices (A-I) (Figure 1.7). Extending from this conserved structure is a highly variable loop. This reactive centre loop (RCL) extends from strand 5A to strand 1C and is the site of cleavage by the proteinase.

The RCL acts as a pseudosubstrate for the proteinase and therefore defines the specificity of the serpin. Using the nomenclature devised by Schechter and Berger the amino acids N-terminal of the cleavage event are designated P_{17} to P_1, while those C-terminal are P_1' to P_{10}' (Schechter and Berger, 1967). The P_1-P_1' peptide bond

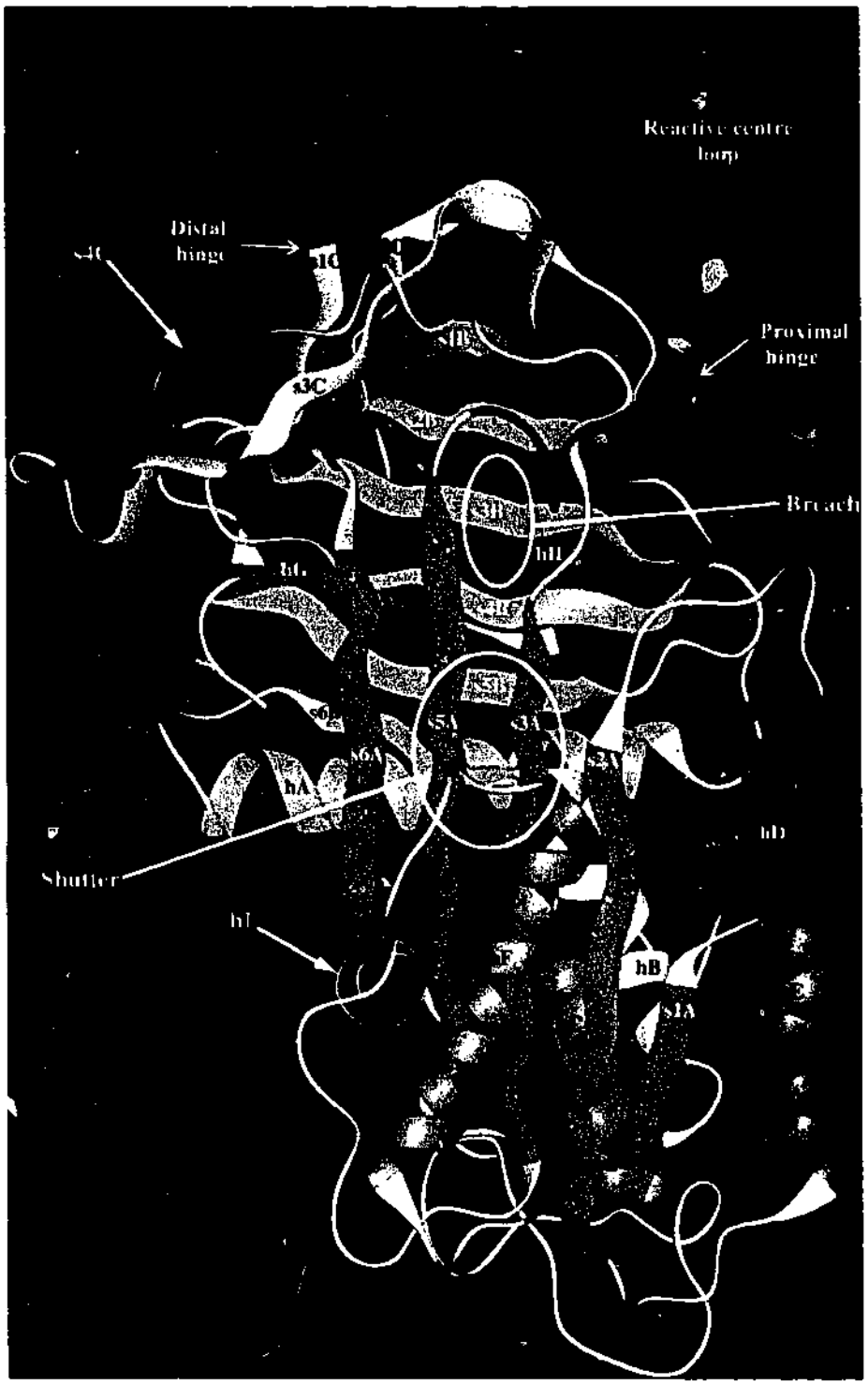

Figure 1.7 Structure of the canonical serpin native antitrypsin. The nine α-helices (hA-I) and the three β-sheets (sA-C) are indicated in separate colours. The reactive centre loop and its adjoining hinge regions which allow the mobility required for inhibitory function, as well as the breach and shutter domain are indicated. Modified from Whisstock *et al.*, 2000.

defines the site of cleavage by the cognate serine proteinase. The P_1 is the major determinant of serpin specificity, while other residues within the RCL contribute to the affinity of the interaction. The Pittsburgh mutant of α_1-AT described above illustrates the importance of the P_1 in determining specificity. The mutation of methionine to arginine occurs at the P_1 position which completely alters the proteinase specificity of the serpin (Owen *et al.*, 1983). However, some serpins can inhibit a number of different serine proteinases by use of alternate P_1 residues in the RCL, for example PI-6 can inhibit trypsin via arginine^{341} (Coughlin *et al.*, 1993) and can also inhibit chymotrypsin via methionine^{340} (Riewald and Schleef, 1996).

The first serpin to be crystallised was α_1-AT cleaved at the P_1-P_1' scissile bond. Unexpectedly, the P_1 and P_1' residues were found to be separated by 67 Å and the residues of the RCL N-terminal to the cleavage site were inserted into β-sheet A to form a 6 stranded β-sheet (Loebermann *et al.*, 1984). Crystallisation of uncleaved serpins demonstrates that the RCL is normally exposed (Stein *et al.*, 1990; Schreuder *et al.*, 1994; Wei *et al.*, 1994) and its insertion into β-sheet A upon cleavage is part of the inhibitory mechanism. This mobility of the RCL is mediated by two flanking hinge regions (proximal and distal) while the insertion of the RCL into β-sheet A is facilitated by the breach, located at the top of the A sheet (Whisstock *et al.*, 2000), and the shutter (illustrated in Figure 1.7). These regions control opening of the A sheet as insertion of the RCL requires movement of the F helix and strands 1-3 of the A sheet (Engh *et al.*, 1990) with strand 3A sliding into the groove of helix B (Stein and Chothia, 1991).

1.6.2 Mechanism of proteinase inhibition by serpins

Proteinase inhibition by serpins follows an essentially irreversible suicide substrate pathway (illustrated in Figure 1.8). The serpin and proteinase bind in a 1:1 ratio following recognition of the serpin RCL by the proteinase. The interaction of the serpin with the proteinase initially involves formation of a reversible Michaelis-Menten complex. The reversible complex is rapidly converted to a covalently locked complex governed by the rate of acylation. This conversion involves cleavage of the RCL at the P_1-P_1' bond, release of the P_1' residue and formation of an ester linkage between the P_1 residue of the serpin and the catalytic serine of the proteinase, trapping the complex as a stable acyl-enzyme intermediate (Lawrence *et al.*, 1995; Wilczynska *et al.*, 1995).

Whether the non-inhibitory or inhibitory pathway is followed depends upon the rate of insertion of the RCL. The non-inhibitory pathway usually results from the interaction of a serpin with a non-cognate proteinase and results in release of active

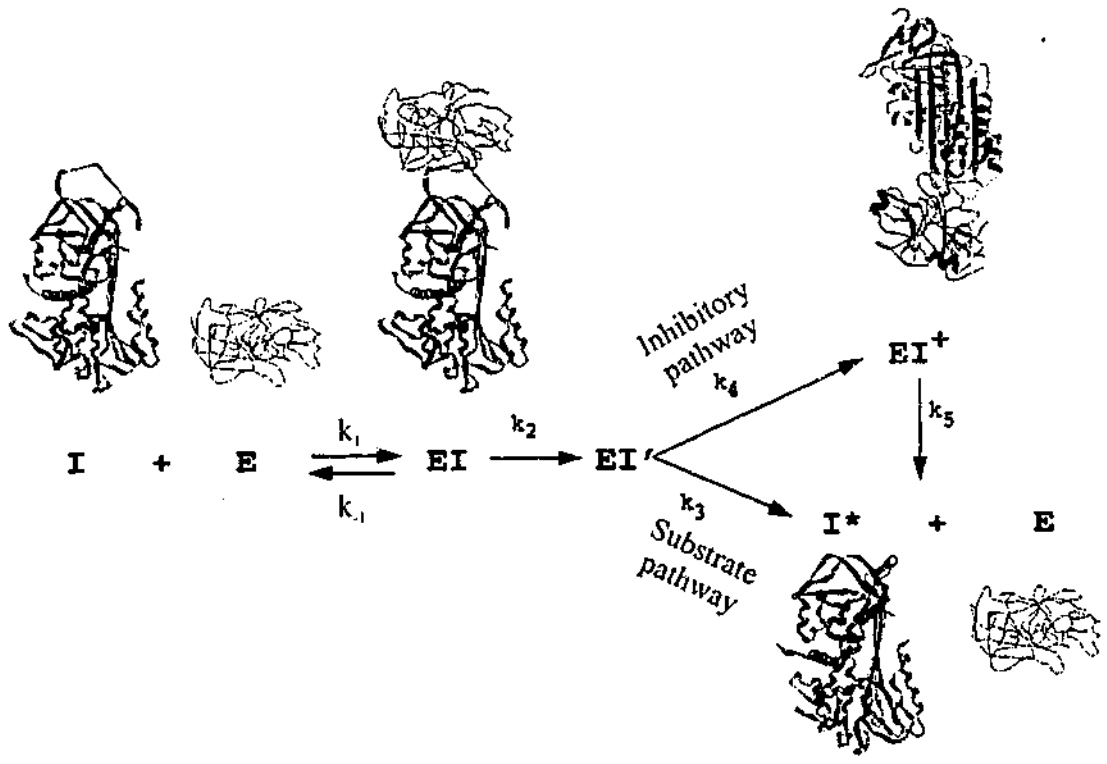

Figure 1.8 The mechanism of proteinase inhibition by serpins. The serpin (I) and proteinase (E) interact to form a noncovalent Michaelis-Menten like complex (EI) which is governed by the equilibrium dissociation constant for the given proteinase-serpin pair (k_1/k_{-1}). This reversible complex is rapidly converted to a covalently locked complex (EI'), governed by the rate of acylation of the serpin (k_2). The choice between the non-inhibitory (k_3) and inhibitory (k_4) pathway is dependent upon the rate of insertion of the RCL. The non-inhibitory pathway usually results from the interaction of a serpin with a non-cognate proteinase and results in release of active proteinase (E) and cleaved, inactive serpin (I*). In the inhibitory pathway, the cleaved RCL inserts into β-sheet A and translocates the proteinase by over 70 Å, to the opposite pole of the serpin (EI^+). Although complexes can be stable for long periods, very slow decay (k_5) of the complex can result in cleaved serpin (I*) and free proteinase (E). Modified from Stratikos and Gettins, 1999 and Huntington *et al.*, 2000.

proteinase and cleaved inactive serpin. In the inhibitory pathway the cleaved RCL rapidly inserts into β-sheet A translocating the proteinase by over 70 Å to the opposite pole of the serpin (Stratikos and Gettins, 1999). The recent solution of the serpin-proteinase complex has confirmed the mechanism by which the proteinase is trapped. The re-orientation of the proteinase results in a 37% loss of structure while the distortion of its catalytic site moves the catalytic serine 6 Å away from the histidine preventing deacylation and trapping proteinase and serpin in a locked complex (Huntington *et al.*, 2000). Although complexes can be stable for long periods, very slow decay of the complex may release in cleaved serpin and active proteinase.

1.6.3 Serpin conformation

Serpins exist in a thermodynamically unfavourable, metastable fold described as the stressed (S) state (Figure 1.9A). The cleavage of the RCL and concomitant insertion of the RCL results in a large conformational change in serpin structure to the more energetically preferred relaxed (R) state (Figure 1.9B) (reviewed in Whisstock *et al.*, 1998). Several serpins can adopt a latent conformation, whereby they adopt the R state due to insertion of their own uncleaved RCL into β-sheet A (Figure 1.9C). PAI-1 can adopt this conformation spontaneously (Mottonen *et al.*, 1992), while heating of antithrombin or α_1-antitrypsin can induce latency (Lomas *et al.*, 1995).

This flexibility of serpin fold can also lead to polymerisation, which occurs spontaneously in a number of genetic variants of serpins, promoting diseases such as emphysema, liver cirrhosis, angio-oedema and thrombosis (reviewed in Carrell and Lomas, 1997). Recently, the polymerisation of a mutant neuroserpin has been shown to result in a form of early onset dementia (Davis *et al.*, 1999).

Polymerisation may occur by one of two proposed mechanisms. The loop A sheet mechanism involves the insertion of the RCL of one serpin molecule into the β-sheet A of another (Mast *et al.*, 1992). Alternatively, the RCL of one serpin may insert into the vacant strand 1C position of another by the loop C sheet mechanism (Carrell *et al.*, 1994). The recent crystallisation of polymers of α_1-antitrypsin shows that polymerisation can occur via the A sheet mechanism (Huntington *et al.*, 1999; Dunstone *et al.*, 2000) and this is confirmed by further *in vitro* analysis of polymerisation (Sivasothy *et al.*, 2000) (Figure 1.9D).

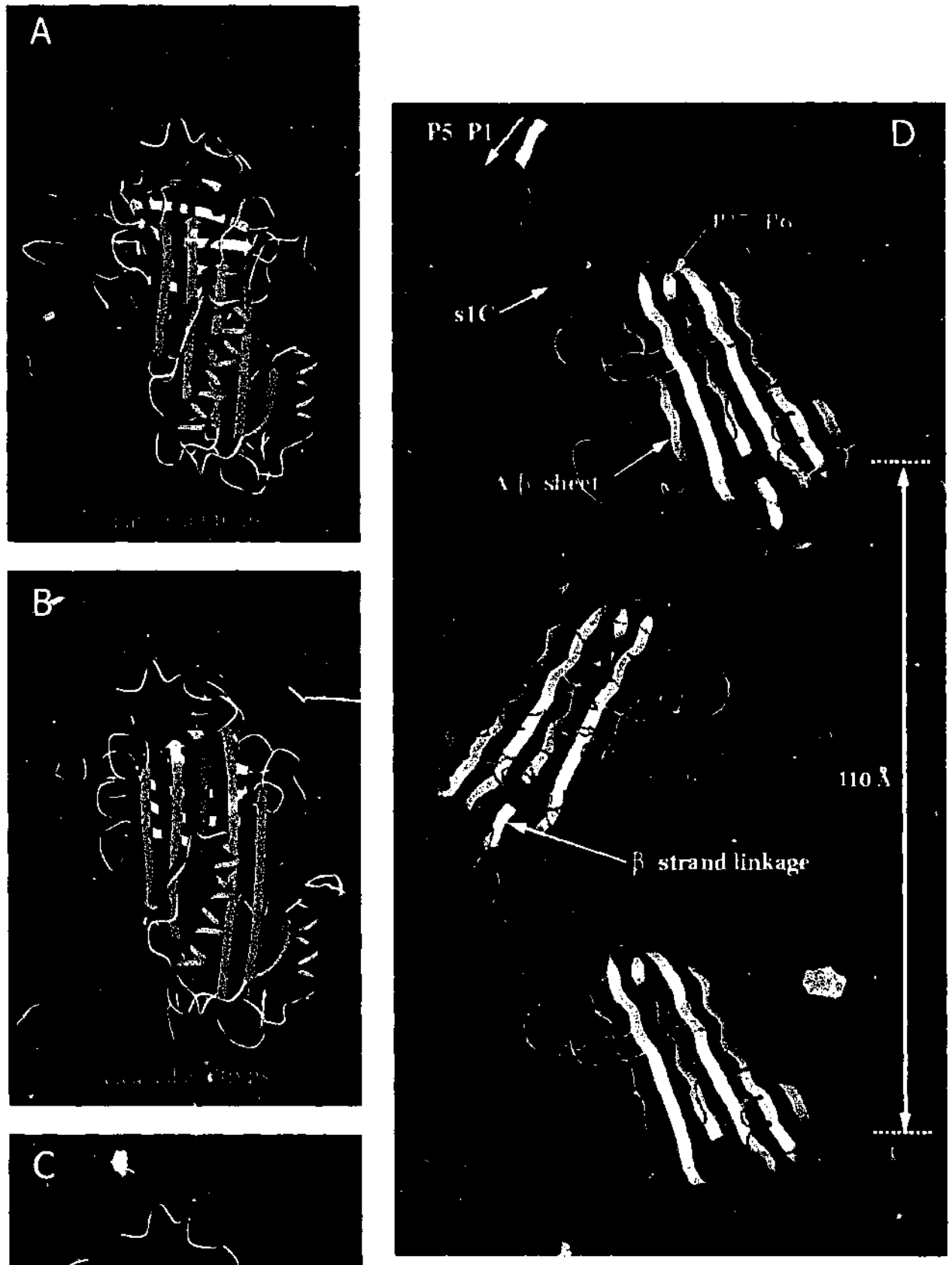

Figure 1.9 Conformations of serpins. In native serpins the RCL is exposed (A) however, upon cleavage of the RCL the serpin undergoes the S to R transition and the RCL is inserted into β-sheet A (B). The insertion of the RCL into β-sheet A can occur spontaneously in a number of serpins to induce latency (C) or polymers (D). Modified from Whisstock *et al.*, 1998 and Dunstone *et al.*, 2000.

1.7 Serpin families

Phylogenetic analysis of 219 full length serpin sequences separates them into 16 clades on the basis of amino acid homology and consensus sequences. These clades represent serpins from higher eukaryotes, nematodes, insects, plants and viruses (Irving *et al.*, 2000). Insect and plant serpins can be described by a single clade each, whereas viral serpins are divided into two clades. Animal serpins represent the majority of the clades (12) with horseshoe crab, nematodes and blood fluke each having a distinct clade. In higher animals the serpins can be divided into eight extracellular clades and a single intracellular clade (Table 1.4). These clades form the basis of a revised nomenclature for serpins (Silverman *et al.*, 2001).

1.7.1 Ov-serpins

Serpins belonging to the single intracellular clade, clade B, are known as the ov-serpins due to their homology to the chicken serpin, ovalbumin (Remold-O'Donnell, 1993). While most of the ov-serpins have been shown to inhibit serine proteinases, a number have been shown to inhibit members of the cysteine proteinase family while some have no known target proteinase (Table 1.5). At present the physiological roles of most of the ov-serpins are unclear, however some have roles in a variety of functions including modulation of inflammation, tumour suppression, protection from apoptosis and cell differentiation (Table 1.5).

The human ov-serpins are found in two gene clusters at chromosome 6p25 and 18q 21-23. *SERPINB1* (Evans *et al.*, 1995; Ooms *et al.*, 1995), *SERPINB6* (Coughlin *et al.*, 1995) and *SERPINB9* (Eyre *et al.*, 1996) are located within a 200 kb cluster on chromosome 6p25 (Figure 1.10A). The second gene cluster spans 800 kb on chromosome 18q21-23 and contains *SERPINB2* (Ye *et al.*, 1989), *SERPINB3*, *SERPINB4* and *SERPINB5* (Schneider *et al.*, 1995), *SERPINB7* (Dr H. Kanai and Dr P. Bird, unpublished results), *SERPINB8* (Scott *et al.*, 1997), *SERPINB10* (Bartuski *et al.*, 1997) and *SERPINB13* (Spring *et al.*, 1999). Two new serpin genes, *SERPINB11* and *SERPINB12*, have recently been identified and localised to 18q21-23 (Askew *et al.*, 2001) (Figure 1.10B).

The ov-serpins can be grouped into two groups based on their gene structure. The first has eight exons and seven introns with identical intron positioning and phasing, while the second has an identical structure except that they lack intron C (Figure 1.10C). The serpins found on 18q21-23 have the eight exon structure, except for *SERPINB5* and *SERPINB8* which share the seven exon structure with the three serpins

Table 1.4 Serpin Clades

Clade	Name
A	antitrypsin-like
B	intracellular
C	antithrombin
D	heparin cofactor II
E	plasminogen activator inhibitor 1 glial derived nexin
F	pigment epithelium-derived factor
G	C1-inhibitor
H	heat shock protein 47
I	neuroserpin

Table 1.5 Human ov-serpins

Gene designation	Protein designation	Distribution	Target proteinases	Possible function(s)
SERPINB1	M/NEI	Monocytes, granulocytes	Elastase, proteinase 3, cathepsin G	Regulate monocyte and granulocyte proteinases
SERPINB2	PAI-2	Monocytes, epithelia	u-PA	Control fibrinolysis and matrix remodeling, protection from TNFα mediated apoptosis
SERPINB3	SCCA-1	Epithelia	Cathepsin K, L, S	Regulate lysosomal proteinases, protection from TNFα mediated apoptosis
SERPINB4	SCCA-2	Epithelia	Cathepsin G, chymase	protection from TNFα mediated apoptosis
SERPINB5	Maspin	Epithelia	t-PA	Tumor suppressor
SERPINB6	PI-6	Epithelia, monocytes, granulocytes, neurons	Cathepsin G, chymotrypsin, thrombin, trypsin, u-PA, plasmin	Regulate monocyte and granulocyte granular proteinases
SERPINB7	Megsin megmat PI-11	Megakaryocytes, dendritic cells	unknown	Megakaryocyte differentiation
SERPINB8	PI-8	Heart, bone marrow, skeletal muscle, liver, lung	Furin, thrombin, chymotrypsin, factor Xa	Regulate protein processing enzymes
SERPINB9	PI-9	Cytotoxic lymphocytes	Granzyme B	Regulate apoptosis
SERPINB10	Bomapin PI-10	Bone marrow	Thrombin, trypsin	Lymphocyte differentiation, protection from TNF-α mediated apoptosis
SERPINB11	Epipin	unknown	unknown	unknown
SERPINB12	Yukopin	Brain, bone marrow, lymph node, heart, liver, lung, pancreas, testis, ovary, intestines	Trypsin, plasmin	unknown
SERPINB13	Hurpin headpin, PI-13	Epithelia	unknown	Tumor suppressor;,keratinocyte differentiation

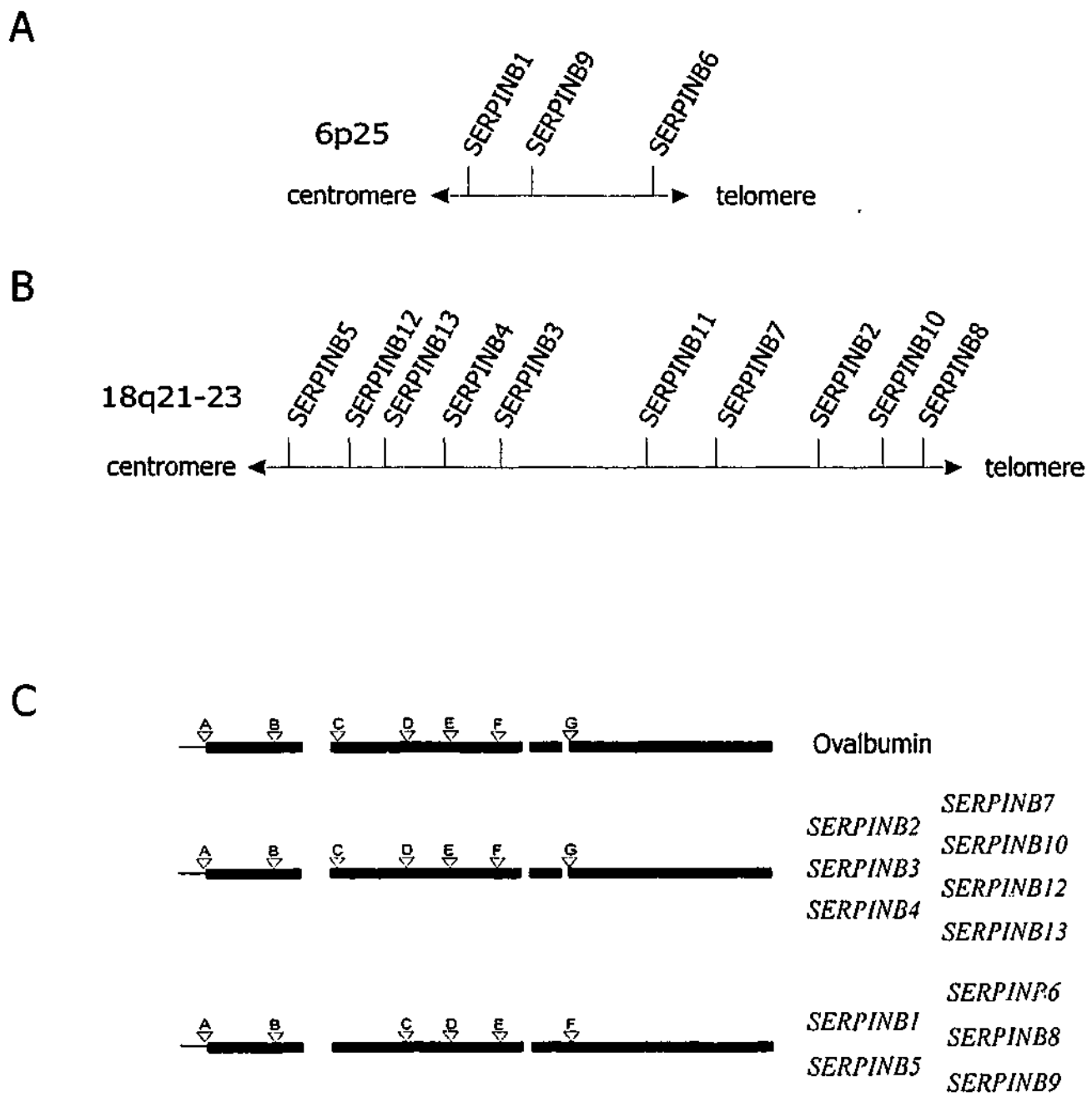

Figure 1.10 Gene localisation and structure of ov-serpins. The ov-serpins are located at two gene loci on chromosome (A) 6p25 (modified from Sun *et al.*, 1998) and (B) 18q21-23 (modified from Askew *et al.*, 2001) (not drawn to scale). (C) The serpins can also be grouped into two families by their gene structure. The first group resembles the ancestral chicken ovalbumin gene and has eight exons and seven introns (consisting of *SERPINB2* (Ye *et al.*, 1989), *SERPINB3* and *SERPINB4* (Schneider *et al.*, 1995), *SERPINB7* and *SERPINB10* (Scott *et al.*, 1999a) *SERPINB12* (Askew *et al.*, 2001) and *SERPINB13* (Nakashima *et al.*, 2000)). The second family lacks intron C and therefore has seven exons and six introns (consisting of *SERPINB1* (Zeng *et al.*, 1998), *SERPINB5* and *SERPINB8* (Scott *et al.*, 1999), *SERPINB6* and *SERPINB9* (Sun *et al.*, 1998)). Filled box indicates coding sequence, line indicates 5'UTR, the position of introns is indicated with an arrow head. Modified from Scott *et al.*, 1999.

located at 6p25. This suggests that *SERPINB5* and *SERPINB8* link the two clusters, which have arisen through interchromosomal and intrachromosomal duplications (Scott *et al.*, 1999a).

1.8 The granzyme B inhibitor, PI-9

PI-9 (*SERPINB9*) was originally cloned by Sprecher and co-workers in 1995, while searching for PI-6-like serpins. They screened a placental cDNA library with a PI-6 cDNA probe at low stringency and identified two novel cDNA sequences. These cDNAs encoded proteins of approximately 42 kDa, which were designated PI-8 and PI-9 (Sprecher *et al.*, 1995). While they observed that PI-9 has an unusual P_1 residue of glutamic acid^{340} and that the RCL shares overall similarity to crmA, a viral serpin that can inhibit graB (Quan *et al.*, 1995), they failed to link these attributes to a graB inhibitor and did not test PI-9 against graB.

Simultaneously, workers in this laboratory independently cloned PI-9 and demonstrated that it is a potent inhibitor of graB with a stoichiometry of interaction of 1 to 1 and an association constant (k_{ass}) of $1.7 \pm 0.3 \times 10^6$ M^{-1} s^{-1}, which is within the range for physiologically significant serpin-proteinase interaction (10^5-10^7 M^{-1} s^{-1} (Travis and Salvesen, 1983)). Analysis of PI-9 mRNA and protein indicates it is abundant in graB expressing CL-like cell lines and IL-2 stimulated PBL, suggesting PI-9 acts as a cytosolic inhibitor of graB, to protect CL from ectopic release of endogenous graB (Sun *et al.*, 1996). PI-9 transcripts can also be detected in the lymphoid organs, spleen and thymus, and in a variety of T, NK and B cell-like cell lines (Sun *et al.*, 1996). As these cells may be exposed to graB during an immune response, it is suggested that PI-9 is expressed to protect bystander cells against mis-directed graB

1.8.1 Tissue distribution of PI-9

Several recent studies have examined the tissue distribution of PI-9 (Bladergroen *et al.*, 2001; Buzza *et al.*, 2001; Hirst *et al.*, 2001). These studies have demonstrated that PI-9 has a restricted distribution consistent with a role in protecting particular cells from inadvertent apoptosis induced by mis-directed graB. PI-9 is present in endothelial and mesothelial cells (Buzza *et al.*, 2001) - lining cells that may be exposed to locally released graB and perforin during an immune response.

PI-9 has also been described in several immune privileged sites including the lens, ovary, testis and placenta (Bladergroen *et al.*, 2001; Hirst *et al.*, 2001). PI-9 is restricted in its expression within these tissues, being present within only a few cell

types. In the ovary, PI-9 is expressed within the granulosa cells surrounding the developing follicle, while in the testis it is present within the Sertoli cells surrounding developing germ cells. PI-9 is also expressed in the trophoblast layers in the placenta. While the expression of PI-9 in these cell types is consistent with PI-9 contributing to the immune privileged status of these tissues, further examination indicates that graB is also expressed in the testis and placenta and that PI-9 might regulate graB in a non-immunological setting (described in Chapter 5 and (Hirst *et al.*, 2001)).

Tissue resident dendritic cells (DC) located in the tonsil, thymus and spleen also express PI-9 (Bladergroen *et al.*, 2001). Many subsets of DC have been described, with varying distributions and functions within tissues, and it is not clear which DC subsets express PI-9 and how this relates to a role in protection from graB mediated apoptosis. The expression of PI-9 in leukocyte populations also has not been further characterised, following the original RNA analysis of leukocyte derived cell lines, the work described in Chapter 6 also describes the expression of PI-9 in peripheral blood leukocytes and DC subsets.

1.8.2 Cellular localisation of PI-9

Like other members of the ov-serpin family, PI-9 lacks a N-terminal, cleavable, signal sequence, suggesting it is not secreted via the conventional secretory pathway. This has been confirmed by indirect immunofluorescence and pulse chase experiments indicating that PI-9 is a cytosolic protein and is not secreted from cells (Sun *et al.*, 1996). Further analysis of its cellular localisation indicates that a proportion of the protein is located within the nucleus, and is directed there via an unconventional mechanism (Bird *et al.*, 2001). This nucleocytoplasmic localisation is consistent with PI-9 inhibiting graB released into the cytoplasm as well as graB that enters the nucleus (Trapani *et al.*, 1994; Jans *et al.*, 1996).

1.8.3 Cytoprotective role for PI-9

The hypothesis that PI-9 protects cells from graB mediated apoptosis is supported by studies on PI-9 transfected cells. Expression of PI-9 in target cells protects from apoptosis induced by either purified graB in the presence of perforin, or by intact CL in a dose-dependent manner (Bird *et al.*, 1998). The protection from graB mediated apoptosis is dependent on the inhibitory mechanism of PI-9 as mutation in the proximal hinge region, required for RCL mobility and inhibitory function (Stein and Carrell, 1995), abrogates protection (Bird *et al.*, 1998). Additionally, mutation of the P_1

glutamic acid to aspartic acid alters the specificity of PI-9 from a potent graB inhibitor to a caspase inhibitor, and modulates its ability to protect from graB mediated apoptosis (Bird *et al.*, 1998).

This cytoprotective function for PI-9 is supported by studies on SPI-6, a mouse homologue of PI-9 (Sun *et al.*, 1997). SPI-6 can form an SDS-stable complex with graB, however the RCL of SPI-6 differs from that of PI-9 and the kinetics with graB (k_{ass} 8 ± 0.8 x 10^4 M^{-1} s^{-1}) are lower than those observed between PI-9 and graB (k_{ass} 1.7 ± 0.3 x 10^6 M^{-1} s^{-1}). However, evidence that SPI-6 is the functional homologue of PI-9 has been demonstrated in the mouse, as DC that express SPI-6 are protected from apoptosis induced by CTL (Medema *et al.*, 2001b). SPI-6 expression in DC is also differentially regulated by T helper cell subsets, with upregulation of SPI-6 induced by CD40-L expressed on T_H1 cells during CTL activation, suggesting that SPI-6 protects DC from the CTL they activate (Medema *et al.*, 2001b).

1.8.4 Regulation of PI-9

The factors that regulate the expression of PI-9 have not been well characterised. The report that PI-9 is an oestrogen inducible gene (Kanamori *et al.*, 2000), with the a unique oestrogen responsive unit 200 bp downstream of the transcription start site (Krieg *et al.*, 2001), is consistent with the expression of PI-9 in reproductive tissue. In endothelial cells, PI-9 is upregulated by the inflammatory stimulus PMA, which mimics activation through PKC pathways (Buzza *et al.*, 2001) however the physiological mediator of this upregulation has not yet been elucidated.

The regulation of PI-9 in leukocyte and DC populations has not been characterised, however the upregulation of SPI-6 in DC is mediated by CD40 CD40-L interaction with T_H1 cells and is suppressed by IL-10 secreted by T_H2 cells (Medema *et al.*, 2001b), suggesting similar mechanisms may exist in humans. The regulation of PI-9 in lymphocytes and DC is examined in greater detail in Chapter 6.

Two recent studies have been published on the dysregulation of PI-9 in cancers suggesting that PI-9 upregulaton is a mechanism employed by epithelial derived carcinomas and lymphomas to evade the immune response mediated through graB (Medema *et al.*, 2001a; Bladergroen *et al.*, 2002). However, both studies failed to analyse the baseline expression of PI-9 in normal cells before concluding that PI-9 was upregulated or abnormally expressed in these cells. The tissue and cellular distribution performed in Chapter 5 and 6 demonstrate that PI-9 is normally expressed in epithelial cells and leukocyte populations.

1.9 Summary and Aims

GraB is a pro-apoptotic serine proteinase that is expressed in NK cells and activated CTL to induce apoptosis in virally infected and tumourigenic cells. GraB can activate a number of intrinsic apoptotic pathways in the cells via cleavage of the caspases, pro-apoptotic members of the Bcl-2 family and substrates in the nucleus. The release of graB into cytoplasm of cytotoxic lymphocytes via leakage from granules, or into bystander and accessory cells would be detrimental to the effectiveness of the immune response.

The intracellular ov-serpin PI-9, is an efficient inhibitor of graB, and the abundant expression of PI-9 in CL suggests it protects from endogenous graB (Sun *et al.*, 1996). Furthermore, studies in transfected cells indicates PI-9 can protect from apoptosis in a dose-dependent manner (Bird *et al.*, 1998). At the commencement of this study little was known about the tissue distribution and baseline expression of PI-9 , beyond its expression in CL.

This thesis describes the study of PI-9 distribution in immune tissues and immune privileged sites. Regulation of PI-9 expression was also examined in T cells and DC both *in vivo* and *in vitro*. These studies required the generation and characterisation of monoclonal and polyclonal antibodies to PI-9. One of these monoclonal antibodies was found to recognise the conserved proximal hinge motif of serpins and was used to investigate changes in serpin structure.

Chapter 2

Materials and Methods

2.1 Materials

Unless otherwise specified all general chemicals were of analytical grade and supplied by Merck BDH Chemicals or Sigma-Aldritch. Materials manufactured overseas were obtained from local subsidiaries or agents of the manufacturer.

Agar, bacteriological	Oxoid
Agarose, ultra pure DNA Grade	Pharmacia Biotech
Ammonium persulfate (APS)	Bio-Rad
Ampicillin	Boehringer Mannheim
Aprotinin	Boehringer Mannheim
BRESAclean DNA purification kit	Bresatec
Calf intestinal alkaline phosphatase	Promega
Cryotubes	Nunc
Deoxynucleoside triphosphates (dNTPs)	Pharmacia Biotech
DIG Labelling Kit	Roche Molecular Biochemicals
Dulbecco's modification of Eagle's medium	Life Technologies
Eagle's Minimal Essential Medium	Life Technologies
FACS™ Lysing solution	BD Bioscience
FACS™ Permeabilizing solution	BD Bioscience
Foetal calf serum (FCS)	Life Technologies
Ficoll-Paque® Plus	Pharmacia Biotech
Fmoc protected amino acids	Auspep
Formamide (deionised)	Pharmacia Biotech

GammaBind™ G Sepharose™	Pharmacia Biotech
GelSlick™	AT Biochem
Gene Editor *in vitro* Site-directed Mutagenesis System	Promega
GeneScreen*Plus*®	NEN Life Science
L-glutamine	Life Technologies
Glycerol vinyl alcohol mounting medium	Zymed
Hypoxanthine, aminopterin and thymidine solution	Life Technologies
Hybond N^+ membrane	Amersham
Hybridoma serum free media	Life Technologies
Interleukin 2, recombinant	Sigma-Aldritch
Klenow fragment	Promega
Leupeptin	Boehringer Mannheim
Liquid DAB Chromogen Substrate System	DAKO
Maxisorp microtiter plates, polystyrene	Nunc
Mouse monoclonal antibody isotyping kit	Amersham
Nitroblue tetrazolium chloride/5-bromo-4-chloro-3-indolyl phosphate substrate	Zymed
Nitrocellulose membrane (Trans-Blot®)	Bio-Rad
PEI-cellulose	Schleicher and Schuell
Penicillin	Life Technologies
Pepstatin	Boehringer Mannheim
Prestained Protein Markers (Broad Range)	New England Biolabs
Prime-a-Gene® labelling system	Promega
Proteinase K	Boehringer Mannheim
Protein assay reagent	Bio-Rad
Rapid-Ag-Stain kit	ICN

Rapid-hyb buffer	Amersham International
Renaissance® Chemiluminescence Reagent	NEN DuPont
Restriction enzymes	New England Biolabs or Promega
RNasin® Ribonuclease Inhibitor	Promega
RosetteSep™ Enrichment cocktails	StemCell Technologies
RPMI 1640 medium	Life Technologies
Streptavidin conjugated to HRP	Chemicon
Streptomycin	Life Technologies
Superfrost Plus slides	Biolabs Scientific
T3 RNA polymerase	Promega
T4 DNA polymerase	New England Biolabs
T4 DNA ligase	Promega
T4 polynucleotide kinase	New England Biolabs
T7 RNA polymerase	Promega
Taq polymerase	Bresatec
Taurine	ICN
N,N,N'N'-tetramethylethylenediamine (TEMED)	Bio-Rad
ThermoSequenase™ Cycle Sequencing Kit	Amersham International
Tissue culture dishes	Nunc
Tissue-Tek	Sakara
TNT® T7 Coupled Wheat Germ Extract System	Promega
Transformer™ Site-Directed Mutagenesis Kit	Clontech
Trypsin	Life Technologies
Tryptone	Oxoid
Twelve well multitest slides	ICN
X-ray film, Curix Ortho, HT-G	AGFA
Yeast extract	Oxoid

2.2 Radiolabelled chemicals

[α^{32}P] deoxycytidine 5'-triphosphate (dCTP) (3000 Ci/mmol)	NEN DuPont
[γ^{32}P] adenosine 5'-triphosphate (ATP) (3000 Ci/mmol)	NEN DuPont

2.3 Buffers, media and solutions

30% (w/v) acrylamide

29:1 ratio of acrylamide:N,N'-methylenebisacrylamide.

50% (w/v) PEG 4000

10 g of PEG 4000 was autoclaved for 20 min then cooled before 10 ml of serum free DMEM was added and mixed well.

50 mM carbonate buffer

15 mM Na_2CO_3 and 35 mM $NaHCO_3$, pH 9.6.

100 mM citrate phosphate buffer

38 mM citric acid, 62 mM sodium phosphate.

Ammonium chloride solution

167 mM NH_4Cl, 1 mM $KHCO_3$ and 0.1 mM EDTA, pH 8.0.

Anode buffer

100 mM Tris-HCl, pH 7.8.

Blotto

5% (w/v) skim milk powder in Tris-HCl Buffer with 0.02% (w/v) sodium azide.

Bouin's fixative

Saturated picric acid, formaldehyde and glacial acetic acid at a ratio of 15:5:1.

Cathode buffer

5.3 mM Tris, 6.8 mM glycine, pH 8.9.

Coomassie Blue

0.25% (w/v) Coomassie Blue R250 in 45% (v/v) methanol and 10% (v/v) acetic acid.

DEAE-dextran/chloroquine (25 x stock)

10 mg/ml DEAE-dextran, 2.5 mM chloroquine, filter sterilised and stored at 4°C.

Destain

10% (v/v) glacial acetic acid, 40% (v/v) methanol.

Diethyl pyrocarbonate (DEPC) treated ddH_2O

ddH_2O was treated with 0.1% (v/v) DEPC for 1 h with stirring. The DEPC was then inactivated by autoclaving for 30 min.

DMEM (Dulbecco's Modified Eagle's Medium), complete

DMEM supplemented with 10% (v/v) heat inactivated fetal calf serum (FCS), 2 mM L-glutamine, 50 U/ml penicillin and 50 µg/ml streptomycin.

DMEM, serum free

DMEM supplememted 2 mM L-glutamine, 50 U/ml penicillin and 50 µg/ml streptomycin.

DNA gel loading buffer

0.1% (w/v) bromophenol blue, 0.1% (w/v) xylene cyanol, 50% (v/v) glycerol.

Dithiothreitol (DTT)

1 M DTT in 10 mM sodium acetate, pH 5.2, stored at -20°C.

Eagle's MEM (Minimum Essential Medium), complete

Eagle's MEM supplemented with 10% (v/v) heat inactivated FCS, 2 mM L-glutamine, 0.1 mM β-mercaptoethanol, 50 U/ml penicillin and 50 µg/ml streptomycin.

Glycerol tolerant gel buffer (GTB; 20 x stock)

1.78 M Tris, 0.58 M taurine, 10 mM $Na_2EDTA.2H_2O$.

Guanadinium thiocyanate solution

4 M guanidine thiocyanate, 25 mM sodium citrate, pH 7.0, 0.5% (w/v) Sarkosyl and 100 mM β-mercaptoethanol.

Laemmli running buffer

25 mM Tris-base, 192 mM glycine, 0.1% (w/v) SDS.

Laemmli sample buffer

62.5 mM Tris-HCl, pH 6.8, 2% (w/v) SDS, 10% (v/v) glycerol, 100 mM DTT and 0.1% (w/v) bromophenol blue.

Luria-Bertani medium (LB)

1% (w/v) tryptone, 0.5% (w/v) yeast extract, 1% (w/v) NaCl.

LB agar

1% (w/v) tryptone, 0.5% (w/v) yeast extract, 1% (w/v) NaCl, 1.5% (w/v) agar.

Modified Laemmli sample buffer

62.5 mM Tris-HCl, pH 6.8, 2% (w/v) SDS, 10% (v/v) glycerol, 100 mM DTT.

MOPS running buffer (10X)

20 mM MOPS, 5 mM sodium acetate, 1 mM EDTA, autoclaved to sterilise.

Native gel sample buffer

125 mM Tris-HCl, 20% (v/v) glycerol, 0.02% (w/v) bromophenol blue.

Native polyacrylamide gels

	4% (w/v) Stacking gel (5 ml)	**10% (w/v) Resolving gel (10 ml)**
0.5 M Tris-HCl, pH 6.8	2.5 ml	-
1.5 M Tris-HCl, pH 8.8	-	2.5 ml
30% (w/v) acrylamide	650 µl	3.25 ml
ddH_2O	1.8 ml	4.1 ml
10% (w/v) APS	50 µl	100 µl
TEMED	5 µl	10 µl

NP-40 lysis buffer

1% (v/v) Nonidet P-40 in 50 mM Tris-HCl, pH 8.0, 10 mM EDTA, pH 8.0 with; 150 µg/ml PMSF, 1 µg/ml aprotinin, 0.5 µM leupeptin and 1 µM pepstatin.

***o*-PD Substrate**

0.4 mg/ml *o*-phenylenediamine in 100 mM citrate phosphate buffer. Immediately before use 0.075% (v/v) H_2O_2 was added.

PBG Mounting fluid

0.1% (w/v) *p*-phenylenediamine, 10% (v/v) PBS, 90% (v/v) glycerol. Adjusted to pH 8.0 with 50 mM carbonate buffer, pH 9.6, stored at -20°C in the dark..

Phosphate buffered saline (PBS)

136 mM NaCl, 2.6 mM KCl, 10 mM Na_2HPO_4, 1.76 mM KH_2PO_4, pH 7.4.

Pre-hybridisation buffer

50% (v/v) deionised formamide, 3 x SSC, 1 x Denhardt's solution, 66 mM phosphate buffer, 10% (w/v) dextran sulfate, 200 µg/ml herring sperm DNA and 100 µg/ml yeast tRNA.

RNA loading buffer

80% (v/v) glycerol, 0.1 mM EDTA, pH 8.0, 0.2% (w/v) xylene cyanol, 0.2% (w/v) bromophenol blue.

RNA sample buffer

50% (v/v) deionised formamide, 20% (v/v) formaldehyde, 10% (v/v) RNA loading buffer in 1 x MOPS buffer.

RPMI 1640 complete medium

RPMI 1640 supplemented with 10% (v/v) heat inactivated FCS, 2 mM L-glutamine, 50 U/ml penicillin and 50 µg/ml streptomycin.

SDS-Polyacrylamide gels

	4% (w/v) Stacking gel (5 ml)	10% (w/v) Resolving gel (10 ml)	12.5 (w/v) % Resolving gel (10 ml)
0.25 M Tris-HCl, pH 6.8	2.5 ml	-	
1.5 M Tris-HCl pH 8.8	-	2.5 ml	2.5 ml
30% (w/v) acrylamide	667 µl	3.33 ml	4.17 ml
10% (w/v) SDS	50 µl	100 µl	100 µl
ddH_2O	1.7 ml	3.9 ml	3.05 ml
10% (w/v) APS	50 µl	100 µl	100 µl
TEMED	4 µl	8 µl	8 µl

SSC buffer (20 x stock)

3 M NaCl, 300 mM tri-sodium citrate. Adjusted to pH 7.0 with 10 M NaOH.

Transfer buffer

25 mM Tris, 192 mM glycine, 20% (v/v) methanol.

Tris-borate buffer (TBE; 5 x stock)

445 mM Tris borate, 10 mM EDTA, pH 8.0.

Tris-EDTA buffer

10 mM Tris-HCl, pH 8.0, 1 mM EDTA, pH 8.0.

Tris-buffered saline (TBS)

20 mM Tris-HCl, pH 7.4, 150 mM NaCl.

Trypsin/EDTA (10 x stock)

0.25% (v/v) Trypsin, 1 mM EDTA, pH 8.0, in PBS.

2.4 Apparatus and equipment

DNA sequencing electrophoresis apparatus, Model S2	Bethesda Research Laboratories
Electrophoresis Power Supply	Pharmacia Biotech
Emax Precision Microplate Reader	Molecular Devices
Flow cytometer (FACS™Calibur)	BD Bioscience

Geiger counter(Mini-monitor)	Mini Instruments
Haemocytometer	Neubauer
Labsonic 1510 sonicator	Braun
Microtome	Leitz
Mini Protean®II Electrophoresis Tank	Bio-Rad
Mini Protean®II Western Blotter	Bio-Rad
Programmable Thermal Controller (PTC-100)	MJ Research
PS3 Protein Technologies Automatic Peptide Synthesizer	Rainin Instrument Company

2.5 Antisera

2.5.1 Rabbit polyclonal antisera

Rabbit anti α_1-antirypsin

Polyclonal antiserum raised in rabbits against human α_1-antirypsin was obtained from Sigma-Aldritch. Rabbit anti α_1-antirypsin was used at a dilution of 1:500 for immunoblotting.

Rabbit anti antithrombin

Polyclonal antiserum raised in rabbits against human antithrombin was obtained from Sigma-Aldritch. Rabbit anti antithrombin was used at a dilution of 1:1000 for immunoblotting and ELISA.

Rabbit anti granzyme B

Polyclonal anti granzyme B antiserum was a kind gift from J. Trapani and is described in Edwards *et al.* 1999. Rabbit anti granzyme B antiserum was used at a dilution of 1:500 for immunoblotting and at 1:250 for immunohistochemistry and indirect immunofluorescence.

Rabbit anti keratin

Polyclonal antiserum raised in rabbit against keratin was a kind gift of R. Boyd and was used at a dilution of 1:200 for indirect immunofluorescence.

Rabbit #11 anti PI-9 antiserum

Polyclonal antiserum was raised in NZW rabbits immunised with recombinant PI-9 (rPI-9) purified from *Pichia pastoris* as described previously (Sun *et al.*, 1996). Rabbit #11 polyclonal anti PI-9 antiserum was used at a dilution of 1:2000 for immunoblotting and indirect immunofluorescence.

Rabbit #12 anti PI-9 antiserum

Rabbit #12 polyclonal anti PI-9 antiserum was produced as described for Rabbit #11 and was used at a dilution of 1:2000 for immunoblotting and at 1:1000 for indirect immunofluorescence.

Rabbit #13 anti PI-6 antiserum

Rabbit #13 polyclonal anti PI-6 antiserum was produced against recombinant PI-6 as described in Scott *et al.*, 1996. Rabbit #13 polyclonal anti PI-6 antiserum was used at a dilution of 1:5000 for immunoblotting and indirect immunofluorescence.

Rabbit #15 anti PI-9 antiserum

Rabbit #15 polyclonal anti PI-9 antiserum was produced against purified rPI-9 mutated at the P_1 residue of the RCL from Glu to Asp. Immunisation was performed as previously described for the Rabbit #11 polyclonal anti PI-9 antiserum. Rabbit #15 polyclonal anti PI-9 antiserum was used at a dilution of 1:2000 for immunoblotting and immunohistochemistry and at 1:1000 for indirect immunofluorescence.

2.5.2 Mouse monoclonal antibodies

1F3 (pan serpin)

The mouse monoclonal antibody, 1F3, was raised against rPI-9 as described in section 2.11. Tissue culture supernatant from the 1F3 hybridoma was used at a 1:20 dilution for indirect immunofluorescence, immunoblotting and immunohistochemistry.

2C5 (anti granzyme B)

The mouse monoclonal antibody, 2C5, raised against human granzyme B was a kind gift of J. Trapani (Apostolidis *et al.*, 1995). 2C5 ascites fluid was used at a dilution of 1:2000 for immunoblotting and at 1:200 for indirect immunofluorescence and immunohistochemistry.

2E7 (anti PI-9)

The mouse monoclonal antibody, 2E7, was raised against rPI-9 as described in section 2.11 Tissue culture supernatant from the 2E7 hybridoma was used neat for the detection of PI-9 by indirect immunofluorescence.

3A (anti PI-6)

The mouse monoclonal antibody 3A was produced by L. Cerruti and characterised by F. Scott (Scott *et al.*, 1998). Tissue culture supernatant from the 3A hybridoma was used neat for immunoblotting and indirect immunofluorescence.

7D8 (anti PI-9)

The mouse monoclonal antibody, 7D8, was raised against rPI-9 as described in section 2.11. Tissue culture supernatant from the 7D8 hybridoma was used neat for the detection of PI-9 by immunohistochemistry and indirect immunofluorescence and at a dilution of 1:10 for immunoblotting.

8D3 (anti PI-9)

The mouse monoclonal antibody, 8D3, was raised against rPI-9 as described in section 2.11. Tissue culture supernatant from the 8D3 hybridoma was used neat for the detection of PI-9 by indirect immunofluorescence and immunohistochemistry and at a dilution of 1:2 for immunoblotting.

CD Markers

CD Marker	Hybridoma designation	Source	Working dilution
CD3	OKT3	ATTC, c/o P. Cameron	Neat†
CD4	Leu3A	BD Bioscience	1:10
CD4-PE*		Diatech	1:25
CD8	OKT8	ATTC, c/o P. Cameron	Neat†
CD8-PE*		Diatech	1:25
CD11b	OKM1	ATTC, c/o P. Cameron	Neat†
CD14	3C10	R. Steinman, c/o P. Cameron	Neat†
CD19	FMC63	ATTC, c/o P. Cameron	Neat†
CD25	AM92.2.1	R. Steinman, c/o P. Cameron	Neat†
CD45-PE*		Diatech	1:25

*Directly conjugated antibodies †Hybridoma supernatant

ELA-5 (anti M/NEI)

Mouse monoclonal anti M/NEI antibody was obtained from Eileen Remold-O'Donnell and was used at a dilution of 1:150 for indirect immunofluorescence.

GrB-7 (anti granzyme B)

Mouse monoclonal anti granzyme B antibody was obtained from Chemicon (original reference (Kummer *et al.*, 1993)) and was used at a dilution of 1:20 for immunohistochemistry.

IgG_1 (isotype control antibody)

An isotype control antibody for 7D8 was obtained from BD Bioscience and was used at a dilution of 1:200 (the same concentration as 7D8) in immunohistochemistry, immunofluorescence and flow cytometry

2.5.3 Other species polyclonal antisera

Chicken anti antithrombin

Polyclonal antiserum raised in chickens against human antithrombin was a kind gift of R. Pike. Chicken anti antithrombin antiserum was used at a dilution of 1:4000 for immunoblotting and ELISA.

2.5.4 Conjugated secondary antibodies

Anti chicken immunoglobulins

HRP-conjugated rabbit anti chicken immunoglobulin (Ig) antiserum was obtained from Sigma-Aldritch and was used for immunoblotting and ELISA at a dilution of 1:20,000.

Anti mouse immunoglobulins

Sheep anti mouse Ig antisera conjugated to either FITC, HRP or Biotin were obtained from Chemicon. Sheep anti mouse Ig antisera conjugated to RITC was obtained from Immunotech. FITC and RITC conjugates were used for indirect immunofluorescence at a dilution of 1:200. The Biotin conjugate was used for immunohistochemistry at a dilution of 1:200. The HRP conjugate was used at a dilution of 1:3000 for immunoblotting.

Anti rabbit immunoglobulins

Sheep anti rabbit Ig antisera conjugated to either FITC, RITC, HRP or Biotin were obtained from Chemicon. FITC and RITC conjugates were used for indirect immunofluorescence at a dilution of 1:200. The Biotin conjugate was used for immunohistochemistry at a dilution of 1:200. The HRP conjugate was used at a dilution of 1:5000 for immunoblotting.

2.6 *Escherichia coli* strains

BL21 (DE3) — F^- *ompT gal [dcm] [lon] hsdS*$_B$, ($r_B^- m_B^-$) with DE3 (λ prophage carrying the T7 RNA polymerase gene) was used for the expression of wildtype and mutant α_1 antitrypsin.

BMH 71-18 — *mutS thi*, *supE*, Δ(*lac-proAB*), [*mutS*:Tn10][F', *proAB*, *lac*I^qZΔM15] was used for site-directed mutagenesis.

DH5α — ϕ80d*lac*ZΔM15, *recA*1, *endA*1, *gyrA*96, *thi*-1, *hsdR*17 (r_k^-, m_k^+), *supE*44, *rel*A1, *deo*R, Δ(*lacZ*YA-*arg*F)U169 was used as the host strain for the propagation and cloning of plasmids.

2.7 Plasmids and vectors

pBluescript KS$^-$	obtained from Stratagene
pBluescript KS$^-$/graB 3'UTR	contains the 3'UTR of granzyme B cloned into the *EcoRI* site of pBluescript KS$^-$. Its production is described in detail in Section 2.19.2.
pBluescript KS$^-$/PI-9	The 3' portion of the PI-9 coding region was cloned into pBluescript KS$^-$. Its production is described in detail in Section 2.19.1.
pCMV2neo/PI-9	obtained from P. Bird and consists of the PI-9 cDNA cloned into the *EcoRI* site of pCMV2/neo.
pCMV2neo/PI-9 P_{14} T-R	obtained from J. Sun and consists of PI-9 cDNA (containing the nucleotide mutations resulting in the substitution of the proximal hinge region P_{14} residue from threonine to arginine) in pCMV2/neo.

pCMV2neo/PI-6	was obtained from P. Bird and consists of the PI-6 cDNA cloned into the *EcoRI* site of pCMV2/neo.
pCR®-Blunt	obtained from Invitrogen.
pEUK/PAI-2	obtained from R. Medcalf and consists of the human PAI-2 cDNA cloned into pEUK.
pGEM-t/HSE 26.1	obtained from J. Trapani and consists of the human granzyme B cDNA cloned into pGEM-t.
pGEM-t/M/NEI	obtained from L. Ooms and consists of M/NEI cDNA cloned into pGEM-t.
pSVTf	obtained from P. Bird (Bird *et al.*, 1987).
pSVTf/M/NEI	pGEM-t/M/NEI was digested with *SacII*, this site filled in with T4 DNA polymerase, then cut with *PstI*, generating a 1.2 kb fragment. This was cloned into the *SmaI* and *PstI* sites of pSVTf.
pSVTf/PI-8	obtained from F. Scott and consists of the placental-derived PI-8 cDNA cloned into pSVTf.
pSVTf/SPI-3	obtained from J. Sun and consists of the SPI-3 cDNA cloned into the *EcoRI* site of pSVTf.
pSVTf/SPI-6	obtained from J. Sun and consists of the SPI-6 cDNA cloned into the *EcoRI* site of pSVTf.

2.8 Recombinant and purified proteins

Protein	Source	Provided by
α_1-ACT	Plasma	M. Pearce
α_1-AT	Plasma	J. Ludeman
	E.coli BL21 (DE3)	J. Ludeman (Hopkins *et al.*, 1997)
AT	Plasma	M. Pearce
CrmA	*P.pastoris*	J. Sun
granzyme B	YT cells	J. Trapani (Trapani *et al.*, 1993)
	P.pastoris	J. Sun (Sun *et al.*, 1999)
Hurpin	*P.pastoris*	H. Abts
MENT	*E.coli* BL21 (DE3)	J. Irving
M/NEI	*P.pastoris*	J. Sun
PAI-2	Recombinant	R. Medcalf
PI-6	*P.pastoris*	J. Sun (Sun *et al.*, 1995)
PI-8	*P.pastoris*	M. Buzza
PI-9	*P.pastoris*	J. Sun
SCCA-1	*E.coli* BL21 (DE3)	D.M. Worrall
SCCA-2	*E.coli* BL21 (DE3)	D.M. Worrall
SPI-3	*P.pastoris*	J. Sun
SPI-6	*P.pastoris*	J. Sun

2.9 Cell lines

COS-1 SV40-transformed African Green Monkey kidney epithelial cell line (Gluzman, 1981) was cultured in complete DMEM.

Hybridomas anti PI-9 hybridomas 1F3, 2E7, 7D8 and 8D3 were cultured in either complete DMEM or Hybridoma serum free medium. Hybridomas specific for the various CD marker (see section 2.5.2; OKT3, OKT8, OKM1, 3C10, FMC63 and AM92.2.1) were cultured in complete DMEM.

HL-60 human promyelocytic cell line (Collins, 1987) was cultured in complete RPMI 1640.

MM-170 human malignant melanoma cell line (Whitehead and Little, 1973) was cultured in complete RPMI 1640.

YT human natural killer-like cell line (Wano *et al.*, 1984) was cultured in complete RPMI 1640 with 0.1 mM β-mercaptoethanol.

2.10 Mammalian cell culture

2.10.1 Cell culture techniques

2.10.1.1 Culture conditions

All cells were maintained at subconfluent densities in 10 cm^2 tissue culture dishes in a 37°C incubator containing a 5% (v/v) CO_2, 95% (v/v) air mixture.

2.10.1.2 Thawing of cells

A vial of cells was taken from liquid nitrogen and rapidly heated until almost completely thawed in a 37°C water bath. Cells were then transferred to a tube containing 10 ml of pre-warmed complete media and centrifuged at 150 *g* for 5 min. The cell pellet was gently resuspended in 10 ml of complete media and transferred to a 10 cm^2 tissue culture dish. The following day the cells were washed to remove dead cells and passaged into fresh complete media.

2.10.1.3 Passaging of cells

Adherent cell lines (COS-1 and MM-170) were passaged at approximately 80% confluency. Monolayers were washed with PBS, 1 ml of trypsin/EDTA was added and the cells incubated at 37°C for 3-5 min or until the cells detached from the dish. 9 ml of complete media was added to neutralise the trypsin and cells were replated to a density of 5 x 10^5 cells/ml in a 10 cm^2 dish.

Non-adherent cell lines (YT, HL-60 and hybridomas) were passaged at subconfluent densities. Cells were transferred into a 10 ml tube, centrifuged at 150 *g* for 5 min, washed in PBS then transferred into complete media at 1:10 and 1:20 dilutions.

2.10.1.4 Storage of cells in liquid nitrogen

A subconfluent dish of adherent cells was harvested with trypsin/EDTA as described above then centrifuged at 150 *g* for 5 min. Alternatively one dish of non-adherent cells at sub-confluent density was transferred into a 10 ml tube then centrifuged at 150 *g* for 5 min. After centrifugation the supernatant was aspirated and the cells resuspended in 2 ml of 10% (v/v) DMSO in heat inactivated FCS. The cell suspension was then aliquoted into 4 cryotubes and placed on ice for 15 min. The vials were then placed onto dry ice for a further 15 min before transfer into liquid nitrogen.

2.10.2 Transient transfection of COS-1 cells

A confluent dish of COS-1 cells was trypsinised and replated at 30-40% confluency. The cells were incubated in complete DMEM at 37°C for 4 h to allow the cells to re-adhere and re-commence growth. The media was aspirated and replaced with 5 ml of serum free DMEM (SF-DMEM) containing 200 µl of DEAE-dextran/chloroquine solution and 1-2.5 µg of plasmid DNA. The dishes were incubated at 37°C for 2.5-3 h. Media was then aspirated and the cells incubated for 2 min in SF-DMEM containing 10% (v/v) DMSO. The DMSO containing medium was aspirated, replaced with complete DMEM, and the cells incubated at 37°C. 48 h later cells were harvested for analysis.

2.10.3 Isolation of purified leukocyte populations from peripheral blood

Highly purified $CD4^+$, $CD8^+$, monocyte and NK cell populations were obtained from whole blood using RosetteSep™ Enrichment cocktails as per the manufacturer's instructions. The purity of each cell population and the presence of any contaminating

cell types was assessed by indirect immunofluorescence using antibodies against CD3, CD4, CD8, CD14, CD19 and CD56.

2.10.4 Isolation of primary leukocytes from peripheral blood

Lymphocytes were isolated using Ficoll-Paque® Plus as per the manufacturer's instructions. Briefly, fresh blood obtained from a volunteer was diluted in an equal volume of PBS before layering over Ficoll-Paque® Plus, then centrifuged for 30 min at 400 *g* at 21°C. The platelet containing serum was aspirated and the "buffy coat" (containing peripheral blood mononuclear cells) at the interface of the Ficoll-Paque® Plus and the serum was collected. Contaminating platelets were removed by three washes in PBS, with centrifugation at 100 *g* for 10 min between each wash step.

2.10.5 Culture of primary leukocytes

Peripheral blood mononuclear cells (PMBC) purified as described above, were cultured at 2 x 10^6 cells/ml in complete RPMI. PBMC were activated by either interleukin 2 at 100 U/ml or a combination of Concanavalin A (ConA) and phorbol 12-myristate 13-acetate (PMA) at 10 µg/ml and 10 ng/ml respectively. Half the culture media was replaced with fresh media containing the appropriate stimulant every four days. At the indicated time points, the activated cells were harvested and cell lysates prepared by lysis in either NP-40 lysis buffer or modified Laemmli sample buffer (Zapata *et al.*, 1998). These lysates were analysed by immunoblotting as described in section 2.13.2.

2.10.6 Culture of primary NK cells

NK cell cultures were provided by H. Warren, and were isolated from peripheral blood and stimulated to proliferate using γ-irradiated MM-170 cells and IL-2 as described previously (Warren and Skipsey, 1991, Warren and Kinnear. 1999).

2.10.6.1 Preparation of irradiated MM-170 cells

MM-170 cells were trypsinised and resuspended at 0.5 x 10^6 cells/ml in Hanks buffered salt solution with 10% (v/v) heat inactivated FCS. Cells were irradiated with 4000 rads from a ^{137}Cs source, centrifuged at 500 *g* and resuspended in complete Eagle's MEM at 1.5 x 10^6 cells/ml. 100 µl of cells was dispensed into a flat bottomed 96 well tray at a final cell density of 3 x 10^4 γ-irradiated MM-170 cells per well.

2.10.6.2 Stimulation of NK cells

Culture generated quiescent NK cells were co-cultured at 1 x 10^4 cells per well with γ-irradiated MM-170 cells (described above) in 200 µl of complete Eagle's MEM supplemented with 200 U/ml IL-2. NK cells were maintained in culture beyond day 8 by the addition of 50 µl of complete Eagle's MEM supplemented with 50 U/ml IL-2.

2.10.6.3 Co-stimulation of NK cultures with CD16

Flat bottomed 96 well plates were coated with 10 µg/ml of affinity isolated sheep anti mouse Ig diluted in 50 mM carbonate buffer overnight at 4°C. Wells were washed four times with PBS then blocked with 5% (v/v) heat inactivated FCS in PBS for 30 min at room temperature. 100 µl of anti CD16 antibody (B73.1 hybridoma supernatant, supplied by H. Warren) was added to the wells and incubated at room temperature for 2 h. The wells were washed with PBS before the addition of the γ-irradiated MM-170 cells followed by the NK cells at the densities described above.

2.11 Production of mouse hybridomas

2.11.1 Preparation of antigen

RPI-9 was emulsified in an equal volume of either complete or incomplete Freund's adjuvant prior to injection. 200 µg of rPI-9 was injected per immunisation. Denatured rPI-9 was prepared by SDS-PAGE as follows. 600 µg of protein was mixed with an equal volume of Laemmli sample buffer, boiled for 5 min, and resolved by 12.5% (w/v) SDS-polyacrylamide gel. Following electrophoresis the gel was placed in ice-cold 0.1 M KCl for 10 min causing the SDS to precipitate around the protein. The protein band was excised, broken up and resuspended in PBS then consecutively passed through an 18, 21 and 24 gauge needle prior to injection.

2.11.2 Immunisation schedule

Each fusion was performed with two BALB/c mice, which were immunised intraperitoneally three or four times at intervals of 2 weeks by V. Sutton. The initial injection consisted of rPI-9 emulsified in Freund's complete adjuvant, the second of rPI-9 emulsified in incomplete Freund's, and the third of rPI-9 mixed with PBS. An additional fourth injection consisting of denatured rPI-9 mixed with PBS was administered in some cases. Three days after the final inoculation the mice were sacrificed and their spleens removed.

2.11.3 Fusion of immune splenocytes to myeloma cells

V. Sutton and J. Trapani performed the fusions. The immune splenocytes were harvested by teasing them into pre-warmed SF-DMEM, then washed once in SF-DMEM, counted and maintained in SF-DMEM at 37°C. NS-1 mouse myeloma cells were maintained in complete DMEM at 2 x 10^5 cells/ml and passaged at log phase prior to the fusion. Feeder cells were prepared from the thymus of 4 four week old CBA mice by teasing into pre-warmed SF-DMEM. Thymocytes were washed twice in SF-DMEM, counted and maintained in SF-DMEM at 37°C.

Immune splenocytes and NS-1 cells were combined at a ratio of 5:1 (approximately 1 x 10^8 splenocytes to 2 x 10^7 NS-1 cells), centrifuged at 100 *g* for 4 min at room temperature and the supernatant aspirated. 800 µl of 50% (w/v) PEG 4000 was added drop by drop over a 45 s period whilst agitating the tube. The cells were then allowed to agglutinate at 37°C for 3 min. The excess PEG was then removed by washing in pre-warmed SF-DMEM and the cells resuspended in complete DMEM with hypoxanthine, aminopterin and thymidine (HAT). 2 x 10^8 feeder cells were added, the volume adjusted to 80 ml with complete DMEM/HAT, resulting in 4 x 10^6 cells/ml. 200 µl of cells were then added to each well of a 96 well plate, to give a final concentration of 8 x 10^5 cells/well.

2.11.4 Screening of hybridomas

HAT-resistant hybridomas were screened, two weeks after the fusion, for production of anti PI-9 antibodies by ELISA as described in section 2.13.1.1. Wells producing reactive antibodies were expanded and screened for specificity to PI-9, this was performed by immunoblotting against a panel of recombinant serpins (as described in section 2.13.2) and indirect immunofluorescence of COS cells transfected with PI-9, PI-8 or PI-6 cDNA (as described in section 2.13.3). Several clones were selected for further analysis. These were expanded and cloned by limiting dilution.

2.11.5 Isotyping of hybridomas

The immunoglobulin isotype of the hybridomas was determined using the mouse monoclonal antibody isotyping kit according to the manufacturer's instructions.

2.12 Purification of immunoglobulin

2.12.1 Purification of 1F3 on Protein G

The 1F3 hybridoma was grown in Hybridoma-serum free media to facilitate the purification of murine IgG_1 without contamination from bovine IgG from foetal calf serum supplemented media.

A column was prepared and packed with GammaBind™ G Sepharose™ to a depth of 2 cm. Before use the column was cleaned with 0.1 M glycine, pH 2.5, then wash with PBS to return to the column to pH 7.4. Hybridoma tissue culture supernatant was added to the column at a flow rate of 1 ml/min and the flow through collected. The column was washed with PBS to remove unwanted proteins and the IgG_1 eluted with 0.1 M glycine, pH 4.5. Fractions of 500 µl were collected and neutralised with 20 µl of 1 M Tris-HCl, pH 8.0. Fractions were assessed by UV spectroscopy at 280 nm and protein containing fractions analysed by SDS-PAGE. Fractions containing IgG_1 were pooled and concentrated. The final concentration of IgG_1 was determined by measurement of UV absorbance at 280 nm with an extinction co-efficient of a solution of 1 mg/ml being 1.4.

2.13 Immunotechniques

2.13.1 Enzyme linked immunosorbant assay (ELISA)

2.13.1.1 Hybridoma screening ELISA

rPI-9 (1 µg/ml) was adsorbed onto polystyrene microtiter plates in 50 mM carbonate buffer, pH 9.6, at 37°C for 1 h. Plates were then washed three times in PBS/0.05% (v/v) Tween-20, (this washing procedure was performed after each incubation step). Non-specific antibody binding to the plate was blocked with 2% (w/v) BSA/PBS for 30 min at 4°C. Hybridoma supernatant was either directly added to the plate or serially diluted in 1% (w/v) BSA/PBS before addition to the plate, then incubated for 45 min at 4°C. Bound antibody was detected with HRP conjugated sheep anti mouse Ig for 45 min at 4°C. This was detected by the addition of the chromogenic *o*-PD substrate, after 10 min the reaction was stopped by the addition of 0.5 M H_2SO_4 and the absorbance was measured at 490 nm.

2.13.1.2 1F3 epitope ELISA

COS-1 cells transiently transfected with pCMVneo/PI-9, pCMVneo/PI-$9_{P16\ Glu\text{-}Lys}$ pCMVneo/PI-$9_{P18\ Asn\text{-}Asp}$, pCMVneo/PI-$9_{P9\ Ala\Delta}$ or pCMVneo/PI-$9_{P9\text{-}P10\ Ala\Delta}$ were lysed in hypotonic lysis buffer followed by three rounds of sonication on ice for 30 sec. Lysates were centrifuged at 16,000 *g* for 5 min to remove cell debris. The total protein concentration for each lysate was determined with the Bio-Rad Protein assay kit. 5 µg of lysate was adsorbed onto each well of a polystyrene microtiter plates in 50 mM carbonate buffer, pH 9.6, at 37°C for 2 h. Plates were then washed three times in PBS/0.05% (v/v) Tween-20, this washing procedure was performed after each incubation step. Non-specific binding to the plate was blocked with 2% (w/v) BSA/PBS for 30 min at 4°C. Bound PI-9 was detected with 1F3, 2E7, 7D8 or 8D3 hybridoma supernatant diluted 1:10 in 1% (w/v) BSA/PBS incubated for 45 min at 4°C. Bound antibody was detected with sheep anti mouse Ig conjugated to horseradish peroxidase for 45 min at 4°C. The chromogenic *o*-PD substrate was added, after 10 min the reaction was stopped by the addition of 0.5 M H_2SO_4 and the absorbance at 490 nm was measured.

The absorbance of each antibody with each mutant of PI-9 was obtained in quadruplicate. The background reactivity of each antibody was also assessed against mock transfected COS-1 cell lysate and subtracted from the readings. The reactivity of 1F3, to each of the mutants, was assessed by calculating the ratio of 1F3 binding to 2E7, 7D8 or 8D3 respectively. This was then normalised to wildtype giving a final measure of 1F3 binding relative to each of the other antibodies, relative to wildtype PI-9.

2.13.1.3 Peptide blocking ELISA

Synthetic PI-9 peptides were synthesised with the assistance of P. Thompson (Department of Medicine, Monash University, Box Hill Hospital) on a PS3 Protein Technologies Automatic Peptide Synthesizer by solid phase chemistry using Fmoc protected amino acids. Analysis and purification of the peptides was performed by reverse phase high performance liquid chromatography and electrospray mass spectroscopy by P. Thompson.

rPI-9 (1 µg/ml) was adsorbed onto polystyrene microtiter plates in 50 mM carbonate buffer, pH 9.6, at 37°C for 1 h. Plates were then washed three times in PBS/0.05% (v/v) Tween-20, this washing procedure was performed after each incubation step. Non-specific binding to the plate was blocked with 2% (w/v) BSA/PBS for 30 min at 4°C.

Peptides at the indicated concentrations were pre-incubated with an equal volume of antiserum for 45 min at room temperature, then serially diluted in 1% (w/v) BSA/PBS before addition to the plate and incubated for 45 min at 4°C. Bound antibody was detected with sheep anti mouse Ig conjugated to horseradish peroxidase for 45 min at 4°C. The chromogenic *o*-PD substrate was added, after 10 min the reaction was stopped by the addition of 0.5 M H_2SO_4 and the absorbance was measured at 490 nm.

2.13.1.4 Antithrombin sandwich ELISA

Rabbit anti human antithrombin (AT) polyclonal antibody (diluted 1:1000) was adsorbed to microtiter plates in 50 mM carbonate buffer, pH 9.6, at 37°C for 1 h. Plates were then washed three times in PBS/0.05% (v/v) Tween-20, this washing procedure was performed after each incubation step. Non-specific binding to the plate was blocked with 2% (w/v) BSA/PBS for 30 min at 4°C. The indicated conformations of AT were then serially diluted (beginning at 5 µg/ml) in 1% (w/v) BSA/PBS and incubated for 45 min at 4°C. Captured AT was detected by either 1F3 (1:10) or chicken anti human AT polyclonal antibody (diluted 1:4000), followed by horseradish peroxidase either conjugated to sheep anti mouse IgG or sheep anti chicken Ig respectively, for 45 min at 4°C. The chromogenic *o*-PD substrate was added, after 10 min the reaction was stopped by the addition of 0.5 M H_2SO_4 and the absorbance was measured at 490 nm.

The conformations tested included AT activated with either heparin or heparin pentasaccharide (as demonstrated by an increase in tryptophan intensity measured at an excitation at 280 nm and emission at 340 nm), AT with the loop peptide of α_1-AT inserted into β-sheet A by incubation at 37°C overnight, and AT cleaved in the RCL by the Arg specific proteinase, gingipain. These conformations of AT were obtained from R. Pike and were verified by native and SDS-PAGE analysis.

2.13.2 Immunoblotting

2.13.2.1 Preparation of cell lysates

Cells were lysed by one of two methods:

- NP-40 lysis buffer: Cells were resuspended in NP-40 lysis buffer, briefly vortexed then placed on ice for 10 min. The lysate was then centrifuged at 12,000 *g* to remove intact nuclei and cell debris. Total protein concentration was determined with the Bio-Rad Protein assay reagent and equal amounts of protein loaded.
- Modified Laemmli sample buffer (Zapata *et al.*, 1998): Cells were resuspended in a small volume of PBS to which the modified Laemmli sample buffer was added.

The lysate was then passed through a 21 gauge needle to shear DNA. The number of cells lysed was noted and equivalent numbers of cells were loaded per lane.

2.13.2.2 Preparation of PI-9/graB complexes

RPI-9 was incubated with or without 25 ng of recombinant graB at 37°C for 10 min then resuspended in an equal volume of Laemmli sample buffer. Complexes from endogenous PI-9 and graB were prepared from the natural killer-like cell line, YT. 1 x 10^6 YT cells were lysed in NP40 lysis buffer or modified Laemmli sample buffer. In some instances YT cells were cultured for 20 h with or without 25 μM calpain inhibitor I (N-Acetyl-Leu-Leu-Norleu) before lysis.

2.13.2.3 Immunodetection

Lysates and purified recombinant proteins were made up to 10 μl with Tris-NaCl buffer, diluted 1:2 with Laemmli sample buffer and boiled for 5 min. The samples were loaded on a 10% or 12.5% (w/v) SDS-PAGE gel alongside prestained SDS-PAGE markers then electrophoresed at 200 V until the dye front migrated to the bottom of the gel. Proteins were then transferred to nitrocellulose membranes using a Mini Protean®II Western Blotter, filled with transfer buffer at 250 mA for 1h. Non-specific antibody binding sites on the membrane were blocked in Blotto at room temperature for 1 h. The membrane was incubated with the indicated primary antibody diluted in Tris-buffered saline with 0.1% (v/v) Tween-20 (TBS/Tween) for 2 h. Unbound primary antibody was removed by washing the membrane three times for 10 min in TBS/Tween. The appropriate HRP-conjugated secondary antibody was diluted (as specified in Section 2.5.4) in TBS/Tween and incubated with the membrane for 1 h. The membrane was again washed three times for 10 min in TBS/Tween, developed with Renaissance® Chemiluminescence reagents and exposed to X-ray film. In some experiments, scanning densitometry was performed and analysed with MCID™ Image Analysis software.

For subsequent hybridisations, the membrane was stripped by incubation in 62.5 mM Tris-HCl, pH 6.8, 2% (w/v) SDS and 100 mM β-mercaptoethanol at 50°C for 30 min. The membrane was then thoroughly washed in TBS/Tween (six times for 10 min) then blocked in Blotto at room temperature for 1 h.

2.13.3 Indirect immunofluorescence of cells

For indirect immunofluorescence of transfected COS-1 cells, the cells were trypsinised 24 h post-transfection, diluted to 1 x 10^5 cells/ml in complete DMEM and 50 µl/well added to a 12 well slide. Cells were allowed to adhere overnight before proceeding with indirect immunofluorescence. Alternatively for the indirect immunofluorescence of non-adherent cells, cells were attached to poly-L-lysine coated slides. Cells were then fixed and permeabilised in either acetone/methanol or formaldehyde followed by Triton X-100.

- Acetone/methanol: Cells were washed twice in PBS then fixed in 1:1 acetone/ methanol for 2 min at room temperature. The acetone/methanol was then aspirated and the slide allowed to dry. Prior to adding the primary antibody the cells were rehydrated in PBS.
- Formaldehyde/Triton X-100: Cells were washed three times in PBS then fixed in 3.7% (v/v) formaldehyde in PBS at room temperature for 20 min then washed twice in PBS. The remaining formaldehyde was quenched in PBS containing 20 mM NH_4Cl for 30 min and then washed twice in PBS. For staining of intracellular antigens, the cells were permeabilised with 0.5% (v/v) Triton X-100 in PBS for 5 min at room temperature, followed by four washes in PBS.

Rabbit polyclonal antisera or mouse monoclonal antibodies were diluted in PBS as specified (Section 2.5) and incubated with the fixed and permeabilised cells for 45 min at room temperature, then washed three times for 5 min with PBS. The appropriate FITC- or RITC-conjugated secondary antibodies were incubated with the cells for 45 min at room temperature, protected from the light. In some cases the cells were counterstained with propidium iodide (1µg/ml) for two minutes. The cells were washed three times for 5 min with PBS, mounted in PBG mounting fluid and viewed under UV light.

- Epifluorescence was observed on an Olympus fluorescence m :op:, with data acquisition via MCID™ Image Analysis software
- Confocal microscopy was observed on a Leica TCS-NT confocal laser scanning microscope.

2.13.4 Indirect immunofluorescence of frozen tissues

Normal human thymus was obtained from R. Boyd. Sections of 6 µm thickness were cut using a cryostat and air-dried onto silanised slides. Sections were washed and blocked in normal goat sera before incubation with 7D8 hybridoma supernatant. Bound

antibody was detected with anti mouse IgG conjugated to FITC. Sections were then stained with either anti CD3, CD4 CD8 or CD45 monoclonal antibodies directly conjugated to phycoerythrin or with rabbit anti wide spectrum keratin, visualised with RITC-conjugated secondary antibody.

2.13.5 Intracellular flow cytometry

Erythrocytes were removed from whole blood by lysis in erythrocyte lysing buffer for 5 min at room temperature, centrifuged at 300 *g* for 5 min and washed twice in PBS. 2.5 x 10^6 leukocytes were fixed in 500 µl of 3.7% (v/v) formaldehyde in PBS for 10 min at room temperature. Cells were centrifuged at 500 *g* for 5 min, the supernatant aspirated and resuspended in 100 µl of FACS™Permeabilizing Solution, incubated in the dark for 10 min at room temperature. The cells were washed in 500 µl of PBS with 1% (w/v) BSA and 0.02% (w/v) NaN_3, centrifuged at 100 *g* for 5 min, the supernatant aspirated and the cell pellet resuspended in 30 µl of 7D8 hybridoma supernatant or isotype control antibody for 45 min. Cells were washed and resuspended in 30 µl of FITC conjugated anti mouse IgG and incubated for 30 min at room temperature. The cells were then washed as described above. Peripheral blood leukocytes were gated into two populations; small lymphocytes and granulocytes, based on the forward and side scatter properties of the cells.

2.13.6 Immunohistochemistry

2.13.6.1 Paraffin embedded tissues

Human tissues fixed in neutral buffered formalin were obtained from the archives of the Pathology Department of Box Hill Hospital. Normal human adult testis fixed in Bouin's fixative was obtained from K. Loveland. Sections of 5 µm thickness were cut using a microtome, floated on ddH_2O and dried onto Superfrost Plus slides.

2.13.6.2 Immunoperoxidase staining

Paraffin embedded sections were dewaxed in two changes of xylene, then rehydrated by two washes in 95% (v/v) ethanol and one wash in 70% (v/v) ethanol. Endogenous peroxidase activity was quenched by treatment in 0.3% (v/v) hydrogen peroxide in methanol for 10 min. Sections were then washed in dH_2O and equilibrated in PBS for 10 min or treated for antigen retrieval by either;

- 50 mM glycine, pH 3.5: Slides were placed into a glass dish containing 50 mM glycine, pH 3.5, the solution was brought to the boil by microwaving on "High" for

2 min, followed by 8 min on "Low". The dish was allowed to cool for 10 min, the slides removed and washed in PBS.

- 10 mM citric acid, pH 6.0: The solution was brought to the boil by microwaving on "High" for 2 min, the slides were then added and the solution brought back to the boil, followed by 12 min on "Low". The dish was allowed to cool for 5 min, the slides removed and washed in PBS.

Sections were then blocked in 2% (w/v) BSA in PBS. Slides were washed in three changes of PBS, these washes were repeated between each incubation step. Primary antibodies were diluted in PBS with 1% (w/v) BSA and incubated overnight in a humidified container. Bound antibody was detected by sheep anti mouse Ig conjugated to biotin for 1 h, followed by Streptavidin conjugated to horseradish peroxidase (diluted 1:200) for 1 h, and visualised using the Liquid DAB Chromogen Substrate System. Sections were counterstained with Harris' haematoxylin and mounted in DPX mounting fluid.

2.14 Molecular biology techniques

The molecular biology and recombinant DNA techniques used in this thesis are standard methods described in detail in "Molecular Cloning, a Laboratory Manual" by Sambrook *et al.*, 1989. The techniques described below are those modified from the standard method.

2.15 Site-directed mutagenesis

2.15.1 Site directed mutagenesis of the proximal hinge of PI-9

Site directed mutagenesis of the proximal hinge of PI-9 was performed by Q. Zhou, using the Transformer™ Site-Directed Mutagenesis Kit based on the technique of Deng and Nickoloff , 1992.

The following list of primers were used to introduce the indicated amino acid substitutions or deletion.

Oligo	5'-3' sequence	Hinge region mutations
PB 433	TGCCTCGGTGCCTTTTTCATTCACCTC	Glu to Lys at the P_{16}
PB 434	GGTGCCTTCTTCATTCACCTCCACAAA	Asn to Asp at the P_{18}
PB 436	AAAGGAGCTCGATGACGCTGCCTC	deletion of Ala at the P_9
PB 437	TACAAAGCAGCTCGACGCTGCCTCGGTGCC	deletion of two Ala at the P_9 and P_{10} positions

Mutagenesis was performed as described in the manufacturer's instructions using the supplied buffers. With the following additions; selection of plasmid DNA containing the desired mutation was performed by *XbaI* endonuclease restriction (digests parental plasmid DNA strand only). Following the final round of selection, positive clones were screened by DNA sequencing across the mutated region.

2.15.2Site directed mutagenesis of the proximal hinge and RCL of α_1-AT

Site directed mutagenesis of the proximal hinge and RCL of α_1-AT was performed using the Gene Editor™ *in vitro* Site-Directed Mutagenesis System according to the manufacturer's instructions. This system utilises antibiotic selection to yield high frequency of mutations. The supplied Selection Oligonucleotide alters the substrate specificity of the wild-type TEM-1 β-lactamase, therefore cells harbouring plasmids that have incorporated this mutation have increased resistance to ampicillin family antibiotics (Venkatachalam *et al.*, 1994).

Oligo	5'-3' sequence	Hinge region mutations
PB 387	CTGACCATCAACGAGGAAGGGACTGAAGCT GCTGCGGCCACCTTAGAGGCCATACC	P_{18} Asp to Asn, P_{16} Lys to Glu, P_{10} Gly to Ala, P_8 Met to Thr and deletion of the P_7 Phe

Mutagenesis was performed as described in the manufacturer's instructions. Following the final selection, clones were screened for successful incorporation of the mutagenesis by *PstI* digests (mutation results in loss of a *PstI* site) then verified by DNA sequencing across the mutated region. Clones containing the correct mutations were then fully sequenced to ensure no second site mutations had occurred.

2.16 DNA sequencing

DNA sequencing was performed using the Thermo Sequenase Cycle Sequencing kit according to the manufacturer's instructions. DNA to be sequenced was isolated from transformed DH5α *E.coli* using a modified alkaline lysis technique (Le Gouill *et al.*, 1994). Sequencing was performed using the radiolabelled primer cycle sequencing protocol.

2.16.1 Preparation of [γ^{32}P] ATP labelled oligonucleotide primers

Oligonucleotides were radiolabelled with [γ^{32}P] ATP. Approximately 20 pmole of oligonucleotide was labelled in T4 polynucleotide kinase buffer with 2 µl of [γ^{32}P] ATP and 10 U of T4 polynucleotide kinase in a total volume of 20 µl, the reaction was incubated at 37°C for 1 h.

The efficiency of labelling was determined by PEI chromatography. A strip of polyethyleneimine (PEI) impregnated microcrystalline cellulose bonded to a plastic backing material was marked with an origin, 2 cm from one end with a soft lead pencil. 1 µl of the labelling reaction was spotted at the origin and the strip placed in a cylinder containing 5 ml of 2 M HCl such that the origin was just above the solvent level. The PEI strip was left until the solvent front approached the top of the strip. Free nucleotides migrate with the solvent front while polynucleotides remain at the origin. The strip was scanned with a hand-held Geiger counter and the efficiency of incorporation estimated by comparing the radioactivity at the origin to the radioactivity at the solvent front. Oligonucleotides were only used if the incorporation was approximately 50% or better.

2.16.2 Sequencing reactions

Sequencing was performed using the cycle sequencing protocol according to the manufacturer's instructions. PCR was performed using a hot start (95°C for 2.5 min) followed by 55 cycles of 95°C for 30 s, 52°C for 30 s and 72°C for 90 s. At the end of the PCR, 4 µl of stop solution was added to each reaction.

2.16.3 Sequencing gel electrophoresis

The gel plates (40 cm in length) were washed thoroughly and one plate coated with GelSlick™ to facilitate its separation from the gel after electrophoresis. Spacers were then set in place and the plates securely held together using a rubber gasket. A 6% (w/v) acrylamide gel mixture was then prepared by dissolving 29.4 g urea, 3.5 ml 20 x glycerol tolerant buffer (GTB) and 26.7 ml dH_2O by heating in a microwave oven. 14 ml of 30% (w/v) acrylamide (38:2 ratio of acrylamide:N,N'-methylenebisacrylamide) was added and this mix was then filtered through filter paper. 400 µl of 10% (w/v) APS and 30 µl TEMED were added and the gel mix carefully poured between the glass plates to avoid the formation of bubbles. The combs were set in place and the gel allowed to set at room temperature for 30 min. Once set, the rubber gasket was removed and the apparatus placed in a gel tank which was then filled with 1 x GTB. The gel was

prewarmed by running at 65 W for 30 min and the wells rinsed of excess urea before loading the samples. The samples were heated to 75°C for 5 min and 2.5 µl of each sample was loaded in separate lanes and electrophoresis continued for 1.5 h at 60 W. Samples were loaded again if more than 100 bp of sequence information was required. The apparatus was dismantled and the siliconised plate removed. The gel was fixed in a solution of 10% (v/v) acetic acid /10% (v/v) methanol for 10 min and rinsed in dH_2O for 20 min. The gel was then dried for 60 min at 80°C under vacuum and exposed to X-ray film overnight at -70°C between intensifying screens.

2.17 Protein analysis

2.17.1 Purification of recombinant α_1-Antitrypsin mutant

α_1-Antitrypsin with the PI-9 hinge was expressed in the *E.coli* strain BL21 (DE3) using the expression vector pTERM and was purified from cell inclusion bodies using guanidinium HCl denaturation and a continual refolding procedure as previously described (Hopkins *et al.*, 1997). Briefly, inclusion bodies were purified from BL21 (DE3) cells by treatment with lysozyme followed by sonication. DNA was removed by DNase treatment and the inclusion bodies washed to remove any contaminating cellular proteins by three washes in 50 mM Tris-HCl, pH 8.0, 300 mM NaCl, 10 mM EDTA with 0.5% (v/v) Triton X-100. The inclusion bodies were dissolved in 6 M guanidinium HCl, 50 mM Tris-HCl, pH 8.0, 100 mM DTT. This solution was then added drop-wise into an excess of refolding buffer (50 mM Tris-HCl, pH 8.0, 50 mM NaCl, 5 mM DTT) with stirring overnight. The refolded protein was further purified by Q-Sepharose chromatography, then eluted with a 50 – 300 mM NaCl gradient. Fractions were assessed by UV spectroscopy at 280 nm and protein containing fraction analysed by native and SDS-PAGE. Fractions containing α_1-AT were pooled and concentrated. The final concentration of α_1-AT was determined by measurement of UV absorbance at 280 nm with an extinction co-efficient of a solution of 1 mg/ml being 0.53. Aliquots were stored at -70°C.

2.17.2 Preparation of polymers of Antithrombin

Polymers of antithrombin purified from plasma were prepared by heating at 55°C at a concentration of 0.2 mg/ml in 100 mM Tris-HCl, pH 7.4, 150 mM NaCl in a total volume of 10 µl for the indicated time, after which the sample was resuspended in an equal volume of pre-chilled native gel sample buffer and stored on ice until analysed by

native PAGE. In some circumstances AT was incubated with an equimolar amount of 1F3 or isotype control antibody (0.65 mg/ml) in a total volume of 10 µl, at 55°C for 3 h.

2.17.3 Native PAGE

Samples were resolved on a 10% (w/v) native polyacrylamide gel using a separate cathode and anode buffer. The gels were electrophoresed at 20 mA per gel for 3 h before being transferred to nitrocellulose or stained with Coomassie Blue.

2.18 RNA analyses

2.18.1 Isolation of total RNA

Isolation of RNA from YT cells was performed using a modification of the guanidinium thiocyanate procedure described by Chomcyznski and Sacchi (Chomczynski and Sacchi, 1987) or by RNAzol™. Adherent cells grown on 10 cm^2 tissue culture dishes were rinsed twice with 2 ml ice cold PBS before being lysed on the dish. Non-adherent cells grown in culture were pellet by centrifugation, them washed in PBS before lysis. Tissue samples were rinsed in several changes of PBS before lysis.

- Guanidinium method: 1 ml of guanidinium thiocyanate solution was added to the sample and incubated on ice for 5-10 min. 100 µl of 2 M sodium acetate, pH 4.0, was added and gently mixed, followed by 1 ml of ddH_2O saturated phenol then 200 µl of chloroform:isoamyl alcohol (49:1), and stored on ice for 15 min. After centrifugation at 10.000 *g* for 15 min at 4°C, the aqueous phase was removed and the phenol/chloroform extraction step repeated. The RNA was precipitated by the addition of an equal volume of isopropyl alcohol and incubation at -20°C for a minimum of 30 min. The RNA was pelleted by centrifugation at 10,000 *g* for 15 min at 4°C and resuspended in 500 µl of guanidinium thiocyanate solution. An equal volume of isopropyl alcohol was added and the RNA sample stored at -20°C until required. Just prior to use the RNA was recovered by centrifugation at 10,000 g for 15 min and dissolved in ddH_2O.
- RNAzol™: Cells were homogenised in 1 ml of RNAzol™ on ice, 0.1 ml of chloroform was added, the mixture vortexed and placed on ice for 5 min before centrifugation at 10,000 *g* for 15 min. The upper aqueous phase was transferred to a fresh tube and an equal volume of iso-propanol added. The RNA was allowed to precipitate on ice for 15 min before centrifugation at 10,000 *g* for 15 min. The RNA

pellet was then washed in 70% (v/v) ethanol, dried briefly under vacuum then dissolved in DEPC treated ddH_2O.

2.18.2 Northern blotting

2.18.2.1 Electrophoresis of RNA

Total RNA samples for YT cells were prepared as above. K. Loveland provided the testis RNA samples. Total RNA was precipitated then resuspended in RNA sample buffer. Dissolved RNA was mixed with RNA loading buffer and heated at 70°C for 5 min then loaded onto a RNA gel consisting of 1% (w/v) agarose containing 2.2 M formaldehyde in 1 x MOPS running buffer. The RNA was electrophoresed at 60 V for 2-4 h. The 18S and 28S ribosomal RNA bands were visualised by ethidium bromide staining of the gel in dH_2O containing 0.5 μg/ml ethidium bromide for 15 minutes. The ethidium bromide was then removed by multiple changes in dH_2O before transfer to nitrocellulose.

2.18.2.2 Transfer of RNA to Hybond N^+ membrane

RNA was transferred to Hybond N^+ membranes using the capillary transfer technique. A piece of membrane was cut to the same size as the gel. A plastic support with a flat surface was placed in a glass tray containing 10 x SSC. Two pieces of 3MM Whatman paper cut slightly larger that the gel were placed over the support with both ends submerged in the 10 x SSC to act as a wick. The gel was placed on the support with the membrane directly on top. Two pieces of 3MM Whatman paper, soaked in 10 x SSC, were placed on top of the membrane followed by plastic wrap to cover the whole apparatus. A scalpel blade was used to remove the plastic directly over the gel. A stack of dry paper towel and a weight of approximately 200 g were placed on top. The following day the apparatus was dissembled and the position of the wells and the 18S and 28S ribosomal RNA bands marked on the membrane. The membrane was rinsed briefly in 2 x SSC and baked at 80°C for 3 h.

2.18.2.3 [α^{32}P] dCTP labelling of cDNA probes

Radioactive probes were prepared using the Prime-a-Gene® Labelling System based on the principle of using random sequence hexanucleotides as primers for DNA synthesis. The PI-9 probe was generated by endonuclease digestion of pBluescript KS$^-$/PI-9 with *EcoRI* and *SacI* and the graB 3'UTR probe by digestion of pBluescript KS$^-$/graB 3'UTR with *EcoRI* (plasmids described in section 2.19.1). Restriction fragments were resolved

on a 2% (w/v) agarose gel, the bands excised and purified with the BRESAclean™ DNA purification kit. Approximately 50 ng of the purified cDNA was then used as a template for the radioactive probe according to the manufacturer's instructions. The efficiency of labelling was determine by PEI chromatography (as described in Section 2.16.1).

2.18.2.4 Hybridisation of radiolabelled probes to Clontech Human RNA Master Blot™

The Clontech Human RNA Master Blot™ was prehybridised in Rapid-hyb buffer at 65°C in a heat-sealed plastic bag for 30 min. The PI-9 probe described above was denatured at 100°C for 5 min and added to the Rapid-hyb buffer to a final concentration of 2 ng/ml. The membrane and probe were incubated at 65°C overnight before washes in SSC at increasing stringency, with a final wash in 2 x SSC, 0.1% (w/v) SDS at 55°C. The membrane was placed in a heat-sealed bag and exposed to X-ray film at -70°C. The signal was then allowed to decay for 6 months before the membrane was reprobed, as described above, with the graB probe.

2.18.2.5 Hybridisation of radiolabelled probes to RNA immobilised on Hybond N^+ membrane

The Hybond N^+ membrane was prehybridised with 8 ml of Rapid-hyb buffer at 65°C in a heat-sealed plastic bag for 15 min. Either the PI-9 or the graB 3'UTR probes described above were denatured at 100°C for 5 min and added to prewarmed Rapid-hyb buffer to a final concentration of 2 ng/ml. The membrane and probe were incubated at 65°C overnight. The membrane was initially washed at room temperature for 20 min with 2 x SSC, 0.1% (w/v) SDS then at 50°C for 10 min with 2 x SSC, 0.1% (w/v) SDS, then in 0.1 x SSC, 0.1% (w/v) SDS at 50°C for 15 min. The membrane was placed in a heat-sealed bag and exposed to X-ray film at -70°C.

2.18.3 Reverse transcription-polymerase chain reaction

2.18.3.1 Reverse transcription reaction

cDNA was synthesised from RNA using Moloney murine leukaemia virus (RNase H minus strain) reverse transcriptase (M-MuLV RT) and oligo(dT). 1 µg of RNA was incubated with oligo(dT_{12-18}) in a total volume of 15 µl for 5 min at 70°C to remove secondary structures, then placed on ice. 500 µM dNTPs, 200 U M-MuLV RT and 25 U RNasin were then added to a total volume of 25 µl in the supplied transcription buffer

and incubated at 42°C for 2 h. A no M-MuLV RT tube was also included to control for contamination by genomic or plasmid DNA.

2.18.3.2 Polymerase chain reaction

The success of the reverse transcription reaction was determined by PCR using primers to GAPDH. This PCR was performed using 20 pmol of primers PB 584 and PB 585 in *Taq* polymerase buffer containing 200 μM dNTPs, 2.5 mM $MgCl_2$ and 2 units of *Taq* polymerase. The PCR was performed for 35 cycles of denaturation at 94°C for 30 s, annealing at 55°C for 30 s, and extension at 72°C for 45 s. PCR to detect PI-9, graB or perforin was performed using the indicated primers under the same conditions.

Oligo	5'-3' sequence	S/AS	Template*	Nucleotides	Exon
PB 584	GACCCCTTCATTGACCTCAAC	S	GAPDH	143-163	3
PB 585	GATGACCTTGCCCACAGCCTT	AS	GAPDH	683-703	8
PB 174	AGATGATGTATCAGGAG	S	PI-9	700-716	6
PB 287	AGTCTGGCTTGGTCCAGG	AS	PI-9	871-888	7
PB 377	GAACAGGAGCCGACCCAGCA	S	graB	257-276	3
PB 378	GGACTTGGCTCCAGAGAAGG	AS	graB	799-818	5
PB 476	AAGTCAGCTCCACTGAAGCT	S	Perforin	329-348	1
PB 477	GGTAGGTTTGGTGGAAGGAG	AS	Perforin	870-889	2

* GenBank Accession numbers for the indicated templates are NM_002046, NM_004155, J04071 and NM_005041 for GAPDH, PI-9, graB and perforin respectively.

2.18.3.3 Transfer to Hybond membrane

Amplified products were resolved on a 2% (w/v) agarose gel by electrophoresis and visualised by ethidium bromide staining. The amplified products were then transferred to nitrocellulose using the capillary transfer technique under alkaline conditions. This is essentially as described in section 2.18.2.2 except 0.4 M NaOH was used instead of 20 x SSC. Following the transfer, the apparatus was dismantled and the position of the wells marked on the membrane with a lead pencil. The membrane was divided into portions containing the products amplified by either PI-9, graB or perforin specific primers, then hybridised with [γ^{32}P] ATP labelled internal oligonucleotides specific for PI-9, graB or perforin respectively.

Oligo	5'-3' sequence	S/AS	Template*	Nucleotides	Exon
PB 286	AGCTGAGCCTGCTGGTG	S	PI-9	787-803	6
PB 279	TGCTTCCTGTAGTTAGTAGC	AS	graB	753-772	4
JT 219	GCCAACTTTGCAGCCCAG	S	Perforin	463-480	1

* GenBank Accession numbers for the indicated templates are NM_004155, J04071 and NM_005041 for PI-9, graB and perforin respectively.

2.18.3.4 Hybridisation of radiolabelled probes to DNA immobilised on Hybond membrane

The membrane was prehybridised with 5 ml of Rapid-hyb buffer at 42°C in a heat-sealed plastic bag for 15 min, then hybridised with 10 ng/ml of [γ^{32}P] ATP labelled oligonucleotide probes (as described in 2.16.1) at 42°C in Rapid-hyb buffer for 1 h. The membrane was initially washed at room temperature for 10 min with 6 x SSC then 6 x SSC at 42°C for 10 min. The membrane was placed in a heat-sealed bag and exposed to X-ray film at -70°C between intensifying screens.

2.19 *In situ* hybridisation

2.19.1 Construction of the PI-9 probe

The probe for PI-9 was generated from nucleotides 827-1388 of human PI-9 cDNA by endonuclease digestion of pCMVneo/PI-9 with *SacI* and *EcoRI*. The 561 bp fragment was gel purified and subcloned into the *SacI/EcoRI* sites of pBluescript II KS$^-$. The resulting plasmid, pBluescriptKS$^-$/PI-9, was verified to be correct by restriction endonuclease mapping and DNA sequencing.

2.19.2 Construction of the granzyme B 3'UTR probe

The probe for graB was generated by amplifying the 3'UTR of graB (nucleotides 747-873) with primer JT 300 and JT 301. This PCR was performed with 20 pmole of each primer with 1 ng of pGEM-t/HSE 26.1 as the template in 1 x *Taq* polymerase reaction buffer containing 2 U of *Taq* polymerase, 2.5 mM $MgCl_2$ and 200 µM dNTPs for 30 cycles of denaturation at 95°C for 90 s, annealing at 50°C for 60°s and extension at 72°C for 30 s. The amplified products were analysed by ethidium bromide agarose gel electrophoresis and the 127 bp product excised from the gel, purified with the BRESAclean™ DNA purification kit and ligated into pCR®-Blunt with T4 DNA ligase. The insert was sequenced as described in Section 2.16 to verify the insert and plasmid.

The 3'UTR of graB was then subcloned into the *EcoRI* site of pBluescript KS$^-$ resulting in pBluescript KS$^-$/graB 3'UTR.

Oligo	5'-3' sequence	S/AS	Template	Nucleotides	Exon
JT 300	TGAAACGCTACTAACTACAG	S	graB	747-766	5
JT 301	GAATAAATACCTCTTAGCTGAGTGG	AS	graB	849-873	5

2.19.3 Digoxigenin-labelling of riboprobes

Digoxigenin (DIG)-labelled riboprobes for both PI-9 and graB were generated following the methods outlined in the DIG Labelling Kit. Plasmids for encoding both graB and PI-9 were linearised either with *SacI* for the antisense direction or *XhoI* for the sense direction. Riboprobes were transcribed with T3 RNA polymerase for the antisense riboprobes and T7 RNA polymerase for the sense riboprobes.

1 µg of linearised plasmid was transcribed using the indicated RNA polymerase using DIG dNTP mix (containing DIG-UTP) in the supplied transcription buffer in a total volume of 20 µl for 2 h at 37°C. The reaction was then terminated by the addition of 2 µl of 0.2 M EDTA, pH 8.0, and the riboprobe precipitated with 2.5 µl of 4 M LiCl and ethanol overnight at -70°C. The riboprobe was pelleted by centrifugation at 10,000 *g* for 15 min, the pellet washed in 70% (v/v) ethanol and resuspended in DEPC treated ddH_2O in the presence of RNasin.

The probe concentration and efficiency of DIG incorporation was assessed by dot blot on Hybond membrane. Serial 2-fold dilutions of the probe were blotted against a supplied control DIG labelled riboprobe. The membrane was microwaved briefly to fix the RNA and the incorporated DIG-UTP was detected by an anti DIG antibody conjugated to alkaline phosphatase. The membrane was then washed and developed with nitroblue tetrazolium chloride/5-bromo-4-chloro-3-indolyl phosphate substrate (NBT/BCIP).

2.19.4 Preparation of sections

Sections of 5 µm thickness were cut from paraffin-embedded tissue of adult human testis using a microtome, floated on DEPC treated ddH_2O and dried onto Superfrost Plus slides. This procedure was performed while wearing latex gloves to minimise RNase contamination of the slides.

Slides were dewaxed in two changes of histosol for 10 min each, then rehydrated in a graded ethanol series (100%, 95% then 70% (v/v)). The sections were incubated in 0.2

M HCl for 20 min and washed twice in DEPC treated ddH_2O. The sections were then treated with a range of proteinase K concentrations (1 – 10 μg/ml diluted in 10 mM Tris-HCl, 1 mM EDTA, pH 8.0) for 30 min at 37°C. This reaction was stopped by incubating the slides in 0.2% (w/v) glycine in PBS at 4°C. The sections were then acetylated in 0.1 M Triethanolamine, 0.25% (v/v) acetic anhydride for 5 min then washed in DEPC treated ddH_2O. The sections were pre-hybridised under coverslips in Pre-Hyb buffer for 2 h at the hybridisation temperate (50°C and 60°C, for PI-9 and graB respectively). Sense and antisense riboprobes were diluted in Pre-Hyb buffer to the indicated concentration (200 – 300 ng/ml), heated to 70°C to remove secondary structures then hybridised under coverslips for 16 h. The slides were washed with increasing stringency in SSC; firstly 2 x SSC at room temperature, followed by a wash in 25 μg/ml RNase in 2 x SSC at 37°C, then 2 x SSC, 1 x SSC and 0.1 x SSC at the hybridisation temperature. The sections were incubated in Blotto, then with an alkaline phosphatase-conjugated anti DIG antibody. Slides were washed, developed with NBT/BCIP then counterstained with haematoxylin and mounted in GVA.

Chapter 3

Production and Characterisation of Antibodies to PI-9

Summary

This chapter describes the production and characterisation of antibodies to PI-9. Polyclonal antisera were raised in rabbits and monoclonal antibodies were produced by fusion of immune splenocytes to NS-1 myeloma cells. Antibodies were assessed for reactivity and specificity to PI-9 by immunoblotting, indirect immunofluorescence and ELISA. Of three polyclonal antisera (Rabbit #11, #12 and #15) raised, Rabbit #15 antiserum had the best specificity to PI-9 and Rabbit #11 antiserum was found to cross-react with a number of related serpins. Of the monoclonal antibodies produced 7D8 and 8D3 gave the greatest specificity across a variety of immunotechniques. 2E7 was specific for PI-9 but it recognises an epitope lost upon denaturation.

Introduction

Although previous RNA analyses indicate that PI-9 transcripts are present in a restricted manner (in immune cells and tissues as well as immune privileged sites) (Sun *et al.*, 1996), a protein distribution study has never been performed. The tissue distribution studies central to this thesis require antibodies specific to PI-9. Members of the serpin superfamily share high homology and have a highly conserved tertiary structure comprising of three β-sheets and nine α-helices. Amongst ov-serpins greater than 40% amino acid homology is observed between PI-9 and most family members, with 62% homology between PI-9, PI-8 and PI-6. Consequently, antibodies raised against PI-9 have a high probability of detecting epitopes conserved on other serpins. As such the process of characterising antibodies to PI-9, performed in this chapter, included investigation of their reactivity and their specificity for PI-9.

Both rabbits and mice were immunised with PI-9 to produce specific antibodies. Polyclonal antisera raised in rabbits were chosen due to the advantages of low cost and short production time. Murine monoclonal hybridomas were also produced, the disadvantages of cost and time offset by the specificity of the antibodies.

3.1 Characterisation of polyclonal antisera to PI-9

Polyclonal antisera to PI-9 were raised in three NZW rabbits with the immunisations performed by J. Sun. Two rabbits (Rabbit #11 and Rabbit #12) were immunised with wildtype recombinant PI-9 (rPI-9) and one rabbit was immunised with a rPI-9 mutant in which the P_1 residue had been mutated from glutamic acid to aspartic acid (Rabbit #15). These rabbit antisera were characterised by a variety of immunological methods to determine their reactivity and specificity towards PI-9.

3.1.1 Analysis of rabbit polyclonal antisera by immunoblotting

Rabbit polyclonal antisera were screened by immunoblotting against a panel of purified recombinant serpins that included the human ov-serpins PI-9, PI-8, PI-6, M/NEI and PAI-2 and the murine ov-serpins SPI-6 and SPI-3, the murine orthologues of PI-9 and PI-6 respectively. At a dilution of 1:500 all three rabbit antisera demonstrated cross-reactivity against all of the ov-serpins tested (illustrated in Table 3.1A). However when the antisera from Rabbit #12 and Rabbit #15 were tested at higher dilutions (1:2000 and 1:5000), specificity to PI-9 was attained in comparison to the other human ov-serpins but cross-reactivity was still detected with the murine ov-

A

Immunoblotting

Serpin	Rabbit #11			Rabbit #12			Rabbit #15		
	1/500	1/2000	1/5000	1/500	1/2000	1/5000	1/500	1/2000	1/5000
PI-9	++++	+++	++	++++	+++	++	++++	+++	++
PI-8	+++	+++	++	+	+/-	-	+	+/-	-
PI-6	++++	+++	++	+++	+	+/-	+++	+	-
M/NEI	++++	+++	++	++	-	-	+	-	-
PAI-2	+++	++	+	+	+/-	-	+	+/-	-
SPI-6	++++	+++	++	+++	++	++	+++	++	++
SPI-3	++++	+++	++	++	+	-	+++	++	+

B

Immunofluorescence

Serpin	Rabbit #11			Rabbit #12			Rabbit #15		
	1/100	1/5000	1/1000	1/100	1/5000	1/1000	1/100	1/5000	1/1000
PI-9	++++	+++	++	++++	+++	++	++++	+++	++
PI-8	+++	+++	++	-	-	-	-	-	-
PI-6	++++	+++	++	-	-	-	-	-	-
M/NEI	++++	+++	++	-	-	-	-	-	-
PAI-2	++	+	+	-	-	-	-	-	-
SPI-6	++++	+++	++	-	-	-	-	-	-
SPI-3	++++	+++	++	-	-	-	-	-	-

Table 3.1 Reactivity of rabbit polyclonal antisera to ov-serpins. (A) 100 ng of each ov-serpin was resolved by reducing 12.5% SDS-PAGE. Gels were transferred to nitrocellulose, immunoblotted with polyclonal antisera from either Rabbit #11, #12 or #15 at the indicated dilutions and detected with HRP conjugated anti mouse IgG and enhanced chemiluminescence. (B) Reactivity of rabbit polyclonal antisera to ov-serpins by indirect immunofluorescence. COS-1 cells transfected with cDNAs for the indicated ov-serpin, were seeded onto slides, fixed, permeabilised and incubated with the indicated dilution of Rabbit #11, #12 or #15 antiserum. Bound antibody was detected with FITC conjugated anti rabbit IgG and visualised with fluorescence microscopy. The reactivity of each dilution of the antiserum was then compared (++++ = very strong, - = negative).

serpins SPI-6 and SPI-3. This cross-reactivity to murine ov-serpins was not considered a problem as these antisera were to be used for analysis of human tissue, however this does illustrate the conservation of structure and epitopes between PI-9 and homologous serpins.

No increase in specificity to PI-9 was demonstrated with the titration of Rabbit #11 antiserum. This indicated that the antiserum predominantly contains antibodies against epitopes common to all of the serpins tested. The cross-reactivity of Rabbit #11 antiserum was examined further by analysis against more distantly related members of the serpin superfamily (Figure 3.1). It was found to recognise the majority of these serpins, with the exception of α_1-antitrypsin (α_1-AT) and the chicken serpin, MENT.

3.1.2 Analysis of rabbit polyclonal antisera by indirect immunofluorescence

The three rabbit antisera were further characterised by indirect immunofluorescence of COS-1 cells transfected with ov-serpin cDNAs that included the human ov-serpins PI-9, PI-8, PI-6, M/NEI and PAI-2 and the murine ov-serpins SPI-6 and SPI-3. Rabbit #11 was found to cross-react with all of the ov-serpins tested, regardless of the dilution (Table 3.1B). This again demonstrated the presence of antibodies directed to a common serpin epitope in Rabbit #11 antiserum. However, Rabbit #12 and #15 antisera were found to be specific for PI-9 at all dilutions tested and even at low dilutions (Table 3.1B). This specificity of Rabbit #12 and #15 antisera to PI-9 by immunofluorescence is not consonant with the cross-reactivity observed by immunoblotting. This apparent contradiction may be due to the exposure of different epitopes under various fixation conditions, illustrating that epitope exposure is crucial in determining cross-reactivity.

As these antisera were to be used for an immunohistochemical tissue survey, it was important to discern which of the above methods would give the best evaluation of antibody specificity to PI-9. Neither of the techniques utilised above accurately reflect the denaturing conditions that PI-9 would be exposed to in tissues that have been fixed in formalin then embedded in paraffin. Would tissue processing more closely resemble immunoblotting, in which the denaturation of serpins results in the exposure of cross-reactive epitopes, or the formaldehyde fixation of transfected COS-1 cells, which does not reveal these cross-reactive epitopes? The simplest way to resolve these questions was to test these antisera by immunohistochemistry on tissue samples for which the distribution of other ov-serpins is known.

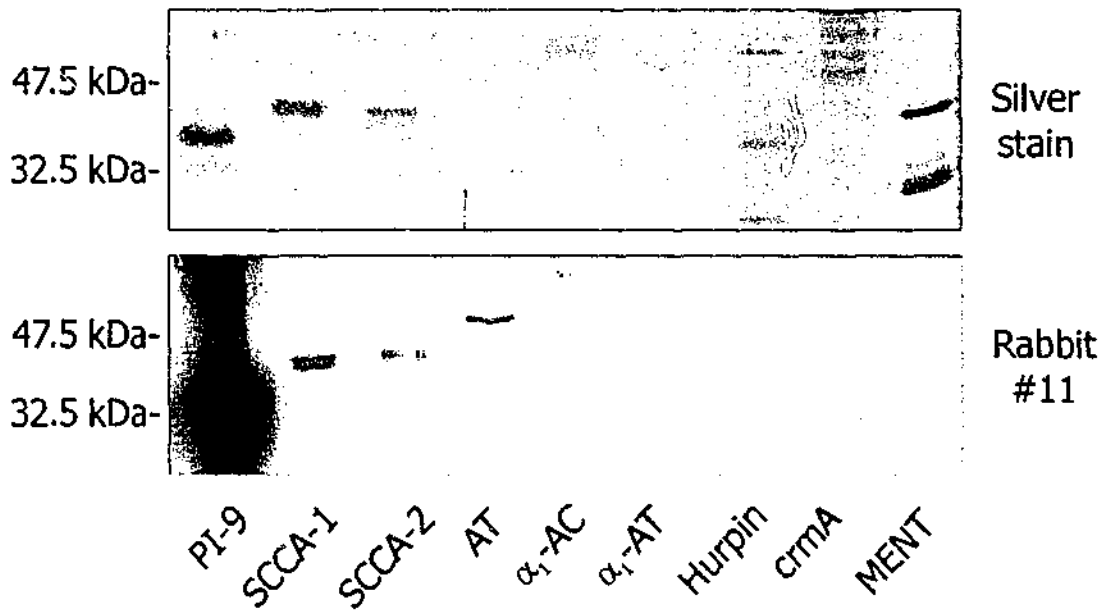

Figure 3.1 Specificity of Rabbit #11 polyclonal antiserum Pan-serpin reactivity of Rabbit #11 antiserum. 100 ng of each serpin was resolved by reducing 12.5% SDS-PAGE, with the exceptions of crmA, Hurpin and MENT for which 500 ng of partially purified recombinant protein was resolved. Duplicate gels were either silver-stained to demonstrate the presence of the indicated serpin or transferred to nitrocellulose and immunoblotted with a 1:2000 dilution of Rabbit #11 polyclonal antiserum and detected with HRP conjugated anti rabbit IgG and enhanced chemiluminescence.

3.1.3 Analysis of rabbit polyclonal antisera by immunohistochemistry

Sections of human skin were chosen to examine the cross-reactivity of rabbit polyclonal antisera to other ov-serpins by immunohistochemistry. Skin is known to contain a number of ov-serpins including PI-6 (in endothelial cells, keratinocytes and sweat glands (Scott *et al.*, 1996; Scott *et al.*, 1998)), PAI-2 (in granular and cornified layers of the epidermis (Lyons-Giordano *et al.*, 1994)), SCCA-1 and -2 (in the suprabasal layers of the epidermis (Cataltepe *et al.*, 2000)) and Hurpin (in keratinocytes (Abts *et al.*, 1999)). As these proteins have a well defined expression pattern in the skin they would provide controls for cross-reactivity to other ov-serpins. The skin sections selected also contained infiltrating lymphocytes, which could act as a positive control for the presence of PI-9. Serial sections of skin were analysed against a series of dilutions for each of the rabbit polyclonal antisera.

At lower dilutions (1:250) Rabbit #12 and #15 antisera non-specifically stained the collagen and elastin fibres in the dermis, although this staining was lost at higher dilutions (Figure 3.2A and B). At a dilution of 1:1000 both antisera exhibited a more restricted staining pattern and stained cells within the lymphocytic infiltrate, with some staining of endothelial cells in the blood vessels and desquamating flakes of keratin. Neither antibody stained the sweat glands or the sebaceous glands (except for Rabbit #15 antiserum which stained one gland near the hair follicle).

The staining observed with Rabbit #12 and #15 antisera did not overlap with previously published distributions of the ov-serpins PAI-2, Hurpin, SCCA-1 or SCCA-2. Skin sections were also stained with Rabbit #13 antiserum (an anti PI-6 polyclonal antiserum) to ensure that anti PI-9 antisera were not cross-reacting with PI-6, the closest paralogue of PI-9 (62% identity at the amino acid level). Dilutions of Rabbit #13 antiserum did not differ markedly in their staining of cell types, detecting PI-6 within endothelial cells of the blood vessels and desquamating flakes of keratin in the skin (Figure 3.2C). The overlap between Rabbit #12 and #15 antisera staining with the distribution of PI-6 suggested that Rabbit #12 and #15 antisera might cross-react with PI-6. However, when Rabbit #12 and #15 antisera were diluted further, the endothelial staining was lost at the same rate as the lymphocyte staining within the infiltrate (data not shown) and further experiments demonstrated that PI-9 is expressed in endothelial cells (Buzza *et al.*, 2001). This illustrates the difficulty in assessing antibodies when the protein distribution is not yet known or when distributions overlap.

A

Rabbit #12

1:250

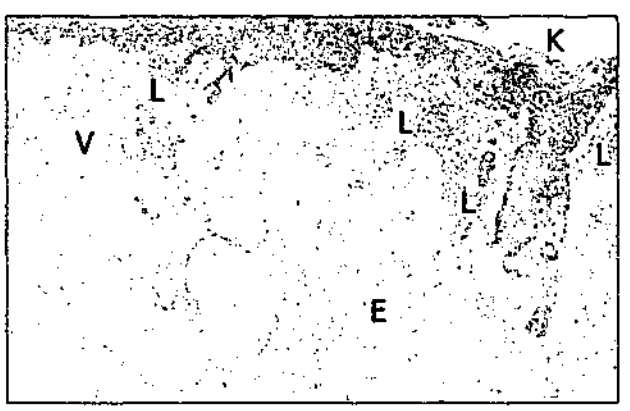

1:500

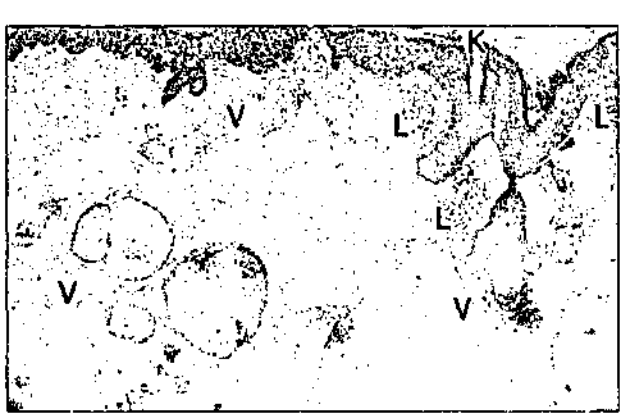

1:1000

B

Rabbit #15

1:250

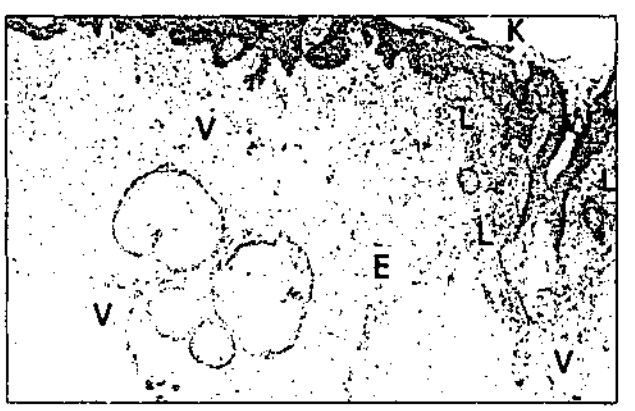

1:500

1:1000

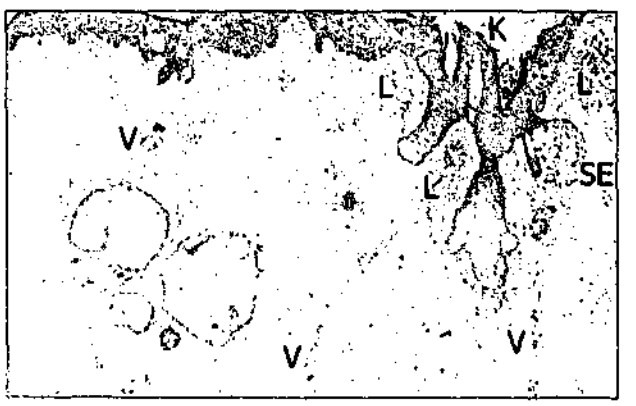

C

Rabbit #11

1:2000

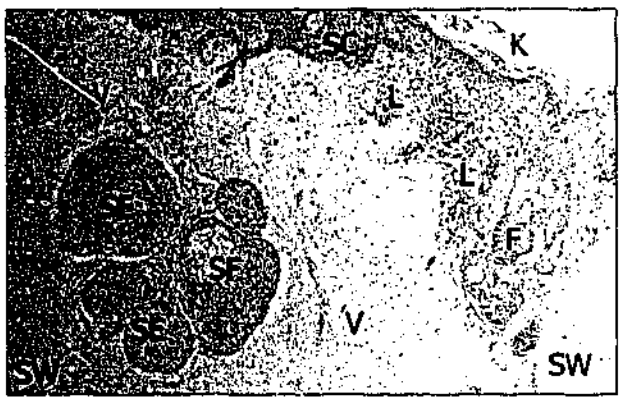

D

Rabbit #13

1:250

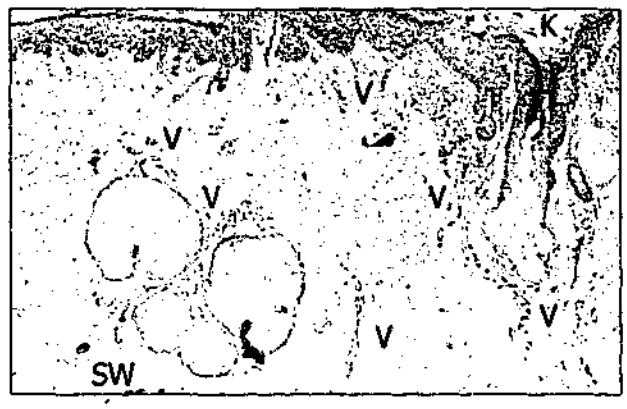

1:500

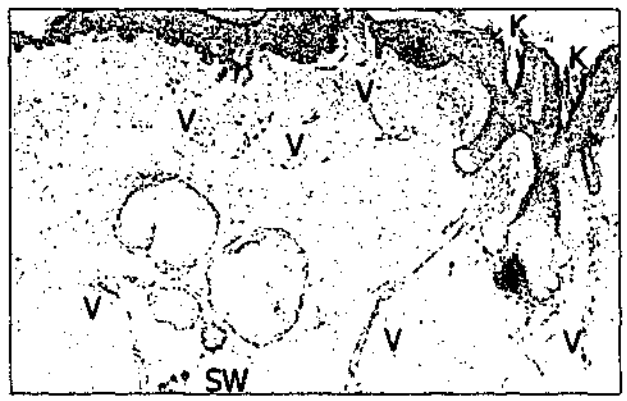

1:1000

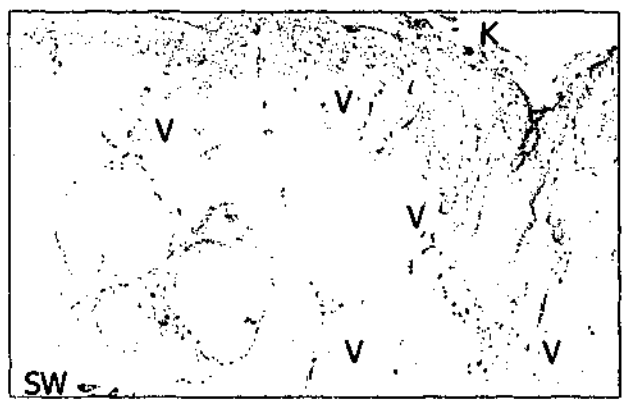

Figure 3.2 Comparison of rabbit polyclonal antisera. Serial sections of skin were examined for reactivity with the rabbit anti PI-9 polyclonal antisera at the indicated dilutions (A-C). These were compared against dilutions of the rabbit anti PI-6 polyclonal antiserum (Rabbit #13; D). Features stained include the sebaceous glands (SE), infiltrating lymphocytes (L), blood vessels (V), hair follicles (F), sweat glands (SW), collagen and elastin fibres in the dermis (E) and layers of the skin including the stratum corneum (SC) and keratin flakes (K).

The pre-immune sera from Rabbit # 12 and #15 were also examined on the these skin sections. The pre-immune sera from Rabbit #12 demonstrated background reactivity with collagen and elastin fibres in the dermis, however the pre-immune sera from Rabbit #15 gave no background staining (data not shown).

The Rabbit #11 antiserum reacted against many cell types and further dilution of the sera did not substantially alter the cell types stained. At a dilution of 1:2000 Rabbit #11 antiserum displayed prominent staining of the sebaceous glands, infiltrating leukocytes, blood vessels, sweat glands and some layers of the skin indicating a wide distribution of serpins within cell types in the skin (Figure 3.2D).

3.1.4 Rabbit polyclonal antisera – in conclusion

The Rabbit #11 antiserum is completely unsuitable as a tool to specifically detect PI-9 as it detects most serpins with equal affinity due to the presence of conserved epitopes. Rabbit #12 and #15 antisera, although cross-reactive by immunoblotting, are both specific to PI-9 by immunofluorescence. Upon closer examination against a wide panel of tissues, Rabbit #15 antiserum stained a more restricted number of cell types than Rabbit #12 antiserum, which occasionally stained other cell types (data not shown). Therefore, Rabbit #15 antiserum appears to be the best candidate for use in PI-9 analysis. However, as Rabbit #15 antiserum does cross-react at lower dilutions, care must be taken when analysing cells expressing high levels of other serpins. This could be a potential problem when carrying out tissue distribution studies, as the tissue distribution of many serpins is not fully characterised, and Rabbit #15 antiserum might exhibit cross-reactivity to other serpins expressed within the cells of interest.

To address the problem of cross-reactivity the antisera could be affinity purified. However as it appears that much of the cross-reactivity is due to immunodominant epitopes conserved amongst ov-serpins, the removal of antibodies to these epitopes would substantially drop the titre of the antisera. Alternative methods of producing specific antibodies include rabbit antisera raised to PI-9 specific peptides or murine monoclonal antibodies. Due to the costs required to produce peptides, murine monoclonal antibodies were produced using rPI-9 as the immunogen. Native and denatured rPI-9 were used to immunise separate mice to ensure that monoclonal antibodies recognising both conformational and linear epitopes were produced.

3.2 Production and characterisation of monoclonal antibodies to native PI-9

Monoclonal antibodies to PI-9 were raised in BALB/c mice immunised with rPI-9 purified from *P.pastoris*. The immunisation schedule consisted of three injections, an initial injection of rPI-9 emulsified in Freund's complete adjuvant, a second of rPI-9 emulsified in incomplete Freund's, and the third of rPI-9 mixed with PBS. Three days after the final inoculation the mice were sacrificed and their spleens removed. V. Sutton and J. Trapani performed the fusion of immune splenocytes to NS-1 myeloma cells.

Two weeks after the fusion, HAT resistant hybridomas were screened for antibody production by ELISA against rPI-9. Eight hybridomas were found to be positive by ELISA, these hybridomas were isotyped and all found to be IgG_1 κ. Antibodies were further characterised by a variety of immunological methods to determine their reactivity and specificity towards PI-9.

3.2.1 Analysis of monoclonal antibodies to native PI-9 by indirect immunofluorescence

Hybridomas positive to PI-9 by ELISA were further examined by indirect immunofluorescence against COS-1 cells transfected with PI-9 or PI-6 cDNA. Only three of the eight hybridomas (1F3, 2E7 and 5C6) recognised PI-9 by immunofluorescence, however 1F3 was found to cross-react with PI-6, suggesting that it recognised a common epitope found on both serpins (Figure 3.3). Of the other five hybridomas, three reacted against mitochondrial or cytoskeletal proteins, similar to that shown by 8B11 (Figure 3.3), and two were negative by immunofluorescence. This lack of reactivity to PI-9 suggested that these hybridomas were reactive to other components of the immunogen, possibly due to contaminating yeast proteins not removed during the purification of rPI-9 from *P.pastoris*.

The three PI-9 reactive hybridomas were then examined for their specificity to PI-9 by indirect immunofluorescence against COS-1 cells transfected with a panel of ov-serpin cDNAs, that included the human ov-serpins PI-9, PI-8 and PI-6 and the murine ov-serpins SPI-6 and SPI-3. Again 2E7 and 5C6 were found to be specific for PI-9, while 1F3 was found to cross-react with all of the other serpins tested (Table 3.2A). This suggested that 1F3, like Rabbit #11 antiserum, recognised a common epitope found in many ov-serpins.

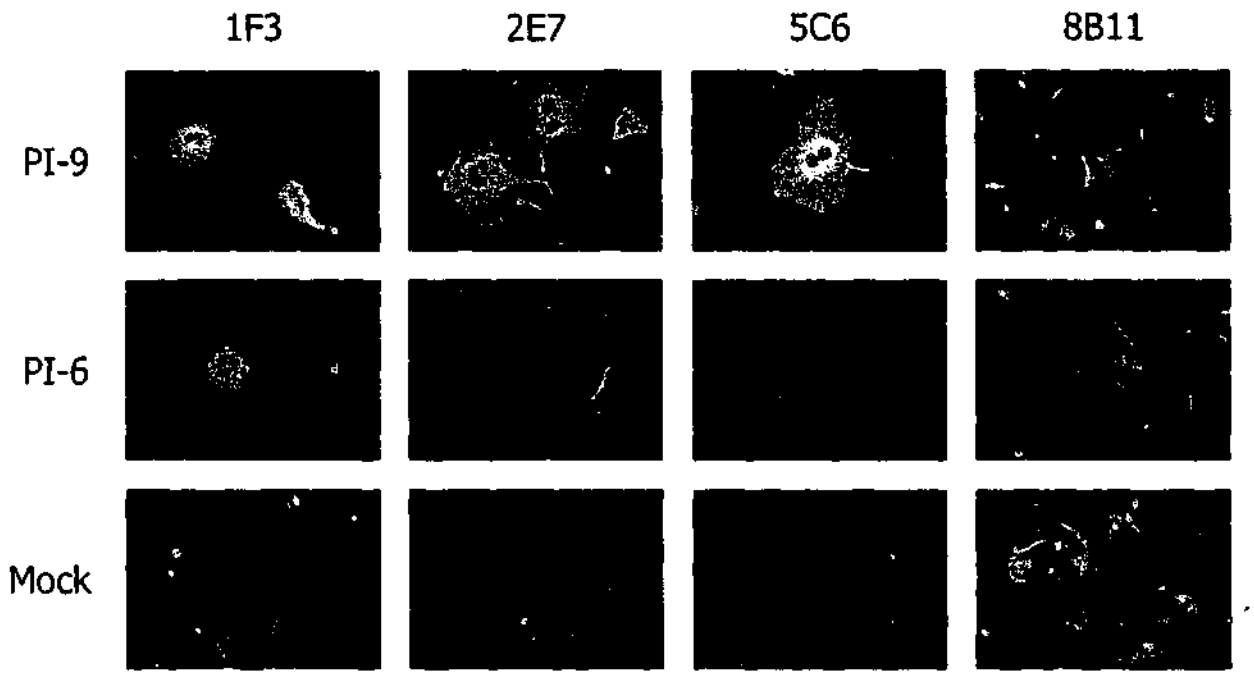

Figure 3.3 The specificity of murine hybridomas to PI-9. COS-1 cells were transiently transfected with PI-9, PI-6 or no cDNA (Mock). 48 h post-transfection cells were seeded onto slides, fixed, permeabilised, and incubated with tissue culture supernatant from the hybridomas 1F3, 2E7, 5C6 or 8B11. Bound antibody was detected with FITC conjugated anti mouse IgG and visualised with fluorescence microscopy.

A

Immunofluorescence

	1F3	2E7	5C6
PI-9	++++	++	+++
PI-8	+++	-	-
PI-6	++++	-	-
SPI-6	++++	-	-
SPI-3	++++	-	-

B

Immunoblotting

	1F3	2E7	5C6
PI-9	++++	-	+++
PI-8	+++	-	+++
PI-6	++++	-	+++
SPI-6	++++	-	-
SPI-3	++++	-	-

C

Fixative	Serpin	7D8	8D3
Formaldehyde/ Triton	PI-9	+++	+++
	PI-6	-	-
Acetone/ Methanol	PI-9	+++	++
	PI-6	-	-
95% Ethanol	PI-9	+++	++
	PI-6	-	-

Table 3.2 Reactivity of murine hybridomas to ov-serpins. (A) COS-1 cells transfected with the indicated ov-serpin cDNAs were seeded onto slides, fixed and permeabilised, and incubated with the indicated hybridoma supernatants. Bound antibody was detected with FITC conjugated anti mouse IgG and visualised with fluorescence microscopy. The intensity of the fluorescence of each hybridoma was then compared. (B) COS-1 cells transfected with indicated ov-serpin cDNAs were lysed in NP-40 lysis buffer and resolved by 12.5% SDS-PAGE. Gels were transferred to nitrocellulose, inmunoblotted with the indicated hybridoma supernatant diluted 1:10 and detected with HRP conjugated anti mouse IgG and enhanced chemiluminescence. The reactivity of each hybridoma was then compared. (C) Effect of fixative on reactivity of murine hybridomas to PI-9. COS-1 cells transfected with PI-9 or PI-6 cDNA were seeded onto slides, fixed and permeabilised using the indicated method, and incubated with the either 7D8 or 8D3 hybridoma supernatant. Bound antibody was detected with FITC conjugated anti mouse IgG and visualised with fluorescence microscopy. The intensity of the fluorescence of each hybridoma was then compared (++++ = very strong, - = negative).

3.2.2 Analysis of monoclonal antibodies to native PI-9 by immunoblotting

Lysates were prepared from COS-1 cells transfected with the panel of ov-serpins described above. These lysates were resolved by 12.5% SDS-PAGE, transferred to membranes and immunoblotted with hybridoma supernatant from 1F3, 2E7 and 5C6 (Table 3.2B). The hybridoma 5C6, although specific for PI-9 by indirect immunofluorescence, was found to cross-react with both PI-6 and PI-8 by immunoblotting. This suggested that the epitope recognised by 5C6 may be destroyed by fixation with formaldehyde by cross-linking residues present in PI-6 and PI-8 but not in PI-9.

The hybridoma 2E7 did not recognise any of the ov-serpins by immunoblotting. Immunoblotting was performed with increasing quantities of rPI-9, but even 6.4 μg was not detected with 2E7 hybridoma culture supernatant or ascites fluid, in comparison to 1F3 and 5C6 which could detect as little 50 ng of rPI-9 (data not shown). This lack of reactivity suggested that 2E7 recognised a conformational epitope found on PI-9 that is lost upon denaturation with SDS.

As previously observed by immunofluorescence, 1F3 was found to cross-react with many of the other serpins tested by immunoblotting. This broad specificity of 1F3 to many of the ov-serpin family mimicked the cross-reactivity seen with Rabbit #11 antiserum, suggesting that 1F3 might also recognise a highly homologous region of serpins. Further analysis of the 1F3 epitope indicated that this antibody recognised the proximal hinge region. The unique properties of 1F3 are described in Chapter 4.

3.2.3 Analysis of monoclonal antibodies to native PI-9 by immunohistochemistry

As the hybridoma 2E7 was the only PI-9 specific monoclonal antibody produced by this fusion, this antibody was tested by immunohistochemistry against a variety of tissues and fixatives. Both formalin fixed paraffin embedded and cryostat prepared samples were tested with 2E7 hybridoma tissue culture supernatant and ascites fluid without success. Also unsuccessful were various methods of antigen retrieval including protease digestion and microwave treatment using low pH buffers. The lack of any 2E7 reactivity to PI-9 by immunohistochemistry indicated that the epitope was sensitive to fixation.

As the ultimate aim of this thesis was to perform tissue distribution studies, 2E7 was unsuitable. An antibody was required that recognised an epitope unaltered by denaturing conditions produced by SDS or the fixatives used in tissue processing such

as formaldehyde. However, 2E7 performs well in settings in which the native conformation of PI-9 is retained, such as immunofluorescence and immunoprecipitation.

3.3 Production and characterisation of monoclonal antibodies to denatured PI-9

During this immunisation, PI-9 was denatured prior to the last two immunisations by resolving rPI-9 by SDS-PAGE before injection into the mouse. The fusion of splenocytes was again performed by V. Sutton and J. Trapani, and resulted in seven hybridomas that were reactive against rPI-9 by ELISA. As antibodies that recognised denatured PI-9 were required, these hybridomas were screened by immunoblotting before further characterisation for specificity to PI-9.

3.3.1 Analysis of monoclonal antibodies to denatured PI-9 by immunoblotting

Only two of the hybridomas tested by immunoblotting demonstrated reactivity to denatured PI-9. These hybridomas, designated 7D8 and 8D3, were isotyped and found to be IgG_1 κ, and were used to immunoblot a panel of ov-serpins to determine their specificity to PI-9. COS-1 cells were transfected with PI-9, PI-8, PI-6, M/NEI, PAI-2, SPI-6 or SPI-3 cDNA. Lysates were prepared, resolved by 12.5% SDS-PAGE, transferred to membranes and immunoblotted with hybridoma culture supernatant from either 7D8 or 8D3 (Figure 3.4). Both of these hybridomas were specific to PI-9, recognising a 42 kDa band only in COS-1 cells transfected with PI-9 cDNA. This indicated that these hybridomas do not cross-react with other ov-serpins, nor do they recognise other cellular proteins found in COS-1 cells.

3.3.2 Analysis of monoclonal antibodies to denatured PI-9 by indirect immunofluorescence

The specificity of the hybridomas 7D8 and 8D3 was confirmed by immunofluorescence of COS-1 cells transfected with the same panel of ov-serpins. Similar to the immunoblotting, neither hybridoma cross-reacted with any of the other ov-serpins or proteins endogenous to COS-1 cells at any dilution (Figure 3.5A and B). As this thesis requires antibodies that would recognise PI-9 by immunohistochemistry, the effect of different fixatives on the recognition of PI-9 by these hybridomas was characterised. The COS-1 cells described above were fixed with formaldehyde and the

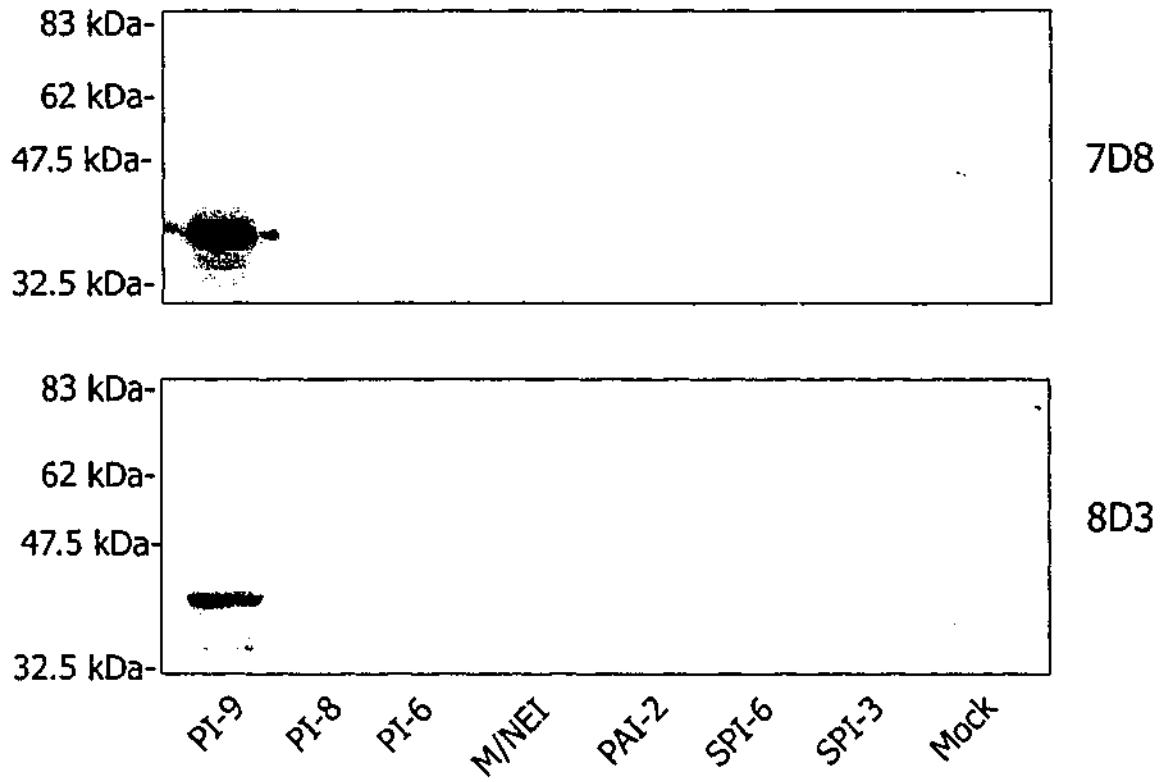

Figure 3.4 Specificity of murine hybridomas to PI-9. COS-1 cells transfected with the indicated cDNAs were lysed in NP-40 lysis buffer and 20 μg of cell lysate was resolved by reducing 12.5% SDS-PAGE. Gels were transferred to nitrocellulose and immunoblotted with either 7D8 or 8D3 hybridoma supernatant diluted 1:10 and detected with HRP conjugated anti mouse IgG and enhanced chemiluminescence.

A

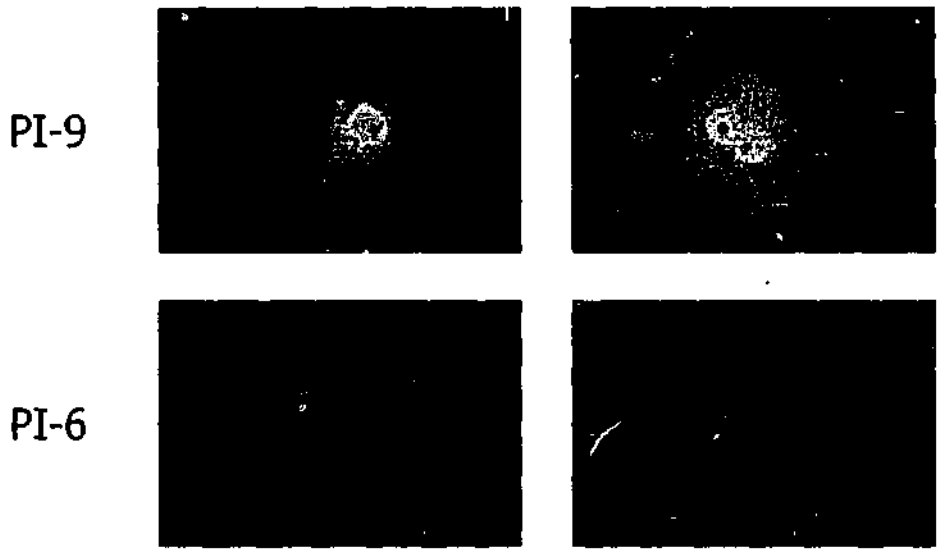

B

	7D8	8D3
PI-9	++++	++++
PI-8	-	-
PI-6	-	-
M/NEI	-	-
PAI-2	-	-
SPI-6	-	-
SPI-3	-	-

Figure 3.5 The specificity of murine hybridomas to PI-9. COS-1 cells transfected with the indicated ov-serpin cDNAs were seeded onto slides, fixed, permeabilised and incubated with either 7D8 or 8D3 hybridoma supernatant. Bound antibody was detected with FITC conjugated anti mouse IgG and visualised with fluorescence microscopy. (A) Photomicrographs of COS-1 cells transfected with either PI-9 or PI-6 cDNA and (B) table of ov-serpins tested against 7D8 and 8D3 indicating the specificity of both murine hybridomas to PI-9.

plasma membrane permeabilised with Triton X-100. This more gentle method of fixation was directly compared to more rigorous methods of fixation; 1:1 acetone:methanol or 95% ethanol. Both 7D8 and 8D3 recognised PI-9 but not PI-6 using all of the fixatives described, although the reactivity of 8D3 to PI-9 was slightly decreased, in comparison to 7D8, by the acetone:methanol and ethanol fixation methods (Table 3.2C).

3.3.3 Analysis of monoclonal antibodies to denatured PI-9 by immunohistochemistry

7D8 and 8D3 were tested by immunohistochemistry using a variety of human tissues and fixatives. Formalin fixed paraffin embedded and cryostat prepared samples of inflamed skin containing infiltrating lymphocytes were tested with 7D8 or 8D3 hybridoma tissue culture supernatant. Regardless of the processing or fixative used, 7D8 and 8D3 stained identical cell types, staining cells within the lymphocytic infiltrate and endothelial cells. However, the signal obtained with 7D8 was consistently stronger than that observed with 8D3, which is consistent with earlier findings that 8D3 is sensitive to some fixatives. In some instances the staining of both 7D8 and 8D3 was quite faint, however this varied between samples of the same tissue and possibly was a result of over-fixation. Various methods of antigen retrieval, including protease digestion and microwave treatment using low pH buffers were found to improve the staining of 7D8, with microwave treatment in 0.1 mM citric acid, pH 6.0 or 0.4 mM glycine, pH 4.0 giving the best results. However 7D8 always out-performed 8D3 by immunohistochemistry regardless of the antigen retrieval method used.

7D8 appeared to be the antibody of choice for the tissue distribution study due to its specificity to PI-9 by immunoblotting, immunofluorescence and immunohistochemistry. As mentioned above, some factors such as over-fixation resulted in poor detection and in these cases Rabbit #15 antiserum could be used to confirm the staining. To ascertain that these antibodies were specific to PI-9 they were tested against a wider range of serpins, including the ov-serpins Hurpin, SCCA-1 and -2, the plasma serpins antithrombin (AT), α_1-antichymotrypsin (α_1-AC) and α_1-antitrypsin (α_1-AT), the viral serpin crmA and the chicken serpin MENT (Figure 3.6). Neither 7D8 nor Rabbit #15 antiserum were found to cross-react with any of the serpins tested (except the previously reported reactivity of Rabbit #15 antiserum to the murine serpins SPI-6 and SPI-3). These two antibodies were used to perform the studies described in Chapters 5 and 6.

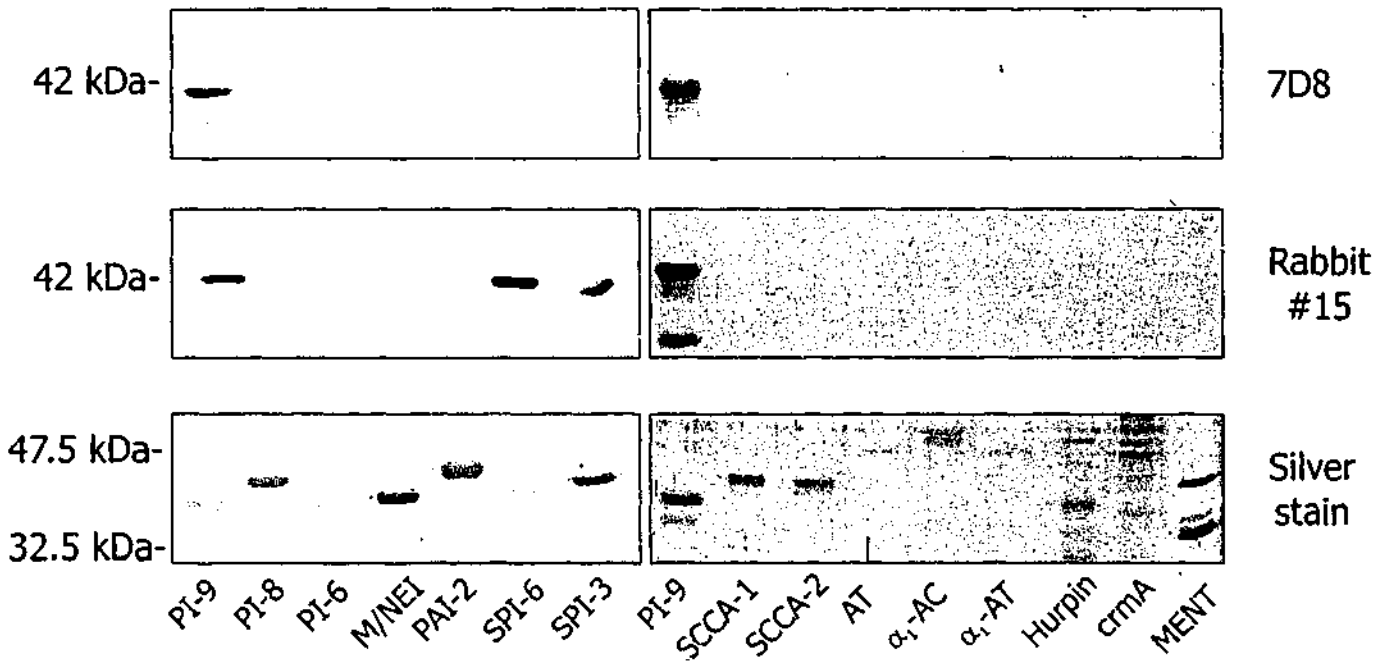

Figure 3.6 The specificity of 7D8 and Rabbit #15 antiserum to PI-9. 100 ng of each serpin was resolved by reducing 12.5% SDS-PAGE, with the exceptions of crmA, Hurpin and MENT for which 500 ng of partially purified recombinant protein was resolved. Duplicate gels were either silver stained to indicate the presence and sizes of the indicated serpins or transferred to nitrocellulose, immunoblotted with 7D8 hybridoma supernatant diluted 1:10 and detected with HRP conjugated anti mouse IgG and enhanced chemiluminescence. The membrane was then stripped and reprobed with Rabbit #15 antiserum diluted 1:2000.

3.4 Recognition of PI-9/granzyme B complex by PI-9 antibodies

It is possible that in some *in vivo* settings that PI-9 is complexed with graB (or other proteinases), as such it is important that the antibodies detect PI-9 in complex as the amount of PI-9 present in a sample may then be underestimated. The interaction of a serpin with its cognate proteinase induces a large conformational change in serpin structure - the S to R transition. This change in structure can radically alter the availability of epitopes, therefore, the reactivity of both monoclonal antibodies and polyclonal antisera to PI-9/graB complexes was examined. Complexes formed by endogenously expressed or recombinant proteins were resolved by SDS-PAGE, transferred to nitrocellulose and immunoblotted with the PI-9' monoclonal antibodies 1F3, 2E7, 7D8 and 8D3 as well as the polyclonal antisera from Rabbit #11, #12 and #15.

The natural killer-like cell line, YT, expresses high levels of endogenous PI-9 and graB. When lysed in NP-40 lysis buffer, the granules are disrupted allowing graB to interact with cytosolic PI-9, and due to the efficiency of the interaction the majority of PI-9 is found in complex with graB. 1F3, 7D8 and 8D3 recognised the complex band of ~63 kDa as well as 42 kDa PI-9 (Figure 3.7A). No bands were detected with 2E7, which is consistent with earlier findings that 2E7 recognises a conformational epitope lost upon SDS denaturation. Immunoblotting with 7D8 and 8D3 indicated that there was very little free PI-9, however a prominent band of 42 kDa was observed with 1F3. This band is most likely free M/NEI, which is also expressed by YT cells.

The polyclonal antisera from Rabbit #11, #12 and #15 detected the prominent complex band (~63 kDa) as well as a 42 kDa band which, as with 1F3, may be M/NEI in addition to low levels of free PI-9. A number of fainter bands were also observed, representing degradation of the complex by free graB and other proteinases found in YT cells (Figure 3.7B).

When PI-9 from transfected COS-1 cells was incubated with recombinant graB a slightly different pattern of bands was observed (Figure 3.8A). 1F3 recognised a number of non-specific bands as well as PI-9 at 42 kDa. Upon the addition of graB, a ~70 kDa complex band was observed, which is higher in molecular weight than the ~63 kDa complex band recognised by 2E7, 7D8 or 8D3. 1F3 recognises the proximal hinge region of PI-9 and therefore can only recognise conformations of PI-9 in which the

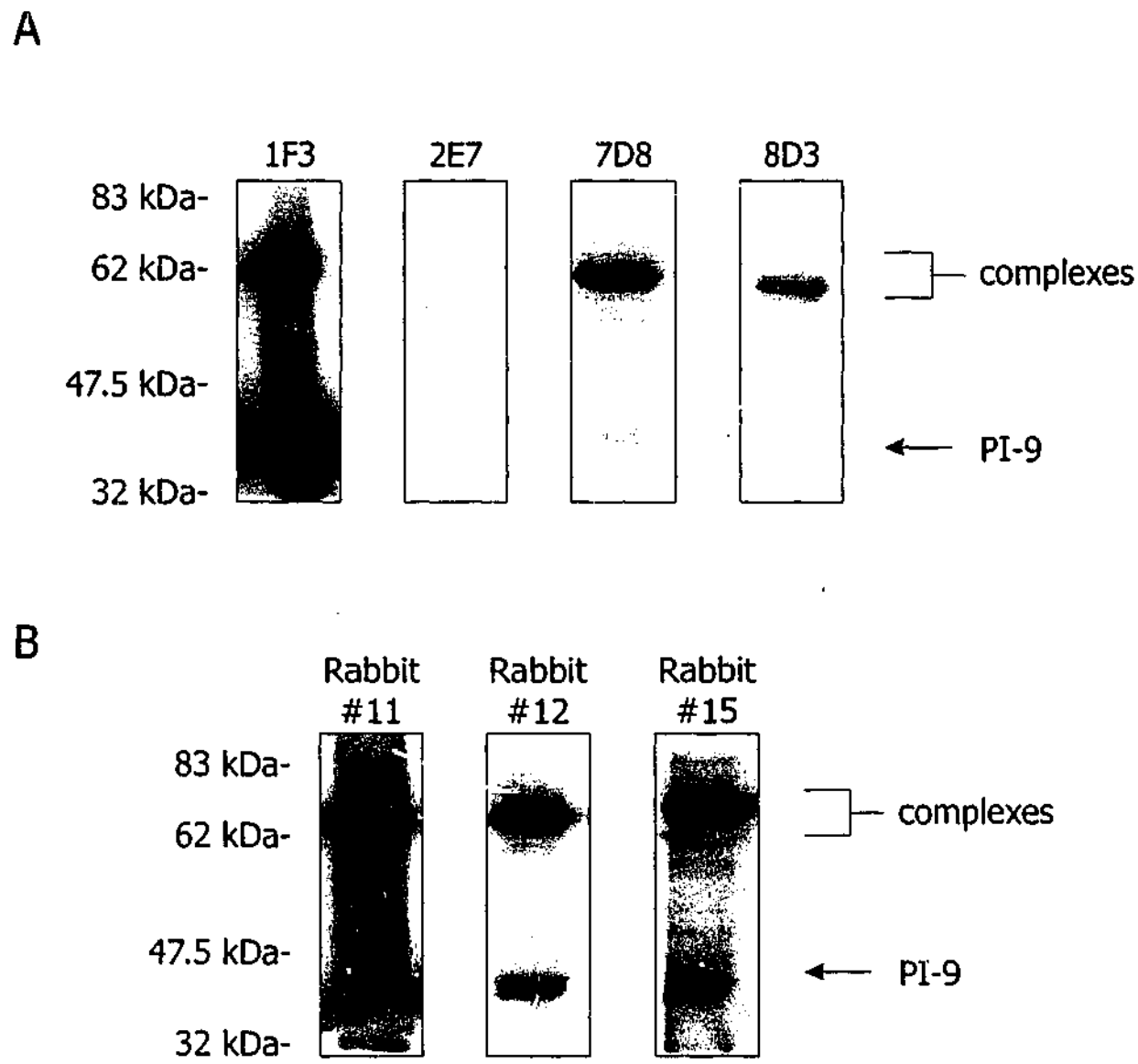

Figure 3.7 Detection of endogenous PI-9 and granzyme B complexes. YT cells were lysed in NP-40 lysis buffer and incubated for 5 min at 37°C. 20 μg of cell lysate was resolved by 12.5% SDS-PAGE. Gels were transferred to nitrocellulose and immunoblotted with either (A) the indicated hybridoma supernatant (1F3 diluted 1:100, 2E7 1:5, 7D8 1:10 and 8D3 1:10) or (B) the indicated rabbit polyclonal antiserum diluted 1:2000 and detected with HRP conjugated anti mouse or rabbit IgG and enhanced chemiluminescence. Arrows indicate the size of free PI-9 and that in complex with graB.

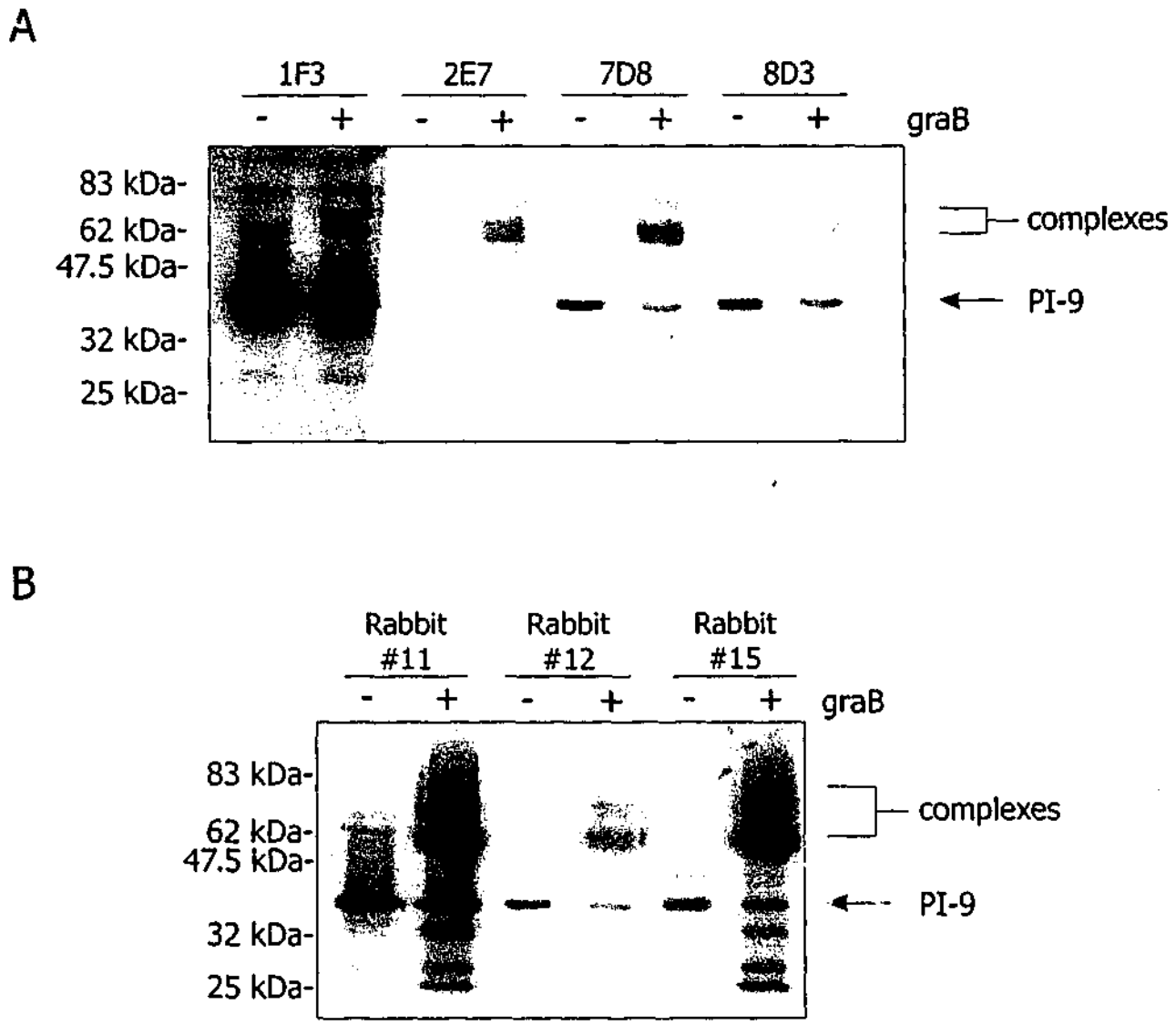

Figure 3.8 Detection of PI-9/granzyme B complexes. COS-1 cells transfected with PI-9 cDNA were lysed in NP-40 lysis buffer. 20 μg of cell lysate was incubated with (+) or without (-) 25 ng of recombinant graB for 10 min at 37°C and resolved by 12.5% SDS-PAGE. Gels were transferred to nitrocellulose, immunoblotted with either (A) the indicated hybridoma supernatant (1F3 diluted 1:100, 2E7 1:5, 7D8 and 8D3 1:10) or (B) the indicated rabbit polyclonal antiserum (diluted 1:2000) and detected with HRP conjugated anti mouse or rabbit IgG and enhanced chemiluminescence. Arrows indicate the size of free PI-9 and that in complex with graB.

hinge region is exposed (described further in Chapter 4). As 1F3 only recognised the higher molecular weight species of the complex, this suggests that the hinge region is available in this larger species of complex but is hidden within the body of the serpin in the ~63 kDa form.

2E7 was able to detect the ~63 kDa complex of rPI-9 and graB, suggesting that its epitope may be stabilised upon complex formation. However, no band was observed in the endogenous complex from YT lysate, possibly due to cleavage of this complex by other proteinases or free graB. Comparison of the PI-9 species detected with 7D8 and 8D3 indicated that, although both hybridomas detected PI-9, 8D3 did not recognise the complex as efficiently as 7D8, suggesting that the epitope recognised by 8D3 is destabilised upon complex formation. The polyclonal antisera demonstrated different affinities for the various complex bands as well as free PI-9 (Figure 3.8B). Although all antisera detected PI-9 and the complex with graB, both Rabbit #11 and #15 antisera recognised the complex with higher affinity than Rabbit #12 antiserum. This preferential recognition of the complex by Rabbit #11 and #15 antisera suggests that novel epitopes are revealed upon complex formation.

3.5 Characterisation of antibodies by flow cytometry

It has previously been shown that PI-9 mRNA is present in IL-2 stimulated peripheral blood leukocytes as well as lymphoid (T, B and NK-like) cell lines, but is absent from myeloid cells (Sun *et al.*, 1996). One way to confirm and extend these observations is to perform intracellular flow cytometry of peripheral blood leukocytes. Therefore the PI-9 monoclonal antibodies were tested for suitability in this technique. Intracellular flow cytometry differs from standard flow cytometry as the cells are fixed then permeabilised prior to incubation with the antibody. This maintains cell integrity, allows the antibody entry into the cell and retains the intracellular antigen within the cell. Therefore the first criterion for the detecting antibody is that it recognises PI-9 after treatment with fixatives.

Several different fixation and permeabilisation reagents were evaluated, including three commercially available reagents: FACS Lysing/FACS Permeabilizing solution (Becton Dickinson), IntraPrep Permeabilisation Reagent (Beckman Coulter) and Cytofix/Cytoperm (BD Pharmigen). Although the exact conponents for these reagents is not specified, the fixation reagents contain formaldehyde while the permeabilisation reagents contain saponin or other detergents to allow the antibody entry into the cell. Non-commercial methods were also tested, which involved fixation

in 4% formaldehyde followed by permeabilisation in either 0.1% saponin or 0.1% Triton X-100. The combination of reagents found to give the most consistent results using 7D8 or 2E7 as standard antibodies was fixation in 4% formaldehyde followed by permeabilisation in freshly diluted FACS Permeabilizing solution (Becton Dickinson).

The performance of the four PI-9 monoclonal antibodies in intracellular flow cytometry was compared between PI-9 positive and negative cell lines. RNA analysis has previously demonstrated that the NK-like cell line, YT, contains high levels of PI-9 transcripts which are undetectable in the myeloid cell line, HL-60 (Sun *et al.*, 1996). 1F3, 2E7, 7D8 and 8D3 all gave approximately equal signals in the PI-9 expressing cell line, YT (Figure 3.9A). However, in the PI-9 negative cell line HL-60, 1F3 was positive, probably due to expression of M/NEI (C. Bird, personal communication). 2E7, 7D8 and 8D3 were all negative against the HL-60 cells, indicating they do not cross-react with M/NEI or other intracellular proteins in this context (Figure 3.9B).

The results of the intracellular flow cytometry were compared to immunoblotting of lysates prepared from HL-60 and YT cells (Figure 3.9C). 1F3 recognised material in both cell lines, consistent with the flow cytometry. In the YT cells, 1F3 recognised PI-9 as a monomer (42 kDa), in complex with graB (~63 kDa) and in the complex breakdown product (~35 kDa). In HL-60 cells, however, 1F3 recognised proteins at 42 and 63 kDa, consistent with 1F3 recognising an ov-serpin expressed in these cells that can form an SDS-stable complex with a proteinase also expressed in these cells. As expected 2E7 did not recognise any proteins by immunoblotting. 7D8 and 8D3 specifically recognised PI-9 and complex in the YT cells and did not recognise any other proteins in either the YT or HL-60 cell lysates.

Although PI-9 is highly expressed by YT cells, the signal observed by intracellular flow cytometry signal was low. When cells stained for PI-9 by the flow cytometry method were attached to poly-L-lysine coated slides and microscopically compared to cells stained on slides by standard indirect immunofluorescence, the amount of fluorescence was visibly less following the flow cytometry method. This indicates that either a portion of the PI-9 is lost during fixation and permeabilisation of the cells, or that the antibody is retarded in its entry into the cell and therefore only a proportion of the PI-9 is labelled.

Examination of the literature reveals that although intracellular flow cytometry is a common technique, it has not been performed on a truly cytosolic protein. Many studies have been performed on the intracellular expression of cytokines, however these proteins are located in the secretory pathway. This protocol requires incubation with

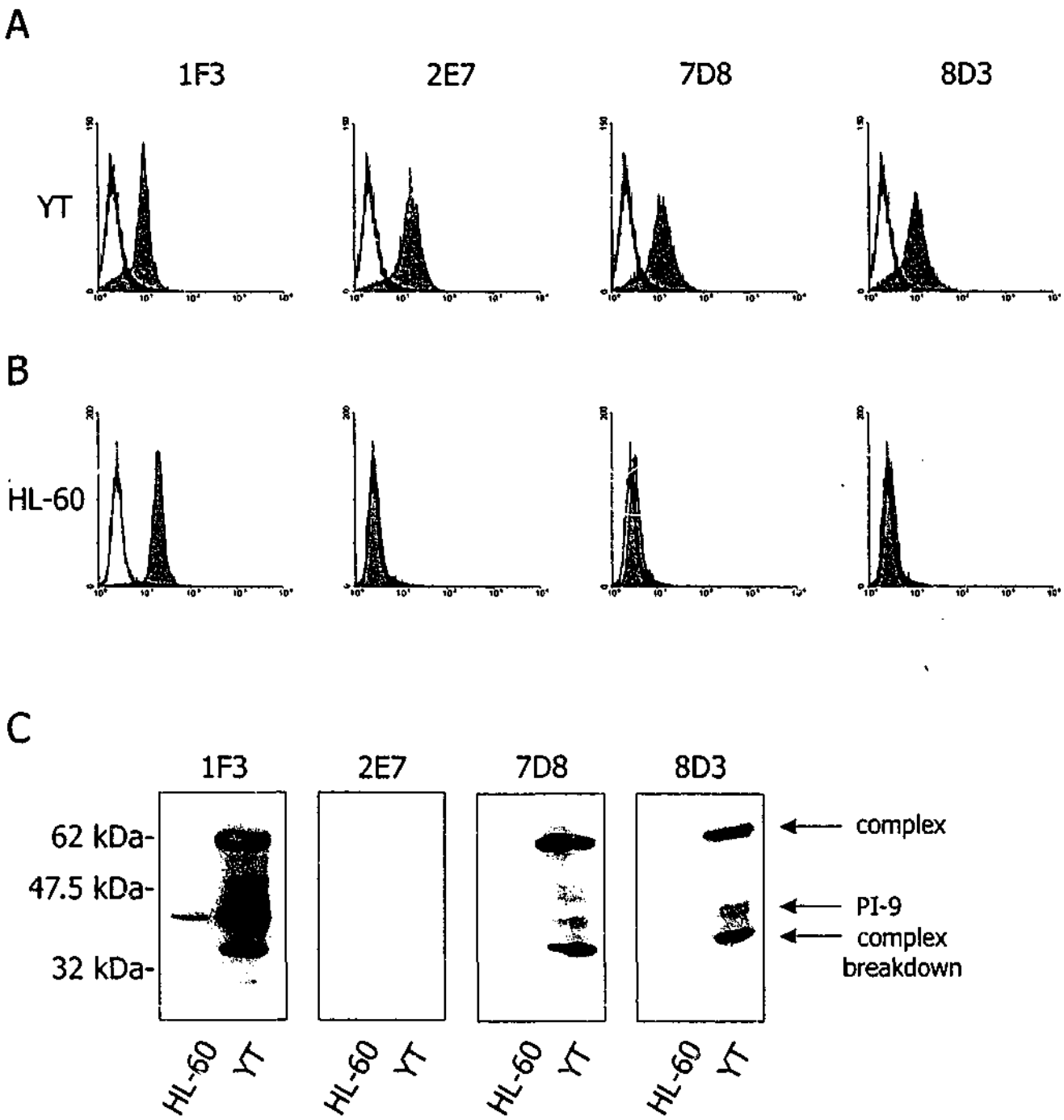

Figure 3.9 Comparison of murine hybridoma supernatants by flow cytometry and immunoblotting Flow cytometric analysis of PI-9 in (A) the PI-9 expressing YT cells and (B) the PI-9 negative HL-60 cells. 0.5 x 10^6 cells were incubated with the indicated hybridoma supernatant or isotype control and detected with anti mouse IgG conjugated to FITC. Samples were run on a FACScalibur and analysed with Cell Quest. PI-9 hybridomas (filled histogram) compared with the isotype control (open histogram). (C) Detection of PI-9 in YT and HL-60 cells. Cells were lysed in NP-40 lysis buffer and 0.5 x 10^6 cells, loaded in quadruplicate and resolved by reducing 12.5% SDS-PAGE and immunoblotted with the indicated hybridoma supernatant (1F3 diluted 1:50, 2E7 diluted 1:2, 7D8 and 8D3 diluted 1:10) and detected with HRP conjugated anti mouse IgG and enhanced chemiluminescence. The positions of free PI-9 (42 kDa), PI-9 in complex with graB (~63 kDa) and complex breakdown (~35 kDa) are indicated on the right.

brefeldin A prior to performing the staining, to retain the cytokines in the Golgi apparatus or endoplasmic reticulum (ER). Studies have also been performed on intracellular graB (Wever *et al.*, 1998), however graB is located within granules and therefore is also not cytosolic. When cells are fixed, cytokines and graB will be cross-linked to the membranes of the ER, Golgi apparatus or granule, respectively. However, PI-9 may be inefficiently cross-linked to cellular structures and lost during the washing procedures.

3.6 Discussion

The antibody characterisation performed in this chapter has identified antibodies that can be used in many techniques to further our knowledge of the biology of PI-9. The specificity displayed by 7D8 in combination with the more robust nature of the Rabbit #15 antiserum will allow immunohistochemical surveys of tissue to be performed to study the cell specific expression of PI-9 (as described in Chapter 5). Furthermore, these antibodies perform well by immunohistochemistry, immunofluorescence and immunoblotting, thereby allowing the examination of PI-9 in cells *in vivo* and *in vitro*. This will permit the study of PI-9 regulation in specific cell types, while antibodies that preferentially recognise complex allow further analysis of the interaction between PI-9 and graB (as described in Chapter 6).

The specificity displayed by 7D8 ensures that the PI-9 analysis will be accurate. The importance of using specific antibodies to characterise the tissue distribution of ov-serpins is illustrated by a recent report on the tissue distribution of SCCA-1 and SCCA-2 (Cataltepe *et al.*, 2000). The squamous cell carcinoma (SCC) antigens were originally identified in patients with SCC (Kato and Torigoe, 1977), with elevated serum levels of SCCA correlating with the severity of the disease (Kato *et al.*, 1979). Subsequently two SCCAs were identified that were 91% identical at the amino acid level (Schneider *et al.*, 1995). Recently it has been demonstrated that these proteins have a much wider tissue distribution than previously reported and also that previous studies used antibodies that do not discriminate between these highly homologous proteins. As such, the correlation between the expression of the SCCAs with cancer is no longer valid (Cataltepe *et al.*, 2000).

Most of the antibodies produced in this study were found to be cross-reactive with other serpins. This illustrates the importance of carefully characterising the specificity of antibodies when analysing serpin distribution by immunohistochemistry. Although these cross-reactive antibodies were not useful for tissue distribution studies

of PI-9, two of the cross-reactive antibodies, 1F3 and Rabbit #11 antiserum, can be used to analyse serpins for which specific antibodies are not yet available. For example, these antibodies can be used for indirect immunofluorescence of transfected cells or analysis of recombinant proteins by immunoblotting.

Chapter 4

Characterisation of an Antibody to the Proximal Hinge Region of Serpins

Summary

In the preceding chapter the murine monoclonal antibody designated 1F3 was found to recognise many serpins, although it was raised against the ov-serpin PI-9. This chapter describes the mapping of the 1F3 epitope to the highly conserved amino acids within the proximal hinge region, specifically within the residues EVNEEGT. Molecular modelling of serpin structure indicates that this epitope is partially buried within a β-turn between strand 5A and the reactive centre loop (RCL). This proximal hinge region is vital to the conformational changes essential to serpin function, and therefore exists in several conformations. As such the ability of 1F3 to differentiate between conformations of serpins was investigated using Antithrombin (AT) as a model. Analysis of AT by both ELISA and native PAGE indicates that 1F3 will only recognise partially unfolded, monomeric AT and does not recognise AT in complex with thrombin, AT binary complex with the loop peptide of α_1-antitrypsin, AT cleaved in the RCL or AT polymers. Furthermore, when AT is polymerised by incubation at 55°C for 4 h, the presence of 1F3 almost completely prevents polymerisation. This antibody therefore provides further evidence for the structures involved in polymerisation, as well as identifying an important mechanism for inhibiting polymerisation.

Introduction

Serpin inhibitory function is mediated through an exposed reactive centre loop (RCL) which acts as a pseudosubstrate for the cognate serine proteinase. Cleavage of the RCL by the proteinase at the P_1-P_1' scissile bond is followed by insertion of the residues N-terminal to the cleavage point into β-sheet A and translocation of the proteinase to the opposite pole of the serpin (Huntington *et al.*, 2000). This results in distortion of the catalytic triad of the proteinase, preventing deacylation and thereby trapping both proteins in an SDS resistant complex.

The RCL is situated between two hinge regions (proximal and distal), which allow the flexibility and mobility necessary for the large conformational change required for inhibitory activity. Serpins exist in a thermodynamically unfavourable, metastable fold, described as the stressed (S) state. The cleavage of the RCL and concomitant insertion of the loop results in a large conformational change in serpin structure to the more energetically preferred relaxed (R) state (reviewed in Whisstock *et al.*, 1998).

This flexibility of the serpin fold can also lead to serpin polymerisation of which there are currently two proposed mechanisms. The loop A-sheet mechanism involves the insertion of the RCL of one serpin molecule into the β-sheet A of another (Mast *et al.*, 1992). Alternatively the RCL of one serpin can insert into the vacant strand 1C position of another by the loop C-sheet mechanism (Carrell *et al.*, 1994). A number of naturally occurring serpin mutants spontaneously undergo polymerisation, which is the underlying cause of diseases such as emphysema, liver cirrhosis, angio-oedema and thrombosis (reviewed in Carrell and Lomas, 1997) and early onset dementia (Davis *et al.*, 1999). The crystallisation of polymers of α_1-AT has advanced our knowledge of the structure of serpin polymers and indicates that they form via loop A-sheet mechanism (Huntington *et al.*, 1999; Dunstone *et al.*, 2000). The mechanism by which polymers form is still not well understood, but is thought to involve opening of β-sheet A prior to the insertion of the polymerogenic RCL (Fitton *et al.*, 1997; James *et al.*, 1999).

4.1 1F3, a monoclonal antibody recognising the proximal hinge of serpins

Routine screening of hybridomas for antibodies specific to PI-9 identified an antibody that recognised not only PI-9 but also the closely related ov-serpins PI-6 and PI-8. This hybridoma, designated 1F3, was further characterised by immunoblotting

against a variety of serpins, and was found to recognise most of the ov-serpins, as well as other members of the serpin superfamily (Figure 4.1). 1F3 recognised these proteins by immunoblotting following denaturing and reducing conditions, suggesting that the epitope is linear. Further characterisation of 1F3 demonstrated that, when compared to other monoclonal antibodies raised to PI-9, it could only immunoprecipitate a fraction of the PI-9 (data not shown). This indicates that although the 1F3 epitope is probably linear, there is some conformational impediment that can block the binding of 1F3 to native serpin.

Sequence alignment of PI-9 with other 1F3 reactive serpins indicated that there were many areas of identity that could contain the 1F3 epitope. However, while using 1F3 to examine PI-9 transfected cells by immunofluorescence, it was observed that 1F3 did not recognise the P_{14} threonine to arginine proximal hinge mutant of PI-9. This was confirmed by indirect immunofluorescence of transfected COS-1 cells and immunoblotting of purified recombinant proteins (Figure 4.2A and B). Other mutations within the RCL, did not affect the binding of 1F3 (Figure 4.2B).

To identify residues that may constitute the 1F3 epitope the proximal hinge region of PI-9 was aligned to the hinge region of the other serpins examined (Table 4.1). As the proximal hinge represents a structurally conserved region of serpins there is a high level of homology in this region. However, when these serpins were divided into 1F3 reactive and non-reactive proteins, as assessed by immunoblotting, the 1F3 reactive serpins demonstrated a very high level of homology to PI-9. The region spanning residues P_{21}-P_9 of PI-9 (VEVNEEGTEAAAA) was found to be highly conserved in the serpins that were 1F3 reactive. Those serpins with lower affinity for 1F3 contained many of these residues, while serpins that were unable to bind 1F3 were most divergent from PI-9 at residues at the N-terminus of this region. This suggests that residues critical for the 1F3 epitope may be contained within the N-terminal portion of the proximal hinge.

4.2 The 1F3 epitope is confined to the sequence EVNEEGT of the proximal hinge region

To further refine the epitope of 1F3, epitope mapping was initially performed by analysis of three overlapping peptides corresponding to the proximal hinge and RCL of PI-9. Two proximal hinge peptides and a single RCL peptide (outlined in Figure 4.3A) were used in an ELISA based peptide-blocking study. Only the P_{21}-P_{10} peptide (VEVNEEGTEAAA) was found to block 1F3 binding to PI-9 (Figure 4.3B). 1F3

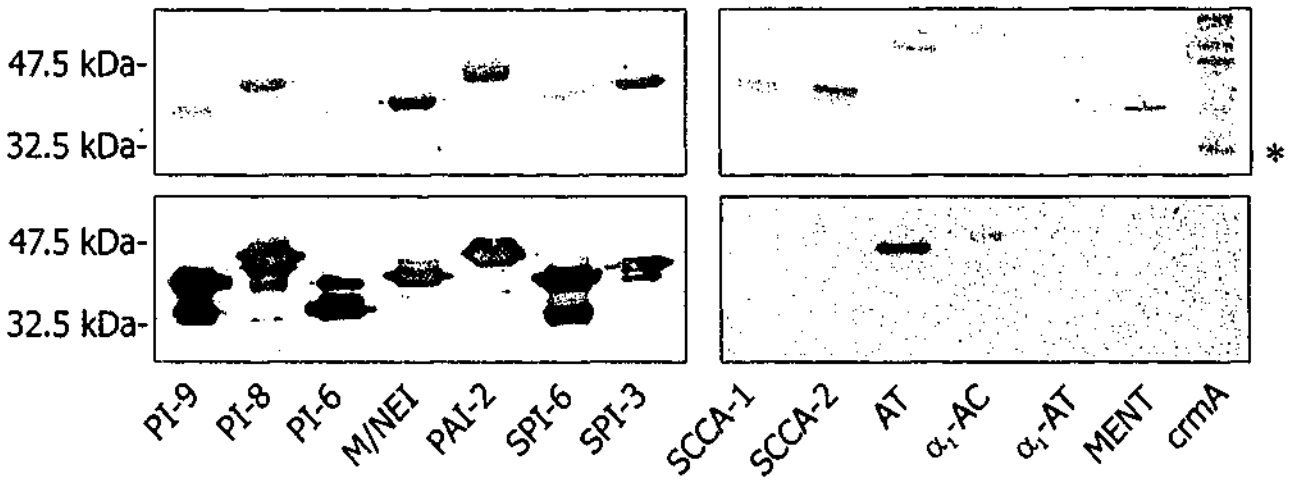

Figure 4.1 Pan-serpin reactivity of 1F3. 100 ng of each serpin was resolved by reducing 12.5% SDS-PAGE, with the exception of crmA in which 500 ng of partially purified crmA extract from *P. pastoris* was resolved (* indicates the position of crmA). Duplicate gels were either silver-stained to demonstrate the presence and size of the indicated serpins (upper panels) or transferred to nitrocellulose and immunoblotted with a 1:100 dilution of 1F3 hybridoma supernatant and detected with HRP conjugated anti mouse IgG and enhanced chemiluminescence (lower panels).

A

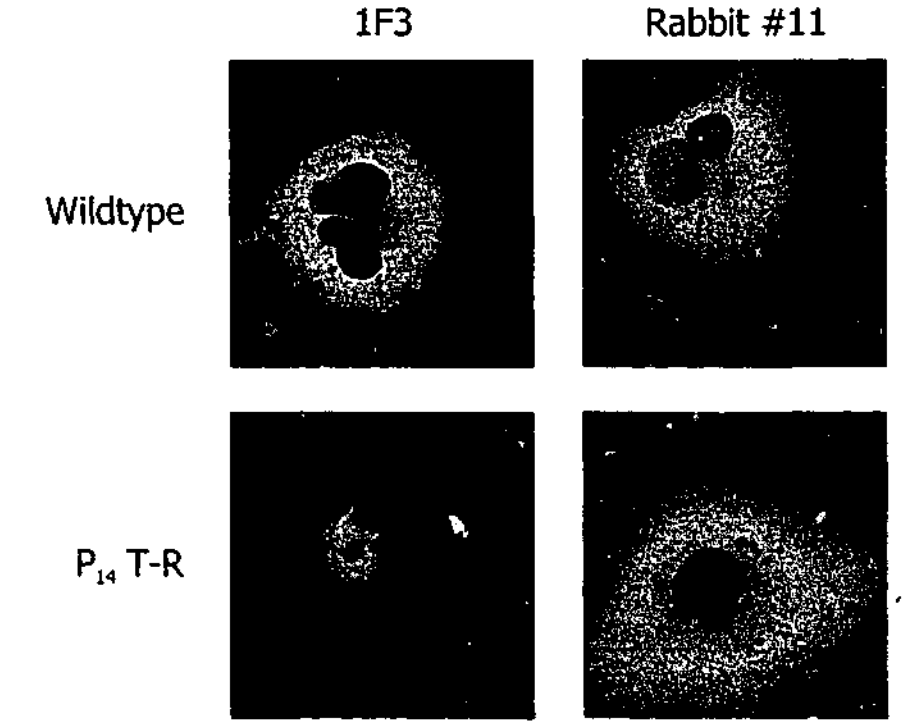

B

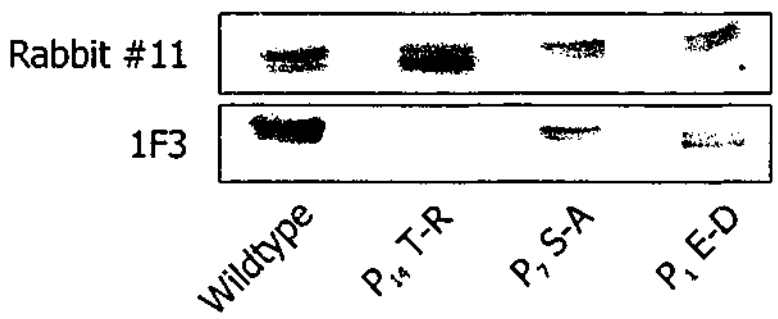

Figure 4.2 Binding of 1F3 to wild type PI-9 and P1-9 mutants. (A) COS-1 cells transiently transfected with either wildtype PI-9 or PI-$9_{PI\ 4T\text{-}R}$ cDNA were seeded onto slides, fixed, permeabilised and incubated with either Rabbit #11 polyclonal antiserum (diluted 1:2000) or 1F3 hybridoma supernatant (diluted 1:20). Bound antibody was detected with FITC conjugated anti mouse or rabbit IgG and visualised with fluorescence microscopy. (B) 50 ng of the indicated PI-9 mutants were resolved by reducing 12.5% SDS-PAGE. Gels were transferred to nitrocellulose and immunoblotted with either Rabbit #11 polyclonal antiserum (diluted 1:2000) or 1F3 hybridoma supernatant (diluted 1:50) and detected with HRP conjugated anti rabbit or mouse IgG and enhanced chemiluminescence.

Serpin	Proximal Hinge Residues	1F3 Reactivity
PI-9	KSFVEVNEEGTEAAAAS	+++
PI-8	KCFVEVNEEGTEAAAAT	+++
PI-6	KSFVEVNEEGTEAAAAT	+++
M/NEI	KSFVEVNEEGTEAAAAT	+++
SPI-6	QSVVEINEEGTEAAAAS	+++
SPI-3	KAFVEVNEEGTEAAAAT	+++
Antithrombin	KAFLEVNEEGSEAAAST	++
Bomapin	SSFVAVTEEGTEAAAAT	+
PAI-2	QAMVDVNEEGTEAAAGT	+
α_1-AC	KAVLDVFEEGTEASAAT	+
SCCA-2	KAFVEVTEEGVEAAAAT	+/-
SCCA-1	KAFVEVTEEGAEAAAAT	-
α_1-AT	KAVLTIDEKGTEAAGAM	-
crmA	KTYIDVNEEYTEAAAPT	-
MENT	QSFVAVDEKGTEAAAAT	-
Hurpin	KAFVEINEQGTEAAAGS	-

Table 4.1 The pan-serpin reactivity of 1F3. The reactivity of 1F3 was tested against the indicated serpin by immunoblotting (as illustrated in Fig 4.1). Semiquantitative binding of 1F3 to each serpin was assessed by comparison to PI-9. The proximal hinge region of each serpin is indicated. Residues identical to PI-9 are red, while non-identical residues are blue. Residues constituting the putative 1F3 epitope are underlined. (+++ = strong reactivity; +/- = very weak reactivity; - = no reactivity).

A

Peptide	PI-9 hinge and RCL residues	Sequence	1F3 blocking
1	P_{19}-P_{12}	VNEEGTEA	-
2	P_{15}-P_2	GTEAAAASSCFVVA	-
3	P_{21}-P_{10}	VEVNEEGTEAAA	+

B

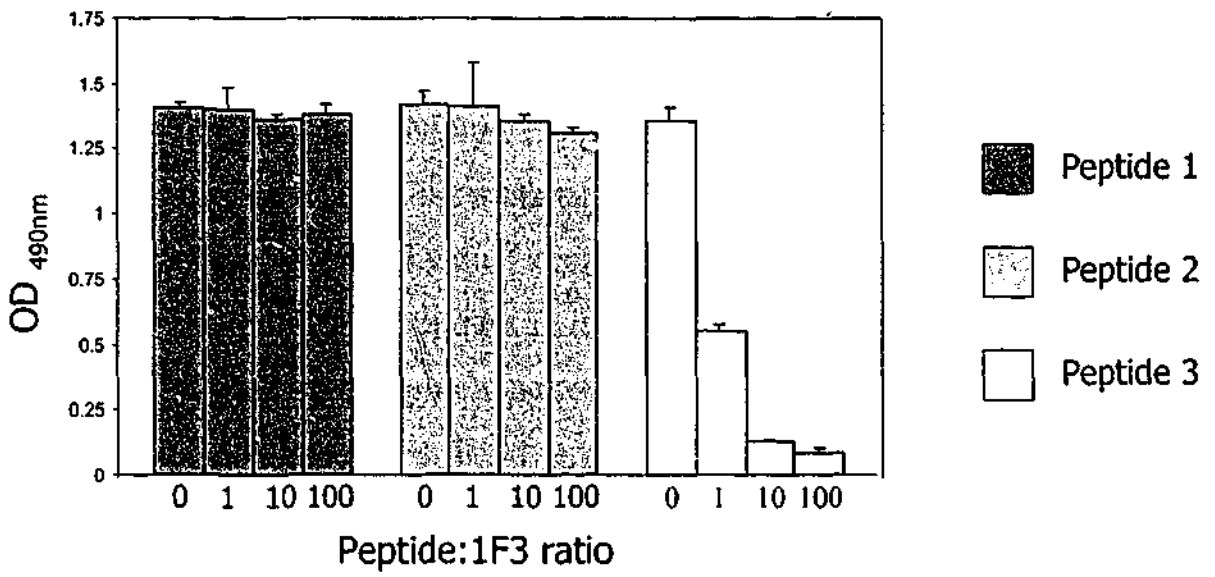

Figure 4.3 1F3 peptide blocking ELISA. (A) Sequence of peptides corresponding to the proximal hinge and RCL of PI-9. (B) 1F3 was pre-incubated with either no peptide (0), equimolar (1), 10-fold (10) or 100-fold (100) molar excess of peptide before incubation with rPI-9 coated microtiter plates. Bound 1F3 was detected with HRP conjugated anti mouse IgG and the ELISA carried out as described in 2.13.1.3. The values plotted are the means of triplicate points plus standard deviation.

binding was not blocked by the smaller P_{19}-P_{12} hinge peptide (VNEEGTEA), which only differs from the longer blocking peptide by two residues at either terminus. This indicates that either the N- or C-terminus of the longer blocking peptide is critical for antibody interaction.

The 1F3 epitope was further defined by site directed mutagenesis of the hinge regions of both PI-9 and α_1-antitrypsin (α_1-AT). α_1-AT is not recognised by 1F3 and its proximal hinge contains many residues that differ from those found in PI-9. As such, mutation of the α_1-AT hinge region to resemble that of PI-9 could result in gain of 1F3 reactivity and conversely, mutation of residues in the PI-9 hinge to those found in α_1-AT could result in loss of 1F3 reactivity.

The hinge region of α_1-AT was mutated at five residues to those amino acids found in PI-9 (outlined in Figure 4.4A). The α_1-AT_{mut} was expressed in BL21 (DE3) *E.coli* and the binding of 1F3 compared to that of wildtype α_1-AT and PI-9 by immunoblotting. These mutations resulted in 1F3 binding to α_1-AT_{mut} (Figure 4.4B), indicating that some or all of the mutated residues are critical for 1F3 reactivity.

To identify which individual amino acids were required for 1F3 reactivity, single amino acid substitutions of residues in the PI-9 hinge were performed. Four mutants of PI-9 were produced, two in which the residues of the hinge region of PI-9 were mutated to the corresponding residues found in α_1-AT (P_{18} asparagine to aspartic acid and P_{16} glutamic acid to lysine) and the deletion of either a single or double alanine residue at the C-terminus of the hinge region (outlined in Figure 4.4A). These mutants were transiently transfected into COS-1 cells and their effect on 1F3 binding was assessed by indirect immunofluorescence and immunoblotting. Mutation of PI-9 at the P_{16} residue (glutamic acid to lysine) resulted in decreased immunofluorescence with 1F3 when compared to wildtype PI-9. However, neither mutation of the P_{18} residue (asparagine to aspartic acid) nor the alanine deletions (P_9 and P_{10}-P_9) appreciably altered the degree of 1F3 immunofluorescence (data not shown).

To quantify the effect of these mutations on 1F3 binding, an ELISA was performed in which the level of 1F3 reactivity was compared to that of other PI-9 monoclonal antibodies. As the epitopes recognised by the three other antibodies are not known, 1F3 was compared to each of the three antibodies to determine a consensus ratio of 1F3 binding relative to wildtype PI-9. This ELISA corroborated the immunofluorescence data, indicating an approximately 50% loss of 1F3 binding to PI-9 mutated at P_{16} from glutamic acid to lysine (Figure 4.4C). The ELISA also

Figure 4.4 Site directed mutagenesis of the proximal hinge regions of α_1-AT and PI-9. (A) Site-directed mutagenesis strategy for the hinge region of α_1-AT and PI-9. The residues of PI-9 thought to contain the 1F3 epitope are indicated in green, the corresponding residues of α_1-AT are indicated in purple. Residues within the α_1-AT hinge were mutated to those found in PI-9, while the PI-9 hinge residues were mutated to those found in α_1-AT. (B) Mutation of the hinge of α_1-AT results in gain of 1F3 reactivity. Wildtype and mutant α_1-AT were expressed in BL21 (DE3) *E.coli* (non-glycosylated recombinant α_1-AT = 44 kDa), cells were lysed in Laemmli sample buffer and resolved by reducing 12.5% SDS-PAGE. Duplicate gels were either transferred to nitrocellulose and sequentially immunoblotted with 1F3 hybridoma supernatant diluted 1:50 (upper panel) then rabbit polyclonal anti α_1-AT antiserum diluted 1:500 (middle panel) and detected with HRP conjugated anti mouse or rabbit IgG and enhanced chemiluminescence; or stained with Coomassie Blue (lower panel). Arrow heads indicate the position of mutant α_1-AT. Recombinant PI-9 (rPI-9) and purified α_1-AT (pα_1-AT, glycosylated plasma α_1-AT = 55 kDa) were used as controls for the cross-reactivity of 1F3. 100 ng of each protein was resolved on the gel for immunoblotting and 500 ng for the Coomassie Blue stain. (C) Mutation of PI-9 hinge residues alters 1F3 reactivity. COS-1 cells were transiently transfected with pCMVneo/PI-9, pCMVneo/PI-9_{P16E-K} pCMVneo/PI-9_{P18N-D}, pCMVneo/PI-$9_{P9A\Delta}$ or pCMVneo/PI-$9_{P9-P10A\Delta}$. Following the transfection, cells were lysed in hypotonic lysis buffer, coated to microtiter plates and detected with 1F3, 2E7, 7D8 or 8D3 hybridoma supernatant diluted 1:10 in 1% (w/v) BSA/PBS and detected as described in 2.13.1.2. The values plotted are the ratio of 1F3 binding relative to 2E7, 7D8 or 8D3 respectively, relative to the binding to wildtype PI-9. The mean plus standard deviation of quadruplicate samples is shown.

A

Mutation	Hinge sequence
α_1-AT	LTIDEKGTEAAGAMF
α_1-AT$_{mut}$	LTINEEGTEAAAAT-
PI-9	VEVNEEGTEAAAASS
PI-9$_{P18\ N\text{-}D}$	VEVDEEGTEAAAASS
PI-9$_{P16\ E\text{-}K}$	VEVNEKGTEAAAASS
PI-9$_{P10\ A\ \Delta}$	VEVNEEGTEAAA-SS
PI-9$_{P9\text{-}P10\ A\ \Delta}$	VEVNEEGTEAA--SS

B

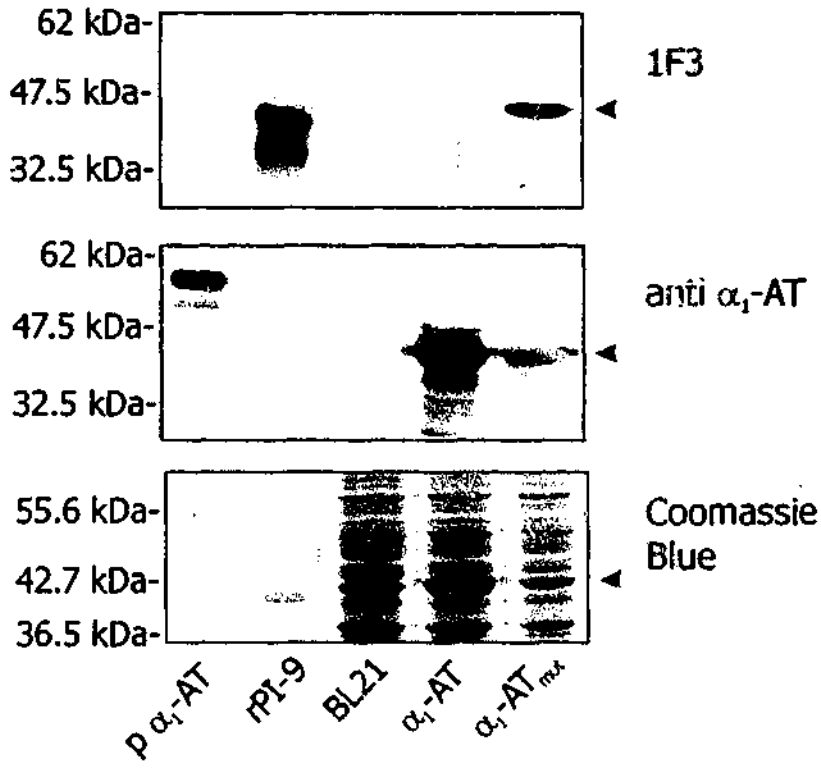

C

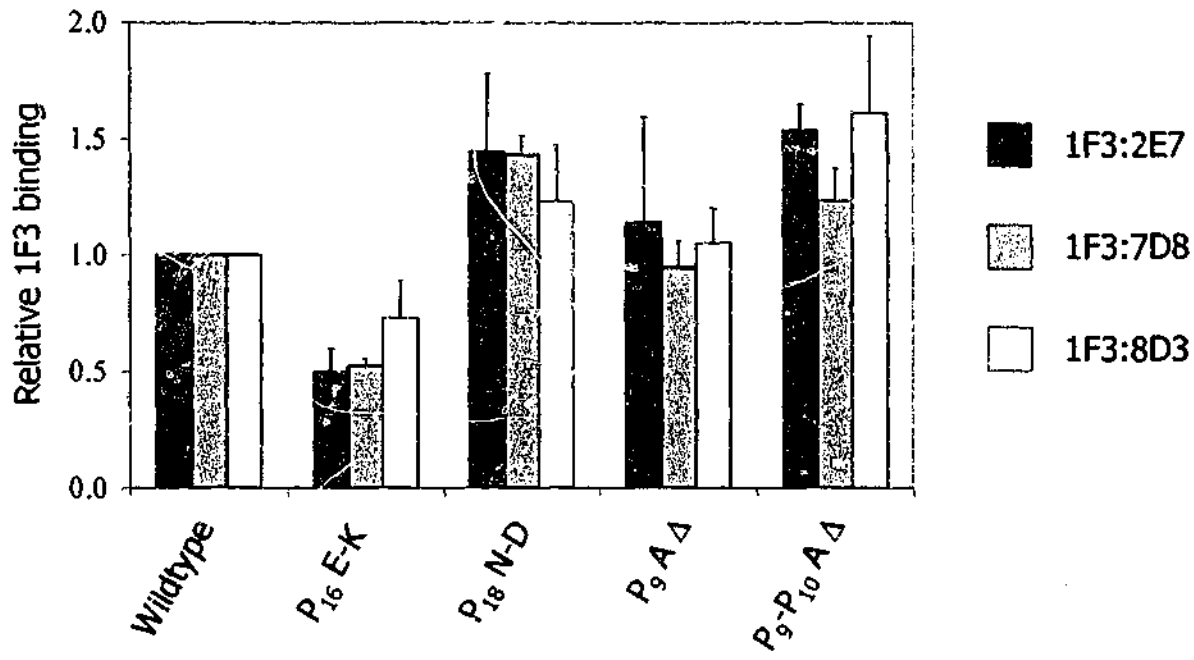

demonstrated that the other mutations did not result in a loss of 1F3 binding, in agreement with the immunofluorescence, indicating that the P_{18} asparagine and the two alanines are not critical to the epitope.

In summary, the 1F3 epitope is contained within the highly conserved proximal hinge region. In determining the minimal epitope necessary for 1F3 reactivity the following results must be considered:

i) the P_{14} threonine to arginine mutation (VEVNEEGREAAA) of PI-9 completely abolished 1F3 binding. Therefore the epitope must contain this residue;

ii) in 1F3 reactive and non-reactive serpins, the greatest divergence was found in the N-terminal part of the hinge region (VEVNEE), implicating these residues at the N-terminus of the hinge as critical for 1F3 binding;

iii) the P_{21}-P_{10} peptide (VEVNEEGTEAAA) blocked 1F3 binding while the P_{19}-P_{12} peptide (VNEEGTEA) did not, implicating either the valine and/or glutamic acid, or the double alanines as being critical to the epitope;

iv) mutation of residues of α_1-AT to those found in PI-9 (α_1-AT_{mut}: LTINEEGTEAAAA) resulted in gain of 1F3 binding, implicating some or all of these residues as being critical;

v) mutation of PI-9 at P_{16} glutamic acid to lysine decreased 1F3 binding (VEVNEKGTEAAA) while other mutations did not lessen 1F3 reactivity (P_{18} asparagine to aspartic acid, single or double P_{10}-P_9 alanine deletion), implicating the P_{16} residue as important for 1F3 binding, while demonstrating that the alanine residues at the C-terminus of this region are not critical.

Therefore, the epitope must include the P_{14} threonine, the P_{16} glutamic acid and extend beyond the N-terminus of the shorter hinge peptide. Hence the minimal epitope is EVNEEGT. Analysis of these residues in 1F3 reactive serpins supports this conclusion (illustrated in Table 4.1), as the six serpins that display equal reactivity to 1F3 contain this sequence. Only SPI-6 has any differences from the identified epitope, however this is a conservative substitution of isoleucine instead of valine. Analysis of the other serpins indicates that reduction and loss of 1F3 reactivity correlates with increasing divergence from the identified EVNEEGT sequence.

4.3 1F3 differentiates between monomeric and polymeric forms of Antithrombin

Serpins can adopt a number of conformational states due to the flexibility and metastable nature of their tertiary fold. The conformational changes in serpin structure are most apparent in the positioning of the RCL. This flexibility is mediated by the proximal and distal hinge regions which themselves undergo changes in structure. As 1F3 recognises the proximal hinge region, the ability of 1F3 to distinguish between various serpin conformations was investigated. Antithrombin (AT) can adopt many conformations, most of which have been verified by crystallisation (Skinner *et al.*, 1997; Skinner *et al.*, 1998). In native AT the P_{14} and P_{15} residues of the RCL are inserted into β-sheet A (Carrell *et al.*, 1994; Schreuder *et al.*, 1994) (illustrated in Figure 4.5A and B). Binding of heparin or heparin derivatives, such as heparin pentasaccharide induces a large conformational change in AT structure. These changes include the expulsion of the P_{14} and P_{15} residues of the RCL (van Boeckel *et al.*, 1994) (illustrated in Figure 4.5C), and the rotation of the bottom half of the serpin relative to the top. This results in an overall conformation of AT that is more similar to other native serpins (Jin *et al.*, 1997) and increases the inhibition of thrombin and factor Xa (Huntington *et al.*, 1996; Jin *et al.*, 1997).

AT can adopt a number of conformations for which structures have been proposed. The 1F3 epitope was mapped onto these conformations, and for each structure the exposure of the epitope was predicted. In native AT the partial insertion of the RCL into β-sheet A would mask the 1F3 epitope (Figure 4.6A), however upon heparin activation and loop expulsion the 1F3 epitope should become exposed (Figure 4.6B). The binary complex of AT with the loop peptide from α_1-AT inserted into β-sheet A should result in expulsion of the RCL and exposure of the 1F3 epitope (Figure 4.6C), while cleaved AT and AT in complex with thrombin should result in complete insertion of the RCL, thereby masking the 1F3 epitope (Figure 4.6D and E). Additionally, coating of AT to electrostatic surfaces has been demonstrated to result in partial unfolding of AT, which results in opening of β-sheet A (Picard *et al.*, 1999). Therefore, 1F3 could be a useful tool to examine models of loop exposure in AT.

The reactivity of 1F3 with AT conformations was initially examined by ELISA. Using a sandwich ELISA, in which AT remains in its natural conformation, 1F3 failed to recognise AT in any of the five conformations tested (native AT, AT activated with either heparin or heparin pentasaccharide, AT with the loop peptide of α_1-AT inserted

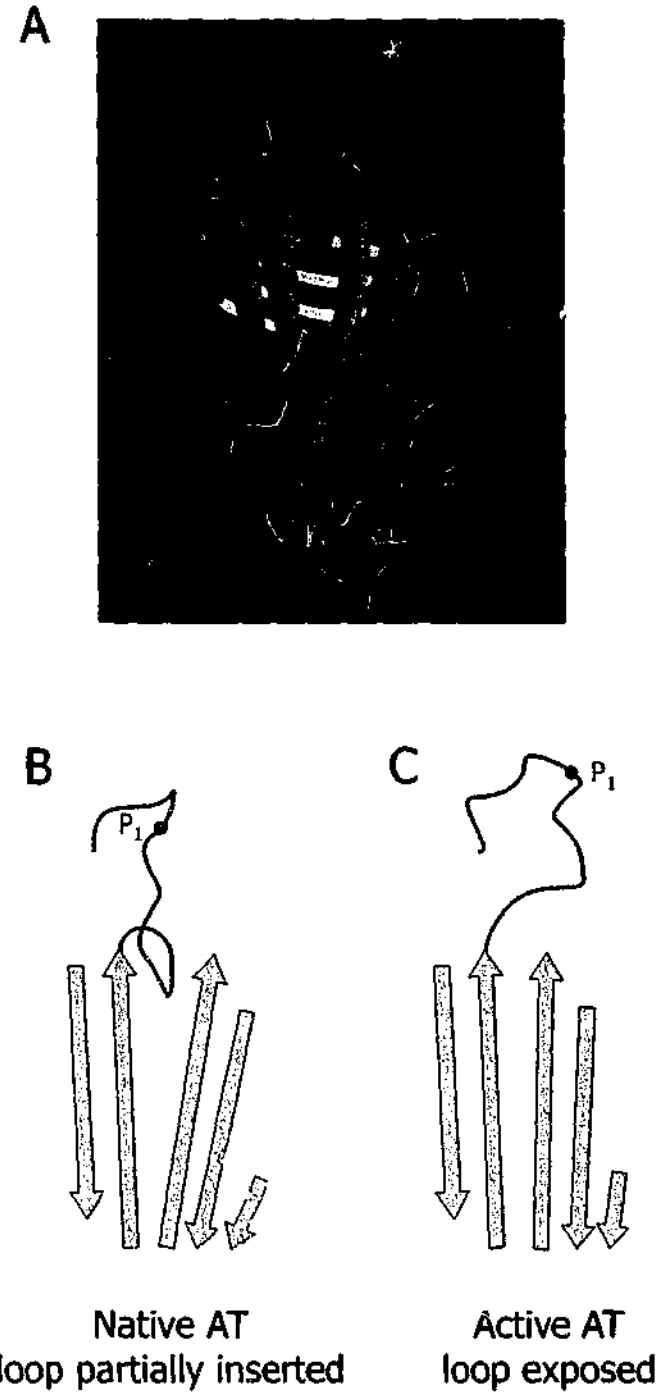

Figure 4.5 Conformational states of Antithrombin. (A) Ribbon diagram of AT in the native state in which the RCL is partially inserted into β-sheet A. (B) Simplified diagram of native AT, the RCL is indicated in red and β-sheet A in green. Partial insertion of the RCL into β-sheet A induces a conformation of the loop in which the P_1 residue is relatively inaccessible to the proteinase. (C) The active conformation of AT. Binding of heparin or heparin derivitives results in expulsion of the RCL and the reoreintation of the P_1 residue making it accessible to the proteinase.

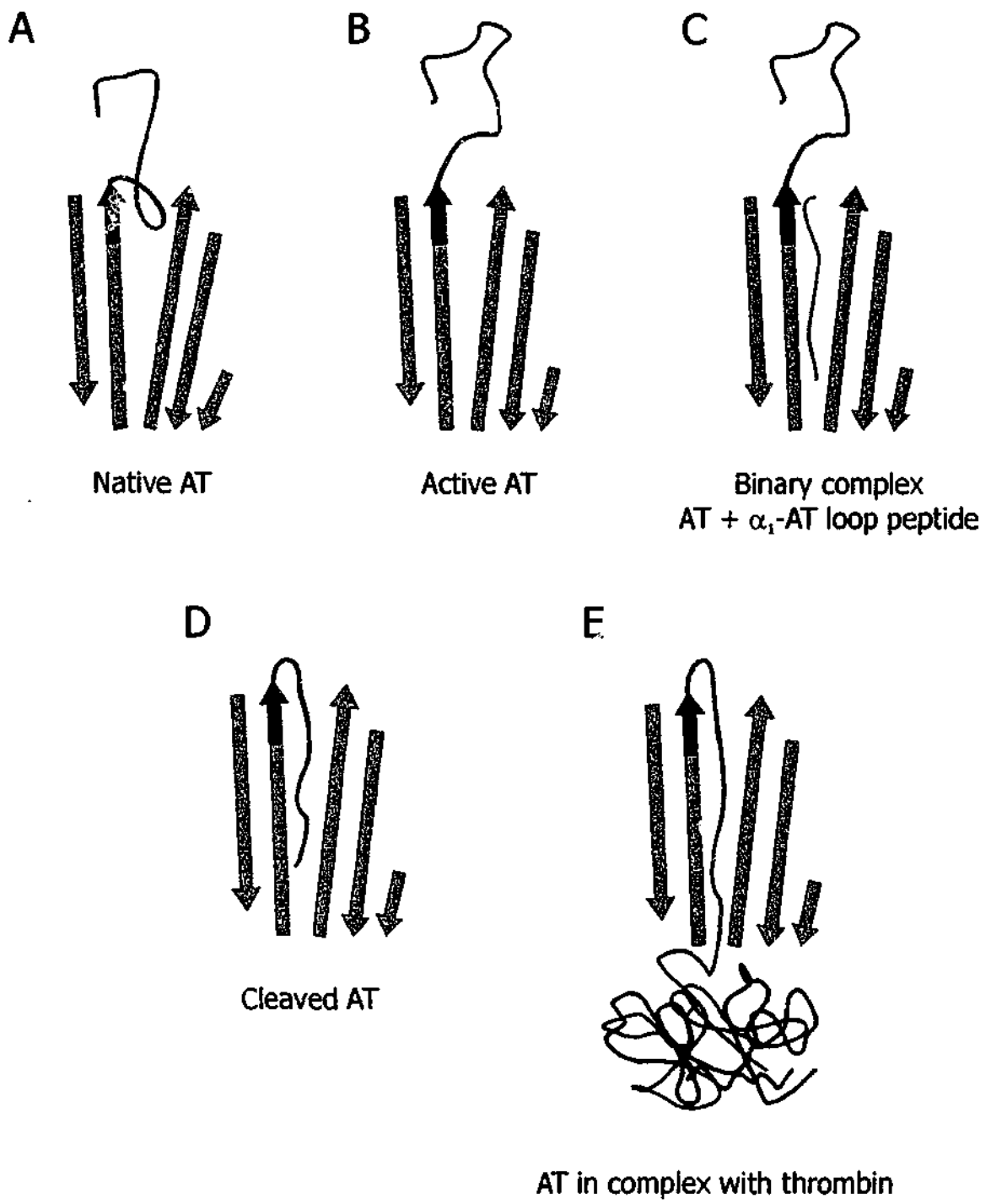

Figure 4.6 Mapping of the 1F3 epitope to conformational states of Antithrombin. Simplified cartoon of AT conformations in which the RCL is indicated in red, β-sheet A in green and the 1F3 epitope in blue. (A) Native AT in which the RCL is partially inserted into β-sheet A. (B) Active AT following the expulsion of the RCL by binding of heparin or heparin derivatives. (C) Binary complex of AT with the loop peptide of α_1-AT (orange) inducing expulsion of the RCL. (D) Cleavage of the loop peptide by gingipain resulting in insertion of the cleaved RCL into β-sheet A. (E) Complex of active AT with thrombin (purple) resulting in insertion of the RCL into β-sheet A and translocation of the proteinase from the top to the bottom of the serpin.

or with the RCL cleaved by gingipain). This suggests that in both activated AT and the binary complex of AT with the loop peptide from α_1-AT, in which the 1F3 epitope was predicted to be exposed, the conformational change in AT structure is not sufficient to allow 1F3 to bind. By contrast, 1F3 could detect AT coated directly onto the microtiter plate (Figure 4.7A). Therefore 1F3 reactivity is dependent upon opening of β-sheet A rather than expulsion of the RCL.

These observations were confirmed by examining conformations of AT by native PAGE and immunoblotting. Again 1F3 recognised the AT monomer, but did not recognise binary complex of AT with the loop peptide from α_1-AT (Figure 4.7B , lower band), although it did recognise the residual monomeric AT (Figure 4.7B , higher band). Furthermore, 1F3 did not recognise either AT with the RCL cleaved or in complex with thrombin. In addition, although 1F3 was able to recognise AT monomer, it was unable to recognise any of the higher molecular weight polymers of AT, induced by heating at 55°C for 4 h (Figure 4.7B). Previous analysis of AT conformations by native PAGE and immunoblotting has demonstrated that binding of monomeric AT to nitrocellulose membranes results in opening of β-sheet A (Picard *et al.*, 1999). As 1F3 only detected monomeric AT by immunoblotting this suggests that 1F3 can only recognise AT that is partially unfolded, and that opening of β-sheet A is necessary to allow 1F3 access to its epitope.

4.4 1F3 prevents polymerisation of Antithrombin but not its inhibitory function

Opening of the A sheet has been described as a prerequisite to the formation of polymers, as analysis of serpin structure using fluorescent probes has indicated that the A sheet opens prior to the insertion of the RCL (Fitton *et al.*, 1997; James *et al.*, 1999). As 1F3 appears to recognise AT only when the A sheet is open, it may bind to its epitope during the initial steps of polymerisation thereby preventing RCL insertion due to steric hindrance.

Incubation of AT at 55°C for 4 hr induces almost complete polymerisation. However, when AT was incubated in the presence of 1F3, although dimers, trimers and multimers were observed the degree of polymerisation was greatly decreased (Figure 4.8A). Densitometric analysis of the residual AT monomer indicated that less than 10% had polymerised. This activity was specific to 1F3 as incubation with an irrelevant antibody of the same isotype was unable to prevent polymerisation (Figure 4.8A).

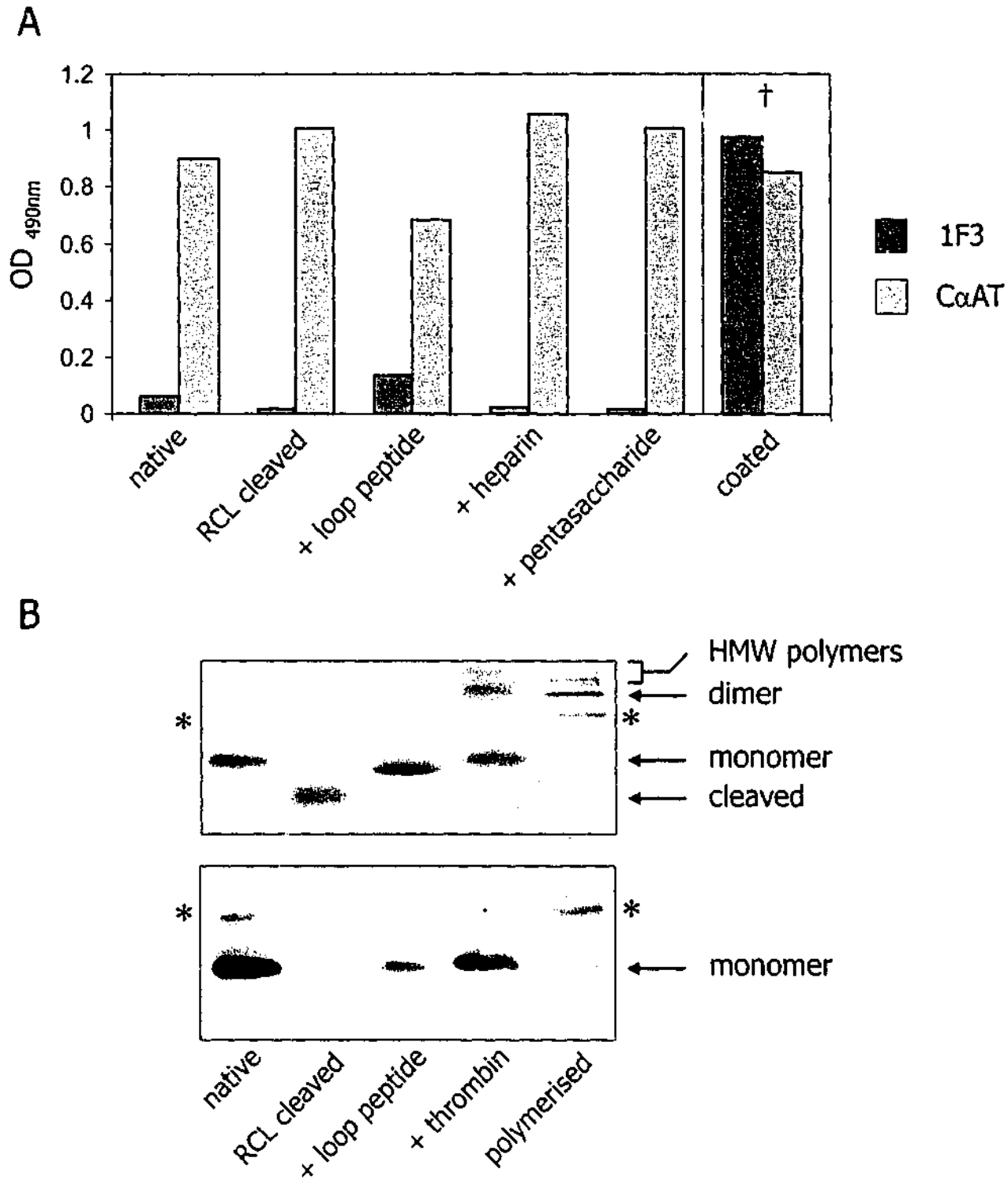

Figure 4.7 Recognition of conformations of Antithrombin by 1F3. (A) The ability of 1F3 to recognise conformations of AT was assessed by sandwich ELISA. Conformations of AT used were: native, RCL cleaved by gingipain, binary complex with the loop peptide of α_1-AT or activated with heparin or pentasaccharide. Conformations of AT were captured with rabbit polyclonal anti AT antiserum (diluted 1:1000) and detected with either chicken anti AT antiserum (diluted 1:4000; CαAT) or 1F3 hybridoma supernatant (diluted 1:10) and the ELISA performed as described in 2.13.1.4. † indicates AT directly coated onto the microtiter plate and demonstrates that 1F3 does recognise AT. (B) 1F3 recognition of AT was further assessed by native PAGE. Conformations of AT used were: native, RCL cleaved with gingipain, binary complex with the loop peptide of α_1-AT, complex with thrombin and polymer induced by heating at 55°C in 20 mM Tris-HCl, pH 7.4, 150 mM NaCl, for 5 h. Duplicate gels were either stained with Coomassie Blue (upper panel) or transferred to nitrocellulose and immunoblotted with 1F3 hybridoma supernatant (diluted 1:20; lower panel) and detected with HRP conjugated anti mouse IgG and enhanced chemiluminescence. * Indicates an uncharacterised high molecular weight form of AT that is present in the purified material.

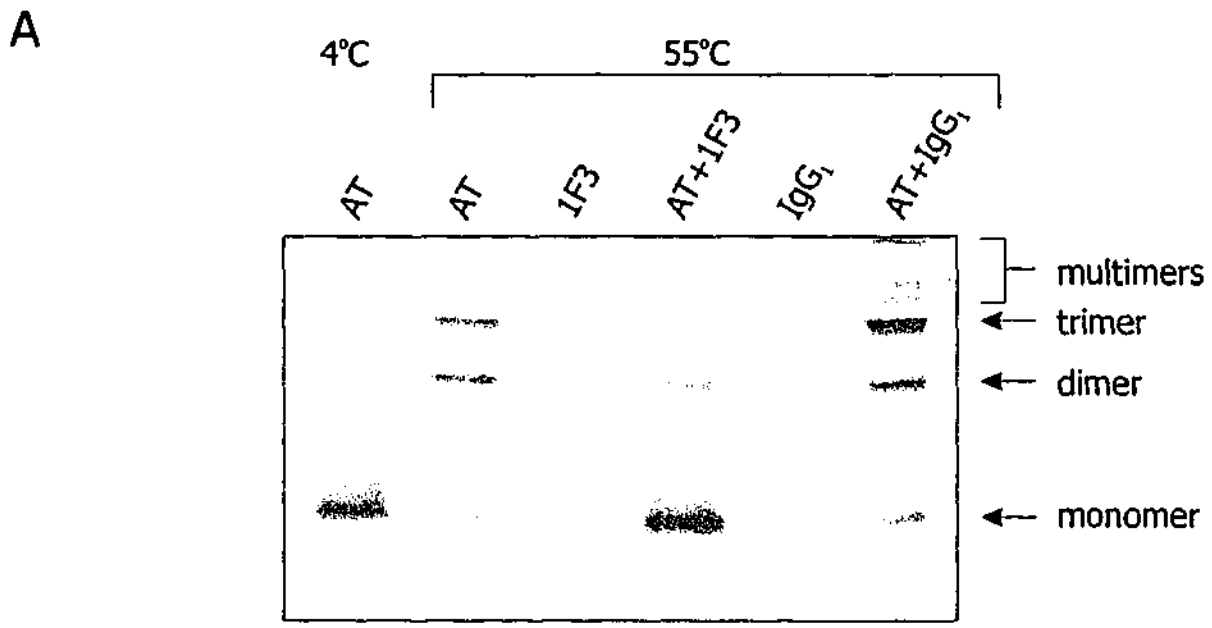

Figure 4.8 Effect of 1F3 on polymerisation and inhibitory function. (A) 1F3 prevents polymerisation of AT. AT (0.2 mg/ml) was incubated at 55°C for 3 h in 20 mM Tris-HCl, pH 7.4, 150 mM NaCl either alone or in the presence of an equimolar amount of 1F3 (0.65 mg/ml) or isotype control antibody (IgG_1). Samples were compared to AT stored at 4°C. Samples were resolved by native PAGE and stained with Coomassie Blue. (B) 1F3 does not prevent the inhibitory activity of AT. AT (2 μg) was incubated with thrombin (1.2 μg) with or without 1F3 (6.5 μg) added prior to incubation with thrombin. Samples were analysed by SDS-PAGE and stained with Coomassie Blue. Species of AT are indicated on the right.

However, as insertion of the RCL into β-sheet A is also a prerequisite to the formation of the serpin-proteinase complex, binding of 1F3 might also prevent the interaction of AT with thrombin. To examine this, AT was pre-incubated 1F3 prior to incubation with thrombin. Incubation of AT with thrombin alone produced the expected complex and complex formation was not disrupted by pre-incubation of AT with 1F3 (Figure 4.8B). This indicates that 1F3 does not block the interaction of AT with its cognate proteinase.

4.5 Discussion

Characterisation of the anti PI-9 monoclonal antibody, 1F3, by immunoblotting after reducing and denaturing conditions indicated that the epitope is linear. Further characterisation demonstrated that 1F3 has pan-serpin reactivity as its epitope is found within the highly conserved proximal hinge region of serpins. Epitope mapping, mutational analysis and the use of blocking peptides indicated that the epitope comprises the P_{20}-P_{14} residues of the proximal hinge region (EVNEEGT) with the P_{16} glutamic acid and the P_{14} threonine being essential residues within the epitope.

1F3 recognises the proximal hinge region, which is a conformationally active region of the molecule. Previous analysis of serpin structure with antibodies has revealed many of the finer details of the conformational changes in structure via the loss or appearance of epitopes (Skriver *et al.*, 1991; Bjork *et al.*, 1993; Nordling and Bjork, 1996; Saunders *et al.*, 1998; Picard *et al.*, 1999). Therefore, analysis of the proximal hinge with 1F3 could be a valuable means to test models of serpin conformation.

Based upon current models of AT structure, 1F3 was expected to be unreactive towards conformations of AT in which the RCL is inserted into β-sheet A (native AT and RCL cleaved AT). Conversely, conformations that result in the expulsion of the P_{14} and P_{15} residue from β-sheet A, allowing AT to adopt a more open conformation of the proximal hinge region, were expected to result in 1F3 reactivity. However, 1F3 did not recognise AT with the loop peptide from α_1-AT inserted or AT activated with heparin or the pentasaccharide derivative, indicating that loop expulsion and the adoption of the active conformation of AT is not sufficient to reveal the 1F3 epitope, and further unfolding of the proximal hinge region is required for 1F3 reactivity.

1F3 will however, recognise AT bound directly to the microtiter plate. Previously it has been observed that binding of AT to electrostatic surfaces (i.e. transferred to nitrocellulose or adsorbed onto plastic) results in opening of β sheet A

(Picard *et al.*, 1999). Thus for 1F3 to have access to its epitope, AT must undergo a more drastic conformational change than transition to the active state, and opening of β-sheet A is required (illustrated in Figure 4.9).

This dependence of 1F3 reactivity upon the opening of β-sheet A raised the possibility that 1F3 could prevent polymerisation, as this is also dependent upon the opening of the A sheet (Fitton *et al.*, 1997; James *et al.*, 1999). 1F3 was shown to inhibit polymerisation induced by heating, suggesting that during polymerisation and A sheet opening, 1F3 can bind to the proximal hinge of the polymerogenic intermediate before another RCL can insert, and therefore prevent polymerisation by steric hindrance.

However, 1F3 does not prevent the inhibitory activity of AT with thrombin which also involves opening of the A sheet, prior to RCL insertion and translocation of the proteinase to the opposite pole of the serpin (Huntington *et al.*, 2000). During AT inhibition of thrombin, the A sheet only opens transiently, during the translocation and insertion of the RCL. Either this translocation is too rapid for 1F3 to bind to its epitope or thrombin bound to the RCL of AT sterically hinders the interaction of 1F3 with the proximal hinge. This suggests that 1F3 can prevent of the polymerisation of serpins without affecting their inhibitory mechanism.

Many naturally occurring serpin mutants spontaneously undergo polymerisation at a number of sites, causing diseases such as emphysema, liver cirrhosis, angio-oedema and thrombosis (reviewed in Carrell and Lomas, 1997). For example, polymerisation of α_1-AT can occur in the endoplasmic reticulum of hepatocytes causing liver cirrhosis while the deficiency in the lung results in emphysema due to unregulated neutrophil elastase activity. Mutations in AT cause polymerisation within the circulation which results in recurrent thromboembolic disease from decreased levels of circulating AT (Stein and Carrell, 1995).

Several studies have identified regions of the serpin structure which are potential targets for drug design to prevent polymerisation (Skinner *et al.*, 1998; Elliott *et al.*, 2000). However, these approaches are based on peptide analogues of the RCL, relying upon insertion of these peptides into the A sheet to prevent polymerisation (Fitton *et al.*, 1997; Mahadeva *et al.*, 2001). Unfortunately, this also results in abrogation of the serpin's inhibitory mechanism.

An alternate approach to the prevention of serpin polymerisation is the use of 'chemical chaperones' or osmolytes. Trimethylamine N-oxide can prevent the heat induced polymerisation of native α_1-AT, however studies on the refolding of denatured α_1-AT demonstrate that it enhances polymerisation (Devlin *et al.*, 2001). Other

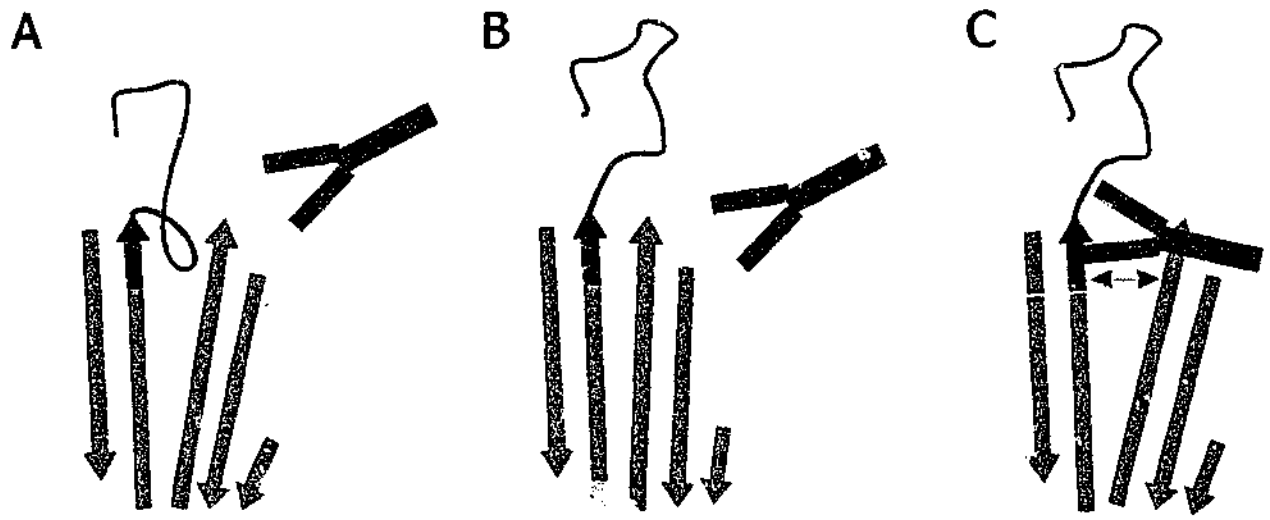

Figure 4.9 Accessibility of the 1F3 epitope in conformationals of Antithrombin.
(A) In native AT in which the RCL is partially inserted into β-sheet A, 1F3 (purple) cannot access its epitope, however expulsion of the loop is not sufficient to allow binding of 1F3 (B), only upon opening of β-sheet A can 1F3 bind to its epitope (C).

osmolytes have also been shown to prevent polymerisation of α_1-AT, however higher concentrations lead to inactive conformations of α_1-AT (Chow *et al.*, 2001). An *in vivo* model of α_1-AT polymerisation has been established in mice which are transgenic for the human Z mutant of α_1-AT. Studies using the chemical chaperone 4-phenylbutyric acid can increase the circulating levels of Z α_1-AT in these mice (Burrows *et al.*, 2000), and although 4-phenylbutyric acid has been used to successful treat urea cycle disorders in neonatal children (Maestri *et al.*, 1991), the long term toxic side effects are not known.

From studies outlined in section, 1F3 appears to be a candidate molecule to prevent serpin polymerisation without affecting serpin inhibitory function and without toxic side effects. To test this further, the effect of 1F3 upon the polymerisation of other serpins should be investigated. For serpins that 1F3 does not recognise, specific antibodies could be raised to the hinge region of the serpin corresponding to the 1F3 epitope in PI-9 (EVNEEGT) and this antibody assessed for anti-polymerogenic effects.

Potential drug therapies need to inhibit polymerisation inside the cell as well as in the circulation. Since antibodies are not cell permeable they cannot be directly used to prevent polymerisation in cells (e.g. polymerisation of the Z mutant of α_1-AT in hepatocytes). However, crystallisation of 1F3 with the polymerogenic intermediate of AT could identify regions of AT that are involved in polymerisation and are amenable to rational drug design.

Chapter 5

Tissue Distribution Studies of PI-9 Reveal a Potential Role for PI-9 and Granzyme B in Testicular Development

Summary

This chapter describes the investigation of PI-9 distribution by RNA analysis and immunohistochemistry, and demonstrates that PI-9 is expressed primarily in immune cells and tissues, and in immune privileged sites, consistent with the hypothesis that PI-9 protects from mis-directed graB during the immune response. However, PI-9 is also expressed in a variety of epithelial cell types, suggesting that PI-9 may play a role in cells outside the immune system. Further analysis of the testis, an immune privileged site, indicates that PI-9 is expressed in the epithelial Sertoli cells. Hypothesising that PI-9 protects these cells from graB-producing, auto-reactive cytotoxic lymphocytes, the testis was also stained for graB. Unexpectedly, graB is observed in spermatogenic cells within the seminiferous tubule of the human testis. This localisation of graB to the testis was verified by *in situ* hybridisation, RT-PCR and RNA hybridisation (Northern blotting). Perforin, which is co-produced with graB by activated cytotoxic lymphocytes and is required for graB release into the target cell, is not detected in the testis using RT-PCR. It is possible that graB has a perforin-independent role in the testis, involving hydrolysis of extracellular matrix components, possibly to facilitate migration of developing germ cells in the tubules or to modulate the complex intercellular signalling between germ cells and Sertoli cells.

Introduction

Previous studies have demonstrated the expression of PI-9 mRNA in a number of immune tissues (spleen, thymus and IL-2 stimulated PBL) (Sun *et al.*, 1996) and immune privileged sites (testis and placenta) (Sprecher *et al.*, 1995; Sun *et al.*, 1996). Further analysis of cell lines indicated that PI-9 mRNA could be detected in lymphoid cells, however no transcripts were detected in myeloid cells. The highest levels of PI-9 mRNA were found in two NK-like cell lines, YT and Lopez T, and in IL-2 stimulated PBL - cells which express graB (Sun *et al.*, 1996). This co-expression with graB is consistent with PI-9 having a protective role in cytotoxic lymphocytes. As well as protecting cytotoxic lymphocytes, PI-9 may also protect bystander cells or antigen presenting cells likely to be exposed to graB during an immune response. To further understand the physiological role of PI-9, it is important to identify specific cells that express PI-9. Therefore tissue distribution studies were performed, initially by expanding the RNA analysis and then by immunohistochemistry of various human tissues.

5.1 Tissue distribution analyses of PI-9

To further investigate the tissue distribution of PI-9 a [α-^{32}P] dCTP labelled PI-9 cDNA probe was hybridised to a multi-tissue mRNA dot blot. The highest levels of PI-9 transcripts were detected in the placenta, lymph node, spleen and thymus (Figure 5.1A), consistent with previous RNA analysis. PI-9 was also detected in the lung, peripheral blood leukocytes (PBL) and testis with low level signals in most other tissues, except the brain. The distribution in foetal tissue mirrored that found in the adult, with PI-9 detected in foetal spleen, lung and thymus. PI-9 transcripts were highest in immune cells as well as immune privileged sites (the placenta and testis) consistent with a role for PI-9 in protecting cells from mis-directed graB during the immune response. However, the low level expression of PI-9 mRNA in many tissues suggests that PI-9 may be expressed in tissue resident DC or NK cells or possibly in cells outside the immune system.

The tissue distribution of PI-9 was compared to that of graB. Although graB is thought to be restricted to cytotoxic lymphocytes (Caputo *et al.*, 1988; Trapani *et al.*, 1988), a comprehensive survey of human tissue has not been reported. Therefore, the multi-tissue mRNA dot blot used above was allowed to decay for 6 months until no

A

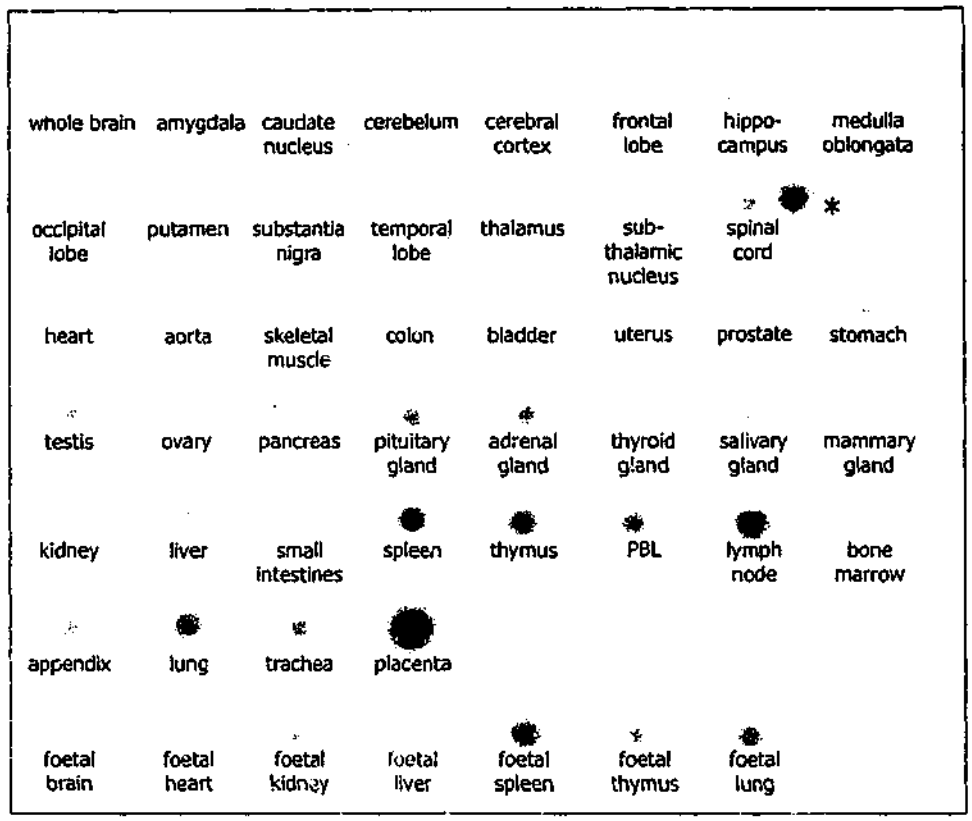

B

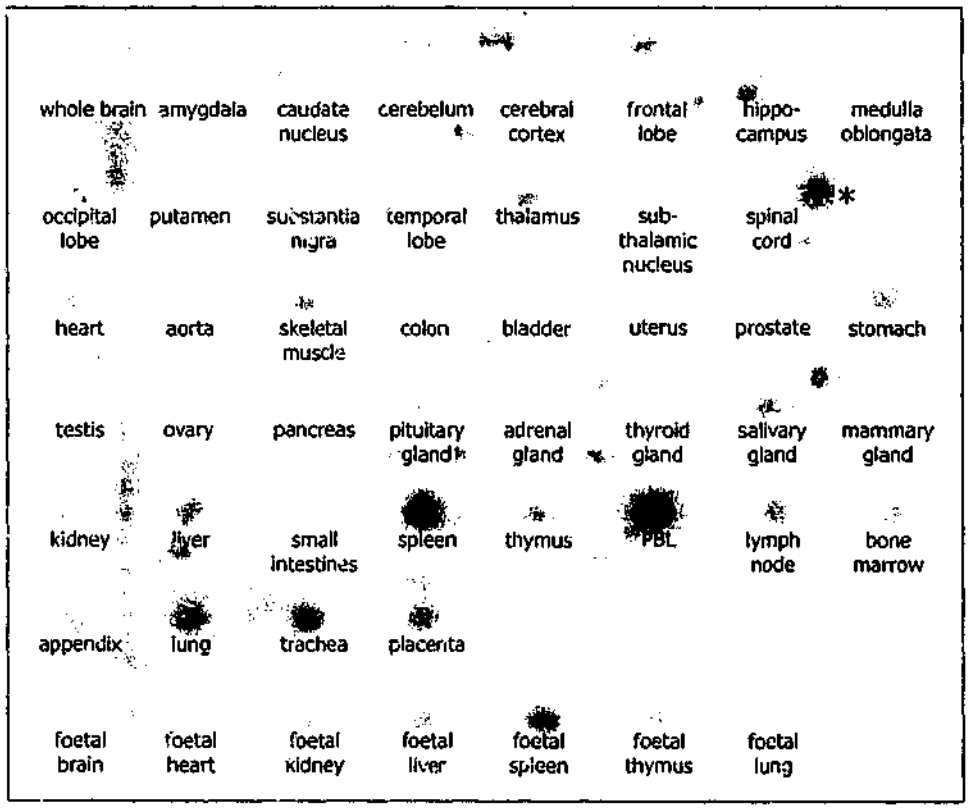

Figure 5.1 Tissue distribution of PI-9 and granzyme B by RNA analysis. A Human RNA Master Blot™ (Clontech) containing mRNA extracted from 50 tissues was hybridised to a [α-^{32}P] dCTP labelled cDNA consisting of either (A) the 3' coding region and 3'UTR of PI-9 at 65°C overnight, after a final wash in 0.2 x SSC at 55°C the blot was exposed to film for 72 hrs; or (B) the 3'UTR of graB at 65°C overnight, after a final wash in 1 x SSC at 65°C the blot was exposed to film for 48 hrs. (* = non specific signal).

residual signal was detectable and was then hybridised with a [α-^{32}P] dCTP labelled cDNA probe consisting of the 3'UTR of graB. The highest levels of graB transcripts were detected in PBL and spleen, with strong signals detected in lung, trachea, foetal spleen, liver and placenta (Figure 5.1B) and low signals in most tissues. The presence of graB transcripts in spleen, PBL and lymph node is consistent with the expression of graB in activated CTL and NK cells, however the presence of graB in thymus, bone marrow and foetal spleen and thymus suggests immature lymphocytes may also express graB. High levels of graB were also detected in trachea, lung, liver and placenta. The high level of graB in liver and placenta may be due to high number of Kupffer cells in the liver and decidual leukocytes in the placenta, however the presence of graB transcripts in the trachea and lung indicates that these tissues may also have high numbers of tissue resident NK cells, or that other cells in these tissues express graB.

Comparison of the tissue distribution of graB and PI-9 suggests that, while their distribution overlaps, this proteinase-inhibitor pair are not co-ordinately expressed. For example, comparison of their expression in immune tissues indicates that PI-9 expression is lower than graB in PBL and spleen but higher in thymus and lymph node. Also, the broad distribution of graB suggests that activated CTL and NK cells are present in many tissues at high levels, or alternatively, other cell types express graB.

To identify specific cell types that produce PI-9, an immunohistochemical survey of normal human tissues was performed using the specific monoclonal antibody 7D8, in parallel with Rabbit #15 polyclonal antiserum. PI-9 expressing cells were observed in a variety of tissues (Table 5.1). In lymphoid tissues, PI-9 was detected in NK cells within the lymph node and in dendritic cell subsets of the tonsil and thymus. These observations and an examination of PI-9 expression in peripheral blood leukocytes are described further in Chapter 6. PI-9 positive cells were also detected in the epithelium, endothelium and mesothelium of all tissues examined. Further examination by M. Buzza, indicated PI-9 is upregulated in reactive mesothelial and endothelial cells, consistent with PI-9 protecting these cells from free graB released during an immune response (Buzza *et al.*, 2001). The expression of PI-9 in lining cells is also consistent with the RNA analysis described above, as the expression of PI-9 in these cells would explain the low signal detected in most tissues.

PI-9 was also detected in foetal pancreas and intestine, and in the fallopian tube (Figure 5.2). In foetal pancreas, PI-9 was detected within the exocrine tissue, specifically the acinar cells (Figure 5.2A). Higher magnification indicated that PI-9 was restricted to the cytoplasm and was not found in all acinar cells within a duct. Acinar

Tissue	Cell types	Intensity[a]
Lymphoid tissues		
Lymph nodes	NK cells	+++
Thymus	Medullary dendritic cells	++
	Hassal's corpuscles	+++
Tonsil	Follicular dendritic cells	+++
Reproductive tissues		
Endometrium[b]	Uterine epithelium	++
	Stromal cells	++
	Large granular lymphocytes	+++
	Glandular epithelium	++
	Myometrium	+
Oviduct	Epithelium	+
Placenta[b]	Syncytial trophoblasts	+++
Testis	Sertoli cells	+++
	Leydig cells	++
Other tissues		
All organs[b]	Mesothelium	+
All tissues[b]	Endothelium	+
Intestine (foetal)	Enterocytes	+
Lung (reactive)[b]	Epithelium	+
Pancreas (foetal)	Ductal acini	+
Skin[b]	Epithelium	+

Table 5.1 Tissue distribution of PI-9. Immunohistochemistry was performed on a variety of tissues using 7D8 and Rabbit #15 polyclonal antiserum. [a] The level of PI-9 staining was compared between the identified cell types (++++ = very strong, - = low). [b] Immunohistochemistry performed by M. Buzza.

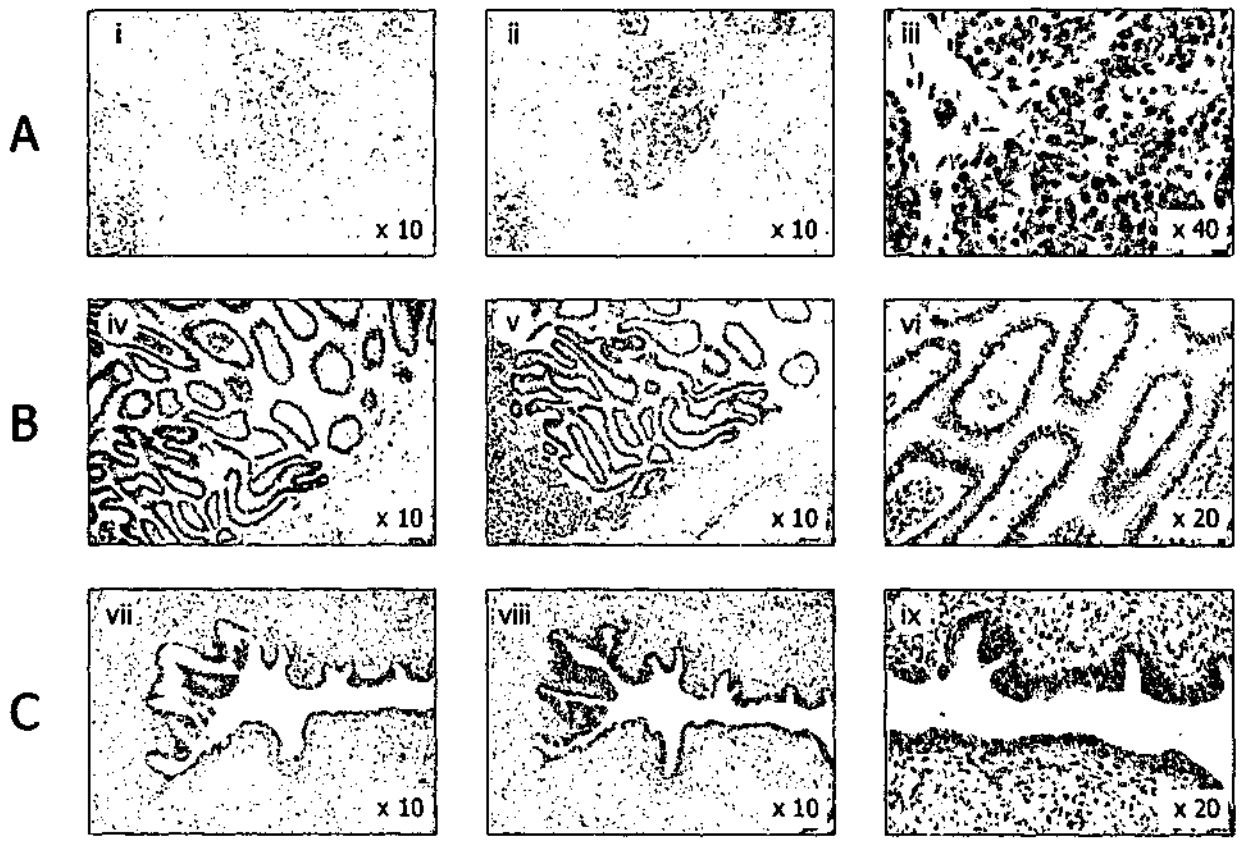

Figure 5.2 Expression of PI-9 in epithelial cells. (A) PI-9 expression in foetal pancreatic acinar cells detected with 7D8 (ii) and (iii), as compared to the isotype matched control antibody (i). (B) Expression of PI-9 in enterocytes of the foetal intestines detected with 7D8 (v) and (vi), and the isotype matched control antibody (iv). (C) PI-9 expression in the ciliated columnar epithelium of the fallopian tube detected with 7D8 (viii) and (ix), as compared to the isotype matched control antibody (vii).

cells are specialised epithelial cells, which produce proteinases as inactive zymogens. These are activated in the small intestine brush border by enterokinase, converting pancreatic trypsinogen into trypsin, which in turn activates pancreatic chymotrypsin and elastase. PI-9 was also detected in the enterocytes of the small intestine (Figure 5.2B). The role for PI-9 in these cells is not clear, however PI-9 may protect these cells from exogenous proteinases. Intraepithelial lymphocytes are often found between enterocytes, where they are thought to play an important part in immune surveillance of the gastrointestinal tract, which may also result in the exposure of enterocytes to cytotoxic proteins (Shiner *et al.*, 1998).

PI-9 was also detected in the ciliated columnar epithelial cells of the fallopian tube (Figure 5.2C) and several different cell types within the female reproductive tract, which is consistent with recent reports indicating that PI-9 is oestrogen responsive (Kanamori *et al.*, 2000; Krieg *et al.*, 2001). PI-9 was also found to be expressed in the placenta. The role of PI-9 in the female reproductive tract is currently under investigation in this laboratory by M. Buzza.

5.2 Expression of PI-9 in the testis

Immunohistochemistry also demonstrated that PI-9 was highly expressed within the tubules of the testis. The structure of the seminiferous tubules and the cell types found within them are illustrated in Figure 5.3A. The PI-9 positive cells were identified as Sertoli cells due to their characteristic shape, extending from the basement membrane to the lumen of the tubule, and their ovoid nucleus with a single nucleolus. The staining for PI-9 was cytoplasmic and nuclear (Figure 5.3B ii and iii), this nucleocytoplasmic distribution of PI-9 has been observed in many cell types (Bird *et al.*, 2001). Because the cytoplasmic extensions of the Sertoli cell wrap around the developing germ cells, it was difficult to identify cell boundaries and definitively rule out PI-9 expression in germ cells. However, careful analysis of a number of serial sections indicated that within the seminiferous tubule, PI-9 is restricted to Sertoli cells. In some normal and inflamed samples however, staining was also observed in infiltrating lymphocytes and Leydig cells within the interstitium.

As the process of spermatogenesis does not begin until puberty, the immune system will not be tolerised to novel antigens expressed by developing germ cells. Sertoli cells form the blood-testis barrier which prevents direct interaction of the immune system with potentially immunogenic germ cells. To further explore a role for

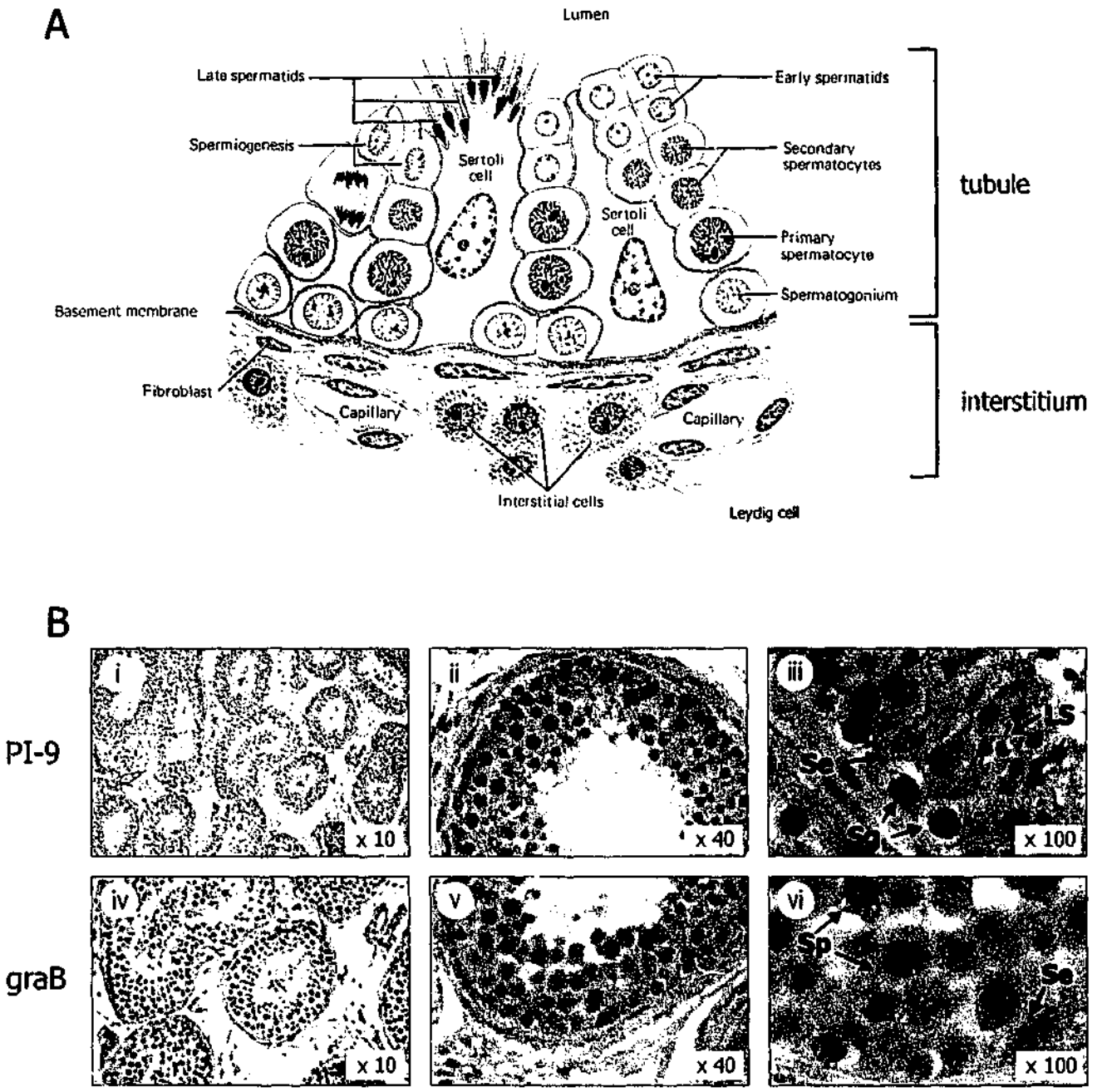

Figure 5.3 Localisation of PI-9 and granzyme B within normal adult human testis. (A) Cartoon illustrating the various cell types present in the seminiferous tubules and interstitium of the human testis. Diagram adapted from Basic Histology 8th ed., Junqueira, Carneiro and Kelley. (B) Immunohistochemistry of normal adult testis using antibodies for PI-9 or graB. Sections stained with the anti PI-9 monoclonal antibody 7D8, indicated the presence of PI-9 in Sertoli cells (Se) but not spermatogonia (Sg) or late spermatids (LS) (ii) and (iii). Sections stained using the anti graB monoclonal antibody 2C5, demonstrated graB expression in both Sertoli cells (Se) and primary spermatocytes (Sp) (v) and (vi). Isotype matched control antibodies are indicated in (i) and (iv).

PI-9 in immune privilege, immunohistochemistry was performed to determine if graB-expressing lymphocytes are normally present in the testis.

5.3 Expression of granzyme B in the testis

Surprisingly, immunohistochemistry of normal human testis using a monoclonal antibody to graB (2C5) indicated expression within the seminiferous tubule (Figure 5.3B v). Like PI-9, graB was observed in Sertoli cells, but graB was also detected in certain cells of the spermatogenic lineage (Figure 5.3B vi). The intensity of staining for graB also varied between cell types. Sertoli cells had diffuse cytoplasmic distribution while primary spermatocytes and early spermatids had more intense cytoplasmic staining. No graB was observed in the nuclei of these cells.

As graB is thought to be restricted to CTL and NK cells (Caputo *et al.*, 1988; Trapani *et al.*, 1988), the immunohistochemistry was confirmed using three other antibodies to human graB. Two commercially available antibodies; sc-1968, (a goat anti graB polyclonal antisera; Santa Cruz Biotechnology) and GrB-7, (a mouse monoclonal antibody; Chemicon) were obtained along with a rabbit anti graB polyclonal antiserum (provided by J. Trapani), and were used in immunohistochemistry. All three were reactive against the graB expressing cell line, YT, and all three demonstrated staining of cells within the seminiferous tubule (data not shown). To determine if graB was present in mature sperm, immunoblotting was performed on sperm isolated from seminal fluid, however no graB was detected (data not shown) suggesting that graB is transiently expressed during spermiogenesis.

5.4 Analysis of PI-9 and granzyme B transcripts in the testis

To eliminate the possibility that the graB antibodies were recognising a highly homologous, but as yet uncharacterised, serine proteinase in the testis, the presence of graB and PI-9 transcripts was confirmed in normal adult testis using a combination of *in situ* hybridisation, RT-PCR and Northern blotting. The RNA analysis performed on the multi-tissue mRNA dot blot described earlier (Figure 5.1B) indicated that very low levels of graB transcripts could be detected within the testis. However, this blot also indicated that very low levels of PI-9 transcripts were present in the testis, which contradicts the previous RNA analysis demonstrating high levels of PI-9 transcripts in the testis and the immunohistochemistry performed above. Therefore, to confirm the presence of graB mRNA in the testis Northern analysis was performed on RNA

extracted from normal human testis (provided by K. Loveland). RNA extracted from YT cells was used as a control for the expected size of graB and the blot was hybridised with a [α-^{32}P] dCTP labelled cDNA probe consisting of the 3'UTR of graB (which is most divergent from other serine proteinases). Due to the very high level of graB transcripts in YT cells it was difficult to visualise the signal from the testis. However, when the lanes were separated, a band was detected in testis RNA following longer exposures (Figure 5.4B). This band appears to be slightly larger than that seen in the YT cells which may represent an alternative splicing event or use of an alternate polyadenylation site within the testis.

The presence of both graB and PI-9 transcripts in normal adult testis was confirmed by RT-PCR from RNA provided by K. Loveland. Amplification using PI-9 specific primers resulted in a product of the expected size (198 bp), which was confirmed as PI-9 by Southern analysis with an oligonucleotide internal to the PCR primers (Figure 5.5A). The graB primers generated several products, one of which was of the correct size (561 bp) and confirmed as graB by Southern analysis (Figure 5.5A). To exclude the possibility that the graB transcripts were derived from contaminating lymphocytes within the tissue sample, co-expression of perforin, which is produced with graB by activated lymphocytes (Liu *et al.*, 1989) was assessed. No products were detected by PCR either visually or by Southern analysis (Figure 5.5B). By contrast, perforin was amplified from cDNA generated from the NK-like cell line, YT (Figure 5.5B). The lack of perforin expression confirmed that graB is produced by non-cytotoxic cells within the testis, and indicates that in this context graB may not act as a cytotoxic proteinase, as its entry into cytoplasm is perforin-dependent (Jans *et al.*, 1996; Shi *et al.*, 1997).

To identify which cell types express PI-9 and graB transcripts, *in situ* hybridisation was performed on normal human adult testis using riboprobes specific for either PI-9 or graB. The PI-9 riboprobe encompassed 561 bp of the 3' coding sequence, spanning the reactive centre loop (the most variable region of a serpin gene) and 149 bp of the 3'UTR. The graB riboprobe comprised the entire 3'UTR (127 bp), which was used above in the Northern blotting. The *in situ* hybridisation confirmed the immunohistochemistry, localising both PI-9 and graB to cells within the testis. Examination of multiple sections indicated that PI-9 mRNA is present in Sertoli cells within the tubules as well as Leydig cells and capillary endothelial cells within the interstitium (Figure 5.5C ii and iii). However, the extended cytoplasmic extensions of the Sertoli cells make it difficult to definitively rule out PI-9 expression in germ cells.

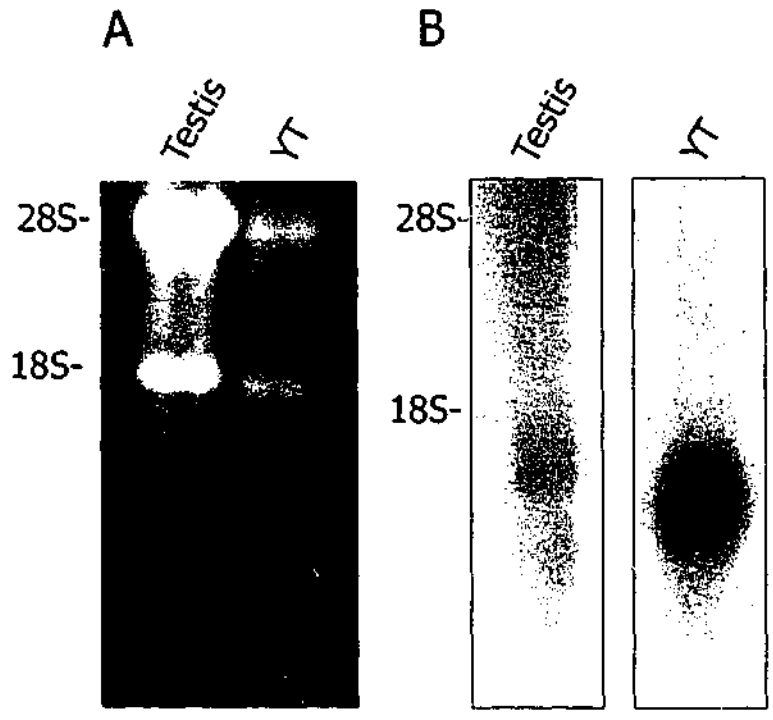

Figure 5.4 Northern analysis of granzyme B in normal testis. 20 μg of total RNA extracted from normal adult testis was resolved with 10 μg of total RNA extracted from the graB expressing cell line, YT. (A) The gel was stained with ethidium bromide to visualise the 28S and 18S ribosomal RNA bands. (B) The RNA was transferred to nitrocellulose and hybridised to a [α-^{3} P] labelled cDNA probe consisting the 3'UTR of human graB at 65°C overnight. After a final wash in 0.1 x SSC at 55°C the blot was exposed to film. Due to the high level of graB mRNA detected in the YT cell line, it was difficult to visualise the signal from the testis without overexposing the YT lane. Therefore the blot was divided in half and exposed to film for different times (testis, 7 days; YT, 12 hrs).

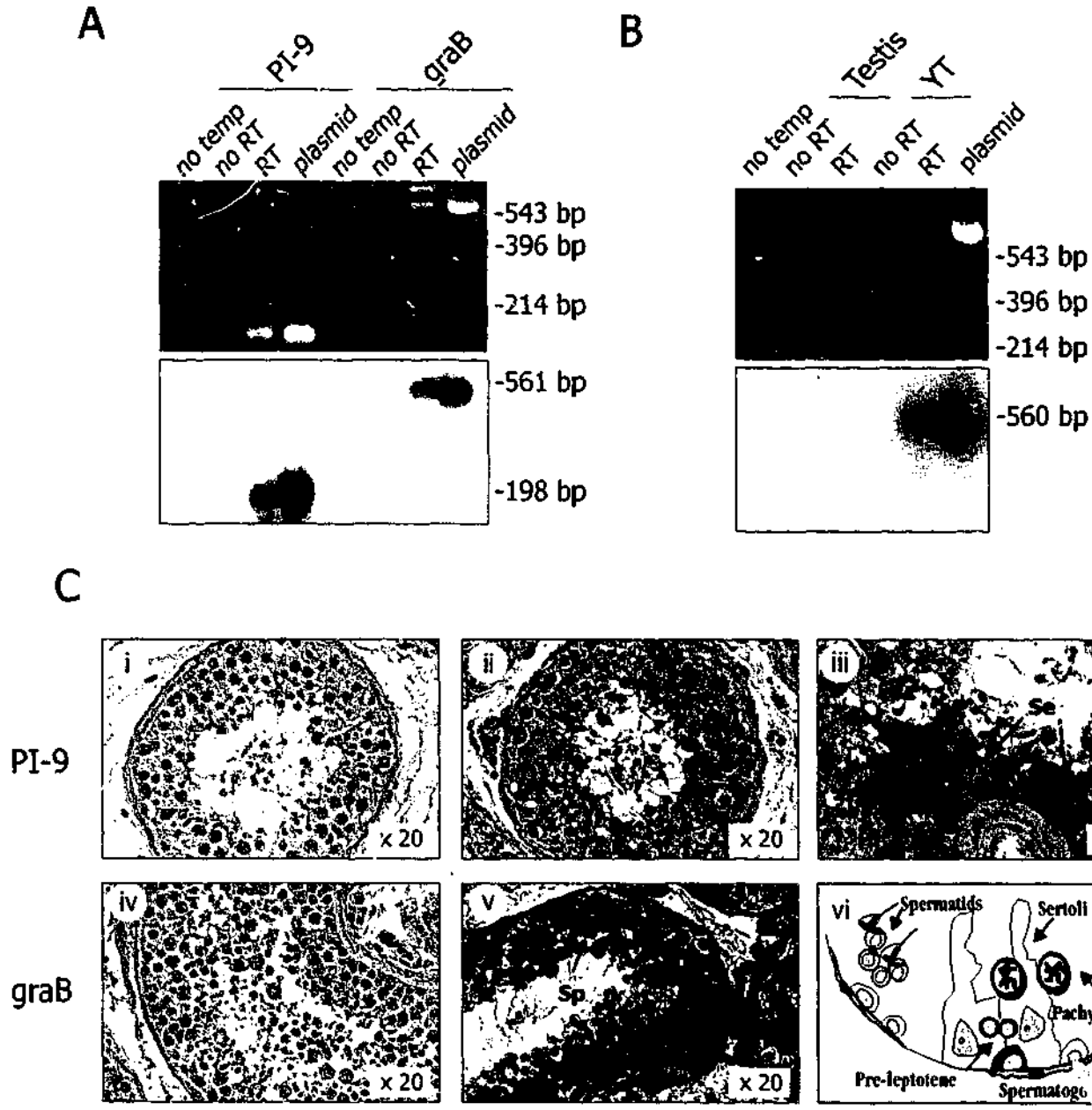

Figure 5.5 Analysis of PI-9, granzyme B and perforin transcripts in normal adult human testis. (A) Detection of Pi-9 and graB mRNA. Total RNA extracted from normal human testis (provided by K. Loveland) was reverse transcribed and used as a template for PCR amplification of PI-9 or graB with primers PB286/PB279 and PB377/PB388 respectively. Plasmids containing the respective cDNA templates were used as a positive control. PCR products were probed with a [γ-^{32}P] labelled oligonucleotide internal to the PCR primers (PB287 for PI-9 or PB279 for graB) following Southern transfer. (B) Detection of perforin mRNA. Total RNA from either normal testis or the NK-like cell line, YT, was reverse transcribed and used as a template for PCR amplification of perforin using primers PB476 and PB477. PCR products were probed with a [γ-^{32}P] labelled oligonucleotide internal to the PCR primers (JT219) following Southern transfer. A plasmid containing the perforin cDNA was used as a positive control. (C) *In situ* hybridisation of normal adult testis using riboprobes specific for PI-9 or graB. The PI-9 antisense riboprobe indicated expression of PI-9 in Sertoli cells (Se) (ii) and (iii). The graB antisense probe indicated the presence of graB mRNA in primary spermatocytes (Sp) (v). Panels (i) and (iv) illustrate the absence of signal obtained using the sense probe for PI-9 or graB, respectively. Panel (vi) is a cartoon of a seminiferous tubule, burgundy illustrates the cell types found to be graB positive.

Analysis of the graB *in situ* hybridisation indicated expression in Sertoli cells as well as in germ cells at various stages of development. Precise identification of the spermatogenic cells expressing graB was difficult due to variation between samples, and their physical interaction with Sertoli cells. Nevertheless, examination of multiple sections indicated that graB positive cell types included some Type A spermatogonia and pre-leptotene spermatocytes, with the most obvious staining in pachytene spermatocytes (Figure 5.5C v). The distribution of graB positive cells, determined from multiple sections, and their location within the tubule is illustrated in Figure 5.5C vi. No graB was detected in late spermatids indicating that graB is lost in the later stages of meiosis and spermiogenesis.

5.5 Dysregulation of granzyme B and PI-9 in disease

To further elucidate the roles of graB and PI-9 in testicular function, their expression was examined in abnormally developed testes. In the maldescent testis either one or both of the testes fails to descend from the abdominal space into the scrotal sac, resulting in exposure to higher temperatures and loss of germ cell progenitors. The maldescent testis has an abnormal appearance, as the only cells present are abnormal Sertoli cells, often with large vacuoles. Both graB and PI-9 were detected in the aberrant Sertoli cells of the maldescent testis by immunohistochemistry (Figure 5.6A).

Analysis of graB and PI-9 gene expression was also performed using RNA extracted from four human testicular germ cell tumour lines (GCT 27C4, 27X1, 48 and 72, provided by M. Pera). Germ cell tumour lines are divided into subclasses on the basis of histology, cell surface antigen expression and their ability to differentiate into other cell types. The four lines chosen represent a spectrum of germ cell tumours; GCT 27C4 and GCT 48 are nullipotent embryonal carcinomas, GCT 27X1 is a multipotent embryonal carcinoma while GCT 72 is a yolk sac carcinoma resembling visceral endoderm (Pera *et al.*, 1987; Pera *et al.*, 1988; Pera *et al.*, 1989). Although the cDNAs were positive for GAPDH, neither graB nor PI-9 were detected by RT-PCR or Southern blotting with an internal oligonucleotide, indicating that both are absent from testicular germ cell tumours (Figure 5.6B). The lack of PI-9 is consistent with its absence from germ cells in normal testis, but the absence of graB suggests that it may be lost during tumourigenesis.

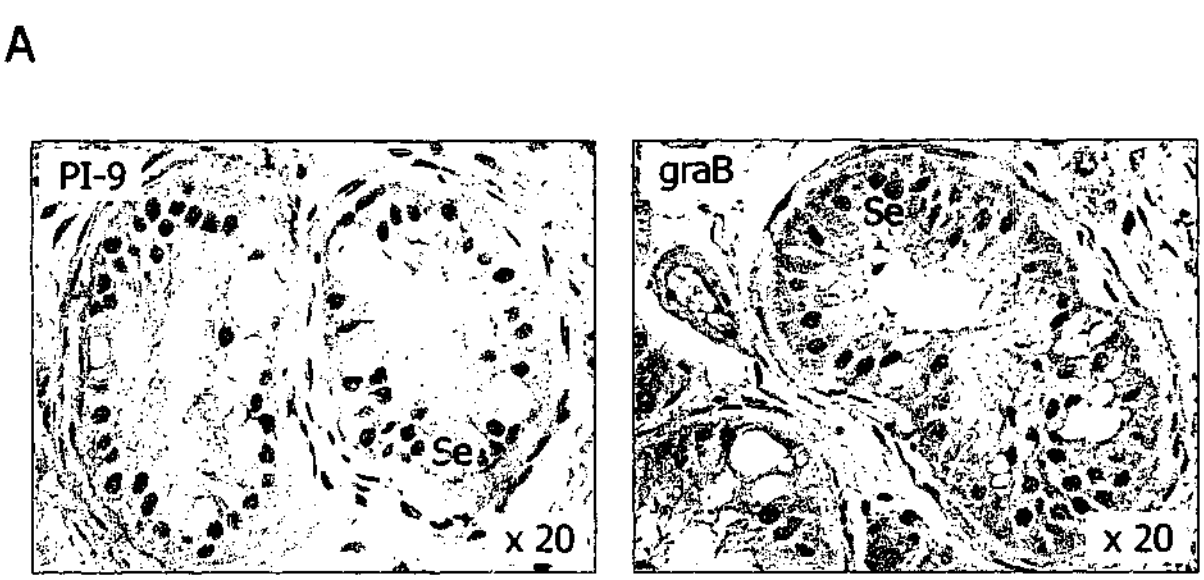

Figure 5.6 Dysregulation of PI-9 and granzyme B in abnormal testis. (A) Immunohistochemistry of maldescent testis using antibodies for PI-9 (7D8) or graB (2C5) demonstrated the presence of PI-9 and graB in Sertoli cells (Se). (B) Detection of PI-9 and graB mRNA in germ cell tumours. RNA from the indicated cell lines was reverse transcribed and used as a template for PCR amplification of both PI-9 and graB using primers PB174/PB287 and PB377/PB378 respectively. Plasmids containing the respective cDNA templates were used as a positive control. PCR products were probed with a [γ-^{32}P] labelled oligonucleotide internal to the PCR primers (PB286 for PI-9 and PB279 for graB) following Southern transfer.

5.6 Rodent models of PI-9 and granzyme B

Human testicular tissue is infrequently available and the work reported here was only possible due to the generosity of K. Loveland and D. de Kretser at the Monash Institute of Reproduction and Development. This lack of testicular material makes further analysis of the role of PI-9 and graB in human testis difficult. To increase understanding of the roles of both PI-9 and graB an animal model would be useful. Rodents are ideal as they are a more available source of tissue and are amenable to genetic manipulation. Furthermore, rodents proceed through an ordered process of spermatogenesis occurring in waves at precise intervals. Therefore at any given time point a defined set of cells are present in the seminiferous tubules. In humans however, spermatogenesis is asynchronous and the tubules contain a mixture of germ cells at various stages of spermatogenesis. The precise regulation of spermatogenesis in rodents allows for stage specific examination of the protein of interest.

Rats rather than mice were chosen as an experimental model, as mice have a greatly expanded repertoire of ov-serpins. The three ov-serpins found in humans on chromosome 6p25 (PI-9, PI-6 and M/NEI) are represented in the mice by 16 ov-serpins (7 PI-9-like, 6 PI-6-like and 3 M/NEI-like genes) on chromosome 13 (Kaiserman *et al.*, 2002). Moreover, the high homology found between members of the ov-serpin family (43 - 98%) makes analysis by immunohistochemistry or *in situ* hybridisation very difficult. Mice also have an expanded repertoire of granzymes, while there are 5 granzyme genes in humans there are 10 in mice, and again the high level of homology exhibited by this family (47 - 89%) complicates analysis. Although genetic analysis of the rat, in terms of the number of serpin and granzyme genes, is less complete than for the mouse, analysis of rat graB indicates it is more closely related to human graB, than mouse graB, and therefore the rat could provide a better model for the function of human graB.

The immunohistochemistry examining the expression of PI-9 in rat testis was performed by K. Loveland, using rabbit polyclonal anti PI-9 antiserum. A restricted cell pattern was detected in the rat testis with this antiserum (Figure 5.7A). In the immature testis (day 3) the strongest staining was observed in the gonocytes, which are the progenitors of the germ cells. Sertoli cells were also positive, consistent with human PI-9, however in the rat, PI-9 staining in Sertoli cells had a much fainter cytoplasmic staining with more prominent nuclear staining. There was also staining in fibroblastic-like cells in the interstitium. In the adult testis (day 40) staining for PI-9 was again most prominent in the nucleus of cells with little staining visible in the cytoplasm. Sertoli

A

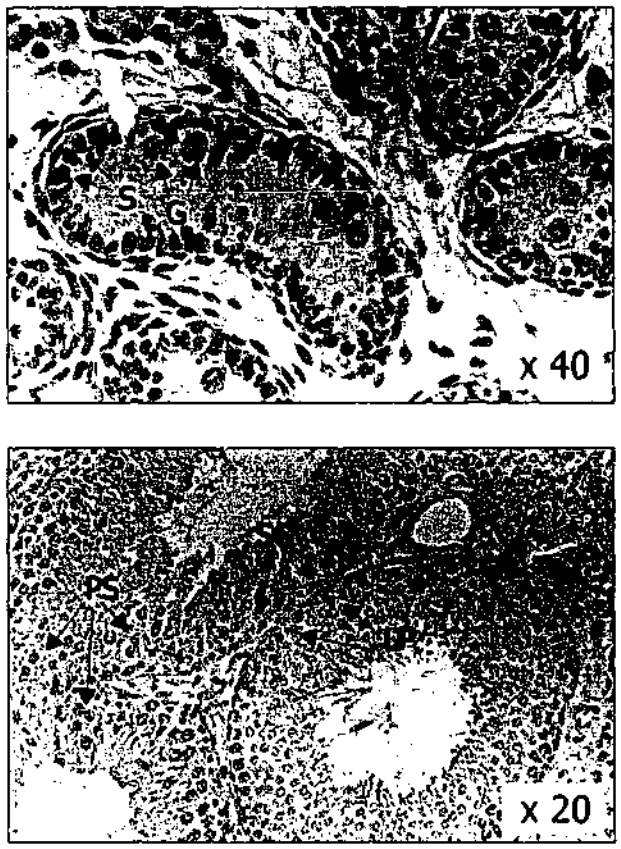

Day 3

Day 40

B

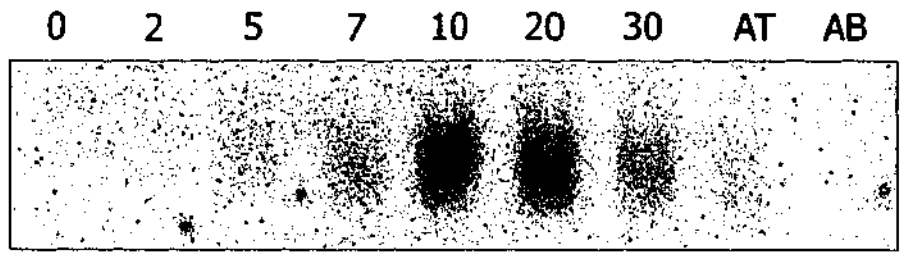

Figure 5.7 Expression of a PI-9-like protein and rat granzyme B mRNA in the rat testis.
(A) Immunohistochemistry of day 3 and day 40 rat testis was performed by K. Loveland. Sections of testis stained with anti PI-9 polyclonal antiserum indicated the presence of a PI-9-like protein in gonocytes (G), Sertoli cells (S), spermatogonia (SG), pre-leptotene spermatocytes (LP) and pachytene spermatocytes (PS). (B) Northern analysis of rat graB was performed by M. Bakker. RNA was extracted from rat testis at the indicated days post-partum as well as from adult testis (AT) and adult brain (AB). 30μg of total RNA was resolved by gel electrophoresis, transferred to nitrocellulose and hybridised with a [α-^{32}P] dCTP labelled probe. This probe was constructed by K. Scarff and consists of the entire 3'UTR of rat graB (RNKP-1).

cells, spermatogonia and pachytene spermatocytes were positive for PI-9, however pre-leptotene spermatocytes were negative. This suggests that PI-9 expression is tightly regulated in a stage specific manner.

Due to the lack of antibodies specific to rat graB, northern analysis was performed on total RNA extracted from the testes of rats over a range of ages, from day 0 (birth) to day 40 (adult), and was performed by M. Bakker. This blot was hybridised with a probe comprised of the 3'UTR of RNKP-1, the rat homologue of human graB (Zunino *et al.*, 1990; Sayers *et al.*, 1992). Rat graB mRNA was detected from day 5 into adulthood, however the highest levels were observed at days 10 and 20 (Figure 5.7B). This expression pattern coincides with the first wave of spermatogenesis in the rat. The differentiation of gonocytes into spermatogonia occurs between days 0 and 5 post partum, some spermatogonia remain as a self-renewing population, while most differentiate into spermatocytes. The initiation of gonocyte differentiation coincides with the onset of graB expression at day 5. By day 10 the spermatogonia have undergone the first meiotic division and have differentiated into spermatocytes, coinciding with the peak graB signal. With the generation of haploid spermatids by day 20, the graB signal was decreased and by day 35, as the first spermatozoa appear, the graB signal was very low.

This preliminary analysis of the rat indicates that PI-9 and graB have similar distributions in the testes of both humans and rats. In particular, the expression of graB in differentiating human germ cells closely matches that observed in the rat (as illustrated in Figure 5.8). As such the rat appears to be a good model for studying the role of PI-9 and graB in testicular development and function.

5.7 Discussion

This study has demonstrated that PI-9 has a restricted distribution, predominantly in immune cells and tissues, as well as in immune privileged sites. This distribution is consistent with earlier findings by Northern analysis, and is also consistent with a recent PI-9 tissue distribution study (Bladergroen *et al.*, 2001). However, PI-9 is not restricted to immune sites as low levels of PI-9 mRNA were found in the majority of tissues, indicating a broader expression pattern. Analysis by immunohistochemistry revealed that this was due to expression of PI-9 in endothelial, mesothelial and epithelial cells in all tissues examined (Buzza *et al.*, 2001). Very high levels of PI-9 mRNA were detected in the immune privileged tissues, the placenta and

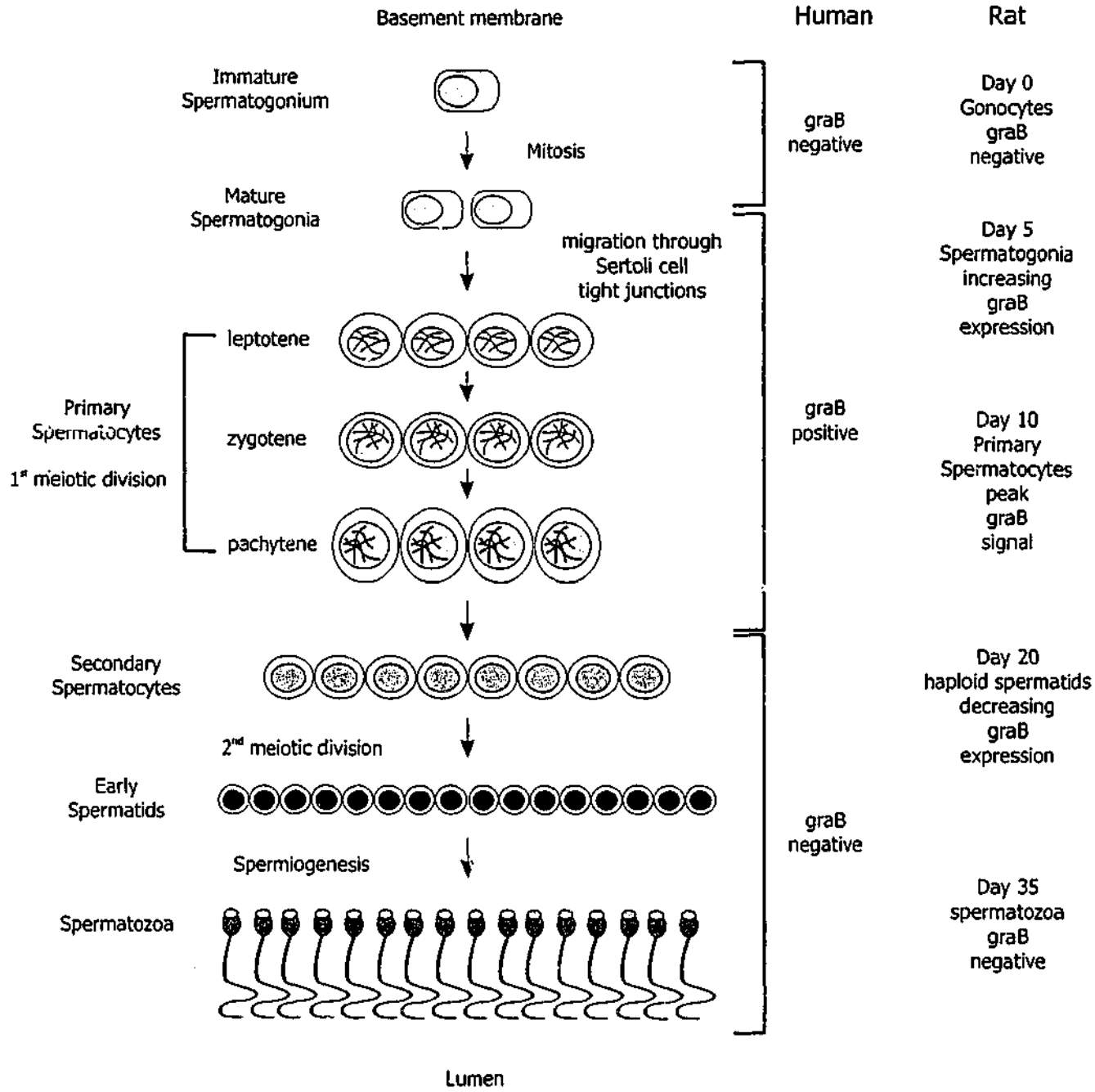

Figure 5.8 Spermatogenesis in the testis. Simplified diagram illustrating the cell types observed in the testis during spermatogenesis. Developing germ cells migrate from the basement membrane towards the lumen of the tubule. This migration coincides with the expression of graB, which is lost in later stages of germ cell development.

testis, and examination by immunohistochemistry indicated a restricted distribution of PI-9 to Sertoli cells in the testis and syncytial trophoblasts in the placenta.

This study demonstrated the expression of PI-9 and the perforin-independent expression of graB in the human testis, in contradiction to the current dogma that graB is confined to NK cells and activated CTL. The view that graB is present only in cytotoxic lymphocytes has arisen because the original analysis of graB mRNA expression was carried out on a panel of haemopoietic cell lines (Trapani *et al.*, 1988). Subsequent analyses have focused exclusively on tissues of the immune system (Held *et al.*, 1990; Hameed *et al.*, 1991; Ebnet *et al.*, 1995b; Kummer *et al.*, 1995). The multi-tissue mRNA dot blot used in this study indicated that graB has a wider than expected distribution, suggesting that activated CTL or NK cells are found in many tissues or that graB may be expressed outside the immune system.

The majority of the studies on graB function have focused on its activation of *intracellular* components, such as BID and caspases. However, a number of studies have indicated that graB is also released into the circulation during the immune response (Spaeny-Dekking *et al.*, 1998; Lauw *et al.*, 2000) and into the synovium during rheumatoid arthritis (Tak *et al.*, 1999; Ronday *et al.*, 2001). Studies have also identified *extracellular* substrates of graB, as graB can degrade components of the extracellular matrix such as the proteoglycan, aggrecan (Froelich *et al.*, 1993), and is able to cause detachment of adherent tumour cell lines (Sayers *et al.*, 1992). Furthermore, in $CD34^+$ peripheral blood progenitor cells, graB may play a role in detachment from bone marrow stromal cells (Berthou *et al.*, 1995). Thus, it is evident that graB has the ability to exert extracellular effects and may have a perforin-independent role in extracellular matrix remodelling. The finding that graB is expressed in the testis in the absence of perforin, suggests such a non-cytotoxic role for graB in reproduction.

GraB is produced as a zymogen which requires processing by dipeptidyl-peptidase-I (DPP-I) for its activity. Although studies on DPP-1 have focused on its role in activation of serine proteinases in immune and inflammatory cells, its expression has been demonstrated in primary spermatocytes (Chung *et al.*, 1998). Thus, the mechanism for graB activation exists in germ cells, further supporting the idea that graB mediated proteolysis occurs in these tissues.

Proteinases and their inhibitors play an important role in testicular development and germ cell maturation (reviewed in Fritz *et al.*, 1993). Controlled proteolytic activity is essential to the remodelling and restructuring of the seminiferous tubule during the

migration of germ cells from the basement membrane to the lumen of the tubule. The plasminogen activators t-PA (tissue type) and u-PA (urokinase) and their cognate inhibitors (PAI-1 and PAI-2) play a role in the degradation of tight junctions between Sertoli cells during testis development (Lacroix *et al.*, 1977). The plasminogen activators are also present in seminal plasma (Astedt *et al.*, 1979) and spermatozoa (Smokovitis *et al.*, 1992), and PAI-1 and PAI-2 are expressed within the seminiferous tubule (Gunnarsson *et al.*, 1999). Acrosomal serine proteinases such as acrosin, TESP-1 and TESP-2 (Kohno *et al.*, 1998) have also been implicated in the degradation of the zona pellucida (the envelope that surrounds the ova) and fertilisation of the ova. Serine proteinases of unknown function are also present in human testis. The proteolytic activity of leydin and testisin are unknown, however their restricted expression to Leydig cells and pachytene spermatocytes respectively, implicates them in testicular function (Hooper *et al.*, 1999; Poorafshar and Hellman, 1999).

Analysis of graB expression by immunohistochemistry and *in situ* hybridisation indicated that the basal population of spermatogonia residing against the basement membrane are graB negative. However, a proportion of the more mature spermatogonia were found to be graB positive. These cells represent the transition from the mitotic population to those cells proceeding into meiosis. This period also involves migration of the developing germ cells through the blood testis barrier towards the tubule lumen, a process that involves the proteolytic degradation of tight junctions between Sertoli cells. Primary spermatocytes were found to be graB positive. This was most apparent in the pachytene spermatocytes, which have a large cytoplasm and are present in most stages of the human seminiferous cycle. However, no graB was detected in secondary spermatocytes, late spermatids or mature spermatozoa, suggesting that graB is lost upon the second meiotic division, with the corresponding loss of cytoplasm that precedes the differentiation into spermatozoa. The expression of graB in germ cells in the early stages of spermatogenesis is consistent with a role for graB in the degradation of tight junctions between Sertoli cells, however the lack of graB in mature sperm suggests that it is not involved in fertilisation (illustrated in Figure 5.8).

The expression pattern of graB in the rat parallels that seen in humans, as graB was observed in spermatogonia and spermatocytes in the first meiotic division but was absent upon differentiation into secondary spermatocytes. Future work in rats will use the rat graB probe, used in the RNA analysis, to perform *in situ* hybridisation and identify the specific cell types expressing graB transcripts. Similarly, the expression of PI-9 in the rat parallels that seen in human. However, the rabbit polyclonal antiserum

use in the immunohistochemistry may be cross-reacting with other PI-9-like serpins. As such these results should be verified using another method, such as using PI-9 cDNA as a probe for *in situ* hybridisation at low stringency. Alternatively, the rat homologue of PI-9 should be identified and used as a specific probe. The isolation and characterisation of rat PI-9 will then allow further analysis into the role of PI-9 in testicular embryogenesis and spermatogenesis.

PI-9 is also expressed in the female reproductive tissue and the placenta. The role of PI-9 in placenta has been further examined by M. Buzza and it has been demonstrated that PI-9 is expressed in the syncytial trophoblast layer of the chorionic villi and in endothelial cells of the term placenta (Hirst *et al.*, 2001). Furthermore, graB is co-expressed with PI-9 in the syncytial trophoblasts. RT-PCR confirmed the expression of graB and PI-9 in syncytial trophoblasts in the absence of perforin. Others have shown that DPP-I is also expressed in human placenta, (Lampelo *et al.*, 1987; Rao *et al.*, 1997) therefore the mechanism to activate graB is also present in these cells. Several other serine proteinases and their inhibitors have been implicated in placental development, during implantation and the matrix remodelling required for invasion of the blastocyst (as reviewed in Salamonsen, 1999). In term placenta, matrix remodelling proteinases and inhibitors are also important during parturition (Tsatas *et al.*, 1998; Athayde *et al.*, 1999; Hu *et al.*, 1999; Riley *et al.*, 1999).

The perforin-independent expression of graB and PI-9 in both testis and placenta suggests a role for graB mediated proteolysis in reproduction. In the testis, graB may facilitate migration of developing germ cells, while in the placenta, it may contribute to extracellular matrix remodelling during implantation or parturition. The presence of PI-9 in Sertoli cells and the syncytial trophoblast layer, which form the blood-tissue barriers, is consonant with its role in cytoprotection against the apoptotic properties of graB. PI-9 may provide protection against graB produced by maternal or self-reactive cytotoxic lymphocytes and thus contribute to immune privilege. Although the entry of graB into the cytoplasm of cells normally requires perforin, other endosomolytic agents or events can mediate its release (Froelich *et al.*, 1996b; Browne *et al.*, 1999). Thus the presence of PI-9 in the cytoplasm and nuclei of cells producing graB (or in closely associated cells) may guard against inappropriate apoptosis in testis and placenta induced by mis-directed graB.

Chapter 6

PI-9 is Upregulated in Activated Cytotoxic Lymphocytes and Antigen Presenting Cells to Inactivate Ectopic Granzyme B

Summary

This chapter describes the expression and regulation of PI-9 in leukocytes, demonstrating expression of PI-9 in $CD4^+$ and $CD8^+$ T cells, NK cells, and at lower levels in B cells and myeloid cells. In CTL, PI-9 is upregulated in response to graB production and degranulation and co-localises with graB containing granules in activated CTL and NK cells. In addition, intracellular complexes of PI-9 and graB can be detected in NK cells and these complexes accumulate in the presence of proteosome inhibitors, demonstrating that there is a pool of cytoplasmic graB that is rapidly inactivated by PI-9. High levels of PI-9 are also present in dendritic cells within the thymic medulla and tonsillar germinal centres. Analysis of DC subsets purified from peripheral blood indicates that PI-9 is also expressed in $CD123^+$ plasmacytoid DC, $CD16^+$ monocyte DC precursors and monocyte derived DC (MDDC), and is upregulated upon TNFα induced maturation of MDDC. The regulated expression of PI-9 in these leukocyte subsets strongly supports the hypothesis that PI-9 protects effector, accessory and bystander cells from ectopic graB during an immune response.

Introduction

PI-9 is a potent inhibitor of graB that is present in graB expressing CTL and NK cells (Sun *et al.*, 1996). Analysis of PI-9 transcripts indicates that PI-9 is also expressed in some non-graB expressing cell lines of lymphoid but not myeloid origin. The expression of PI-9 in lymphocyte subsets is supportive of a role for PI-9 in protecting cells from mis-directed graB during the immune response. This model is corroborated by experiments which demonstrate that PI-9 transfected cells are protected from graB mediated apoptosis (Bird *et al.*, 1998).

During granule mediated apoptosis the granular contents are directed towards the target cell via the "immunological synapse" (Stinchcombe and Griffiths, 2001) and graB is endocytosed into the target cell primarily by the mannose 6-phosphate receptor (M6PR) (Motyka *et al.*, 2000). However, some graB may escape from the intercellular space, as indicated by the presence of free graB in the sera of patients with elevated CTL responses (Spaeny-Dekking *et al.*, 1998) and in those with severe Gram negative bacterial infections (Lauw *et al.*, 2000). Hence cells in the localised area of the immune response are also at risk from graB.

The expression of PI-9 in endothelial and mesothelial cells, which is upregulated by inflammatory stimuli, suggests that PI-9 protects bystander cells during the immune response (Buzza *et al.*, 2001). Other cells found at the site of the immune response include accessory cells such as antigen presenting cells, B cells and $CD4^+$ T helper cells. These cells provide the appropriate secondary signals and cytokine environment to support the immune response. For example, naïve $CD8^+$ T cells require activation by antigen presenting cells before they are able to differentiate into CTL, which involves the rapid induction of graB and perforin (Liu *et al.*, 1989; Oehen and Brduscha-Riem, 1998).

However, the presentation of MHC class I and peptide by the DC, which is necessary for the induction of effector function, also results in the DC becoming a potential CTL target. Indeed, several studies have shown that DC can be killed by activated CTL (Hermans *et al.*, 2000; Ludewig *et al.*, 2001). To counter this, DC express a number of anti-apoptotic proteins including Bcl-2 family members (Bjorck *et al.*, 1997; Wong *et al.*, 1997) and FLIP (Ashany *et al.*, 1999; Willems *et al.*, 2000). These proteins protect DC from Fas mediated pathways of apoptosis, however little is known about protection from apoptosis mediated by granule components.

6.1 The distribution of PI-9 in peripheral blood leukocytes

To extend previous observations that PI-9 is primarily expressed within lymphoid but not myeloid cells (Sun *et al.*, 1996), PI-9 expression was measured in peripheral blood leukocytes (PBL) by intracellular flow cytometry. PI-9 was evident in the majority of PBL, in both mononuclear cells (T and B lymphocytes) and in granulocytes (monocytes, neutrophils, basophils and eosinophils) (Figure 6.1A). The level of PI-9 detected in mononuclear cells varied - while the majority of cells were clearly positive, some had very low amounts of PI-9. Granulocytes also appeared to have very low amounts of PI-9, with only a slight positive shift apparent over the isotype control. Comparison of the fluorescence intensities indicated that the majority of mononuclear cells express at least 5-fold more PI-9 than granulocytes.

The PI-9 gene is located at chromosome 6p25 with two other genes encoding the closely related serpins, proteinase inhibitor 6 (PI-6) and monocyte/neutrophil elastase inhibitor (M/NEI) (Sun *et al.*, 1998). PI-6 is a potent inhibitor of cathepsin G (catG), and is expressed in monocytes and granulocytes to protect from the leakage of catG from azurophilic granules (Scott *et al.*, 1999b). M/NEI inhibits neutrophil elastase, catG and proteinase 3 which are also expressed in monocytes and neutrophils (Remold-O'Donnell *et al.*, 1989; Sugimori *et al.*, 1995). The inhibitory properties of this cluster of intracellular ov-serpins suggests that they protect leukocytes from endogenous granular proteinases (reviewed in Bird, 1999).

To establish the relative levels of PI-9, PI-6 and M/NEI in leukocyte subsets, the expression of these proteinase inhibitors was examined in cells purified from peripheral blood by indirect immunofluorescence (Figure 6.1B). Consistent with the flow cytometry data, this demonstrated that PI-9 is primarily restricted to lymphoid cells with small amounts in myeloid cells (monocytes and granulocytes). The highest levels of PI-9 were evident in NK and T cells ($CD4^+$ and $CD8^+$ T cells expressed equivalent levels), while B cells had very low levels. By contrast, PI-6 is highly expressed in the myeloid cells and is virtually absent from lymphoid cells, although it was detected at low levels in both NK cells and $CD8^+$ T cells. Contrary to previous reports that it is restricted to monocytes and neutrophils (Remold-O'Donnell *et al.*, 1989), M/NEI was evident in all leukocyte subsets examined, although the levels were highest in monocytes and granulocytes.

Thus, these highly homologous ov-serpins are expressed in leukocytes in a distinct but overlapping manner. The restricted expression pattern of PI-9 and PI-6 implicates these serpins in regulating distinct cognate proteinases expressed in similarly

A

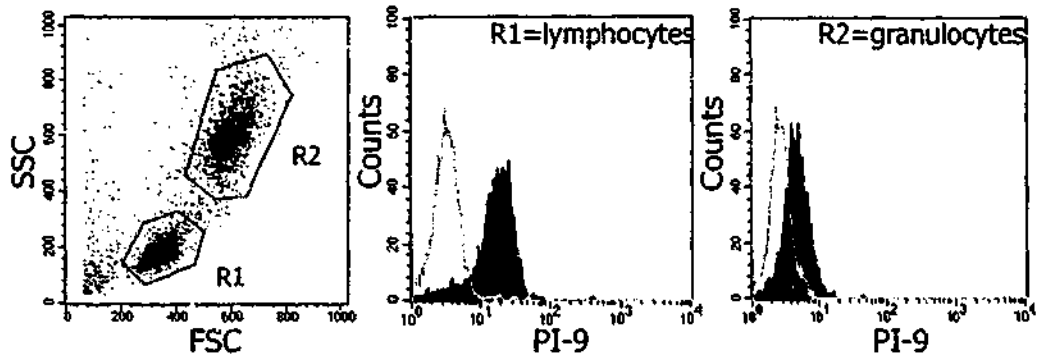

B

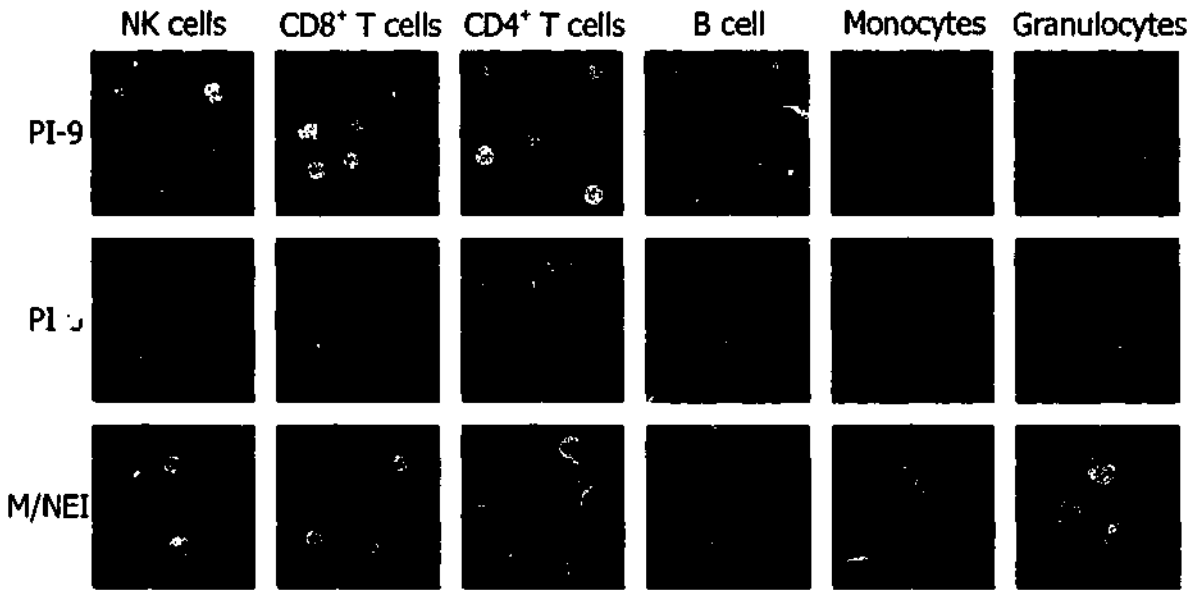

Figure 6.1 Distribution of ov-serpins in peripheral blood leukocytes (A) Flow cytometry analysis of PI-9 in PBL. PBL purified from healthy volunteers were stained with 7D8 (filled histogram) compared against the isotype control (gray line). Both the lymphocytic (R1) and granulocytic (R2) populations were positive for PI-9. This figure is representative of 4 different donors. (B) Relative distribution of ov-serpins in PBL. Purified leukocyte subsets were isolated as described in section 2.10.3. Indirect immunofluorescence was performed with a monoclonal antibody specific to each of the indicated serpins detected with FITC conjugated anti mouse IgG (green). The nuclei were counterstained with propidium iodide (red) and images obtained using laser scanning confocal microscopy. Relative levels of serpins are demonstrated as all images were obtained at the same time using the same instrument settings. This figure is representative of three separate experiments.

restricted subsets. The expression of M/NEI is broader than the distribution of neutrophil elastase, proteinase 3 or catG, suggesting this serpin regulates a yet to be identified proteinase(s) that is more widely expressed.

6.2 The intracellular localisation of PI-9 in granzyme B expressing cells

To further understand the role of PI-9 in protecting graB expressing cytotoxic lymphocytes from endogenous graB, the intracellular localisation of PI-9 in CL was examined. Indirect immunofluorescence and laser scanning confocal microscopy of activated CTL indicated that PI-9 was localised in punctate patches within the cytoplasm (Figure 6.2A), in addition to its previously reported cytoplasmic and nuclear distribution (Bird *et al.*, 2001). To determine whether this co-localised with graB, two-colour indirect immunofluorescence was performed. Confocal microscopy of cultured NK cells incubated with targets and stained for graB demonstrated a punctate staining pattern consistent with the localisation of graB in granules (Figure 6.2B). Further analysis indicated that graB was present in granules (secretory lysosomes) within these cells, as it co-localised with the granule marker LAMP-1, and not with markers for the ER or Golgi apparatus (data not shown). When cells were stained for PI-9 they again demonstrated a punctate pattern, which co-localised with the graB staining (Figure 6.2B). However, PI-9 is not in granules and therefore must be associating with the cytoplasmic face. This overlapping distribution of PI-9 and graB was also observed in the NK-like cell line, YT, which expresses very high levels of both PI-9 and graB (Figure 6.2C).

Due to the potent pro-apoptotic properties of graB, any graB entering the cytotoxic cell cytoplasm would need to be rapidly inhibited. As such the localisation of PI-9 to granules suggests that graB may leak from granules, and that PI-9 can protect cytotoxic lymphocytes in this context. To investigate this further, YT cells were examined for evidence of free cytoplasmic graB. When YT cells are lysed in NP40 lysis buffer, graB is released from granules and can complex with cytoplasmic PI-9 post-lysis (Bird *et al.*, 1998; Bird *et al.*, 2001). However, lysis in buffers containing SDS rapidly denatures graB preventing post-lysis interactions (Zapata *et al.*, 1998). Lysis of YT cells in SDS lysis buffer will prevent any artificial association between PI-9 and graB, and hence any complex detected in SDS-treated YT extracts must be formed before lysis.

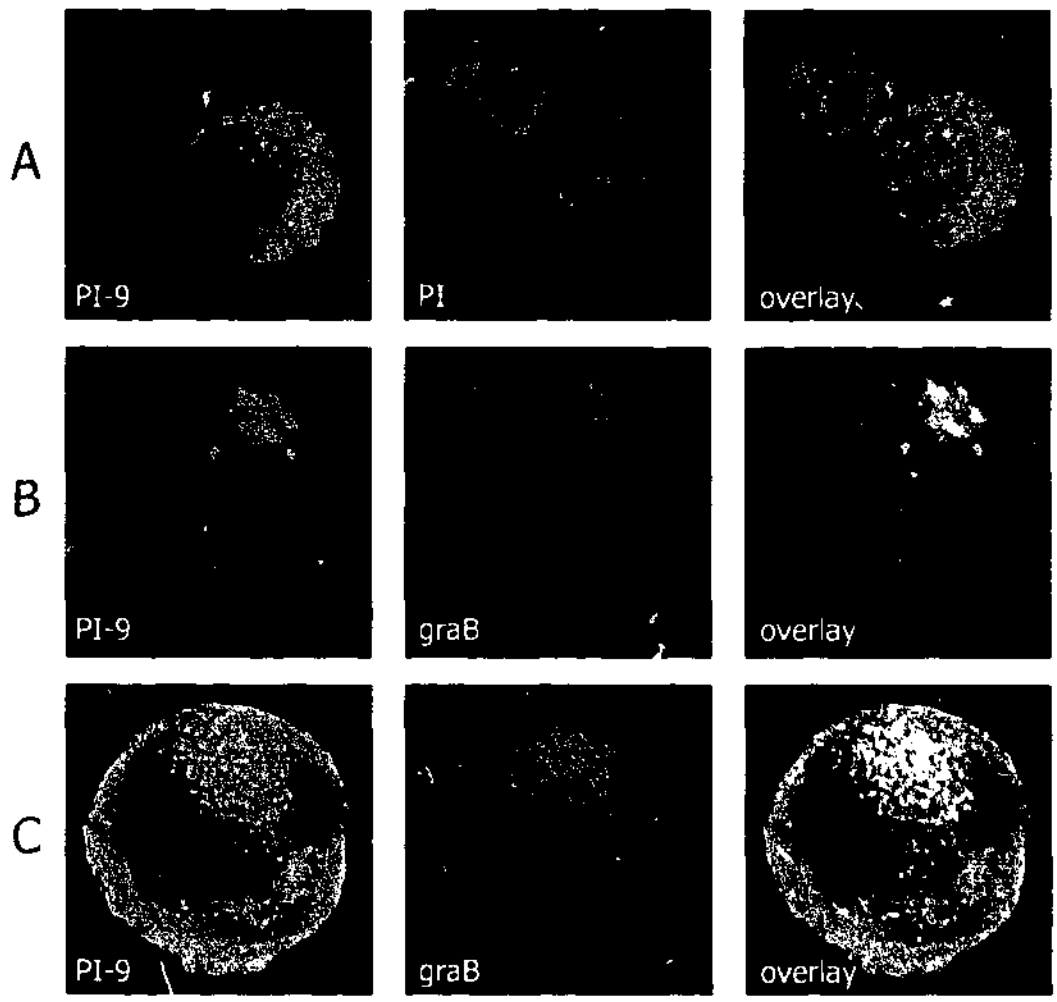

Figure 6.2 Co-localisation of PI-9 and granzyme B in cytotoxic lymphocytes. (A) Activated CTL were stained for PI-9 (7D8, green) and the nucleus counterstained with propidium iodide (PI, red). (B) Activated NK cells were stained for PI-9 (7D8, green) and graB (Rabbit anti graB/H, red). (C) YT cells were stained for PI-9 (Rabbit anti PI-9, green) and graB (2C5, red). Two-colour images were obtained using laser scanning confocal microscopy. (A) and (B) illustrate a single section through the cell, (C) is a projected view of multiple scans through the depth of the cell at 1 μm intervals to give a 3D representation of the entire cell.

PI-9/graB complexes in lysed YT cells were detected with the anti PI-9 polyclonal antisera Rabbit #12 and #15. Rabbit #15 has higher affinity for PI-9 than Rabbit #12 and preferentially recognizes the PI-9/graB complex (see Chapter 3, Figure 3.8B). Lysis of YT cells with NP40 lysis buffer generated a post-lysis complex of approximately 70 kDa, as well as complex breakdown products that were detected by both antisera but more efficiently by Rabbit #15. By contrast, when cells were lysed in SDS buffer a small amount of complex was detected by Rabbit #15 (Figure 6.3). This indicates that there is a pool of extra-granular graB in the cytoplasm of YT cells that interacts with PI-9.

Since serpin/proteinase complexes are essentially irreversible and involve conformational distortion of the proteinase (Huntington *et al.*, 2000), it was predicted that cytoplasmic PI-9/graB complexes would be recognized and rapidly degraded by the ubiquitin-proteosomal machinery. Cells cultured in the presence of a proteosome inhibitor should therefore accumulate complexes. Indeed, greater amounts of complexes were detected when cells were incubated in the presence of the proteosomal inhibitor, calpain inhibitor I (Figure 6.3). This also supports the idea that some graB enters the cytoplasm of YT cells during normal cellular function, and is rapidly inactivated by PI-9.

6.3 Regulation of PI-9 in granzyme B expressing cells

The hypothesis that PI-9 protects graB-expressing cells from endogenous graB is supported by the observations above that PI-9 associates with graB containing granules and extra-granular graB is detected in effector cells. Therefore it was predicted that upon cytotoxic cell stimulation, which increases the level of graB, there should be a corresponding increase in PI-9. The regulation of PI-9 was examined in T and NK cells under stimuli known to induce graB synthesis and release. T cells were stimulated with IL-2, which expands and activates T cells, or a combination of ConA and PMA, which activates T cells and causes granule exocytosis. Both of these stimuli induced graB expression, peaking at day 6 and day 3 respectively (Figure 6.4A and B). No significant increase in PI-9 was observed in T cells stimulated with IL-2 alone (Figure 6.4A), however, stimulation of T cells with ConA/PMA resulted in a three-fold induction of PI-9 over endogenous levels (Figure 6.4B). This stimulation also generated a higher molecular weight form of graB (35 kDa) that is only observed following T cell degranulation (Isaaz *et al.*, 1995). Thus, *in vitro*, PI-9 upregulation is associated with increased graB release rather than increased graB transcription.

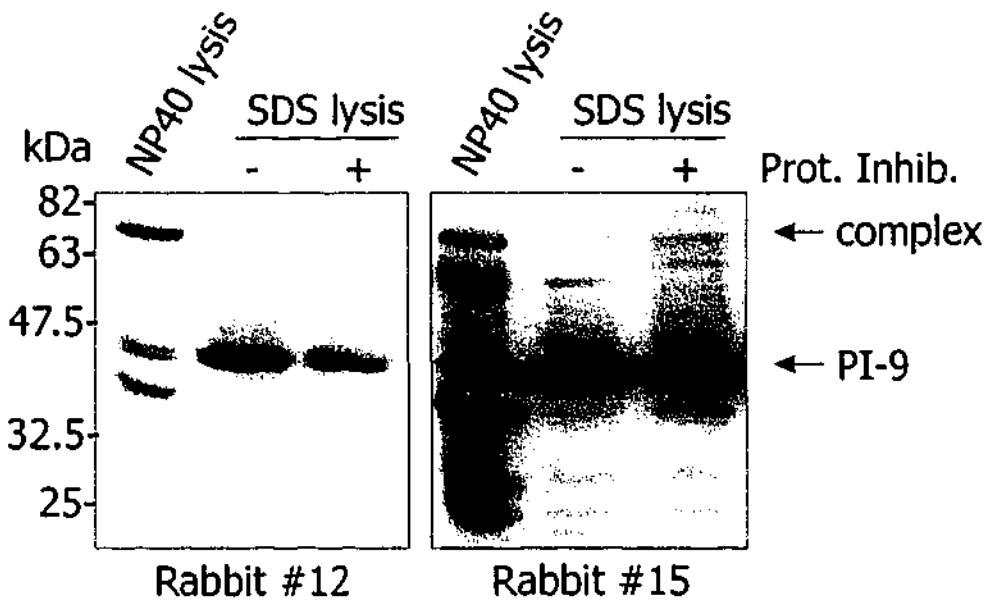

Figure 6.3 Detection of preformed complexes in cytotoxic cells. YT cells were incubated in the presence (+) or absence (-) of a proteosome inhibitor (Prot. Inhib.) then lysed in NP40 or SDS lysis buffer. Cell lysates were immunoblotted with Rabbit #15 diluted 1:2000 and detected with HRP conjugated anti rabbit Ig and enhanced chemiluminescence, then stripped and reprobed with Rabbit #12 diluted 1:2000. The position of free PI-9 (42 kDa) and that in complex with graB (60-75 kDa) is indicated on the right.

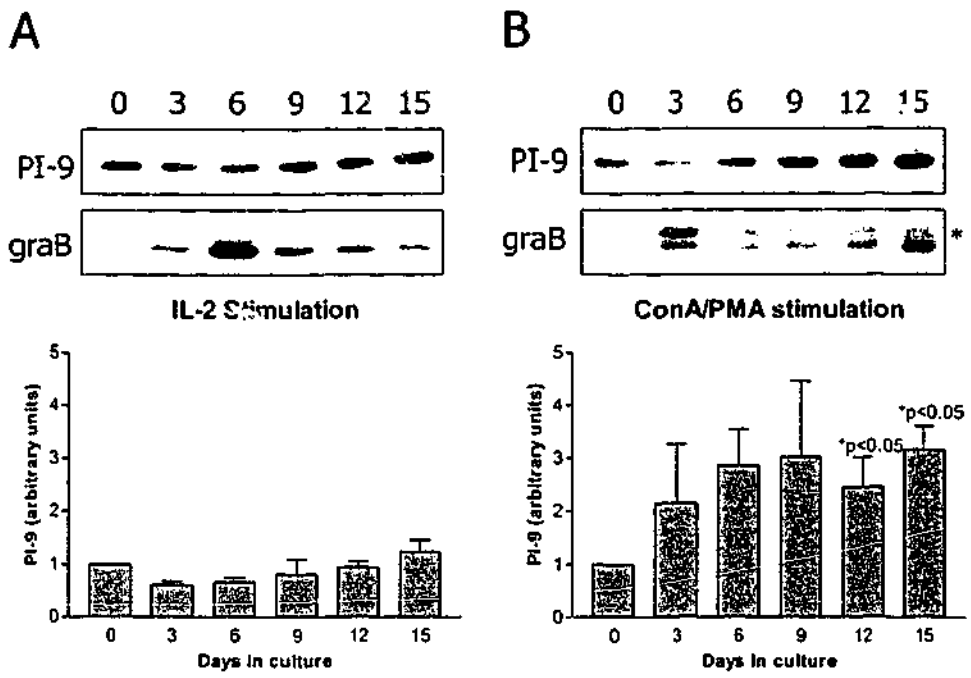

Figure 6.4 Regulation of PI-9 expression in activated cytotoxic lymphocytes. PBMC were activated in the presence of (A) 100 U/ml IL-2 or (B) a combination of ConA and PMA (10 µg/ml and 10 ng/ml respectively). (C) Culture generated quiescent NK cells were activated in the presence of irradiated MM [illegible] cells and [illegible] U/ml IL-2. On the indicated days cells were harvested and lysates prepared. 0.5 x 10^6 cells were loaded per lane, resolved by reducing 12.5% SDS-PAGE and sequentially immunoblotted with monoclonal antibodies to PI-9 (7D8, hybridoma supernatant diluted 1:10) and graB (2C5, diluted 1:2000) and detected with HRP conjugated anti mouse IgG and enhanced chemiluminescence. * Indicates the presence of the 35 kDa form of graB. Densitometric analysis was performed on immunoblots from four separate stimulations and the relative levels of PI-9 plotted (mean + standard deviation).

The regulation of PI-9 was also investigated in NK cells. Culture generated quiescent NK cells were activated by incubation with targets (irradiated MM-170 cells) in the presence of IL-2. These NK cells constitutively express both PI-9 and graB as evident on day 1 of the stimulation (Figure 6.4C). While activated NK cells killed MM-170 cells and upregulated graB, which peaked at day 3, no significant increase in PI-9 was detected over the time course.

Taken together, the above results suggest that constitutive levels of PI-9 in activated NK cells and proliferating, non-degranulating T cells are sufficient to protect them from low level, ectopic graB. However, the increase in PI-9 expression during degranulation suggests that granule exocytosis is associated with increased entry of graB into the effector cell cytoplasm, and that degranulating cells consequently require higher levels of PI-9.

Since PI-9 be upregulated in response to T cell degranulation *in vitro*, its expression was also investigated in activated T cells to determine if this occurred *in vivo*. Analysis was performed by immunohistochemistry of normal and inflamed human tissues. When normal spleen was examined using the specific PI-9 monoclonal antibody, 7D8, in standard immunohistochemical procedures, no PI-9 positive lymphocytes were detected (Figure 6.5b, c). However, when lymphocytes were extracted from freshly isolated spleen, and stained for PI-9 using the more sensitive technique of indirect immunofluorescence, PI-9 positive cells were apparent (Figure 6.5a). This indicated that the level of PI-9 expressed in resting lymphocytes was below the level of *immunohistochemical* detection using this antibody.

By contrast, when inflamed tissue samples were examined by immunohistochemistry, PI-9 positive cells were clearly evident within lymphocytic infiltrates. For example, PI-9 positive lymphocytes were observed in sections of a ductal carcinoma of the breast (Figure 6.5d). These cells were also positive for graB (Figure 6.5e) confirming that they were cytotoxic lymphocytes. Thus it appears that PI-9 is upregulated in graB-expressing effector cells *in vivo*.

6.4 Expression of PI-9 in dendritic cell populations

The protection hypothesis predicts that, in addition to protecting cytotoxic lymphocytes from endogenous graB, PI-9 should protect accessory and bystander cells from exogenous graB. In support of this idea, PI-9 positive dendritic cells were evident in tonsillar germinal centres using the immunohistochemical procedures described above (Figure 6.6b and c). PI-9 positive dendritic cells were also detected by two-colour

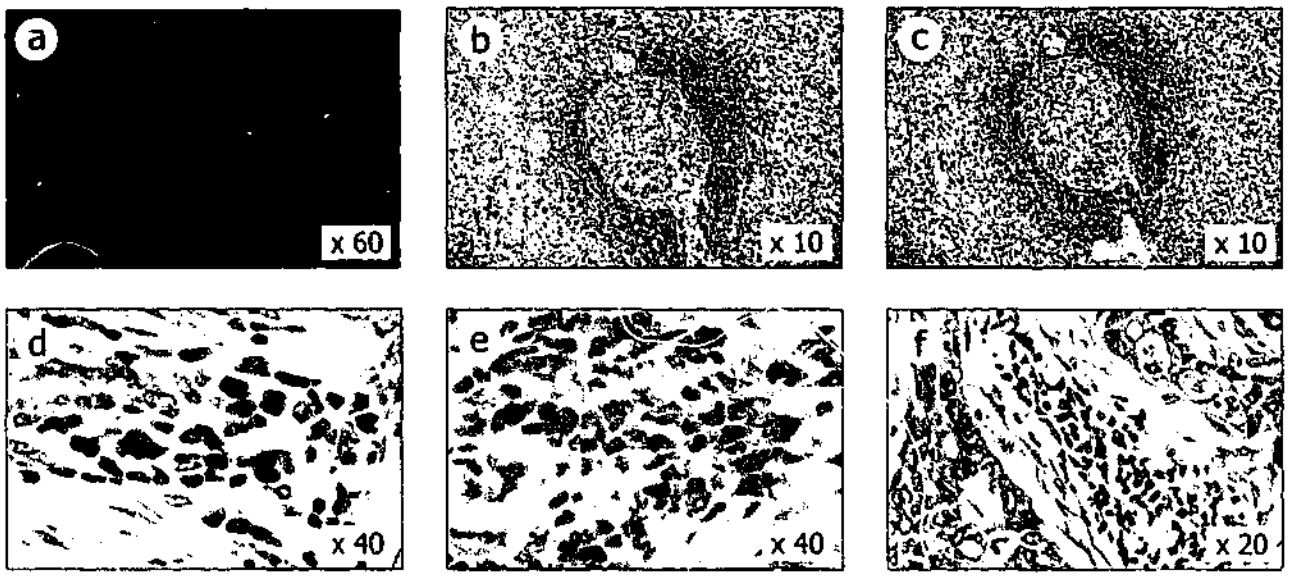

Figure 6.5 Expression of PI-9 in activated lymphocytes. (a) Indirect immunofluorescence of PI-9 (green) in lymphocytes isolated from normal spleen, (b) PI-9 is undetectable in formalin fixed, paraffin embedded normal spleen and (c) isotype control of a serial section of normal spleen. (d) Immunohistochemistry of PI-9 in activated lymphocytes in ductal breast carcinoma, (e) co-expression of graB in activated lymphocytes and (f) isotype control.

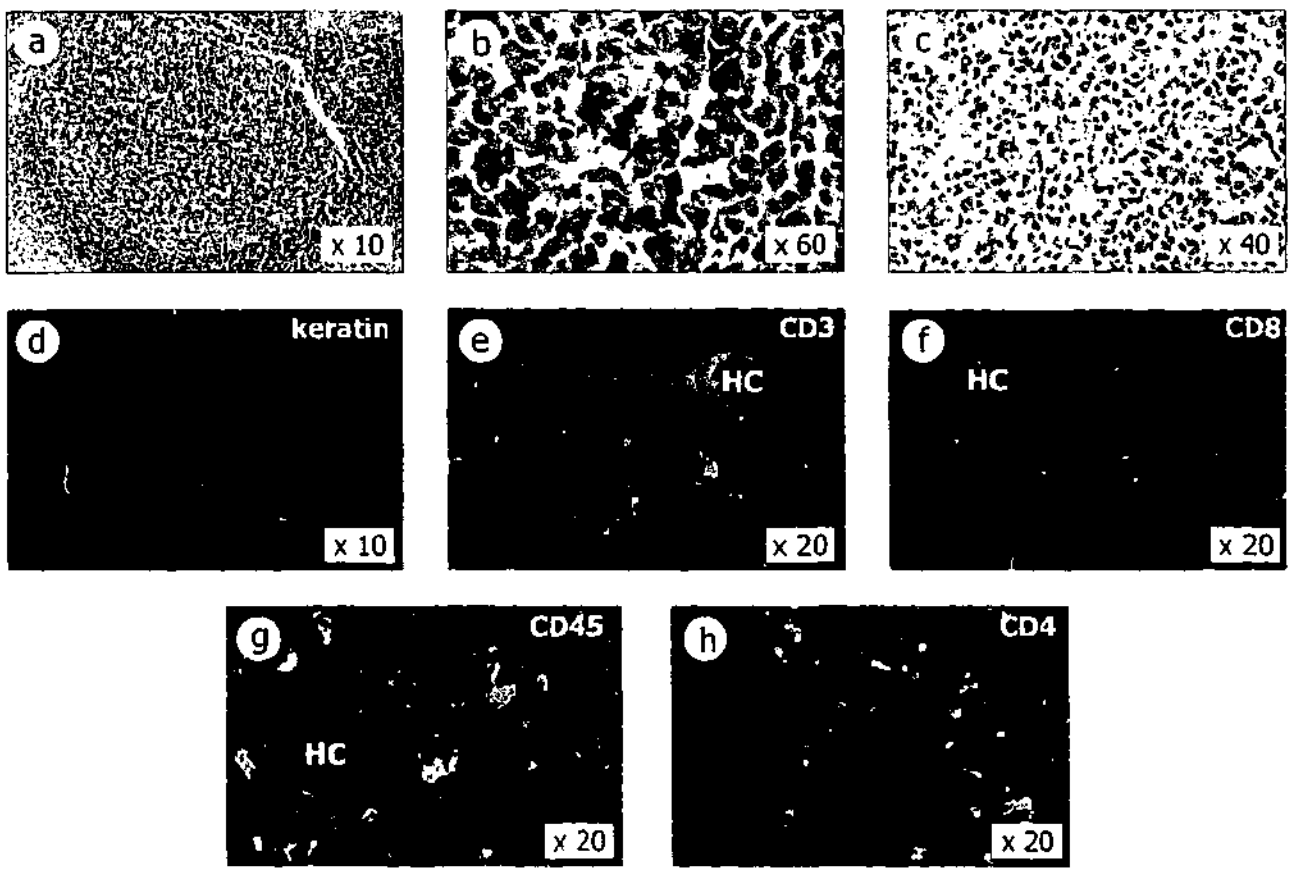

Figure 6.6 Expression of PI-9 and dendritic cells. (a) Localisation of PI-9 to dendritic cells within a tonsillar germinal centre, (b) higher magnification illustrating the dendritic morphology of the PI-9 positive cells and (c) isotype control. Localisation of PI-9 positive cells within the thymus. PI-9 positive cells (green) are located within the keratin negative medulla (d, red) which is also identified by the presence of Hassall's corpuscles (HC). PI-9 does not co-localise with $CD3^-$ thymocytes (e, red) or $CD8^-$ thymocytes (f, red) but slight co-localisation is noted where cytosolic PI-9 overlaps with membrane CD45 (g, red) and CD4 (h, red) expressed on dendritic cells.

immunofluorescence in the thymus. These thymic PI-9 positive cells were $CD3^-$ $CD8^-$ $CD4^+$ $CD45^+$ with dendritic cell morphology, and were located in the keratin negative medulla (Figure 6.6d - h). The morphology and phenotype of these PI-9 positive DC is consistent with several populations of human thymic DC recently described (Vandenabeele *et al.*, 2001). It is important to note that no PI-9 positive lymphocytes were detected in either tonsil or thymus, suggesting that DC constitutively express higher levels of PI-9 than resting or immature lymphocytes.

Since immunohistochemistry is not a quantitative technique, highly purified DC subpopulations and precursor populations were assessed for their relative levels of PI-9. These populations were isolated from whole blood and provided by P. Cameron. Consistent with the flow cytometry data, low levels of PI-9 were present in monocytes purified from PBL. IL-4 and GM-CSF induced differentiation of these cells into immature monocyte-derived dendritic cells (MDDC) resulted in a significant increase in PI-9 expression (Figure 6.7A). Maturation of MDDC by incubation with TNFα resulted in a further increase in the expression of PI-9 (Figure 6.7B). By densitometric analysis, this increase in PI-9 in MDDC was approximately 4-fold over monocytes, and increased a further 3.5-fold upon maturation with TNFα.

To identify specific DC types that express PI-9, subpopulations purified from whole blood (provided by P. Cameron) were examined for PI-9 by immunoblotting. The $CD16^+$ monocytic precursors of tissue DC (Grage-Griebenow *et al.*, 2001; Sanchez-Torres *et al.*, 2001) expressed higher levels of PI-9 than $CD16^-$ monocytes (Figure 6.7B). Lineage negative DC purified from peripheral blood expressed PI-9 at an intermediate level between monocytes and MDDC (Figure 6.7A). These lineage negative DC contain two major populations; $CD1b/c^+$ Langerhans cell precursors (Ito *et al.*, 1999) (the resident DC in the skin) and $CD123^+$ plasmacytoid DC (Olweus *et al.*, 1997) (which reside in secondary lymphoid organs). The plasmacytoid DC expressed an intermediate level of PI-9 while Langerhans cell precursors expressed virtually no PI-9 (Figure 6.7B).

The differential expression of PI-9 in DC populations from both the myeloid and lymphoid lineages is illustrated in Figure 6.7C. This suggests that expression is not limited by ancestry, and that differing requirements for protection from graB during antigen presentation to naïve $CD8^+$ T cells, and the induction of effector functions regulate PI-9 expression.

Figure 6.7 Expression of PI-9 in primary dendritic cells and monocyte derived dendritic cells. (A) 50 μg of cell lysate prepared from elutriated monocytes (Mono), sorted monocytes (sMono), lineage negative dendritic cells (lin^- DC), monocyte derived dendritic cells (MDDC), T cells or (B) sorted monocytes further divided into $CD16^+$ and $CD16^-$ populations, lineage negative DC divided into $CD1b/c^+$ (Langerhans cell precursors) and $CD123^+$ (plasmacytoid DC), and MDDC cultured in the presence (+) or absence (-) of TNFα (10 ng/ml) for 2 days were resolved by 12.5% reducing SDS-PAGE, transferred to nitrocellulose and immunoblotted for PI-9 with 7D8 hybridoma supernatant diluted 1:10, detected with anti mouse IgG and enhanced chemiluminescence. (C) Simplified diagram illustrating the differentiation of DC from either a myeloid or lymphoid precursor. Boxed populations were assessed for PI-9 by immunoblotting and immunohistochemistry (shades of grey represent relative levels of PI-9). Chequered boxes indicate that while PI-9 positive DC were observed in the thymus, the phenotype of these DC is not yet known. Dashed arrows indicate *ex vivo* stimulation. Modified from Ardavin *et al.*, 2001 with additional information from Grouard *et al.*, 1996, Sanchez-Torres *et al.*, 2001, Summers *et al.*, 2001 and Vandenabeele *et al.*, 2001.

A

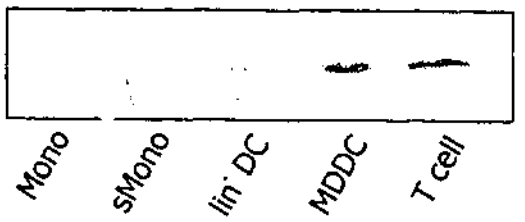
Mono
sMono
lin⁻ DC
MDDC
T cell

B


CD16⁻
CD16⁺
CD1b/c⁺
CD123⁺
- TNF
+ TNF
sMono
lin⁻ DC
MDDC

C

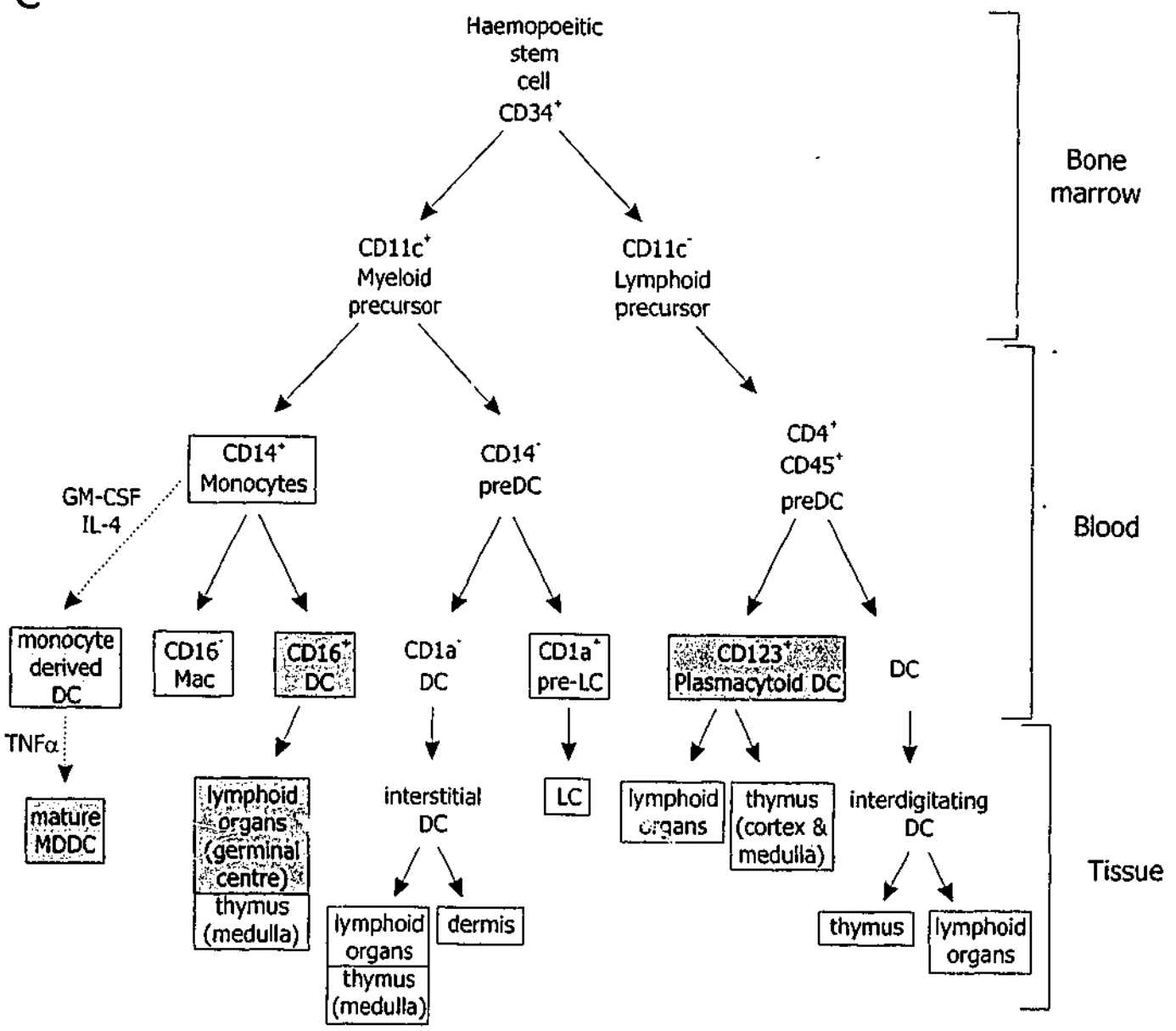
Haemopoeitic stem cell CD34⁺
CD11c⁺ Myeloid precursor
CD11c⁻ Lymphoid precursor
CD14⁺ Monocytes
CD14⁻ preDC
CD4⁺ CD45⁺ preDC
GM-CSF IL-4
monocyte derived DC
CD16⁻ Mac
CD16⁺ DC
CD1a⁻ DC
CD1a⁺ pre-LC
CD123⁺ Plasmacytoid DC
DC
TNFα
mature MDDC
lymphoid organs (germinal centre) thymus (medulla)
interstitial DC
LC
lymphoid organs
thymus (cortex & medulla)
interdigitating DC
lymphoid organs thymus (medulla)
dermis
thymus
lymphoid organs
Bone marrow
Blood
Tissue

6.5 Discussion

Cells have evolved a number of mechanisms to prevent inappropriate apoptosis. For example, IAPs inhibit caspases directly (Deveraux *et al.*, 1997) while c-FLIP blocks Fas mediated apoptosis (Kataoka *et al.*, 1998) and the Bcl-2 family members regulate apoptosis at the mitochondria (reviewed in Adams and Cory, 2001; Shi, 2001). It has been proposed that PI-9 is another protective mechanism employed by cells, to provide protection from mis-directed graB (Sun *et al.*, 1996; Bird *et al.*, 1998; Buzza *et al.*, 2001; Hirst *et al.*, 2001). Furthermore, there is mounting evidence that PI-9 and the other intracellular serpins are part of the anti-apoptotic machinery of specific cell types, particularly those involved in, or exposed to, the cellular immune response (Bird, 1999; Scott *et al.*, 1999b; Bladergroen *et al.*, 2001; Medema *et al.*, 2001b).

Expression and regulation of PI-9 in cytotoxic lymphocytes

A role for PI-9 in protecting graB expressing cells is supported by the unusual intracellular distribution of PI-9 described in the first part of this chapter. In addition to its cytoplasmic and nuclear localisation (Bird *et al.*, 2001), PI-9 in cytotoxic lymphocytes is associated with graB containing granules. This co-localisation is not due to direct contact between PI-9 and graB, as PI-9 is not present within the granule (Sun *et al.*, 1996). Therefore PI-9 must associate with the cytoplasmic face of the granule. PI-9 has only been observed to associate with the granules of CTL and NK cells. This suggests that PI-9 interacts with a specific granular membrane protein or lipid that is not found in other membrane bound organelles. (The lipid content of the granule membrane differs from that of the plasma membrane and other organelles (Takai *et al.*, 1997)).

GraB is stored as an active proteinase (Pham and Ley, 1999), and therefore leakage from the granules would allow active graB access to its cytoplasmic substrates, inducing apoptosis. The positioning of PI-9 at the granule surface and the low level of PI-9/graB complexes that were detected in cells suggests that these granules do leak and that PI-9 is present to rapidly inactivate graB. Granules are modified lysosomes containing lysosomal hydrolases in addition to the granzymes and perforin (Burkhardt *et al.*, 1990; Peters *et al.*, 1991; Page *et al.*, 1998). While there is no direct evidence to suggest that granules leak, lysosomal rupture can be induced by oxidative stress leading to apoptosis (discussed in Brunk *et al.*, 1997; Brunk *et al.*, 2001). Increased levels of reactive oxygen species have been observed in activated CL which, under certain circumstances, can lead to apoptosis (Hildeman *et al.*, 1999), suggesting that granule leakage may occur during effector cell activation and/or function.

The protective role of PI-9 is also supported by the significant increase in PI-9 detected during degranulation induced by ConA/PMA. Once granule exocytosis is triggered the granules are refilled with newly synthesised graB. However, some graB bypasses the granule pathway and is secreted as a 35 kDa form (Isaaz *et al.*, 1995) (observed in Figure 6.4B). This 35 kDa form of graB is a convenient marker of degranulating cells, and its appearance along with an increase in PI-9 suggests that graB mis-direction occurs during T cell degranulation.

Release of graB into the effector cell cytoplasm need not only occur from leaking granules. It is possible that secreted graB is endocytosed by effector cells. The uptake of graB into target cells is mediated primarily by the 300 kDa mannose-6 phosphate receptor (M6PR) (Motyka *et al.*, 2000). The M6PR is expressed in all nucleated cells with up to 20% present at the cell surface at steady state (Willingham *et al.*, 1983; Geuze *et al.*, 1984; Geuze *et al.*, 1985; Braulke *et al.*, 1987; Griffiths *et al.*, 1990), and therefore T cells have the potential to internalise graB via the M6PR. Furthermore, the M6PR is upregulated on activated T cells (Hindmarsh *et al.*, 2001), which would potentially *increase* their susceptibility to secreted graB.

The association of PI-9 with granules observed here, in addition to its previously noted nucleocytoplasmic distribution of PI-9 in CL (Bird *et al.*, 2001) suggests that PI-9 can protect CL from graB at distinct sites. The expression of PI-9 in the nucleus indicates that it may protect CL from graB that is rapidly translocated to nucleus (Trapani *et al.*, 1994; Jans *et al.*, 1996), while PI-9 associated with cytotoxic granules may protect from leakage of active graB into the cytoplasm (Figure 6.8A i). The upregulation of PI-9 during degranulation may protect CL from leakage of graB into the cytoplasm, during the fusion of the granule to the plasma membrane (Figure 6.8A ii). Furthermore, after exocytosis of granular contents, PI-9 can rapidly inactivate any graB that is re-internalised via the M6PR (Figure 6.8A iii).

Expression of PI-9 in accessory and bystander cells

The cellular immune response involves a complex interplay between many cell types. Antigen presenting or accessory cells (DC, macrophages and B cells) induce the differentiation of naïve T cells into cytotoxic or helper T lymphocytes by secretion of cytokines and expression of co-stimulatory molecules. However, these accessory cells are closely associated with CTL and are therefore likely to be exposed to graB and perforin during an immune response (as illustrated in Figure 6.8B).

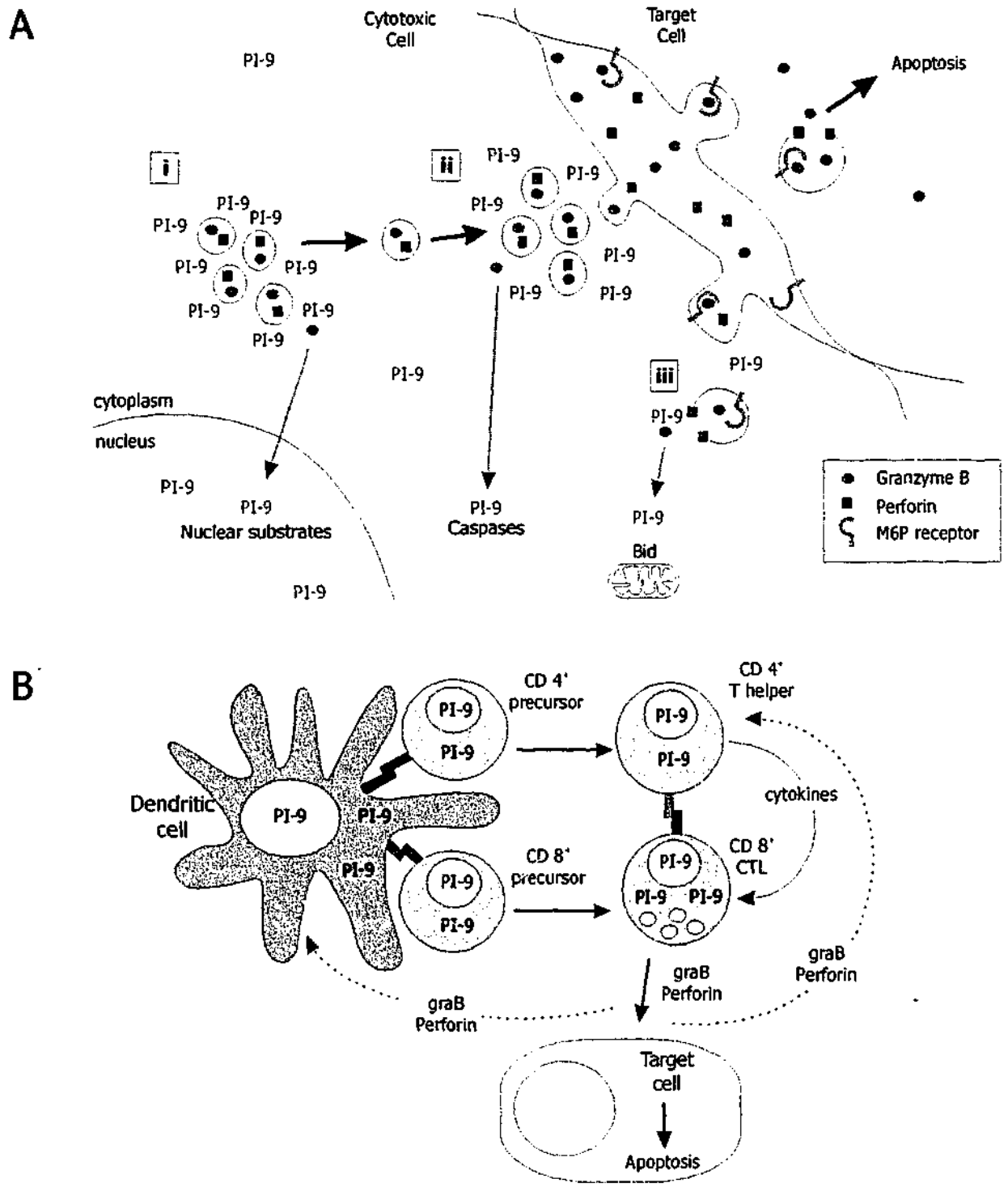

Figure 6.8 PI-9 protects cells from mis-directed granzyme B. (A) PI-9 protects cytotoxic lymphocytes from mis-directed granzyme B. PI-9 protect CL at a number of levels. (i) PI-9 is associated with the cytotoxic granules to protect from leakage of active graB into the cytoplasm. (ii) PI-9 is upregulated during degranulation to protect CL from leakage graB into the cytoplasm during the fusing of the granule to the plasma membrane and (iii) from any graB that is reinternalised via the M6PR. Thus, PI-9 protects cells from graB mediated cleavage of nuclear substrates, the caspases or mitochondrial proteins such as Bid. (B) PI-9 protects bystander and accessory cells from mis-directed graB. The antigen specific interaction of precursor $CD4^+$ and $CD8^+$ T cells with MHC Class II and I on dendritic cells results in differentiation into effector cells. $CD4^+$ T helper cells can provide the appropriate cell-cell contact and cytokines for the expression of the effector molecules (graB and perforin) in $CD8^+$ CTL. During effector functions and release of granule contents towards the target cell graB may escape from the immunological synapse and affect surrounding cells. The nucleocytoplasmic expression of PI-9 in $CD4^+$ T cells and dendritic cell populations is consistent with protecting these cells from mis-directed graB.

Tissue resident immature DC are efficient antigen scavengers which, upon maturation, upregulate MHC class I / II and co-stimulatory molecules and migrate to the draining lymph node to present antigen. DC have established roles in presenting antigen to $CD4^+$ T helper cells and eliciting T_H1 (CTL) or T_H2 (B cell) responses. However, distinct DC subpopulations have also been shown to directly interact with B cells or $CD8^+$ CTL. For example, follicular dendritic cells in the germinal centre directly contribute to B cell proliferation and differentiation (Grouard *et al.*, 1995) while virally infected DC and DC purified from blood can directly present to $CD8^+$ T cells in the absence of $CD4^+$ T helper cells (Young and Steinman, 1990; Bhardwaj *et al.*, 1994). However, this T helper independent activation of naïve $CD8^+$ is dependent upon upregulation of CD40-L by the DC (Bennett *et al.*, 1998; Schoenberger *et al.*, 1998).

This close association of activated CTL with DC may result in elimination of DC by effector CTL, as effector functions in CTL are rapidly induced (Liu *et al.*, 1989; Oehen and Brduscha-Riem, 1998). Although elimination of DC in normal mice is not usually observed, presumably due to protective mechanisms, the elimination of antigen specific DC by cognate CTL has been observed in several transgenic mouse models (Hermans *et al.*, 2000; Ludewig *et al.*, 2001), demonstrating that DC are *potentially* susceptible to CTL. However, there is controversy as to how this CTL dependent clearance of DC is mediated. One study found DC elimination to be independent of Fas and perforin (Ludewig *et al.*, 2001), while another reports that it is mediated partly by the perforin pathway (Loyer *et al.*, 1999)..

DC express a number of anti-apoptotic proteins. They are protected from Fas mediated apoptosis through expression of FLIP (Ashany *et al.*, 1999; Willems *et al.*, 2000), upregulation of Bcl-2 (Bjorck *et al.*, 1997) and upregulation of Bcl-xL mediated by TRANCE (Wong *et al.*, 1997). This laboratory and others have suggested that the expression of PI-9 in DC is consistent with a role in preventing graB mediated apoptosis during antigen presentation to CTL (Bird, 1999; Bladergroen *et al.*, 2001). This is further supported by the recent report that SPI-6, one of seven murine PI-9 homologues (Kaiserman *et al.*, 2002), protects murine DC from CTL induced apoptosis (Medema *et al.*, 2001b).

As shown in this study, PI-9 is not expressed in all DC subtypes but is restricted to specific subpopulations. PI-9 is expressed in both lymphoid derived plasmacytoid DC and myeloid derived $CD16^+$ precursor DC populations, indicating that PI-9 is not restricted to cells of lymphoid origin. In MDDC, PI-9 expression is upregulated upon maturation with TNFα, consistent with a role for PI-9 in protection of DC during

antigen presentation. PI-9 is also expressed in tissue resident DC in the thymus and germinal centre, however at this time it is unknown whether these cells are of lymphoid or myeloid origin.

Thymic medullary DC comprise three different subsets: a major $CD11b^-$ subset of lymphoid origin, a minor $CD11b^+$ subset of myeloid origin (Vandenabeele *et al.*, 2001) as well as a population of plasmacytoid DC. The $CD11b^+$ thymic DC resemble tonsillar germinal centre DC (Grouard *et al.*, 1996) and are thought to be phenotypically and morphologically related to them (Vandenabeele *et al.*, 2001). Considering this relationship, it is likely that the PI-9 positive DC observed in the thymus (Figure 6.6) are related to the PI-9 positive DC located in the tonsil. Both of these DC populations are thought to be derived from $CD16^+$ myeloid precursors (Almeida *et al.*, 2001; Grage-Griebenow *et al.*, 2001; Sanchez-Torres *et al.*, 2001). PI-9 is highly expressed in $CD16^+$ monocytes, which is consistent with PI-9 expression in the $CD11b^+$ thymic DC and tonsillar germinal centre DC.

The differential expression of PI-9 in DC suggests a differential requirement for protection from graB mediated apoptosis in DC subsets. Thymic medullary DC are essential in the positive and negative selection of thymocytes. GraB positive cells are present in the thymic medulla with graB transcripts detected in double positive ($CD4^+$ $CD8^+$) thymocytes, (Held *et al.*, 1990) and in both $CD4^+$ and $CD8^+$ single positive thymocytes (Ebnet *et al.*, 1995b). This suggests that thymocytes undergoing selection express graB and are capable of cytotoxic functions. Thus the presence of PI-9 in thymic medullary DC is consistent with a role in protecting these DC from graB mediated apoptosis.

Some subsets of germinal centre DC are involved in presentation and activation of T cells directly (Grouard *et al.*, 1996) while plasmacytoid DC are interferon-producing cells (Cella *et al.*, 1999; Siegal *et al.*, 1999; Kadowaki *et al.*, 2000) that respond rapidly to initiate potent T_H1 (CTL) responses (Cella *et al.*, 2000). The expression of PI-9 in these cells suggests that DC populations that present to, and activate, $CD8^+$ precursor T cells are at risk from the effector functions of the T cells they activate. This is also supported by the upregulation of PI-9 in MDDC upon TNFα induced maturation, suggesting that antigen presenting cells require protection from inappropriate apoptosis.

It would be advantageous for other accessory or bystander cells to express PI-9 to protect against mis-directed graB released during the immune response. PI-9 is expressed in endothelial and mesothelial cells suggesting that it protects bystander cells.

(Buzza *et al.*, 2001). As shown here, PI-9 is also present in accessory cells including $CD4^+$ T cells, B cells, monocytes and granulocytes. The expression of graB and perforin has been demonstrated in human $CD4^+$ CTL (Susskind *et al.*, 1996; Yasukawa *et al.*, 2000), suggesting that PI-9 may also have a cytoprotective role in some $CD4^+$ T cells. The level of PI-9 expressed in B cells, monocytes and granulocytes is lower than that seen in cytotoxic lymphocytes or DC and it is unlikely that they would be protected from direct CTL attack. Hence these cells have sufficient PI-9 to cope with low level mis-directed graB but could still be cleared by CTL if they become virally infected or tumourigenic.

Expression of PI-9 related serpins in leukocytes

Finally, analysis of the distribution of serpins closely related to PI-9 in PBL has also provided insight into their physiological roles. The highest levels of M/NEI and PI-6 were observed in granulocytes and monocytes. M/NEI can inhibit the azurophilic granular proteinases elastase, proteinase 3 and catG (Remold-O'Donnell *et al.*, 1989; Sugimori *et al.*, 1995) while PI-6 is a potent inhibitor of catG (Scott *et al.*, 1999b). CatG can activate the pro-apoptotic caspase, procaspase-7 (Zhou and Salvesen, 1997) and cleave the nuclear protein, brm (Biggs *et al.*, 2001), while elastase can induce apoptosis of neutrophils (Trevani *et al.*, 1996) and endothelial cells (Yang *et al.*, 1996). Therefore, the uncontrolled release of these pro-apoptotic proteinases into the cytosol of monocytes and granulocytes would be detrimental as they could activate intrinsic apoptotic pathways.

In addition to the reported expression of M/NEI in monocytes and granulocytes (Remold-O'Donnell *et al.*, 1989), M/NEI was found in all leukocytes examined and low levels of PI-6 were detected in $CD8^+$ T cells and NK cells. These cell types do not express catG or elastase, however these proteinases are released from monocytes and granulocytes during the immune response (Campbell *et al.*, 1989). Therefore, PI-6 and M/NEI may protect bystander cells from exogenous catG and elastase in a manner analogous to that of PI-9. Alternatively, M/NEI and PI-6 may inhibit other granular proteinases. Both PI-6 and M/NEI can inhibit multiple serine proteinases through use of alternate P_1 residues (Coughlin *et al.*, 1993; Riewald and Schleef, 1996; Cooley *et al.*, 2002), and thus may inhibit as yet unidentified granular or lysosomal proteinases expressed in these cells.

Chapter 7

The Endogenous Granzyme B Inhibitor, PI-9

The tissue distribution studies performed in this thesis have revealed that PI-9 is expressed in NK cells and $CD8^+$ and $CD4^+$ T cells and is also detected in lower amounts in B cells, monocytes and neutrophils. Furthermore, PI-9 is upregulated in response to CL degranulation and co-localises with graB containing granules, consistent with a role in protecting CL from leakage of endogenous graB. Analysis of DC subsets purified from peripheral blood indicates that PI-9 is expressed in DC of lymphoid and myeloid origin, and is upregulated upon TNFα induced maturation of monocyte derived DC. The regulated expression of PI-9 in leukocyte subsets is consistent with a role for PI-9 in protecting effector, accessory and bystander cells from ectopic graB during an immune response.

PI-9 is not only expressed in cells of the immune system as it is also detected in cells of epithelial origin and in immune privileged sites such as the testis and placenta. Expression of PI-9 in these sites is also consistent with a role for PI-9 in protecting bystander cells from ectopic graB during an immune response, or from inadvertent apoptosis induced by auto-reactive or allogeneic T cells. However, the co-expression of graB with PI-9 in the testis suggests that graB may have a non-immune function, involving hydrolysis of extracellular matrix components to facilitate the migration of developing germ cells.

7.1 PI-9 protects cytotoxic lymphocytes from endogenous granzyme B

The high level expression of PI-9 in CTL and NK cells is consistent with PI-9 protecting CL from apoptosis induced by endogenous graB. This is further supported by analysis of the subcellular localisation of PI-9 in CL, which indicates that PI-9 is associated with cytotoxic granules, and is upregulated in activated CTL undergoing degranulation. This suggests that PI-9 can protect cells from graB mediated apoptosis induced by the entry of graB into the cytoplasm either via leakage from the granule or reflux following degranulation.

Recent work on the induction of memory $CD8^+$ T cells has provided supporting evidence of a role for PI-9 in protecting CL. This work suggests that T cells that survive the effector phase of the immune response are precursors of memory cells (Opferman *et al.*, 1999). Classically, memory T cells were thought to be a separate cell lineage that were dependent upon persistence and presentation of antigen by DC for their survival (Gray and Matzinger, 1991; Oehen *et al.*, 1992). However, the expression of perforin in memory $CD8^+$ T cells (Geisberg and Dupont, 1992; Opferman *et al.*, 1999) suggests that memory cells are effector CTL that remain following clearance of activated T cells by activation induced cell death (AICD; reviewed in Ashton-Kickardt and Opferman, 1999). Several mechanisms have been proposed for initiating AICD, such as fratricide mediated by Fas and other TNF family members (reviewed in Janssen *et al.*, 2000), however it has recently been suggested that cytotoxic molecules expressed by the effector cell are responsible for AICD (Spaner *et al.*, 1998; Opferman *et al.*, 2001). Furthermore, it has been suggested that the survival of memory T cells may be related to an intracellular graB inhibitor, such as PI-9 (Opferman *et al.*, 2001).The amount of PI-9 expressed by a CTL may determine the number of targets that can be deleted before the CTL is overwhelmed by endogenous graB.

7.2 PI-9 may protect accessory cells and bystander cells from exogenous granzyme B

During granule mediated apoptosis the granular contents are directed towards the target cell via the immunological synapse (Stinchcombe and Griffiths, 2001). However, some graB may escape from the intercellular space as indicated by the presence of graB in the sera of patients with elevated CTL responses (Spaeny-Dekking *et al.*, 1998) and in those with severe Gram negative bacterial infections (Lauw *et al.*, 2000). Hence, cells in the localised area of the immune response may also be at risk from graB, including accessory cells that provide the appropriate cytokine environment and secondary signals (by direct cell-cell contact) to support the immune response as well as bystander cells. The expression of PI-9 in accessory cells such as DC, B cells and $CD4^+$ T helper cells and bystander cells such as endothelial and mesothelial cells suggests that PI-9 protects these cells during the immune response.

A cytoprotective role for PI-9 is further supported as the expression of PI-9 in endothelial and mesothelial cells can be upregulated by inflammatory stimuli (Buzza *et al.*, 2001). Furthermore, studies on transfected cells demonstrate that expression of PI-9

in target cells protects, in a dose dependent manner, from apoptosis induced by either purified graB and perforin or cytotoxic lymphocytes (Bird *et al.*, 1998).

7.3 The interaction of PI-9 with other proteinases

The tissue distribution studies performed in Chapter 5 and 6 indicate that PI-9 is expressed in cells that do not express graB such as B cells, DC and epithelial cells. This suggests that PI-9 may also inhibit proteinases (other than graB) expressed within these cells. PI-9 can interact with a number of other proteinases, although not all of these interactions exhibit association rate constants within the physiologically relevant range (between 10^5 and 10^7 M^{-1} s^{-1}; Travis and Salvesen, 1983). The association rate constant reported for PI-9 with elastase (1.5×10^5 M^{-1} s^{-1}) is within this range, however a 1400:1 ratio of elastase to PI-9 is required to form an SDS-stable complex (Dahlen *et al.*, 1999) rather than the 1:1 ratio normally associated with serpin inhibition. This suggests that PI-9 is a substrate of elastase rather than an inhibitor.

PI-9 has also been reported to inhibit subtilisin A, an endopeptidase produced by *Bacillus subtilis*. The association rate constant reported for this interaction ($2.4 \pm 0.1 \times 10^6$ M^{-1} s^{-1}; Dahlen *et al.*, 1997) is greater that that observed between PI-9 and graB ($1.7 \pm 0.3 \times 10^6$ M^{-1} s^{-1}), however the relevance of PI-9 inhibiting a bacterial proteinase is not clear. However, subtilisin A is related to the mammalian proprotein convertases, which are expressed in the secretory pathway to process a wide variety of prohormones and propeptides (reviewed in Steiner, 1998). A mammalian member of this family, furin, is inhibited by the closely related ov-serpin PI-8 (Dahlen *et al.*, 1998b), suggesting that PI-9 may interact with other mammalian proprotein convertases, although no interactions have been reported to date. Alternatively, the expression of PI-9 in epithelial cells of the skin, intestines and reproductive system suggests that PI-9 may have a role in protecting epithelial layers from bacterial proteinases during infection.

PI-9 has also been reported to inhibit the activity of some caspases (caspase-1, -4 and -8), however the kinetics of these interactions are dependent on time rather than the concentration of PI-9 (Annand *et al.*, 1999) and the association rate constant for PI-9 and caspase-1 is very low (7×10^2 M^{-1} s^{-1}). However, this laboratory has also investigated the interaction of PI-9 with the caspases and found that caspase-4 is the only caspase that is inhibited to any significant degree (Bird *et al.*, 1998 and N. Thornberry, personal communication).

Caspase-1 and -4 belong to the cytokine-processing group of caspases. If PI-9 does inhibit these proteinases, it may have additional roles in regulating inflammatory cytokines. However, very high levels of PI-9 would be required to effectively inhibit these caspases *in vivo*. Young and co-workers have suggested a role for PI-9 in regulating IL-1β processing by caspase-1, with the dysregulation of PI-9 expression in the smooth muscle cells surrounding arteries contributing to the inflammatory response and the generation of atherosclerotic plaques (Young *et al.*, 2000). However, the rabbit polyclonal antisera used to detect PI-9 in this study may have been cross-reactive, as subsequent tissue distribution studies have failed to observe expression of PI-9 in smooth muscle cells of the vasculature, although expression is observed in the endothelium (Bladergroen *et al.*, 2001; Buzza *et al.*, 2001).

So while PI-9 has been described to interact with a number of proteinases, convincing evidence that these interactions occur *in vivo* has yet to be described. Therefore it appears that the major function of PI-9 is to inhibit mis-directed graB.

7.4 The role of granzyme B and PI-9 in the reproductive system

The expression of PI-9 in immune privileged sites (Bladergroen *et al.*, 2001; Hirst *et al.*, 2001) is consistent with PI-9 protecting these sites from inappropriate targeting by autoreactive T cells. However, the perforin independent expression of graB in the testis and placenta suggests an extracellular function for graB, possibly in the matrix remodelling required for migration of developing germ cells and invasion of the blastocyst into the uterine wall. This extracellular role for graB is supported by reports implicating graB in the degradation of aggrecan proteoglycan (Froelich *et al.*, 1993) and detachment of bone marrow stromal cells (Berthou *et al.*, 1995). It is unlikely that PI-9 is involved in regulating the extracellular functions of graB, as PI-9 would have limited activity once released from cells due to the oxidation of cysteine residues in the RCL.

Sertoli cells express both graB and PI-9, suggesting that PI-9 is present to inhibit apoptosis induced by mis-directed graB, however the post-mitotic stages of developing germ cells express graB independently of PI-9. Whether these cells require protection from graB mediated apoptosis is not known. Loss of Sertoli cells, which provide structural and nutritional support to the developing germ cells, would be detrimental to the functioning of the testis and therefore these cells need to be maintained. However, due to the large numbers of germ cells produced in the testis every day, the loss of a few

germ cells by graB mediated apoptosis would not affect overall sperm production. Alternatively germ cells may have developed other mechanisms to protect themselves from inadvertent apoptosis, such as expression of Bcl-2 family members (Print and Loveland, 2000; Meehan *et al.*, 2001).

Analysis of PI-9 expression in the rat indicates that it is expressed in neonatal gonocytes and adult spermatogonia. These cells reside at the basement membrane and represent the self-renewing populations which differentiate to give rise to cells that undergo spermatogenesis. The maintenance of these cells is imperative to reproduction as their loss would result in sterility. The first wave of spermatogenesis coincides with the initiation of graB transcription on day 5. At this time, the spermatogonia would be in close association with primary spermatocytes that express graB and hence require a protective mechanism. Further analysis of the stage specific expression of PI-9 and graB in the rat will help to elucidate their roles in testicular development and function.

7.5 PI-9 and granzyme B in disease

No naturally occurring mutations of PI-9, or diseases involving dysregulation of PI-9, have been described, nor have they been described for graB. This suggests that defects in either of these proteins is deleterious for survival. By contrast, loss of perforin expression has been linked to one disorder.

Haemophagocytic lymphohistiocytosis (HLH) is a complex disorder that is characterised by excessive immune activation. The disorder can be divided into two categories, a hereditary form (Familial HLH (FHLH)), and an acquired condition which is associated with immunosuppressive therapy, malignancy and viral infection (Henter and Elinder, 1995). FHLH occurs during early childhood and can be rapidly fatal if not treated with chemotherapy and bone marrow transplantation (Bolme *et al.*, 1995). Two loci have been genetically linked to FHLH, 9q21-3-q22 (Ohadi *et al.*, 1999) and 10q22 (Dufourcq-Lagelouse *et al.*, 1999) with the defect at 10q22 recently shown to be due to mutations within the perforin gene which result in loss of perforin expression (Stepp *et al.*, 1999). Other cases of FHLH however, are not linked to either of these loci and it is interesting to speculate whether defects in PI-9 (at 6p25) or graB (at 14q11) are associated with this disease, or other disorders involving cytotoxic lymphocytes.

7.5.1 PI-9 dysregulation in cancer

The dysregulation of PI-9 in cancer has been reported, with studies suggesting that expression of PI-9 in carcinomas and lymphomas is a mechanism that protects them

from immune clearance (Medema *et al.*, 2001a; Bladergroen *et al.*, 2002). However, while these studies examined the expression of PI-9 in melanoma and carcinomas of the breast, colon, and cervix (Medema *et al.*, 2001a) as well as T, B and Hodgkin lymphomas (Bladergroen *et al.*, 2002) they failed to analyse the expression of PI-9 in normal epithelium and lymphocytes.

This thesis and other work performed in this laboratory (Buzza *et al.*, 2001) indicates that PI-9 is expressed in epithelial cells in normal tissue, and it has been specifically observed in the ductal tissue of the breast, the columnar epithelia of the colon and the ciliated columnar epithelial lining the female reproductive tract. Therefore, the expression in carcinomas derived from these cells is not unexpected. The level of PI-9 expressed by these carcinomas was determined by semiquantitative RT-PCR, and as the study performed by Medema and co-workers did not compare the level detected in carcinomas to normal cells it is not possible to conclude that PI-9 is upregulated in carcinoma. Medema and co-workers also reported the expression of PI-9 in melanomas. The expression of PI-9 in skin has been observed (M. Buzza, personal communication), and as these melanoma lines were generated by culturing of dissected tumour material, the presence of PI-9 as detected by RT-PCR may reflect expression of PI-9 in contaminating normal skin cells or dendritic cells within the skin.

Work presented in Chapter 6 of this thesis describes the expression of PI-9 in leukocyte populations and demonstrates expression of PI-9 in both T and B cells. Hence, PI-9 expression in T and B cell lymphomas is to be expected. Furthermore, of the 224 biopsies examined by Bladergroen and co-workers, only 62 (28%) were positive for PI-9 and the percentage of PI-9 positive cells within the biopsy varied, such that only 39 (17%) of the cases contained a majority of tumour cells positive for PI-9. The lack of PI-9 in the majority of these lymphomas suggests that PI-9 overexpression is *not* a widespread mechanism of immune evasion. Additionally, when these biopsies were analysed for co-expression of PI-9 and graB, less than 50% of the graB positive T cell lymphomas were positive for PI-9. The graB positive T cell lymphomas that have lost PI-9 expression would be *more* susceptible to clearance by CL, and therefore PI-9 cannot be considered as a mechanism by which lymphomas evade immune surveillance.

Therefore, future studies on the association of PI-9 with cancer or disease must use detection methods that are quantitative and can distinguish the *upregulation* of PI-9 over baseline expression in normal cells.

7.6 Intracellular serpins protect cells from the release of granular pro-apoptotic serine proteinases

The role of PI-9 in protecting CL from leakage of graB from cytotoxic granules is supported by analysis of two closely related ov-serpins, PI-6 and M/NEI. PI-9 is located at the same locus as PI-6 and M/NEI on 6p25 (Sun *et al.*, 1998), and they are 62% and 51% identical to PI-9 at the amino acid level, respectively. M/NEI inhibits the azurophilic granule proteinases elastase, proteinase 3 and catG (Remold-O'Donnell *et al.*, 1989; Sugimori *et al.*, 1995), while PI-6 can inhibit catG (Scott *et al.*, 1999b).

Azurophilic granule proteinases are expressed in monocytes and neutrophils, and are involved in the destruction of phagocytosed material following fusion of the azurophilic granule with the phagosome. They can also be secreted into the extracellular environment where they are implicated in degradation of a range of extracellular matrix components (reviewed in Shapiro *et al.*, 1991). However, some may also have pro-apoptotic functions as catG can activate procaspase-7 (Zhou and Salvesen, 1997) and cleave the nuclear protein, brm (Biggs *et al.*, 2001), while elastase can induce apoptosis of neutrophils (Trevani *et al.*, 1996) and endothelial cells (Yang *et al.*, 1996). As such, the uncontrolled release of these pro-apoptotic proteinases into the cytosol of monocytes and neutrophils could result in activation of intrinsic apoptotic pathways.

Whether leakage of these pro-apoptotic granular proteinases occurs has not been investigated in monocytes, neutrophils or CTL. However, studies in fibroblasts provide evidence that oxidative stress induces lysosomal rupture and release of lysosomal contents into the cytoplasm (Brunk *et al.*, 1997). As azurophilic and cytotoxic granules are modified lysosomes (Page *et al.*, 1998) it is possible that they too are sensitive to oxidative stress. Reactive oxygen species are generated by monocytes and neutrophils following phagocytosis of bacterium and also by activated CTL during effector functions, which in some circumstances is associated with induction of AICD (Hildeman *et al.*, 1999). Therefore, these cells can be exposed to oxidative stress and are potentially at risk from it.

Alternatively, pro-apoptotic proteinases may be mis-directed into the cytoplasm during the fusion of granules with the phagolysosome or the plasma membrane, or following granule exocytosis and re-internalisation by endocytosis. The expression of PI-9, PI-6 and M/NEI in the cytoplasm of cytotoxic lymphocytes, monocytes and neutrophils places them in an ideal location to inhibit the activity of pro-apoptotic proteinases that enter the cytoplasm.

7.7 Ov-serpins and the regulation of apoptosis

PI-9 protects cells from graB mediated apoptosis in a dose dependent manner (Bird *et al.*, 1998) and other ov-serpins have also been shown to protect cells from apoptosis. PAI-2 can protect cells from TNFα mediated apoptosis (Kumar and Baglioni, 1991; Dickinson *et al.*, 1995) and apoptosis induced by *Mycobacterium avium* infection (Gan *et al.*, 1995). This anti-apoptotic ability is dependent upon the inhibitory activity of PAI-2, as mutation at the P_1 residue in the RCL abrogates protection (Dickinson *et al.*, 1995). Furthermore, mutations in the C-D interhelical loop of PAI-2, which do not affect its inhibitory activity, also result in loss of protection (Dickinson *et al.*, 1998), suggesting that the proteinase requires the C-D interhelical loop for stabilisation.

Proteinase inhibitor 10 (PI-10), which is restricted in distribution to bone marrow and myeloid leukaemias (Riewald and Schleef, 1995; Riewald *et al.*, 1998) has been recently shown to protect cells from TNFα mediated apoptosis (Schleef and Chuang, 2000). Protection from TNFα correlates with the level of PI-10 expressed and the formation of an SDS-stable complex. However the identity of the interacting proteinase in not yet known.

Both SCCA-1 and -2 can protect cells from TNFα mediated apoptosis (Suminami *et al.*, 2000, McGettrick *et al.*, 2001). Overexpression of SCCA-1 can protect cells from apoptosis induced by drugs (SN-38 and etoposide) or by IL-2 stimulated NK cells and can protect tumour cells *in vivo* (Suminami *et al.*, 2000). However, how this is mediated is not yet clear, as no interacting proteins have been identified. The protection mediated by SCCA-2 is dependent upon the inhibitory function, as mutations in the RCL abrogate protection (McGettrick *et al.*, 2001). CatG expression is upregulated during TNFα treatment and as SCCA-2 can inhibit catG (Schick *et al.*, 1997), this suggests that SCCA-2 may protect cells via inhibition of catG. However, no intracellular complexes of SCCA-2 with catG have been detected in TNFα treated cells.

Although a number of ov-serpins have been shown to protect cells from cell death, the mechanism through which this is mediated is not yet clear. PI-9 remains the only ov-serpin for which the mechanism of protection is known.

7.8 Future directions

This thesis provides further evidence that PI-9 functions to protect CL from graB that may gain access to the cytoplasm via leakage from granules or re-internalisation following degranulation. The expression of PI-9 in DC indicates that they may require protection from graB during the stimulation of precursor CTL, while its expression in the testis suggests a role for PI-9 in reproduction. These hypotheses can be confirmed by examining various 'loss of function' models.

7.8.1 What is the consequence of PI-9 deficiency?

PI-9 deficiency could best be studied by the generation of PI-9 null mice by disrupting the gene encoding the murine homologue of PI-9. However, recent analysis of the mouse genome has indicated the presence of multiple PI-9-like genes (Kaiserman *et al.*, 2002). Therefore, the functional murine homologue of PI-9 needs to be identified and the possibility of redundancy assessed before proceeding with this approach. There is however, some evidence that SPI-6 is the functional homologue of PI-9, as DC transfected with SPI-6 are protected from CTL induced apoptosis (Medema *et al.*, 2001b).

The predicted phenotype of the murine PI-9 (mPI-9) null mouse would predominantly involve cytotoxic lymphocytes, although it may also affect other cell types. Possible outcomes of mPI-9 deficiency include:

a) reduced CTL and NK cell numbers in the blood due to cell death induced by unregulated graB leakage.

b) reduced CTL and NK cell numbers upon induction of effector functions and degranulation, as CTL and NK cells may only be susceptib following the upregulation of graB or during granule mediated killing,

c) lack of cell mediated immunity due to los en presenting DC populations,

d) reduced fertility due to loss of Sertoli cells and germ cell progenitors in the testis.

An alternative approach would be to use the Cre-lox recombinase system (reviewed in Sauer, 1998) to generate mice that allow examination of the loss of PI-9 in specific cell types. For instance, PI-9 deficiency could be examined in cytotoxic lymphocytes, by placing the Cre recombinase gene downstream of a $CD8^+$ T cell specific promoter. The effect of mPI-9 deficiency in reproduction could also be examined by use of a testis-specific promoter. Another strategy would be to abrogate or

decrease the level of PI-9 in a cell line that expresses graB, such as YT cells. Transfection with a vector containing antisense PI-9 cDNA or a gene targeting vector designed to disrupt the PI-9 gene could be employed. The viability of PI-9 deficient YT cells during normal cellular functions and in killing assays could then be assessed.

7.8.2 Do proteinases leak from granules?

The appearance of PI-9/graB complexes in cells incubated with a proteosome inhibitor suggests that granules do leak. This is confirmed by the localisation of PI-9 to the cytoplasmic face of the granule, where it can rapidly inhibit any graB entering the cytoplasm. However, the leakage of graB from cytotoxic granules needs to be more vigorously tested. This could be examined by monitoring graB redistribution from the granule to the cytoplasm of cytotoxic cells at rest and during effector functions. Analysis via cell fractionation and immunoblotting can be difficult due to cross contamination of samples and may not detect small amounts of leakage. The analysis could be simplified by the expression of graB tagged with green fluorescent protein. Stable transfection of this construct into YT cells could be used to monitored the release of a graB from granules by confocal microscopy under various conditions.

olecular Human Reproduction Vol.7, No.12 pp. 1133–1142, 2001

Perforin-independent expression of granzyme B and proteinase inhibitor 9 in human testis and placenta suggests a role for granzyme B-mediated proteolysis in reproduction

Claire E.Hirst[1,*], Marguerite S.Buzza[1,*], Vivien R.Sutton[2], Joseph A.Trapani[2], Kate L.Loveland[3] and Phillip I.Bird[1,4]

[1]Department of Biochemistry and Molecular Biology, Monash University, Clayton, 3800, [2]The Peter MacCallum Institute, East Melbourne, 3002 and [3]Monash Institute of Reproduction and Development, Monash University, Clayton, 3168, Australia

[4]To whom correspondence should be addressed at: Department of Biochemistry and Molecular Biology, Building 13B, Room G09, Monash University, Clayton, 3800, Australia. E-mail: phil.bird@med.monash.edu.au

*Both authors contributed equally to this work

Granzyme B (graB) plays a pivotal role in cytotoxic lymphocyte granule-mediated apoptosis through cleavage of intracellular proteins in target cells. Proteinase inhibitor-9 (PI-9) is a potent inhibitor of graB and is highly expressed in cytotoxic lymphocytes. Here, we show by immunohistochemistry that PI-9 is also abundantly expressed in human testicular Sertoli cells and placental syncytial trophoblasts. Postulating that PI-9 protects these tissues from graB-producing auto- or allo-reactive cytotoxic lymphocytes, we also stained sections for graB. Unexpectedly, graB was observed in non-cytotoxic cells in both tissues. In the adult human testis, graB was present in spermatogenic cells within the seminiferous tubule, and this was verified by in-situ hybridization and reverse transcription–polymerase chain reaction (RT–PCR). Immunohistochemical analysis of term placentae demonstrated graB in syncytial trophoblasts, and this was confirmed by RT–PCR on primary trophoblasts from term placenta. Perforin, which is co-produced with graB by activated cytotoxic lymphocytes and is required for graB release into the target cell, was not detected in either testis or placenta. We postulate that, in these organs, graB has a perforin-independent role, involving hydrolysis of extracellular matrix components. In the testis, graB may facilitate migration of developing germ cells, while in the placenta, it may contribute to extracellular matrix remodelling during parturition.

Key words: extracellular matrix remodelling/granzyme B/perforin/proteinase inhibitor 9 (PI-9)/serpin

Introduction

The serine proteinase granzyme B (graB) is highly expressed in cytotoxic T cells (CTLs) and natural killer (NK) cells. It is stored in granules of activated CTLs and NK cells with a number of other cytotoxins, including the pore forming protein perforin. When CTLs or NK cells recognise and adhere to virus-infected or malignant cells, these granules migrate to the site of cell contact and their contents are released into the intercellular space. Cytotoxins are endocytosed by the target cell and perforin mediates their release into the cytoplasm by disrupting the endocytic vesicles. Once released from endocytic vesicles into the cytoplasm, graB initiates apoptosis by cleaving the Bcl-2 family member, BID (Alimonti *et al.*, 2000; Barry *et al.*, 2000; Heibein *et al.*, 2000; Sutton *et al.*, 2000), as well as caspases (Andrade *et al.*, 1998; Yang *et al.*, 1998). GraB also has substrates in the nucleus (Pinkoski *et al.*, 1996; Trapani *et al.*, 1998) and is necessary for rapid fragmentation of target cell DNA (Heusel *et al.*, 1994).

At the end of an immune response, excess CTLs and NK cells are removed from the circulation by activation-induced cell death. However, during target cell killing it is important that CTLs and NK cells are resistant to their own cytotoxins so that they do not undergo premature apoptosis. To protect against misdirected graB they produce an intracellular serpin, proteinase inhibitor 9 (PI-9), which is a member of a large superfamily of metazoan and viral proteinase inhibitors. We have shown that PI-9 is a potent graB inhibitor and that expression of PI-9 in the cytoplasm and nuclei of cells affords protection from graB-mediated apoptosis (Bird *et al.*, 1998). PI-9 inhibitory function is mediated through a C-terminal reactive centre loop (RCL) which resembles a graB substrate (Sun *et al.*, 2001). Cleavage of the PI-9 RCL by graB causes a rapid conformational change in the serpin, resulting in the formation of a stable serpin–proteinase complex (Sun *et al.*, 1996). The recent crystallization of a serpin–proteinase complex has shown that the proteinase is substantially distorted

during complex formation and that catalysis of the RCL is not completed, leaving the two molecules covalently linked and inactive (Huntington *et al.*, 2000).

As well as protecting cytotoxic lymphocytes, PI-9 may also protect bystander cells or antigen-presenting cells likely to be exposed to graB during an immune response. The presence of PI-9 in non-cytotoxic cells such as B cells (Sun *et al.*, 1996), monocytes (Young *et al.*, 2000) and endothelial and mesothelial cells (Buzza *et al.*, 2001) is consistent with such a role. Furthermore, very high levels of PI-9 transcripts are present in placenta and testis, suggesting a role in maintaining the privileged immune status of these tissues (Sun *et al.*, 1996).

To further understand the physiological role that PI-9 plays in bystander protection and immune privilege, it is important to identify specific cells that express PI-9. In this study we have surveyed various human tissues for PI-9, focusing on testis and placenta. We show that PI-9 is present in Sertoli cells and syncytial trophoblasts, consistent with a role in maintaining immune privilege. Surprisingly we also detect perforin-independent expression of graB in and around these cells. This is the first description of graB expression outside lymphocytes, and suggests a novel role for this proteinase in reproductive function.

Materials and methods

Materials

All reagents were of analytical grade and were purchased from either Sigma Chemicals, St Louis, MI, USA or Merck BDH Chemicals, Darmstadt, Germany unless otherwise specified. All reagents were obtained from local subsidiaries or agents of the manufacturers. The recombinant human serpins PI-9, PI-8 and PI-6, monocyte-neutrophil elastase inhibitor (MNEI), murine serine proteinase inhibitor 6 and 3 (SPI-6 and SPI-3) and the viral serpin cytokine response modifier A (CrmA) were expressed in *Pichia pastoris* and purified following methods described previously (Sun *et al.*, 1995). Recombinant human plasminogen activator 2 (PAI-2) was obtained from Dr R.Medcalf (Monash University Department of Medicine, Box Hill Hospital). Recombinant human squamous carcinoma cell antigens 1 and 2 (SCCA-1 and -2) were a kind gift of Dr D.M.Worrall (Department of Biochemistry, University College, Dublin). Dr S.Bottomley and Dr R.Pike provided purified human α_1-antitrypsin (α_1-AT), α_1-antichymotrypsin (α_1-AC) and antithrombin (AT). J.Irving provided recombinant myeloid and erythroid nuclear termination stage specific protein (MENT) (Department of Biochemistry and Molecular Biology, Monash University). Dr H.Abts provided recombinant Hurpin (Department of Dermatology, Heinrich-Heine-University). YT, a human NK-like cell line (Wano *et al.*, 1984), was cultured in RPMI 1640 with 10% heat inactivated fetal calf serum, 2 mmol/l L-glutamine, 50 IU/ml penicillin and 50 µg/ml streptomycin. Antibodies used to detect graB were 2C5 (Apostolidis *et al.*, 1995) and rabbit polyclonal anti-graB (Edwards *et al.*, 1999). GrB-7 was obtained from Chemicon, Temecula, CA, USA (Kummer *et al.*, 1993), and goat polyclonal anti-graB (C-19) was from Santa Cruz Biotechnologies, Santa Cruz, CA, USA.

Monoclonal antibody production

BALB/c mice were immunized by intraperitoneal injections of recombinant PI-9 (rPI 9) at 2 week intervals. The initial injection consisted of rPI-9 emulsified in Freund's complete adjuvant, the second of rPI-9 emulsified in incomplete Freund's, and the third of sodium dodecyl sulphate (SDS)-denatured rPI-9 mixed with phosphate-buffered saline (PBS). Three days after the final inoculation, splenocytes were recovered and fused to NS-1 myeloma cells as described previously (Apostolidis *et al.*, 1995). HAT resistant hybridomas were screened by ELISA and immunoblotting against purified rPI-9. Positive hybridomas were expanded and cloned by limiting dilution.

Specificity of PI-9 monoclonal antibodies

The specificity of the hybridoma 7D8 to PI-9 was determined by immunoblotting against a panel of purified serpins. The indicated serpins (100 ng of each) were separated on duplicate 12.5% SDS-polyacrylamide gels under reducing conditions. One gel was silver-stained (Rapid-Ag-Stain, ICN, Costa Mesa, CA, USA) to verify equal loading of proteins. Proteins on the second gel were transferred to nitrocellulose and immunoblotted with hybridoma supernatant. Bound antibody was detected by horse-radish peroxidase (HRP) conjugated sheep anti-mouse IgG (Chemicon) and enhanced chemiluminescence (NEN DuPont, Boston, MA, USA).

Preparation of tissue from normal human adult testis and term placenta

Samples of human adult testes were obtained with informed consent following the guidelines of the Monash Human Ethics Committee. Immediately upon collection, part of the testis was fixed for 5 h in Bouin's fixative, then rinsed and stored in 70% ethanol before dehydration and paraffin embedding. The histological specimens were cut into 5 µm sections, floated on diethyl pyrocarbonate (DEPC)-treated MilliQ water and dried onto slides (Superfrost Plus, Biolabs Scientific, Clayton, Vic, Australia). These sections were used for both immunohistochemistry and in-situ hybridization analyses. Another sample of testis material was snap frozen immediately upon collection and stored at −70°C until use for RNA analysis. S.Black (Monash University Department of Medicine, Box Hill Hospital) provided formalin-fixed paraffin-embedded term placental blocks obtained from routine Caesarean sections. Sections of 5 µm were cut onto glass slides (Menzel-Glaser, Braunscheig, Germany) and used for immunohistochemistry.

Immunohistochemistry

Various tissue blocks (other than listed above) were obtained from the Box Hill Hospital, Department of Anatomical Pathology archive. Endometrial tissue sections were provided by Dr P.Rogers (Monash University Department of Obstetrics and Gynaecology, Monash Medical Centre). Sections were dewaxed, rehydrated and treated with 0.3% hydrogen peroxide. Antigen retrieval was then performed by heating sections at 100°C for 10 min in 50 mmol/l glycine, pH 3.5 (testis sections), or 10 mmol/l citric acid, pH 6.0 (placental sections). Slides were washed three times in Tris-buffered saline (TBS: 10 mmol/l Tris-HCl, 150 mmol/l NaCl, pH 7.6), and these washes were repeated between each incubation step. Sections were blocked in 5% normal sheep serum diluted in TBS with 0.1% bovine serum albumin (BSA; testis sections), or with 2% BSA in TBS (placental sections), for 20 min. Primary antibodies were diluted in TBS/0.1% BSA and incubated overnight in a humidified container. Bound antibody was detected by biotinylated sheep anti-mouse or anti-rabbit IgG (Chemicon) for 1 h, followed by HRP conjugated streptavidin (Chemicon) for 1 h or in some cases Vectastain® Elite ABC Kit (Vector Laboratories, Burlingame, CA, USA), and visualized using the Liquid DAB Chromogen Substrate System (DAKO). Sections were counterstained with Harris' haematoxylin and mounted in DPX mounting fluid (Merck BDH).

Table I. Oligonucleotides used in PCR, RT–PCR and Southern blotting

Oligo	5′–3′ sequence	S/AS[a]	Template[b]	Nucleotides	Exon
PB 174	AGATGATGTATCAGGAG	S	PI-9	700–716	6
PB 286	AGCTGAGCCTGCTGGTG	S	PI-9	787–803	6
PB 287	AGTCTGGCTTGGTCCAGG	AS	PI-9	871–888	7
PB 279	TGCTTCCTGTAGTTAGTAGC	AS	graB	753–772	4
PB 377	GAACAGGAGCCGACCCAGCA	S	graB	257–276	3
PB 378	GGACTTGGCTCCAGAGAAGG	AS	graB	799–818	5
PB 476	AAGTCAGCTCCACTGAAGCT	S	perforin	329–348	1
PB 477	GGTAGGTTTGGTGGAAGGAG	AS	perforin	870–889	2
PB 584	GACCCCTTCATTGACCTCAAC	S	GAPDH	178–198	3
PB 585	GATGACCTTGCCCACAGCCTT	AS	GAPDH	718–738	8
JT 219	GCCAACTTTGCAGCCCAG	S	perforin	463–480	1
JT 300	TGAAACGCTACTAACTACAG	S	graB	747–766	5
JT 301	GAATAAATACCTCTTAGCTGAGTGG	AS	graB	849–873	5

[a]S/AS indicates whether the oligonucleotide is sense (S) or antisense (AS) with respect to the coding strand. [b]GenBank accession numbers for the indicated templates are NM_004155, J04071, NM_005041 and XM_006959 for PI-9, graB, perforin and GAPDH respectively.

In-situ hybridization

Riboprobes for PI-9 were generated from nucleotides 827–1388 of a human PI-9 cDNA subcloned into the *SacI*/*Eco*RI sites of pBluescript II KS⁻ (Stratagene) by digestion with *Sac*I and *Eco*RI. Riboprobes for graB 3′ UTR were generated by amplifying nucleotides 747–873 of human graB with primers JT 300 and JT 301 (Table I). This fragment was subcloned into pCR®-Blunt (Invitrogen), excised with *Eco*RI and cloned into the *Eco*RI site of pBluescript II KS⁻. Digoxigenin-labelled riboprobes for both graB and PI-9 were generated following the methods outlined in the dUTP-DIG Labelling Kit (Roche Molecular Biochemicals, Mannheim, Germany). The in-situ hybridization was performed essentially as previously described (Meinhardt *et al.*, 1998).

Reverse transcription–polymerase chain reaction (RT–PCR) for PI-9, graB and perforin

Primary placental cytotrophoblasts were isolated from fresh term placentae by S.Black by enzymatic digestion and Percoll gradient centrifugation, essentially as previously described (Kliman *et al.*, 1986), except that the cells were cultured in RPMI 1640. Most cells had formed syncytial structures 48 h after plating. Prior to RNA extraction the cells were washed thoroughly with PBS to remove any contaminating non-adherent leukocytes or erythrocytes and observed microscopically to verify purity. RNA isolated from testicular germ cell tumour lines was provided by Dr M.Pera (Monash Institute of Reproduction and Development). Total RNA was extracted from YT cells, normal testis tissue and placental syncytial trophoblasts using RNAzol™ B (Tel-Test) according to manufacturer's instructions. M-MuLV reverse transcriptase (New England Biolabs) and oligo dT (Amersham) were used to synthesize cDNA from 1 µg of total RNA. PCR was performed using 20 pmol of the indicated primer in 50 mmol/l KCl, 10 mmol/l Tris-HCl, pH 9.0, 0.1% Triton X-100 containing 2.5 mmol/l $MgCl_2$, 200 µmol/l dNTPs and 2 IU of *Taq* polymerase (GeneWorks, Thebarton, SA, Australia) for 35 cycles of 94°C for 30 s, 55°C for 30 s and 72°C for 45 s. The PCR primers were designed to amplify across intron/exon boundaries, thereby allowing discrimination of genomic DNA contamination in the cDNA. PCRs were performed with the primers indicated in Table I and amplification of glyceraldehyde-3-phosphate dehydrogenase (*GAPDH*) was used as a control for reverse transcription reactions. Amplified products were resolved on a 2% Agarose gel by electrophoresis and transferred to nitrocellulose under alkaline conditions. Membranes were hybridized with [γ-^{32}P] ATP-labelled oligonucleotides specific for PI-9, graB or perforin that were internal to the amplifying primers (PB 286, PB 279 and JT 219 respectively).

Results

Production and characterization of monoclonal antibodies to PI-9

Due to the high sequence and structural similarities between serpins, a polyclonal antiserum raised to one serpin will often cross-react with other family members. To reliably identify cells expressing PI-9 by immunohistochemistry, monoclonal antibodies were generated by immunizing mice with recombinant PI-9. Four hybridomas producing antibodies to PI-9 were identified by ELISA and screened for specificity to PI-9 by indirect immunofluorescence, immunoblotting and immunoprecipitation against a panel of serpins. One antibody, designated 1F3, recognised the majority of the serpins tested. Further analyses indicated that 1F3 recognises the highly conserved serpin proximal hinge region (data not shown).

Of the three other hybridomas, 2E7 and 8D3 reacted poorly against denatured PI-9 as assessed by immunoblotting and indirect immunofluorescence on acetone/methanol fixed cells. By contrast, 7D8 detected PI-9 under denaturing conditions, suggesting that it would be suitable for immunohistochemistry. 7D8 (IgG_1 κ) was assessed for cross-reactivity to a range of serpins including members of the ov-serpin family to which PI-9 belongs (Sun *et al.*, 1996). Following immunoblotting, a 42 kDa protein was detected only in the lanes containing rPI-9, demonstrating that 7D8 is specific for PI-9 (Figure 1).

Expression of PI-9 and graB in the testis

To identify cells that produce PI-9, an immunohistochemical survey of normal human tissues was performed using the specific monoclonal antibody 7D8. As indicated in Table II, PI-9-expressing cells were observed in a variety of tissues. In lymphoid tissue, PI-9 was restricted to lymphocytes and dendritic cells, while in reproductive and other tissues PI-9 was found in a number of epithelial and stromal cells. This distribution is consistent with its proposed role in cytotoxic cells and bystander protection during an immune response

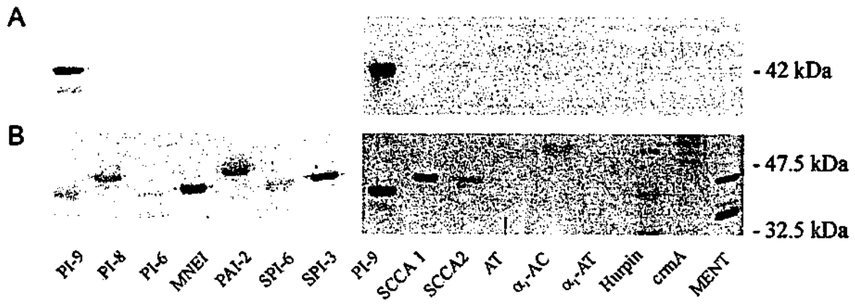

Figure 1. The monoclonal antibody 7D8 is specific for PI-9. The indicated serpins (100 ng) were resolved by 12.5% SDS–PAGE and were either (**A**) transferred to nitrocellulose and immunoblotted with 7D8 hybridoma supernatant diluted 1:10, or (**B**) silver stained to indicate the presence and sizes of the indicated serpins.

Table II. Tissue distribution of PI-9 (immunohistochemistry was performed on a variety of tissues using antibodies specific for PI-9)

Tissue	Cell types	Intensity[a]
Lymphoid tissues		
Lymph nodes	NK cells	+++
Thymus	Medullary dendritic cells	++
	Hassal's corpuscles	+++
Tonsil	Follicular dendritic cells	+++
Reproductive tissues		
Endometrium	Uterine epithelium	++
	Stromal cells	++
	Large granular lymphocytes	+++
	Glandular epithelium	++
	Myometrium	+
Oviduct	Epithelial cells	+
Placenta	Syncytial trophoblasts	+++
Testis	Sertoli cells	+++
	Leydig cells	++
Other tissues		
All organs	Mesothelium	+
All tissues	Endothelium	+
Intestine (fetal)	Enterocytes	+
Lung (reactive)	Epithelium	+
Pancreas	Ductal acini	+
Skin	Infiltrating lymphocytes	+++
	Epithelium	+

[a]The level of PI-9 staining was compared between the identified cell types.

(Bird *et al.*, 1998; Buzza *et al.*, 2001). As previously indicated by RNA analysis (Sun *et al.*, 1996), PI-9 was also observed in testis and placenta. As these are known to be sites of immune privilege, they were the focus of our subsequent investigations.

Analysis of normal human testis by immunohistochemistry indicated that PI-9 is present within seminiferous tubules (Figure 2Aii). Under higher magnification, the most prominent staining for PI-9 was apparent in Sertoli cells (Figure 2Aiii) extending from the basement membrane to the lumen. There was also pronounced nuclear staining for PI-9, which we have previously observed in many cell types (Bird *et al.*, 2001). As the cytoplasmic extensions of the Sertoli cell wrap around the developing germ cells, it was difficult to identify cell boundaries and definitively rule out PI-9 expression in germ cells in a single section. However, careful analysis of a number of serial sections indicated that within the seminiferous tubule, PI-9 is restricted to Sertoli cells. In some sections however, staining was also observed in Leydig cells and lymphocytes within the interstitium.

As Sertoli cells form the blood–testis barrier, the presence of PI-9 in these cells suggested that PI-9 contributes to the maintenance of the immune privileged status of the testis. By expressing PI-9, Sertoli cells would be resistant to graB produced by activated cytotoxic lymphocytes responding to the developing and potentially immunogenic germ cells. To further explore this role for PI-9 in immune privilege, we performed immunohistochemistry to determine if graB-expressing lymphocytes are normally present in the testis. Surprisingly, immunohistochemistry on normal human testis using a monoclonal antibody to graB indicated expression of the proteinase within the seminiferous tubule (Figure 2Av). As with PI-9, graB was observed in Sertoli cells, but in contrast, it also appeared in a number of different cells of the spermatogenic lineage (Figure 2Avi). The intensity of staining for graB varied between cell types; Sertoli cells had a diffuse cytoplasmic distribution while primary spermatocytes and round spermatids had a more intense cytoplasmic staining. No graB was visible in the nuclei of these cells. To determine if graB was present in mature spermatozoa, immunoblotting was performed on spermatozoa isolated from seminal fluid; however, no graB was detected in these samples (data not shown). As graB is thought to be restricted to CTLs and NK cells (Caputo *et al.*, 1988; Trapani *et al.*, 1988), we confirmed the immunohistochemistry using three other antibodies to human graB (both monoclonal and polyclonal) and all three demonstrated graB within the seminiferous tubule (data not shown).

Analysis of PI-9 and graB transcripts in the testis

To eliminate the possibility that the graB antibodies were in fact recognising some highly homologous but as yet uncharacterized serine proteinase in the testis, we examined whether graB and PI-9 transcripts could be detected by in-situ hybridization using riboprobes, or by RT–PCR performed on RNA extracted from normal adult testis.

In-situ hybridization was performed using probes specific for either PI-9 or graB on normal human adult testis. The PI-9 probe encompassed the region including the reactive centre loop, which is the most variable region of a serpin gene. The

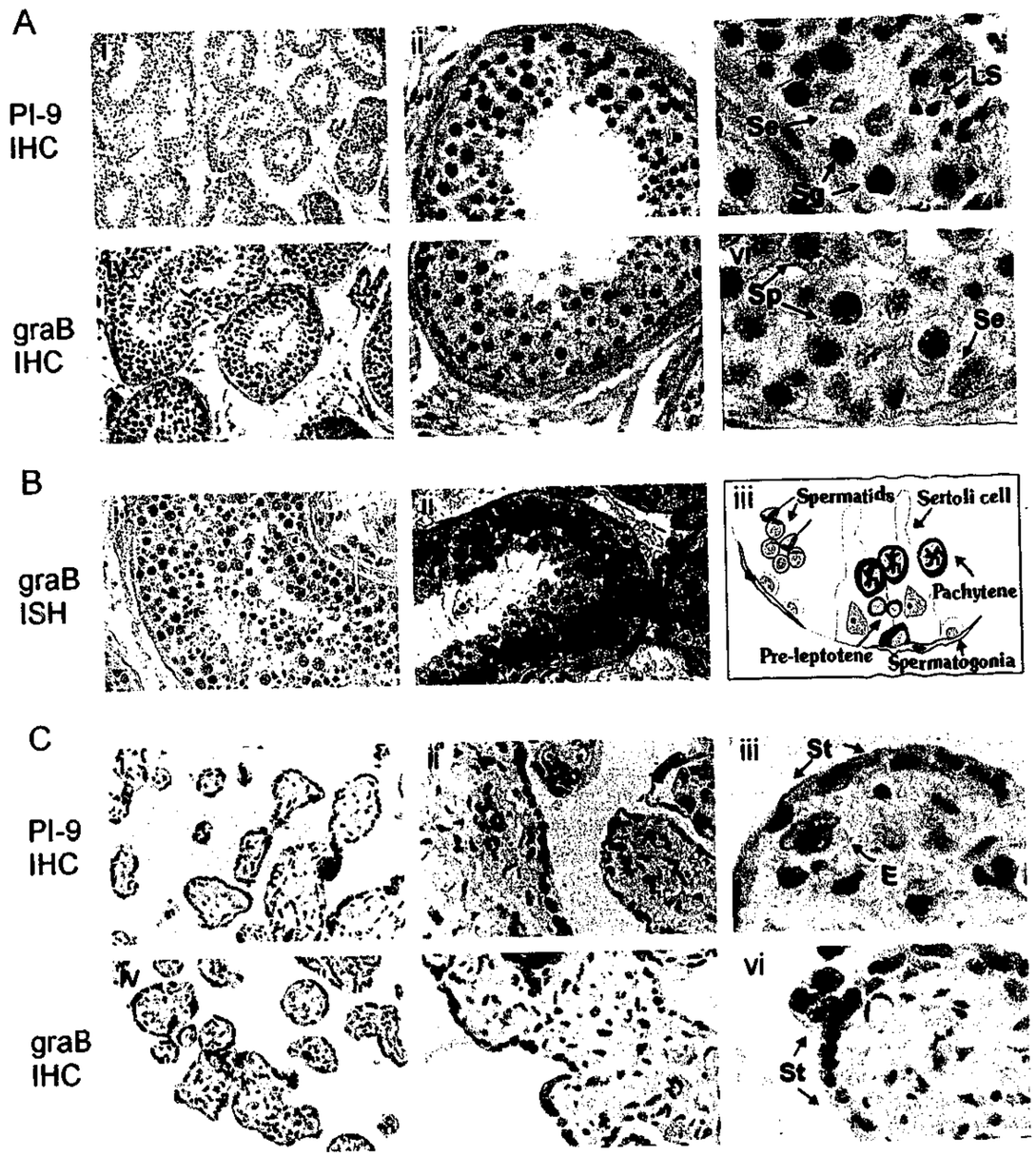

Figure 2. Localization of PI-9 and graB within normal human adult testis and term placenta. (**A**) Immunohistochemistry (IHC) of normal adult testis stained using antibodies for PI-9 or graB. Panels (ii) and (iii) show sections stained with the anti-PI-9 monoclonal antibody 7D8, indicating the presence of PI-9 in Sertoli cells (Se) but not in spermatogonia (Sg) or late spermatids (LS). Panels (v) and (vi) show sections stained using the anti-graB monoclonal antibody 2C5, demonstrating graB expression in both Sertoli cells (Se) and primary spermatocytes (Sp). Isotype matched control antibodies are indicated in (i) and (iv). Original magnification of micrographs are: (i) ×100, (iv) ×200, (ii) and (v) ×400, (iii) and (vi) ×1000. (**B**) In-situ hybridization (ISH) of normal adult testis using graB riboprobes. Panel (ii) demonstrates the graB antisense probe indicating the presence of graB mRNA in primary spermatocytes. Panel (i) illustrates the absence of signal obtained using the sense probe for graB. Panel (iii) is an illustration of a seminiferous tubule with purple showining the cell types found to be graB positive. Original magnification of micrographs are ×400. (**C**) Immunohistochemistry of normal term placentae. PI-9 expression in syncytial trophoblasts (St) and endothelial cells (E) detected with monoclonal antibody 7D8 (ii) and (iii), as compared with the isotype matched control antibody (i). Expression of graB in the placental syncytial trophoblast detected with monoclonal antibody GrB-7 (v and vi), as compared with no primary antibody control (iv). Original magnification of micrographs are: (i) and (iv) ×200; (ii) and (v) ×400, (vi) ×600 and (iii) ×800.

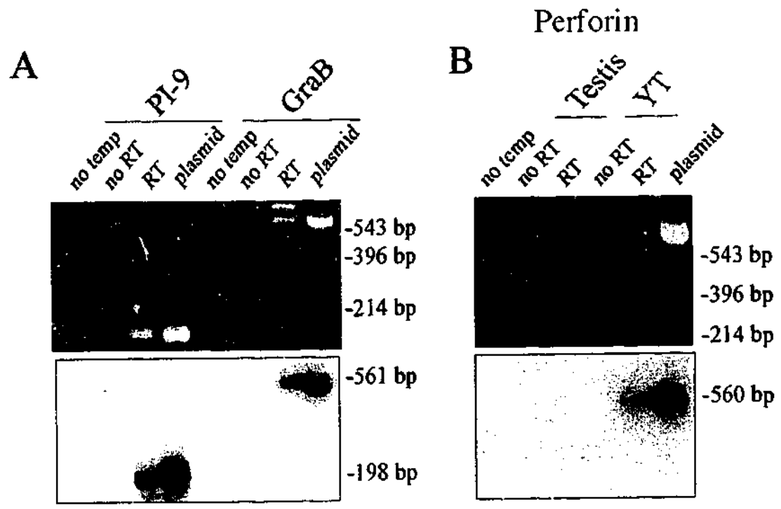

Figure 3. RT–PCR analysis of PI-9, graB and perforin expression in normal adult human testis. (**A**) Detection of PI-9 and graB mRNA. Total RNA extracted from normal human testis was reverse transcribed and used as a template for PCR amplification of PI-9 or graB respectively. (**B**) Detection of perforin mRNA. RNA was extracted from either normal testis or the natural killer-like cell line, YT. Total RNA was reverse transcribed and used as a template for PCR amplification of perforin. Plasmids containing the respective cDNA templates were used as a positive control. PCR products were probed with an internal oligonucleotide following Southern transfer.

graB probe was generated from the 3′ untranslated region, which is most divergent from other serine proteinases. In-situ hybridization confirmed the results of the immunohistochemistry, localising both PI-9 and graB to cells within the testis. Careful examination of multiple sections from both the immunohistochemistry and in-situ hybridization studies indicated that PI-9 is present in Sertoli cells within the tubules and Leydig cells and capillary endothelial cells within the interstitium. Endothelial cell expression of PI-9 has been previously observed (Buzza *et al.*, 2001).

Analysis by in-situ hybridization indicated that graB is expressed in Sertoli cells as well as in germ cells at various stages of development (Figure 2Bii). There was also some staining of interstitial cells within the testis consisting of scattered lymphocytes and endothelial cells. Precise identification of the spermatogenic cells expressing graB was difficult due to variation between samples, and the fact that the cytoplasmic extensions of Sertoli cells are intimately involved with the developing germ cells, making it difficult to delineate intercellular boundaries. Nevertheless, cell types positive for graB included some spermatogonia and pre-leptotene spermatocytes with the most obvious staining found in pachytene spermatocytes (Figure 2Bii). No signal was detected in the various stages of spermatid development, indicating that graB is restricted to germ cells in the early stages of meiotic division.

The presence of both graB and PI-9 transcripts in normal adult testis was confirmed by RT–PCR. Amplification using PI-9-specific primers resulted in a product of the expected size (188 bp), which was confirmed as PI-9 by Southern blotting with an internal oligonucleotide (Figure 3A). RT–PCR using graB primers resulted in several products, one of which was of the correct size (561 bp) and was confirmed to be graB by Southern blotting with an internal oligonucleotide (Figure 3A). To exclude the possibility that the graB transcripts were derived from contaminating lymphocytes within the tissue sample, we tested for co-expression of perforin, which is produced with graB by activated lymphocytes (Liu *et al.*, 1989). No products were detected by PCR either visually (Figure 3B upper panel) or by Southern blotting with an internal oligonucleotide to perforin (Figure 3B lower panel). By contrast, perforin was amplified from cDNAs generated from the NK-like cell line YT at the same time as the testis cDNA (Figure 3B). The lack of perforin expression confirmed that graB is produced by non-cytotoxic cells within the testis, and indicates that in this context graB may not act as a cytotoxic proteinase, as its entry into cells is perforin-dependent (Jans *et al.*, 1996; Shi *et al.*, 1997).

Dysregulation of graB and PI-9 in disease

To further elucidate the role of graB and its inhibitor, PI-9, in testicular function, we examined their expression in abnormally developed testes. In the maldescent testis, either one or both of the testes fails to descend from the abdominal space into the scrotal sac, and developing germ cells are exposed to higher temperatures causing loss of germ cell progenitors. Due to the interplay between the developing germ cells and Sertoli cells, this also results in abnormal Sertoli cell development. The expression of both graB and PI-9 (as determined by immunohistochemistry) was decreased in the aberrant Sertoli cells of maldescent testis (data not shown).

Analysis of graB and PI-9 gene expression was also performed on RNA extracted from four human testicular germ cell tumour lines (GCT 27C4, 27X1, 48 and 72) (Pera *et al.*, 1987, 1988, 1989). Although *GAPDH* cDNA was detected by RT–PCR, neither graB nor PI-9 were detected by RT–PCR or Southern blotting with an internal oligonucleotide, indicating

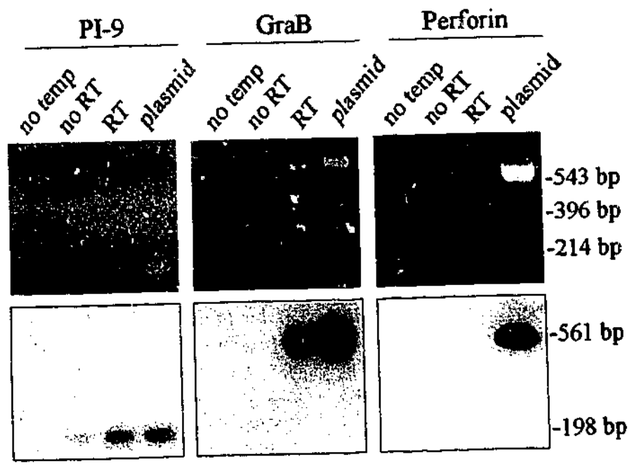

Figure 4. Expression of PI-9 and graB mRNA in primary trophoblasts. Cytotrophoblasts isolated from a term placenta were allowed to fuse into syncytial trophoblasts over 48 h in culture. Total RNA was extracted, reverse transcribed and used as a template for detection of PI-9, graB and perforin cDNA by PCR. Plasmids containing the respective cDNA templates were used as a positive control. PCR products were probed with an internal oligonucleotide following Southern transfer.

that these proteins are absent from testicular germ cell tumours (data not shown). The lack of PI-9 is consistent with its absence from germ cells in normal testis, but the absence of graB suggests that it may be lost during tumorigenesis.

Expression of PI-9 and graB in placental trophoblasts

We have previously shown that high levels of PI-9 mRNA are produced in human placenta (Sun *et al.*, 1996). To identify the cells expressing PI-9, we performed immunohistochemical analysis of normal term placentae using PI-9 specific antibodies. As shown in Figure 2C, PI-9 was highly expressed in the multi-nucleated syncytial trophoblast layer (syncytium) of the chorionic villi and in endothelial cells (Figure 2Cii,iii).

Given the unexpected finding of graB in the human testis, we also examined term placentae for graB expression, and it was detected in syncytial trophoblasts (Figure 2Cv,vi), with weak staining of endothelial cells occasionally observed. It is unlikely that the graB staining was due to antibody cross-reaction with a similar protein, as graB was detected in these cells with three other antibodies. To confirm this finding, we performed RT–PCR for graB on primary cultured syncytial trophoblasts. Primary cytotrophoblasts were isolated from human term placenta and after 48 h of culture, most had fused to form multi-nucleated syncytial trophoblasts. RT–PCR using RNA extracted from these cells yielded appropriately sized products for both PI-9 and graB, which were verified by Southern blotting with internal oligonucleotides (Figure 4). To eliminate the possibility that the graB products arose from RNA of contaminating lymphocytes in the trophoblast preparation, RT–PCR for perforin was performed and no product was detected (Figure 4).

Discussion

This study has demonstrated the presence of both graB and its cognate inhibitor, PI-9, in adult human testis and term placenta, in contradiction to the current dogma that graB is confined to NK cells and activated CTLs. The view that graB is present only in cytotoxic lymphocytes has arisen because the original analysis of graB mRNA expression was carried out on a panel of haemopoietic cell lines (Trapani *et al.*, 1988). Subsequent immunohistochemical analyses have also focused exclusively on tissues of the immune system (Held *et al.*, 1990; Hameed *et al.*, 1991; Ebnet *et al.*, 1995; Kummer *et al.*, 1995). A comprehensive survey of human graB expression has apparently never been carried out, so its presence in non-immune tissues and any additional physiological functions has not been considered.

GraB has a preference for cleavage after acidic amino acids, particularly aspartic acid (Poe *et al.*, 1991). It is this 'Asp-ase' activity that allows cleavage of BID, caspases and other intracellular components during apoptosis. However, a number of studies have indicated that graB is also released into the circulation during inflammation (e.g. rheumatoid arthritis) (Tak *et al.*, 1999; Ronday *et al.*, 2001) and have identified extracellular substrates of graB. For example, graB has the ability to degrade components of the extracellular matrix such as the proteoglycan, aggrecan (Froelich *et al.*, 1993), and it is able to cause detachment of adherent tumour cell lines (Sayers *et al.*, 1992). In $CD34^+$ peripheral blood progenitor cells, graB may play a role in detachment from bone marrow stromal cells (Berthou *et al.*, 1995). Thus, it is evident that graB has the ability to exert extracellular effects and may have a perforin-independent role in extracellular matrix remodelling. Our finding that graB is expressed in the testis and placenta in the absence of perforin suggests a non-cytotoxic role for graB in reproduction. As discussed below, in the testis graB may contribute to migration of developing germ cells through Sertoli cell tight junctions, while in the term placenta syncytial trophoblast expression of graB may contribute to extracellular matrix remodelling during parturition.

GraB is produced as a zymogen which is activated by the cysteine proteinase dipeptidyl-peptidase-I (DPP-I, cathepsin C). DPP-1 is present in cytotoxic lymphocyte granules and removes an N-terminal Gly-Glu dipeptide from the graB zymogen (Brown *et al.*, 1993; Smyth *et al.*, 1995). Although studies on DPP-1 have focused on its role in activation of serine proteinases in immune and inflammatory cells, it has nonetheless been demonstrated in primary spermatocytes (Chung *et al.*, 1998) and in human placenta (Lampelo *et al.*, 1987; Rao *et al.*, 1997). Thus, the mechanism for graB activation exists in both germ cells and placenta, further supporting the idea that graB-mediated proteolysis occurs in these tissues.

Proteases and their inhibitors play an important role in testicular development and germ cell maturation (Fritz *et al.*, 1993). Controlled proteolytic activity is essential to the remodelling and restructuring of the seminiferous tubule during the migration of germ cells from the basement membrane to the lumen of the tubule. The plasminogen activators t-PA (tissue type) and u-PA (urokinase) and their cognate inhibitors (PAI-1 and PAI-2) play a role in the degradation of tight junctions between Sertoli cells during testis development (Lacroix *et al.*, 1977). The plasminogen activators are also present in seminal plasma (Astedt *et al.*, 1979) and spermatozoa (Smokovitis *et al.*, 1992), and PAI-1 and PAI-2 are expressed within the seminiferous tubule (Gunnarsson *et al.*, 1999). Acrosomal serine proteinases such as acrosin, TESP-1 and TESP-2 (Kohno *et al.*, 1998) have also been implicated in the degradation of the zona pellucida and fertilization of the ova.

Serine proteinases of unknown function are also present in human testis. The proteolytic activity of leydin and testisin are unknown. However, their restricted expression to Leydig cells and pachytene spermatocytes respectively, implicates them in testicular function (Hooper *et al.*, 1999; Poorafshar and Hellman, 1999). Loss of testisin expression has also been associated with the development of testicular germ cell tumours. Interestingly, graB shares a similar expression pattern to testisin, as it is also expressed in pachytene spermatocytes and is absent from germ cell tumour lines. Perhaps loss of graB is also associated with germ cell tumour progression.

The expression of graB in cells that represent the transition from mitotic to meiotic division suggests that graB is involved in germ cell maturation. Developing germ cells must also migrate through the blood–testis barrier in a process that involves proteolytic degradation of the tight junctions between Sertoli cells and it is possible that graB is involved in this process. However, the lack of graB in mature spermatozoa suggests that it is not involved in fertilization.

Serine proteinases are intimately involved in placental development, particularly during implantation. During this process the trophectoderm (which comprises the outer layer of the blastocyst) and invasive cytotrophoblasts secrete a myriad of extracellular matrix degrading proteases. Of these, the serine proteinases uPA, tPA, kallikrein, cryptase and elastase contribute to the extensive matrix remodelling required for invasion of the blastocyst through the endometrial wall and stroma, and eventually into maternal blood vessels. Expression of the serpins PAI-1 and PAI-2, and tissue inhibitors of metalloproteinases (TIMPs) by trophoblasts and endometrial decidual cells is thought to regulate the extent of invasion (Salamonsen, 1999; for review). It will be of interest to determine whether graB is expressed by invasive cytotrophoblasts and contributes to implantation. In the term placenta matrix remodelling proteases and their inhibitors are also important during parturition. Here, matrix metalloproteinases and TIMPs, as well as plasminogen activators and their inhibitors, are thought to regulate this process (Tsatas *et al.*, 1998; Athayde *et al.*, 1999; Hu *et al.*, 1999; Riley *et al.*, 1999), and graB may also contribute to this process.

The presence of PI-9 in Sertoli cells and the syncytial trophoblast layer, which form the blood–tissue barriers, is consonant with its role in cytoprotection against graB. PI-9 may provide protection against graB produced by maternal or self-reactive cytotoxic lymphocytes and thus contribute to immune privilege. Although the entry of graB into the cytoplasm of cells normally requires perforin, other endosomolytic agents or events can mediate its release (Froelich *et al.*, 1996; Browne *et al.*, 1999). Thus the presence of PI-9 in the cytoplasm and nuclei of cells producing graB (or in closely associated cells) may guard against inappropriate apoptosis in testis and placenta induced by misdirected graB.

Finally, it is possible that the role of graB and PI-9 in reproduction or immune privilege may be further elucidated by careful study using rodent models. At present it is not known whether graB or PI-9 orthologues are expressed in mouse testis or placenta. However, using polyclonal antisera raised against PI-9 we have demonstrated staining in rat and mouse seminiferous tubules (data not shown). These findings should be tempered by the observation that, compared with humans, rodents have a significantly expanded repertoire of both granzymes (Smyth *et al.*, 1996) and serpins (Sun *et al.*, 1997), and that the functions of these genes may be duplicated, shared or redundant. This difficulty is illustrated by the graB-null mice which have an immune deficiency but are fertile (Heusel *et al.*, 1994), implying that in rodents either graB is unimportant for reproduction or it is functionally redundant. Nonetheless it should be noted that these mice have not been thoroughly analysed for reproductive function in terms of organ or embryonal development, fecundity or litter size. As was the case with FSH-null mice, FSH was predicted to be essential for spermatogenesis. However, more detailed investigations revealed that FSH-deficient males were fertile despite having markedly reduced testis weight (Kumar *et al.*, 1997). Similar investigations may uncover a reproductive defect in the graB-null mice.

In conclusion, our work clearly suggests roles for graB and PI-9 beyond the immune system in human reproductive function. The targets and precise function of graB in this context remain to be determined, but it is likely to involve extracellular matrix remodelling in germ cell maturation and trophoblast invasion.

Acknowledgements

We are grateful to Dr P.Hosking (Department of Anatomical Pathology, Box Hill Hospital) for providing archival tissues, S.Black (Monash University, Box Hill Hospital) for the placental trophoblasts and tissue blocks, Dr P.Rogers (Monash University, Monash Medical Centre) for the endometrial sections and Prof. D.M.de Kretser Monash Institute of Reproduction and Development) for access to the testis material. We would also like to thank T.Meehan for help with the preparation of figures. This work was funded by the National Health and Medical Research Council of Australia. C.Hirst and M.Buzza are recipients of the Australian Postgraduate Award.

References

Alimonti, J.B., Shi, L., Baijal, P.K. *et al.* (2000) Granzyme B induces BID-mediated cytochrome c release and mitochondrial permeability transition. *J. Biol. Chem.*, **12**, 6974–6982.

Andrade, F., Roy, S., Nicholson, D. *et al.* (1998) Granzyme B directly and efficiently cleaves several downstream caspase substrates: implications for CTL-induced apoptosis. *Immunity*, **8**, 451–460.

Apostolidis, V.A., Browne, K.A., Smyth, M.J. *et al.* (1995) The peptide loop consisting of amino acids 139–157 of human granzyme B (fragmentin 2) contains an immunodominant epitope recognized by the mouse. *Mol. Immunol.*, **32**, 909–917.

Astedt, B., Wallen, P. and Aasted, B. (1979) Occurrence of both urokinase and tissue plasminogen activator in human seminal plasma. *Thromb. Res.*, **16**, 463–472.

Athayde, N., Romero, R., Gomez, R. *et al.* (1999) Matrix metalloproteinases-9 in preterm and term human parturition. *J. Matern. Fetal Med.*, **8**, 213–219.

Barry, M., Heibein, J.A., Pinkoski, M.J. *et al.* (2000) Granzyme B short-circuits the need for caspase 8 activity during granule-mediated cytotoxic T-lymphocyte killing by directly cleaving Bid. *Mol. Cell Biol.*, **20**, 3781–3794.

Berthou, C., Marolleau, J.P., Lafaurie, C. *et al.* (1995) Granzyme B and perforin lytic proteins are expressed in CD34+ peripheral blood progenitor cells mobilized by chemotherapy and granulocyte colony-stimulating factor. *Blood*, **86**, 3500–3506.

Bird, C.H., Sutton, V.R., Sun, J. *et al.* (1998) Selective regulation of apoptosis: the cytotoxic lymphocyte serpin proteinase inhibitor 9 protects against granzyme B-mediated apoptosis without perturbing the Fas cell death pathway. *Mol. Cell Biol.*, **18**, 6387–6398.

Bird, C.H., Blink, E.J., Hirst, C.E. *et al.* (2001) Nucleocytoplasmic distribution of the ovalbumin serpin PI-9 requires a nonconventional nuclear import pathway and the export factor Crm1. *Mol. Cell Biol.*, **21**, 5396–5407.

Brown, G.R., McGuire, M.J. and Thiele, D.L. (1993) Dipeptidyl peptidase I is enriched in granules of *in vitro*- and *in vivo*-activated cytotoxic T lymphocytes. *J. Immunol.*, **150**, 4733–4742.

Browne, K.A., Blink, E., Sutton, V.R. *et al.* (1999) Cytosolic delivery of granzyme B by bacterial toxins: evidence that endosomal disruption, in addition to transmembrane pore formation, is an important function of perforin. *Mol. Cell Biol.*, **19**, 8604–8615.

Buzza, M.S., Hirst, C.E., Bird, C.H. *et al.* (2001) The granzyme B inhibitor, PI-9, is present in endothelial and mesothelial cells, suggesting a role in bystander cell protection during an immune response. *Cell Immunol.*, **210**, 21–29.

Caputo, A., Fahey, D., Lloyd, C. *et al.* (1988) Structure and differential mechanisms of regulation of expression of a serine esterase gene in activated human T lymphocytes. *J. Biol. Chem.*, **263**, 6363–6369.

Chung, S.S., Zhu, L.J., Mo, M.Y. *et al.* (1998) Evidence for cross-talk between Sertoli and germ cells using selected cathepsins as markers. *J. Androl.*, **19**, 686–703.

Ebnet, K., Levelt, C.N., Tran, T.T. *et al.* (1995) Transcription of granzyme A and B genes is differentially regulated during lymphoid ontogeny. *J. Exp. Med.*, **181**, 755–763.

Edwards, K.M., Kam, C.M., Powers, J.C. *et al.* (1999) The human cytotoxic T cell granule serine protease granzyme H has chymotrypsin-like (chymase) activity and is taken up into cytoplasmic vesicles reminiscent of granzyme B-containing endosomes. *J. Biol. Chem.*, **274**, 30468–30473.

Fritz, I.B., Tung, P.S. and Ailenberg, M. (1993) Proteases and antiproteases in the seminiferous tubule. In Russell, L.D. and Griswold, M.D. (eds) *The Sertoli Cell*, Cache River Press, Clearwater, pp. 217–236.

Froelich, C.J., Zhang, X., Turbov, J. *et al.* (1993) Human granzyme B degrades aggrecan proteoglycan in matrix synthesized by chondrocytes. *J. Immunol.*, **151**, 7161–7171.

Froelich, C.J., Orth, K., Turbov, J. *et al.* (1996) New paradigm for lymphocyte granule-mediated cytotoxicity. Target cells bind and internalize granzyme B, but an endosomolytic agent is necessary for cytosolic delivery and subsequent apoptosis. *J. Biol. Chem.*, **271**, 29073–29079.

Gunnarsson, M., Lecander, I. and Abrahamsson, P.A. (1999) Factors of the plasminogen activator system in human testis, as demonstrated by in-situ hybridization and immunohistochemistry. *Mol. Hum. Reprod.*, **5**, 934–940.

Hameed, A., Truong, L.D., Price, V. *et al.* (1991) Immunohistochemical localization of granzyme B antigen in cytotoxic cells in human tissues. *Am. J. Pathol.*, **138**, 1069–1075.

Heibein, J.A., Goping, I.S., Barry, M. *et al.* (2000) Granzyme B-mediated cytochrome c release is regulated by the bcl-2 family members bid and Bax. *J. Exp. Med.*, **192**, 1391–1402.

Held, W., MacDonald, R. and Mueller, C. (1990) Expression of genes encoding cytotoxic cell-associated serine proteases in thymocytes. *Int. Immunol.*, **2**, 57–62.

Heusel, J.W., Wesselschmidt, R.L., Shresta, S. *et al.* (1994) Cytotoxic lymphocytes require granzyme B for the rapid induction of DNA fragmentation and apoptosis in allogeneic target cells. *Cell*, **76**, 977–987.

Hooper, J.D., Nicol, D.L., Dickinson, J.L. *et al.* (1999) Testisin, a new human serine proteinase expressed by premeiotic testicular germ cells and lost in testicular germ cell tumors. *Cancer Res.*, **59**, 3199–3205.

Hu, Z.Y., Liu, Y.X., Liu, K. *et al.* (1999) Expression of tissue type and urokinase type plasminogen activators as well as plasminogen activator inhibitor type-1 and type-2 in human and rhesus monkey placenta. *J. Anat.*, **194**, 183–195.

Huntington, J.A., Read, R.J. and Carrell, R.W. (2000) Structure of a serpin–protease complex shows inhibition by deformation. *Nature*, **407**, 923–926.

Jans, D.A., Jans, P., Briggs, L.J. *et al.* (1996) Nuclear transport of granzyme B (fragmentin-2). Dependence of perforin *in vivo* and cytosolic factors *in vitro*. *J. Biol. Chem.*, **271**, 30781–30789.

Kliman, H.J., Nestler, J.E., Sermasi, E. *et al.* (1986) Purification, characterization, and *in vitro* differentiation of cytotrophoblasts from human term placentae. *Endocrinology*, **118**, 1567–1582.

Kohno, N., Yamagata, K., Yamada, S. *et al.* (1998) Two novel testicular serine proteases, TESP1 and TESP2, are present in the mouse sperm acrosome. *Biochem. Biophys. Res. Commun.*, **245**, 658–665.

Kumar, T.R., Wang, Y., Lu, N. *et al.* (1997) Follicle stimulating hormone is required for ovarian follicle maturation but not male fertility. *Nature Genet.*, **15**, 201–204.

Kummer, J.A., Kamp, A.M., van Katwijk, M. *et al.* (1993) Production and characterization of monoclonal antibodies raised against recombinant human granzymes A and B and showing cross reactions with the natural proteins. *J. Immunol. Methods*, **163**, 77–83.

Kummer, J.A., Kamp, A.M., Tadema, T.M. *et al.* (1995) Localization and identification of granzymes A and B-expressing cells in normal human lymphoid tissue and peripheral blood. *Clin. Exp. Immunol.*, **100**, 164–172.

Lacroix, M., Smith, F.E. and Fritz, I.B. (1997) Secretion of plasminogen activators by Sertoli cell enriched cultures. *Mol. Cell Endocrinology*, **9**, 227–236.

Lampelo, S., Lalu, K. and Vanha-Perttula, T. (1987) Biochemical studies on dipeptidyl peptidases I to IV of the human placenta. *Placenta*, **8**, 389–398.

Liu, C.C., Rafii, S., Granelli-Piperno, A. *et al.* (1989) Perforin and serine esterase gene expression in stimulated human T cells. Kinetics, mitogen requirements, and effects of cyclosporin A. *J. Exp. Med.*, **170**, 2105–2118.

Meinhardt, A., O'Bryan, M.K., MacFarlane, J.R. *et al.* (1999) Localization of follistatin in the rat testis. *J. Reprod. Fertil.*, **112**, 233–241.

Pera, M.F., Blasco Lafita, M.J. and Mills, J. (1987) Cultures stem cells from human testicular teratomas: the nature of human embryonal carcinoma and its comparison with two types of yolk-sac carcinoma. *Int. J. Cancer*, **40**, 334–343.

Pera, M.F., Blasco Lafita, M.J., Cooper, S. *et al.* (1988) Analysis of cell-differentiation lineage in human teratomas using new monoclonal antibodies to cytostructural antigens of embryonal carcinoma cells. *Differentiation*, **39**, 139–149.

Pera, M.F., Cooper, S., Mills, J. *et al.* (1989) Isolation and characterization of a multipotent clone of human embryonal carcinoma cells. *Differentiation*, **42**, 10–23.

Pinkoski, M.J., Winkler, U., Hudig, D. *et al.* (1996) Binding of granzyme B in the nucleus of target cells. Recognition of an 80-kilodalton protein. *J. Biol. Chem.*, **271**, 10225–10229.

Poe, M., Blake, J.T., Boulton, D.A. *et al.* (1991) Human cytotoxic lymphocyte granzyme B. Its purification from granules and the characterization of substrate and inhibitor specificity. *J. Biol. Chem.*, **266**, 98–103.

Poorafshar, M. and Hellman, L. (1999) Cloning and structural analysis of leydin, a novel human serine protease expressed by the Leydig cells of the testis. *Eur. J. Biochem.*, **261**, 244–250.

Rao, N.V., Rao, G.V. and Hoidal, J.R. (1997) Human dipeptidyl-peptidase I. Gene characterization, localization, and expression. *J. Biol. Chem.*, **272**, 10260–10265.

Riley, S.C., Leask, R., Denison, F.C. *et al.* (1999) Secretion of tissue inhibitors of matrix metalloproteinases by human fetal membranes, decidua and placenta at parturition. *J. Endocrinol.*, **162**, 351–359.

Ronday, H.K., van der Laan, W.H., Tak, P.P. *et al.* (2001) Human granzyme B mediates cartilage proteoglycan degradation and is expressed at the invasive front of the synovium in rheumatoid arthritis. *Rheumatology*, **40**, 55–61.

Salamonsen, L.A. (1999) Role of proteases in implantation. *Rev. Reprod.*, **4**, 11–22.

Sayers, T.J., Wiltrout, T.A., Sowder, R. *et al.* (1992) Purification of a factor from the granules of a rat natural killer cell line (RNK) that reduces tumor cell growth and changes tumor morphology. Molecular identity with a granule serine protease (RNKP-1). *J. Immunol.*, **148**, 292–300.

Shi, L., Mai, S., Israels, S. *et al.* (1997) Granzyme B (GraB) autonomously crosses the cell membrane and perforin initiates apoptosis and GraB nuclear localization. *J. Exp. Med.*, **185**, 855–866.

Smokovitis, A., Kokolis, N., Taitzoglou, I. *et al.* (1992) Plasminogen activator: the identification of an additional proteinase at the outer acrosomal membrane of human and boar spermatozoa. *Int. J. Fertil.*, **37**, 308–314.

Smyth, M.J., McGuire, M.J. and Thia, K.Y. (1995) Expression of recombinant human granzyme B. A processing and activation role for dipeptidyl peptidase I. *J. Immunol.*, **154**, 6299–6305.

Smyth, M.J., O'Connor, M.D. and Trapani, J.A. (1996) Granzymes: a variety of serine protease specificities encoded by genetically distinct subfamilies. *J. Leukoc. Biol.*, **60**, 555–562.

Sun, J., Coughlin, P., Salem, H.H. *et al.* (1995) Production and characterization of recombinant human proteinase inhibitor 6 expressed in Pichia pastoris. *Biochem. Biophys. Acta*, **1252**, 28–34.

Sun, J., Bird, C.H., Sutton, V. *et al.* (1996) A cytosolic granzyme B inhibitor related to the viral apoptotic regulator cytokine response modifier A is present in cytotoxic lymphocytes. *J. Biol. Chem.*, **271**, 27802–27809.

Sun, J., Ooms, L., Bird, C.H. *et al.* (1997) A new family of 10 murine ovalbumin serpins includes two homologs of proteinase inhibitor 8 and two homologs of the granzyme B inhibitor (proteinase inhibitor 9). *J. Biol. Chem.*, **272**, 15434–15441.

Sun, J., Whisstock, J.C., Harriott, P. *et al.* (2001) Importance of the P4′ residue in human granzyme B inhibitors and substrates revealed by scanning mutagenesis of the PI-9 reactive center loop. *J. Biol. Chem.*, **276**, 15177–15184.

Sutton, V.R., Davis, J.E., Cancilla, M. *et al.* (2000) Initiation of apoptosis by granzyme B requires direct cleavage of bid, but not direct granzyme B-mediated caspase activation. *J. Exp. Med.*, **192**, 1403–1414.

Tak, P.P., Spaeny-Dekking, L., Kraan, M.C. *et al.* (1999) The levels of soluble granzyme A and B are elevated in plasma and synovial fluid of patients with rheumatoid arthritis (RA). *Clin. Exp. Immunol.*, **116**, 366–370.

Trapani, J.A., Klein, J.L., White, P.C. *et al.* (1988) Molecular cloning of an inducible serine esterase gene from human cytotoxic lymphocytes. *Proc. Natl Acad. Sci. USA*, **85**, 6924–6928.

Trapani, J.A., Jans, D.A., Jans, P.J. *et al.* (1998) Efficient nuclear targeting of granzyme B and the nuclear consequences of apoptosis induced by granzyme B and perforin are caspase-dependent, but cell death is caspase-independent. *J. Biol. Chem.*, **273**, 27934–27938.

Tsatas, D., Baker, M.S., Moses, E.K. *et al.* (1998) Gene expression of plasminogen activation cascade components in human term gestational tissues with labour onset. *Mol. Hum. Reprod.*, **4**, 101–106.

Wano, Y., Uchiyama, T., Fukui, K. *et al.* (1984) Characterization of human interleukin 2 receptor (Tac antigen) in normal and leukemic T cells: co-expression of normal and aberrant receptors on Hut-102 cells. *J. Immunol.*, **132**, 3005–3010.

Yang, X., Stennicke, H.R., Wang, B. *et al.* (1998) Granzyme B mimics apical caspases. Description of a unified pathway for trans-activation of executioner caspase-3 and -7. *J. Biol. Chem.*, **273**, 34278–34283.

Young, J.L., Sukhova, G.K., Foster, D. *et al.* (2000) The serpin proteinase inhibitor 9 is an endogenous inhibitor of interleukin 1beta-converting enzyme (caspase-1) activity in human vascular smooth muscle cells. *J. Exp. Med.*, **191**, 1535–1544.

Received on May 11, 2001; accepted on September 12, 2001

C ular Immunology **210**, 21–29 (2001)
d· :10.1006/cimm.2001.1806, available online at http://www.idealibrary.com on IDEAL®

The Granzyme B Inhibitor, PI-9, Is Present in Endothelial and Mesothelial Cells, Suggesting That It Protects Bystander Cells during Immune Responses

Marguerite S. Buzza,* Claire E. Hirst,* Catherina H. Bird,* Patrick Hosking,† Joseph McKendrick,‡ and Phillip I. Bird*

**Department of Biochemistry and Molecular Biology, Monash University, 3800 Victoria, Australia; and †Department of Anatomical Pathology and ‡Department of Oncology, Box Hill Hospital, Box Hill, 3128 Victoria, Australia*

Received February 27, 2001; accepted May 8, 2001

Proteinase inhibitor 9 (PI-9) is a 42-kDa human intracellular serpin present in cytotoxic lymphocytes (CLs). PI-9 is an extremely efficient inhibitor of the pro-apoptotic CL granule proteinase granzyme B and is thought to function in the cytosol of CLs to protect against apoptosis induced by endogenously expressed or released granzyme B, particularly during target cell killing. Here we show by immunohistochemistry that PI-9 is also present in endothelial cells, in every tissue examined. Cultured endothelial cells express functional PI-9 (as assessed by binding to recombinant granzyme B) localized to the cytoplasm and nucleus. Immunohistochemistry also showed PI-9 in mesothelial cells, and this was confirmed by analysis of primary cells cultured from pleural and serous effusions. Granzyme B expression was not detected in either endothelial or mesothelial cells. In both cell types, PI-9 is up-regulated at the mRNA and protein level by exposure to the phorbol ester PMA, consistent with a response to inflammatory stimuli. We postulate that PI-9 is present in these lining cell types to protect against misdirected, free granzyme B released during a local immune response. © 2001 Academic Press

Key Words: **PI-9; granzyme B; cytotoxic lymphocyte; bystander cell; apoptosis; endothelial cell; mesothelial cell; serpin.**

INTRODUCTION

Granule-mediated apoptosis is an important mechanism used by cytotoxic lymphocytes (CTL and NK cells) for the clearance of virally infected and malignant cells. Upon recognition and conjugation with a target cell, cytotoxic lymphocyte (CL) granule contents are released into the intercellular space. Internalization of granule cytotoxins occurs, followed by their release into the target cell cytoplasm via perforin-induced rupture of endocytic vesicles (1). The major granule effector molecule is the serine proteinase granzyme B (graB). GraB rapidly induces apoptosis of the target cell via by directly activating apical pro-apoptotic caspases (2, 3) and by cleaving the pro-apoptotic molecule Bid, leading to mitochondrial dysfunction and cytochrome C release (4–6).

We have recently described a potent inhibitor of graB; proteinase inhibitor 9 (PI-9), which is highly expressed by CLs (7). PI-9 is an intracellular protein belonging to the serpin superfamily. Serpins regulate the activity of serine proteinases by the formation of an irreversible (SDS-stable) complex. The specificity of inhibition achieved by a particular serpin is dependent on the amino acids present in an exposed peptide loop (reactive center loop, RCL), which acts as a pseudosubstrate for the target protease. Cleavage of the RCL by the protease occurs, followed by a large conformational change in the serpin that translocates and distorts the protease, leaving it inactive and susceptible to proteolysis (8). PI-9 is an extremely efficient inhibitor of graB (rate constant (K_{ass}) 1.7 ± 0.3 × 10^6 M^{-1} s^{-1}), with which it forms a 1:1 SDS-stable complex, typical of a serpin–serine proteinase interaction. Ectopic expression of PI-9 in target cells effectively protects against CL–granzyme B mediated apoptosis. As PI-9 is highly expressed in CL cytosol, we have proposed a role for PI-9 in self-protection from endogenously expressed and released granzyme B (9).

Although it is commonly thought that CL granule release is unidirectional into the target cell, there is *in vitro* evidence that shows that nontarget or bystander cells in the proximity of the killing reaction can also undergo apoptosis in a granule-dependent mechanism (10). *In vivo*, in situations in which a CTL response is occurring, local serum concentrations of graB are highly elevated (11). Thus, bystander cells in the vicinity of an immune response are likely to be exposed to locally released perforin and graB, and it would be detrimental for these normal cells to be inadvertently killed. Consistent with this is evidence that PI-9 is

0008-8749/01 $35.00

produced by other cells of the immune system which do not endogenously express graB, such as B cells (7) and monocytes (12).

Lining cells such as endothelial and mesothelial cells are in close contact with activated lymphocytes during an immune response. Both are mesodermally derived simple squamous epithelial cells. Endothelial cells line the lumen of the vasculature, and mesothelial cells line the body cavities and outer surfaces of internal organs. These cells are both thought to actively participate in local immune responses through production of inflammatory cytokines and presentation of antigen (reviewed in 13, 14). As PI-9 expression does not appear solely restricted to CLs, we sought to examine whether this graB inhibitor is also expressed by endothelial and mesothelial cells that may also require protection from locally released graB during an immune response.

MATERIALS AND METHODS

Antibodies. Monoclonal anti-PI-9 antibody (7D8) (characterized by C. Hirst, manuscript in preparation) and rabbit 15 anti-PI-9 antiserum (extensively characterized against a large panel of related serpins) were produced in this laboratory. Monoclonal anti-granzyme B (2C5) antibody was provided by Dr. J. Trapani and has been previously described (15). Mouse IgG1 isotype control was purchased from Pharmingen. Other antibodies used for the identification of mesothelial and endothelial cells were mouse anti-cytokeratin 8 (CAM5.2, Becton–Dickenson), rabbit anti-PAN cytokeratin (Zymed), mouse anti-vimentin (clone LN6, Sigma), rabbit anti-vWF (provided by Dr. S. Jackson), mouse anti-CD45 (Sigma), mouse anti-CD3 (Diatec), and mouse anti-CD14 (Diatec).

Primary endothelial cells and cell lines. Human umbilical vein endothelial cells (HUVEC) were isolated from fresh umbilical cords by collagenase digestion as previously described (16). HUVECs and the spontaneously transformed HUVEC cell line C11STH (17) were maintained on dishes precoated with 0.2% gelatin in M199 medium containing 20% FCS (Gibco-BRL), as described in (17). Human myometrial microvascular endothelial cells were provided by Dr. P. Rogers and cultured in M199 medium (Gibco-BRL) with 15% pooled male serum and 5% FCS, according to (18). YT cells (ATCC) were maintained in RPMI medium with 10% FCS, 2 mM glutamine, 1 mM pyruvate, and 55 μM mercaptoethanol (Gibco-BRL).

Processing and culture of mesothelial cells from serous effusions. Serous effusions (pleural or peritoneal) were obtained from patients in the Box Hill Hospital Oncology Department, with hospital ethics committee approval (No. 99/078). Cells in approximately 400 ml of fluid were pelleted at 150*g*, resuspended in erythrocyte lysis buffer (168 mM NH_4Cl, 10 mM $KHCO_3$, 0.1 mM EDTA, pH 7.3, for 5 min at RT, repelleted, and washed in PBS. For cytospin preparations, cells were resuspended at 2×10^6 cells/ml, and 100 μl was cytospun onto glass slides. For culture of mesothelial cells, nonerythrocytes were resuspended at 1×10^6 cells/ml in RPMI medium (Gibco-BRL) containing 10% FCS and allowed to adhere to tissue culture dishes (Nunc). Mesothelial cells formed confluent monolayers within 1–2 weeks. Nonadherent leukocytes and malignant cells were removed through changes of medium, and any adherent macrophages were diluted out with passaging. Cells were subcultured routinely at 1:3 for up to six passages after which they became senescent.

Identification of mesothelial cells and indirect immunofluorescence. Cytospin preparations were stained with hemotoxylin and eosin (H&E) to observe cellular morphology. Cytospin preparations or cultured mesothelial/endothelial cells seeded onto glass slides were used for indirect immunofluorescence. Cells were fixed in 3.7% formaldehyde for 20 min and permeabilized in 0.5% Triton X-100 for 5 min. Cells were incubated with primary antibodies for 30 min at RT, followed by incubation with a 1:200 dilution of the appropriate secondary antibody, FITC-conjugated sheep anti-rabbit Ig (Silenus) or RITC-conjugated goat anti-mouse Ig (Immunotech), for 30 min at RT. Mesothelial cells were identified by expression of the intermediate filaments cytokeratin (CK) (CAM5.2, 1:10 or rabbit anti-CK 1:200), and vimentin (1:25). In addition, mesothelial cells were negative for the endothelial marker vWF (1:500), the pan-leukocyte marker CD45 (1:25), the T cell marker CD3 (1:25), and the macrophage marker CD14 (1:25). Monoclonal anti-PI-9 antibody hybridoma supernatant (neat) was used to detect PI-9 and mouse IgG1 (1:200) was used as an isotype-matched negative control.

Cell lysates and immunoblotting. Trypsinized cells were lysed in 1% NP-40 on ice for 15 min, and insoluble material was pelleted by centrifugation at 15,800*g*. Unless otherwise stated, 80 μg of soluble protein was electrophoresed on 12.5% SDS–polyacrylamide gels and transferred to nitrocellulose membrane (Bio-Rad). For each cell type, 50 ng of recombinant human graB (19) was added to 80 μg of cell lysate and incubated for 10 min at 37°C, prior to the addition of sample buffer. Recombinant PI-9 (7) alone (50 ng) or preincubated with 50 ng of graB were also used as controls for complex formation. The blot was incubated with primary antibody overnight at 4°C followed by detection with sheep anti-mouse Ig conjugated to horseradish peroxidase (1:200, Silenus) and enhanced chemiluminescent detection (NEN). PI-9 was detected using monoclonal hybridoma supernatant (1:10) and graB was detected using a monoclonal antibody (2C5) ascites fluid at 1:2000 after stripping the membrane.

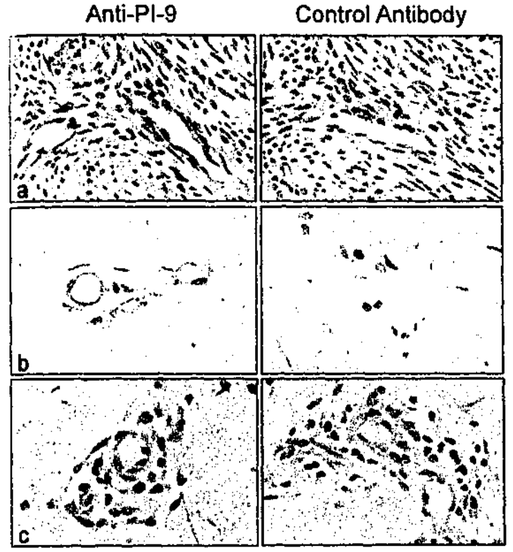

FIG. 1. PI-9 expression in endothelial cells of various human tissues. PI-9 was detected using a rabbit polyclonal (a and b) or mouse monoclonal (c) anti-PI-9 antibody. Control antibody is preimmune serum (a and b) or IgG1 isotype control (c). Endothelial cells in the myometrium (a), breast (b), and a dermal capillary heamangioma (c) are shown.

Immunohistochemistry. Most formalin-fixed paraffin-embedded tissue samples were obtained from the Box Hill Hospital Anatomical Pathology Department, provided by the chief pathologist Dr. P. Hosking. Human endometrial tissue was provided by Dr. P. Rogers (Monash Medical Centre). Human skin sections were provided by Dr. F. Scott. Sections (5 μm) were cut, dewaxed, and rehydrated according to standard procedures. For some antibodies/tissue sections, antigen retrieval was required. This involved incubation in 10 mM citric acid, pH 6.0, and boiling by microwaving for 10 min. After being blocked in 2% BSA in phosphate-buffered saline (PBS), sections were incubated with primary antibody in 1% BSA overnight at RT, washed in PBS containing 0.1% Tween, and incubated for 30 min in biotinylated sheep anti-mouse or anti-rabbit Ig (1:200, Silenus). After being washed in PBS, sections were incubated in streptavidin–horseradish peroxidase (1:200, Silenus) for 30 min. Sections were washed and developed using diaminobenzidine (Dako) and counterstained with Mayer's hemotoxylin. Primary antibody dilutions were as follows: mouse monoclonal anti-PI-9 hybridoma supernatant, neat; rabbit anti-PI-9 serum or preimmune, 1:2000; mouse anti-CK 8 (CAM5.2), 1:20.

Northern blotting and stimulation of cultured cells with PMA. A nitrocellulose membrane containing 5 μg of total RNA from C11STH cells which had been stimulated with 5 nM PMA (4β-phorbol 12-myristate 13-acetate, Sigma) for 0, 6, and 24 h was kindly provided by Dr. M. Costa in the laboratory of Dr. R. Medcalf. The membrane was hybridized to a [^{32}P]dATP-labeled (Prime-a-gene labeling system, Promega) PI-9 cDNA probe in Rapid-hyb buffer (Amersham) at 68°C. The membrane was washed in 0.1× SSC at 68°C and exposed to X-ray film. To control for RNA loading, the membrane was also hybridized with a β-actin cDNA probe (provided by Dr. R. Medcalf). For protein analysis, semiconfluent second passage HUVECs and third passage pleural mesothelial cells were stimulated with 25 nM PMA for 6 or 24 h, respectively. After this time,

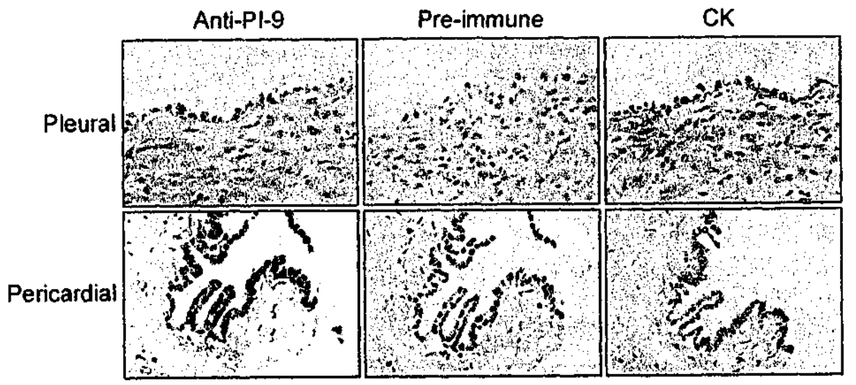

FIG. 3. PI-9 is expressed in reactive/activated mesothelium in inflamed sites. Tissue sections containing mesothelium in diseased states were stained for PI-9 using rabbit anti-PI-9 serum and for cytokeratin (CK) for identification. Pleural mesothelial cells both on the surface and caught up in fibrous tissue covering the lung of a patient with pleurisy (top) and pericardial mesothelium from a patient with a metastatic lung carcinoma which had invaded the pericardial space (bottom) are shown.

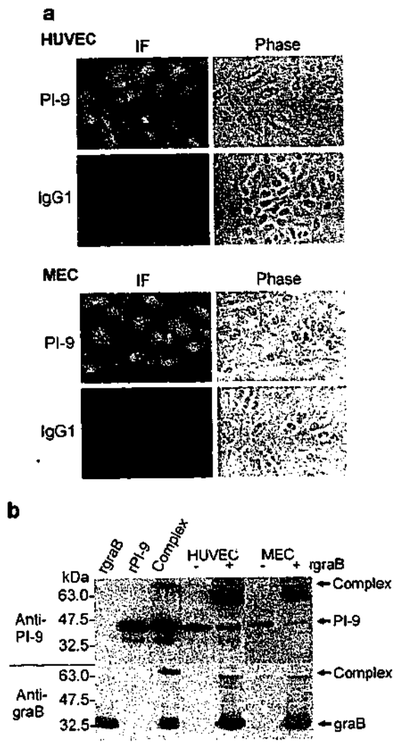

FIG. 2. Expression of PI-9 by large and small vessel endothelial cells. (a) Primary human umbilical vein endothelial cells (HUVEC) and microvascular endothelial cells (MEC) from the myometrium were stained with monoclonal anti-PI-9 antibody or IgG1 control antibody by indirect immunofluorescence (IF). (b) Detection of active PI-9 in HUVEC and MEC lysates. Lysates were incubated with (+) or without (−) recombinant human graB (rgraB) at 37°C for 10 min prior to analysis by 12.5% SDS–PAGE, followed by immunoblotting. As controls, recombinant PI-9 (rPI-9) and rgraB alone or in complex are also shown. Following blotting with monoclonal anti-PI-9, the membrane was stripped and reprobed with a monoclonal anti-graB antibody.

cells were lysed in 1% NP-40 lysis buffer and 80 μg of stimulated and unstimulated cell lysates were analyzed by immunoblotting with the monoclonal anti-PI-9 antibody. Quantitation by densitometry was performed using the Gel-Pro Analyzer (3.1) program.

RESULTS

Normal Human Endothelial Cells Produce PI-9

During an immunohistochemical survey of human tissues for PI-9 expression, it was noted that PI-9 is produced by endothelial cells. Positive staining for PI-9 in endothelial cells was observed in all tissues examined using either a mouse monoclonal or a rabbit polyclonal anti-PI-9. Normal tissues examined included the uterus (Fig. 1a), breast (Fig. 1b), placenta, testis, and dermis (not shown). Other tissues examined had some associated pathological condition but also clearly showed PI-9 in endothelial cells. These included lung, lymph node, tonsil, and ovary (not shown). Shown in Fig. 1c is a dermal lobular capillary hemangioma surrounded by leukocytes, some of which are also positive for PI-9. Normal dermal capillary endothelial cells showed positive but weaker staining. Thus, it appears PI-9 is ubiquitously expressed by endothelial cells throughout the body. As immunohistochemistry is not a quantitative assay, the level of PI-9 in normal compared to inflamed/activated endothelial cells was not determined.

PI-9 Is Produced by Primary Cultured Human Endothelial Cells

To confirm the findings by immunohistochemistry, primary cultured human endothelial cells were examined for PI-9 expression. Two primary endothelial cell types were analyzed; large vessel human umbilical vein endothelial cells from term umbilical cords and microvascular endothelial cells (MECs) from the human myometrium (staining shown in Fig. 1a). Cells were examined for PI-9 expression by indirect immunofluorescence using a monoclonal anti-PI-9 antibody. As shown in Fig. 2a, both cultured primary endothelial cell types show positive staining for PI-9 (cytosolic and nuclear) compared to the isotype-matched control.

Immunoblotting of cultured endothelial cell lysates confirmed PI-9 expression. Figure 2b shows a 42-kDa band representing PI-9 in the HUVEC and MEC cell lysates. In order to confirm that this protein was PI-9 and that it is active in endothelial cells, recombinant graB was added to the lysates. Inhibition of graB by PI-9 occurs through the formation of a SDS-stable PI-9-graB complex. This is shown in Fig. 2b, in which recombinant PI-9 has been incubated with recombinant graB (32 kDa), resulting in the expected 67-kDa complex. Upon addition of recombinant graB to the lysates, most of the 42-kDa protein has shifted in MW, indicating complex formation with graB, which demonstrates the presence of active PI-9 in endothelial cells. However, the complex is partially degraded due to the presence of excess graB. Figure 2b (lower panel) shows the same membrane reprobed with a monoclonal anti-graB antibody. This blot shows that endothelial cells do not endogenously produce detectable levels of granzyme B. PI-9 is also produced by the spontaneously transformed HUVEC cell line C11STH (see Fig. 6).

Expression of PI-9 in Activated Mesothelium

As mesothelial cells are morphologically and functionally similar to endothelial cells, particularly in relation to an immune response, mesothelial cells in human tissue sections were examined for expression of PI-9. Mesothelial cells are known to become activated or reactive when they are in an inflamed environment, such as during the production of ascites or pleural fluid. Expression of cytokeratin filaments was used to identify mesothelial cells in these tissues. Figure 3 shows expression of PI-9 in cytokeratin-positive reactive mesothelium surrounding the lung from a patient with pleurisy (top panel) and the heart in a patient with a lung carcinoma which had spread to the pericardial space (lower panel). Tissues containing normal resting mesothelium could not be examined due to difficulty in obtaining tissues that had not been removed due to some degree of inflammation or disease.

To further examine whether PI-9 expression was a common feature of reactive mesothelium, cells in serous effusions (mainly due to malignancy) were stained for PI-9 using a monoclonal antibody (Fig. 4). Pleural or peritoneal effusions generally contained a mixture of lymphocytes, neutrophils and macrophages, and a small proportion (approx. <10%) of mesothelial cells, which have sloughed off into the fluid. Mesothelial cells in cytospin preparations were identified first by morphology in H&E-stained samples (Fig. 4a, indicated by an arrow). These cells are distinguished by their size, abundant cytoplasm, round central nuclei, and a ruffled membrane due to the presence of microvilli. Expression of low-molecular-weight cytokeratins (Fig. 4b) and the intermediate filament vimentin (data not shown) were also used to identify mesothelial cells. PI-9 was observed in mesothelial cells in six pleural and six peritoneal serous effusions from different patients. Figure 4b shows an example of a peritoneal effusion double stained for cytokeratin expression and PI-9 using a monoclonal antibody (panel 1) or for cytokeratin and IgG1 isotype control (panel 2). PI-9 is clearly observed in the cytokeratin-positive mesothelial cells compared to the isotype control.

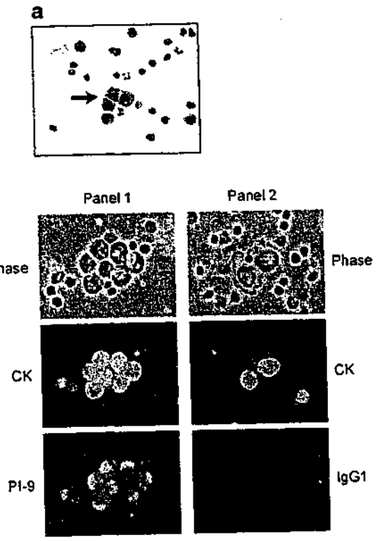

FIG. 4. Mesothelial cells in serous effusions express PI-9. (a) H&E-stained cytospin preparation from a peritoneal effusion. A group of mesothelial cells are indicated by the arrow. (b) Cytospin preparations from a peritoneal effusion, showing PI-9 expression by cytokeratin (CK)-positive mesothelial cells by indirect immunofluorescence. Cells were first stained with rabbit anti-PAN cytokeratin, which was detected with FITC-conjugated anti-rabbit Ig, followed by staining with a monoclonal antibody to PI-9 (panel 1) or IgG1 isotype control (panel 2) which was detected with RITC-conjugated anti-mouse Ig. The specificity of PI-9 staining in cytokeratin positive cells is shown by negative staining with the IgG1 isotype-matched control.

PI-9 Is Produced by Cultured Mesothelial Cells

As there are very few mesothelial cell lines, the serous effusions were also used as a source of primary mesothelial cells. Mesothelial cells were cultured from serous effusions and formed confluent, contact inhibited monolayers (Fig. 5a) with an epitheloid-like morphology as previously described (20). After approximately three to four passages, cultures were free of contaminating lymphocytes and neutrophils (nonadherent) and any adherent macrophages had been diluted out. The identity of mesothelial cells was confirmed by staining for various markers by indirect immunofluorescence. Cultured cells were positive for both cytokeratin (Fig. 5a, top panel) and vimentin (not shown) consistent with a mesothelial phenotype, and not that of contaminating fibroblasts or endothelial cells (21). In addition, cells were also negative for the endothelial marker vWF, the pan-leukocyte marker CD45, the T cell marker CD3, and the macrophage marker CD14 (not shown).

Pure mesothelial cell cultures were obtained from two pleural and two peritoneal serous effusions and were examined for PI-9 expression using the monoclonal anti-PI-9 antibody. Figure 5a is an example of cultured pleural mesothelial cells stained for PI-9. In these cells (and in cytospin preparations), PI-9 is located in both the cytosol and the cell nucleus, as is observed in endothelial cells (Fig. 2a). This is consistent with the cellular distribution of PI-9 in other cell types, in which a proportion of PI-9 is invariably located in the cell nucleus (C. Bird, in press). All four cultured mesothelial cells samples were PI-9 positive, and immunoblotting of the cell lysates confirmed PI-9 expression. Figure 5b (upper panel) shows 42-kDa PI-9 in a peritoneal mesothelial cell lysate. Upon addition of recombinant graB to the lysate, a proportion of the PI-9 is shifted to the expected 67-kDa PI-9–graB complex. This complex is also observed when the same membrane is reprobed with the monoclonal anti-graB antibody (Fig. 5b, lower panel). Similar to endothelial cells,

this blot also shows that mesothelial cells do not endogenously produce graB. Figure 5c shows PI-9 expression in two pleural and two peritoneal mesothelial cell lysates from different patients. The variation in the amount of PI-9 in mesothelial cells from different patients may simply be due to the different number of passages required to purify the cells or possibly the degree of inflammation in each patient.

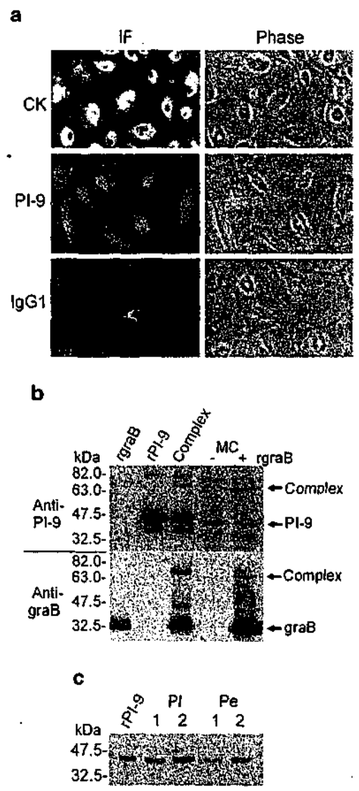

FIG. 5. Cultured mesothelial cells produce PI-9. (a) PI-9 expression by pure, cultured, cytokeratin (CK)-positive pleural mesothelial cells by indirect immunofluorescence. Cells were stained for CK, PI-9, or isotype-matched control (IgG1) as described in Fig. 4b. (b) Detection of active PI-9 in mesothelial cell lysates by complex formation with graB. Pure cultured mesothelial cell (MC) lysates were incubated with (+) or without (−) recombinant human graB (rgraB) at 37°C for 10 min prior to analysis by 12.5% SDS–PAGE, followed by immunoblotting. As controls, recombinant PI-9 (rPI-9) and graB (rgraB) alone or in complex are also shown. Following blotting with monoclonal anti-PI-9, the membrane was stripped and reprobed with monoclonal anti-graB antibody. (c) PI-9 is detected in mesothelial cells cultured from two pleural (Pl) and two peritoneal (Pe) effusions from different patients.

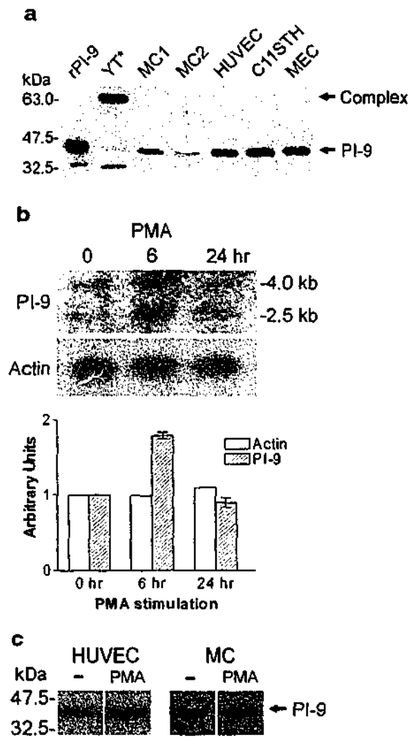

FIG. 6. (a) Lining cell types produce less PI-9 than cytotoxic cells. A total of 80 μg of protein from the highest (MC1) and lowest (MC2) PI-9-expressing mesothelial cell samples, human umbilical vein endothelial cells (HUVEC), a transformed HUVEC cell line (C11STH), and microvascular endothelial cells (MEC) was loaded alongside 8 μg of protein (10-fold less) from a lysate of a human NK leukemia cell line (YT*) on a 12.5% SDS–PAGE gel and immunoblotted with monoclonal anti-PI-9 antibody. PI-9 in YT cells, which also produce graB, is predominantly found in complex with PI-9. (b) PI-9 mRNA is elevated approximately 2-fold in C11STH endothelial cells stimulated with 5 nM PMA at 6 h. The membrane was probed with a [^{32}P]dATP-labeled PI-9 cDNA probe. The membrane was also probed for β-actin as a control for RNA loading. Scanning densitometry was used to quantitate the degree of up-regulation (bottom). (c) HUVEC and mesothelial cells were stimulated for 6 and 24 h, respectively, with 25 nM PMA. Equivalent amounts of protein from unstimulated and PMA-stimulated cells were loaded and blotted for PI-9 as in (a). Densitometric analysis shows a 2.5-fold increase in PI-9 protein levels in HUVECs and a 0.6-fold increase in mesothelial cells in response to PMA.

PI-9 Is Up-regulated by PMA in Endothelial and Mesothelial Cells

It has previously been shown that CLs, which produce graB, also express high levels of PI-9 (7). The level of PI-9 produced by cultured endothelial and mesothelial cells was compared to PI-9 production in the human NK leukemia cell line YT. Figure 6a shows the relative amounts of PI-9 produced by these cells by

immunoblot. Tenfold less YT cell protein was loaded, and after lysis essentially all PI-9 in these cells is in complex with graB. From this blot, it was estimated that endothelial and mesothelial cells produce 10- to 20-fold less PI-9 than YT cells.

To gain an insight into whether PI-9 may be up-regulated in an inflammatory environment, preliminary stimulation experiments on endothelial and mesothelial cells were performed with the cytokine IL-1β, which is known to activate these cells (22, 23). However under these conditions, no change in PI-9 levels was detected (data not shown). As the regulation of PI-9 expression may require other factors, we employed a more general cell activator, the phorbol ester PMA. Although it is not a physiological stimulus, PMA activates the protein kinase C (PKC) pathway through which many inflammatory mediators act to induce cellular effects (24–26). PMA is therefore commonly used to mimic the intracellular signaling utilized by these agents. As shown in Figs. 6b and 6c, PI-9 expression is up-regulated in response to PMA, at both the RNA and the protein level. In the endothelial cell line C11STH, PI-9 mRNA is elevated approximately 2-fold, with a peak at 6 h after stimulation. The presence of two PI-9 transcripts (4 and 2.5 kb) has been previously observed (7) and may reflect differential promoter use or alternate transcription termination sites. As shown in Fig. 6c, PI-9 protein levels were elevated 2.5-fold in HUVECs compared to 0.6-fold in mesothelial cells. This difference may be explained by the observation that mesothelial cells cultured from effusions are in a semi-activated or primed state (27).

DISCUSSION

PI-9 expression in CLs is thought to provide protection from unwanted self-induced apoptosis by misdirected graB that may reach the CL cytosol during degranulation or via granule leakage (9). Here, we have shown that endothelial and mesothelial cells produce PI-9 in the absence of graB expression. The expression of PI-9 in these noncytolytic cells is consistent with previous reports of PI-9 expression in leukocytes (B cells, monocytes), which do not themselves produce graB (7, 12). Like other cells of the immune system, the role of endothelial and mesothelial cells in a local immune response is now well documented, including production of inflammatory cytokines/chemokines, antigen presentation/T cell activation, and passaging of activated CLs (reviewed in 13, 14). We have shown that in endothelial and mesothelial cells the level of PI-9 is significantly lower than in CLs. Therefore, it is unlikely that these levels of PI-9 would protect a cell from direct CL–graB-mediated attack. However, PI-9 may be synthesized in these cells (and other leukocytes) to provide protection from lower levels of free locally released graB.

CL killing of target cells via degranulation is often portrayed as a unidirectional process during which granule contents are released from the killer cell directly into the target. However, during *in vitro* CL killing assays, extracellular/free graB activity is detected in culture supernatants (28). *In vivo* evidence also demonstrates the presence of extracellular granzyme B. Patients with an active CTL response have significantly elevated serum graB levels, such as during viral infections with EBV and HIV1, particularly during the acute phase of the infection (11). Markedly high levels of granzymes are also found in the synovial fluid of patients with active rheumatoid arthritis (11, 29). In addition, serum graB is also significantly elevated in patients with a severe infection with Gram-negative bacteria and in experimental human endotoxemia (30).

The presence of extracellular graB is thought to contribute to bystander or non-target-cell killing by CLs which is frequently observed in *in vitro* CL killing assays (31–33). Like directed cell killing, bystander killing may arise through extracellular graB/perforin, FasR engagement, or TNF receptor engagement. However, it has been shown that a granule-dependent mechanism is at least in part responsible for bystander killing (10, 34). It is conceivable that granule contents may be released extracellularly as a CL engages with one target, degranulates, and then moves on to kill another target. Free graB and subsequent bystander killing may also be due to newly synthesized graB/perforin that is nonspecifically secreted via the constitutive endocytic pathway after degranulation (34). In addition, inadvertent release of graB may occur in response to CTL/NK chemokines in the absence of target cell conjugation. For example, the MCP1 and MIP-1 chemokines, both of which are produced by activated endothelium and mesothelium, have been shown not only to activate NK cells, but also to induce degranulation *in vitro* (35–38).

It is clear that during a CL response "normal" cells in close proximity to the reaction are likely to be exposed to free graB/perforin. PI-9 expression in bystander cells such as endothelial and mesothelial cells, monocytes, and B cells may be required to protect these cells from inadvertent graB-mediated apoptosis. It is of interest, therefore, to determine whether PI-9 levels are up-regulated in an inflammatory situation. The preliminary stimulation experiments performed using the phorbol ester PMA indeed suggest this, as many inflammatory mediators act through the PKC pathway. The effect of exposure to individual cytokines on PI-9 expression has not yet been fully examined, and a quantitative immunohistochemical study on normal versus reactive/inflamed tissues is required. Given the anti-apoptotic properties of PI-9, it will also be of interest to examine dysregulation of this protein in malignancies such as hemangioma, mesothelioma, and B

cell lymphoma in which PI-9 may contribute to prolonged survival of these cells.

ACKNOWLEDGMENTS

M. Buzza and C. Hirst are recipients of Australian Postgraduate Awards. This work was funded by the National Health and Medical Research Council of Australia and the Box Hill Hospital Oncology Research Fund in memory of Prue Leyden. We are grateful to Dr. P. Rogers and Dr. C. Gargett (Monash University) for providing the human endometrium tissue sections and microvascular endothelial cells, Dr. F. Scott (Monash University) for providing human skin sections, and Dr. M. Costa/Dr. R. Medcalf (Monash University) for the C11STH Northern membrane. We also thank S. Black (Monash University) for assistance with HUVEC preparations and Dr. J. Chong (Box Hill Hospital) for assistance with serous effusion.

REFERENCES

1. Froelich, C. J., Orth, K., Turbov, J., Seth, P., Gottlieb, R., Babior, B., Shah, G. M., Bleakley, R. C., Dixit, V. M., and Hanna, W., New paradigm for lymphocyte granule-mediated cytotoxicity. Target cells bind and internalise granzyme B, but an endosomolytic agent is necessary for cytosolic delivery and subsequent apoptosis. *J. Biol. Chem.* **46,** 29073–29079, 1996.
2. Medema, J. P., Toes, R., Scaffidi, C., Zheng, T. S., Flavell, R. A., Melief, C., Pete, M., Offringer, R., and Krammer, P. H., Cleavage of FLICE (caspase-8) by granzyme B during cytotoxic T lymphocyte induced apoptosis. *Eur. J. Immunol.* **27,** 3492–3498, 1997.
3. Yang, X., Steinnicke, H., Wang, B., Gren, D., Janicke, R., Shrinivasan, A., Seth, P., Salvesen, G., and Froelich, C., Granzyme B mimics apical caspases. Description of a unified pathway for trans-activation of executioner caspase-3 and -7. *J. Biol. Chem.* **273,** 34278–34283, 1998.
4. Barry, M., Heibein, J. A., Pinkoski, M. J., Lee, S-F., Moyer, R. W., Green, D. R., and Bleakley, R. C., Granzyme B short circuits the need for caspase 8 activity during granule-mediated cytotoxic T-lymphocyte killing by directly cleaving Bid. *Mol. Cell. Biol.* **20,** 3781–3794, 2000.
5. Heibien, J. A., Goping, I. S., Barry, M., Pinoski, M. J., Shore, G. C., Green, D. R., and Bleakley, R. C., Granzyme B-mediated cytochrome C release is regulated by the bcl-2 family members bid and bax. *J. Exp. Med.* **192,** 1391–1402, 2000.
6. Sutton, V. R., Davis, J. E., Cancilla, M. M., Johnstone, R. W., Ruefli, A. A., Sedelies, K., Brown, K. A., and Trapani, J. A., Initiation of apoptosis by granzyme B requires direct cleavage of bid, but not direct granzyme B-mediated caspase activation. *J. Exp. Med.* **192,** 1403–1414, 2000.
7. Sun, J., Bird, C. H., Sutton, V., McDonald, L., Couglin, P. R., De Jong, T. A., Trapani, J. A., and Bird, P. I., A cytosolic granzyme B inhibitor related to the viral apoptotic regulator cytokine response modifier A is present in cytotoxic lymphocytes. *J. Biol. Chem.* **271,** 27802–27809, 1996.
8. Huntington, J. A., Read, R. J., and Carrell, R. W., Structure of a serpin–protease complex shows inhibition by deformation. *Nature* **407,** 923–926, 2000.
9. Bird, C. H., Sutton, V. R., Sun, J., Hirst, C. E., Novak, A., Kumar, S., Trapani, J. A., and Bird, P. I., Selective regulation of apoptosis: The cytotoxic lymphocyte serpin proteinase inhibitor 9 protects against enzyme B mediated apoptosis without perturbing the Fas cell death pathway. *Mol. Cell. Biol.* **18,** 6387–6398, 1998.
10. Kuwano, K., and Arai, S., Involvement of two distinct killing mechanisms in bystander target cell lysis induced by a cytotoxic T lymphocyte clone. *Cell. Immunol.* **169,** 288–293, 1996.
11. Spaeny-Dekking, E. H., Hanna, W. L., Wolbink, A. M., Wever, P. C., Kummer, A. J., Swaak, A. J., Middeldorp, J. M., Hack, C. E., Froelich, C. J., and Hack, C. E., Extracellular granzymes A and B in humans: Detection of native species during CTL responses in vitro and in vivo. *J. Immunol.* **160,** 3610–3616, 1998.
12. Young, J. L., Sukhova, G. K., Foster, D., Kisiel, W., Libby, P., and Schonbeck, U., The serpin proteinase inhibitor 9 is an endogenous inhibitor of the interleukin 1β-converting enzyme (caspase-1) activity in human vascular smooth muscle cells. *J. Exp. Med.* **191,** 1535–1544, 2000.
13. Pober, J. S., Immunobiology of human vascular endothelium. *Immunol. Res.* **19,** 225–232, 1999.
14. Antony, V. B., and Mohammed, K. A., Pathophysiology of pleural space infections. *Semin. Respir. Inf.* **14,** 9–17, 1999.
15. Trapani, J. A., Brown, K. A., Dawson, M. J., and Smyth, M. J., Immunopurification of a functional Asp-ase (natural killer granzyme B) using a monoclonal antibody. *Biochem. Biophys. Res. Commun.* **195,** 910–920, 1993.
16. Warren, J. B., Large vessel endothelial isolation. *In* "The Endothelium: An Introduction to Current Research," pp. 263–265. Wiley–Liss, New York, 1990.
17. Cockerill, G. W., Meyer, G., Noack, L., Vadas, M. A., and Gamble, J. R., Characterization of a spontaneously transformed human endothelial cell line. *Lab. Invest.* **71,** 497–509, 1994.
18. Gargett, C. E., Bucak, K., and Rogers, P. A. W., Isolation, characterization and long term culture of human myometrial microvascular endothelial cells. *Hum. Reprod.* **15,** 293–301, 2000.
19. Sun, J., Bird, C. H., Buzza, M. S., McKee, K. E., Whisstock, J. C., and Bird, P. I., Expression and purification of recombinant human granzyme B from *Pichia Pastoris*. *Biochem. Biophys. Res. Commun.* **261,** 251–255, 1999.
20. Pronk, A., Leguit, P., van Papendrecht, A., Hagelen, E., van Vroonhoven, T., and Verbrugh, H. A., A cobblestone cell isolated from the human omentum: The mesothelial cell; isolation, identification, and growth characteristics. *In Vitro Cell. Dev. Biol* **29A,** 127–134, 1993.
21. Poltzch, B., Grulich-Henn, J., Rossing, R., Wille, D., and Muller-Berhaus, G., Identification of endothelial and mesothelial cells in human omental tissue and omentum derived cultured cells by specific cell markers. *Lab. Invest.* **63,** 841–852, 1990.
22. Bevilacqua, M. P., Pober, J. S., Wheeler, M. E., Cotran, R. S., and Gimbrone, M. A., Interleukin-1 activation of vascular endothelium. Effects on procoagulant activity and leukocyte adhesion. *Am. J. Pathol.* **121,** 394–403, 1985.
23. Lanfrancone, L., Boraschi, D., Ghiara, P., Falini, B., Grignani, F., Peri, A., Mantovani, A., and Pelicci, P. G., Human peritoneal mesothelial cells produce many cytokines (granulocyte colony-stimulating factor [CSF], granulocyte-monocyte-CSF, macrophage-CSF, interleukin-1 [IL-1], and IL-6) and are activated and stimulated to grow by IL-1. *Blood* **80,** 2835–2842, 1992.
24. Rahman, A., Anwar, K. N., and Malik, A. B., Protein kinase C-zeta mediates TNF-alpha-induced ICAM-1 gene transcription in endothelial cells. *Am. J. Physiol. Cell. Physiol.* **279,** C906–C914, 2000.
25. Patterson, C. E., Stasek, J. E., Bahler, C., Verin, A. D., Harrington, M. A., and Garcia, J. G., Regulation of IL-1-stimulated GMCSF mRNA levels in human endothelium. *Endothelium* **6,** 45–59, 1998.
26. Mattila, P., and Renkonen, R., Protein kinase C regulates MHC-class II expression on endothelial cells. *Scand. J. Immunol.* **34,** 153–160, 1991.
27. Zhang, X., Pettengell, R., Nasiri, N., Kalia, V., Dalgleish, A. G., and Barton, D. P., Characteristics and growth patterns of human peritoneal mesothelial cells: Comparison between advanced epithelial ovarian cancer and non-ovarian cancer sources. *J. Soc. Gynecol. Invest.* **6,** 333–340, 1999.
28. Takayama, H., Trenn, G., Humphrey, W., Bluestone, J. A., Henkart, P. A., and Sitkovsky, M. V., Antigen receptor-triggered secretion of a trypsin-type esterase from cytotoxic T lymphocytes. *J. Immunol.* **138,** 566–569, 1987.
29. Young, L. H., Joag, S. V., Lin, P. Y., Luo, S. F., Zeng, L. M., Liu, C. C., and Young, J. D., Expression of cytolytic mediators by synovial fluid lymphocytes in rheumatoid arthritis. *Am. J. Pathol.* **140,** 1261–1268, 1992.
30. Lauw, F. N., Simpson, A. J., Hack, C. E., Prins, J., Wolbink, A., van Deventer, S. J., Chaowagul, W., White, N. J., and van der Poll, T., Soluble granzymes are released during human endotoxemia and in patients with severe infection due to Gram-negative bacteria. *J. Infect. Dis.* **182,** 206–213.
31. Fleischer, B., Lysis of bystander target cells after triggering of human cytotoxic T lymphocytes. *Eur. J. Immunol.* **16,** 1021–1024, 1986.
32. Duke, R. C., Self recognition by T cells. I. Bystander killing of target cells bearing syngeneic MHC antigen. *J. Exp. Med.* **170,** 59–71, 1989.
33. Burrows, S. R., Fernan, A., Argaet, V., and Suhrbier, A., Bystander apoptosis induced by CD8+ cytotoxic T cell (CTL) clones: Implications for CTL lytic mechanisms. *Int. Immunol.* **5,** 1049–1058, 1993.
34. Isaaz, S., Baetz, K., Olsen, K., Podack, E., and Griffiths, G. M., Serial killing by cytotoxic T lymphocytes: T cell receptor triggers degranulation, refilling of the lytic granules and secretion of lytic proteins via a non-granule pathway. *Eur. J. Immunol.* **25,** 1071–1079, 1995.
35. Volk, T., Hensel, M., Schuster, H., and Kox, W. J., Secretion of MCP-1 and IL-6 by cytokine stimulated production of reactive oxygen species in endothelial cells. *Mol. Cell. Biochem.* **206,** 105–112, 2000.
36. Antony, V. B., Hott, J. W., Kunkel, S. L., Godbey, S. W., Burdick, M. D., and Strieter, R., Pleural mesothelial cell expression of C-C (monocyte chemotactic peptide) and C-X-C (interleukin-8) chemokines. *Am. J. Respir. Cell. Mol. Biol.* **12,** 581–588, 1995.
37. Taub, D. D., Ortaldo, J. R., Turcovski-Corrales, S. M., Key, M. L., Longo, D. L., and Murphy, W. J., Beta chemokines costimulate lymphocyte cytolysis, proliferation, and lymphokine production. *J. Leukocyte Biol.* **59,** 81–89, 1996.
38. Loetscher, P., Seitz, M., Clark-Lewis, I., Baggiolini, M., and Moser, B., Activation of NK cells by CC chemokines. Chemotaxis, Ca^{2+} mobilization, and enzyme release. *J. Immunol.* **156,** 322–327, 1996.
39. Bird, C. H., Blink, E. J., Hirst, C. E., Buzza, M. S., Steele, P S., Sun, J., Jans, D. A., and Bird, P. I. Nucleocytoplasmic distribution of the Ovalbumin serpin PI-9 requires a non-conventional nuclear import pathway and the export factor Crm1. *Mol. Cell. Biol.*, in press.

MOLECULAR AND CELLULAR BIOLOGY, Aug. 2001, p. 5396–5407 Vol. 21, No. 16
0270-7306/01/$04.00+0 DOI: 10.1128/MCB.21.16.5396–5407.2001

Nucleocytoplasmic Distribution of the Ovalbumin Serpin PI-9 Requires a Nonconventional Nuclear Import Pathway and the Export Factor Crm1

CATHERINA H. BIRD,[1] ELIZABETH J. BLINK,[2] CLAIRE E. HIRST,[1] MARGUERITE S. BUZZA,[1] PAULINE M. STEELE,[1] JIURU SUN,[1] DAVID A. JANS,[2] AND PHILLIP I. BIRD[1]*

Department of Biochemistry and Molecular Biology, Monash University, Victoria 3800,[1] and Nuclear Signaling Laboratory, John Curtin School of Medical Research, Australian National University, Canberra ACT 2601,[2] Australia

Received 17 May 2001/Accepted 18 May 2001

Proteinase inhibitor 9 (PI-9) is a human serpin present in the cytoplasm of cytotoxic lymphocytes and epithelial cells. It inhibits the cytotoxic lymphocyte granule proteinase granzyme B (graB) and is thought to protect cytotoxic lymphocytes and bystander cells from graB-mediated apoptosis. Following uptake into cells, graB promotes DNA degradation, rapidly translocating to the nucleus, where it binds a nuclear component. PI-9 should therefore be found in cytotoxic lymphocyte and bystander cell nuclei to ensure complete protection against graB. Here we demonstrate by microscopy and subcellular fractionation experiments that PI-9 is present in the nuclei of human cytotoxic cells, endothelial cells, and epithelial cells. We also show that the related serpins, PI-6, monocyte neutrophil elastase inhibitor (MNEI), PI-8, plasminogen activator inhibitor 2 (PAI-2), and the viral serpin CrmA exhibit similar nucleocytoplasmic distributions. Because these serpins lack classical nuclear localization signals and are small enough to diffuse through nuclear pores, we investigated whether import occurs actively or passively. Large (~70 kDa) chimeric proteins comprising PI-9, PI-6, PI-8, MNEI, or PAI-2 fused to green fluorescent protein (GFP) show similar nucleocytoplasmic distributions to the parent proteins, indicating that nuclear import is active. By contrast, CrmA-GFP is excluded from nuclei, indicating that CrmA is not actively imported. In vitro nuclear transport assays show that PI-9 accumulates at a rate above that of passive diffusion, that it requires cytosolic factors but not ATP, and that it does not bind an intranuclear component. Furthermore, PI-9 is exported from nuclei via a leptomycin B-sensitive pathway, implying involvement of the export factor Crm1p. We conclude that the nucleocytoplasmic distribution of PI-9 and related serpins involves a nonconventional nuclear import pathway and Crm1p.

Proteolysis mediated by serine proteinases is crucial to processes such as blood coagulation, fibrinolysis, complement activation, embryo implantation, extracellular matrix remodeling, and cell differentiation. Homeostatic regulation of serine proteinases is mainly achieved through interactions with inhibitors belonging to the large metazoan, plant, and virus serpin superfamily (44). Inhibitory serpins have a common structure and mode of action: each contains a variable C-terminal-reactive center loop resembling the substrate of its cognate proteinase. On proteinase binding, the serpin is cleaved between two residues in the loop designated P_1 and P_1', and it undergoes a conformational change that distorts the proteinase and irreversibly locks the serpin-proteinase complex (27). The P_1 residue is crucial and largely dictates the specificity of the serpin-proteinase interaction, while residues surrounding the cleavage site contribute to the affinity of the interaction (66).

The best-characterized serpins are involved in the regulation of extracellular proteolysis in vertebrates (reviewed in references 44 and 54); however, there is an emerging, more widespread subgroup resembling chicken ovalbumin (ov-serpins) which includes serpins that function intracellularly and some that target other proteinase classes, such as caspases and papains (14, 45, 48, 57). Ov-serpins display complex patterns of cellular distribution that probably reflect diverse physiological functions. Most are intracellular, with roles that are as yet unclear, but some are efficiently secreted to regulate cell-cell and cell-matrix interactions, and others exist in both intracellular and extracellular forms (5, 35, 71). Two of the intracellular ov-serpins, chicken MENT and human bomapin, accumulate efficiently in nuclei via classical nuclear localization sequences (NLSs) resembling the signal on the simian virus 40 large tumor antigen (T-ag) (13, 21). MENT is involved in chromatin condensation, but the nuclear role of bomapin is unknown (21).

Two other intracellular serpins, poxvirus CrmA and human proteinase inhibitor 9 (PI-9), are involved in the regulation of apoptosis (reviewed in reference 7). Cytotoxic lymphocytes (CLs) kill abnormal cells by using either one of two proapoptotic systems (37, 53). One system involves Fas ligand on the surface of the CL binding to Fas/Apo1/CD95 (Fas) on the target cell, resulting in receptor trimerization and recruitment of cytoplasmic adapter molecules to the receptor complex. The initiator caspase zymogen, procaspase 8, then binds to the complex, is activated, and in turn activates downstream effector caspases. CrmA efficiently inhibits caspase 8 (70) and potentially protects poxvirus-infected cells against CL Fas-mediated apoptosis (7).

The second cytotoxic system requires perforin to mediate

* Corresponding author. Mailing address: Department of Biochemistry and Molecular Biology, P.O. Box 13D, Monash University, Victoria 3800, Australia. Phone: 61 3 9905 3771. Fax: 61 3 9905 4699. E-mail: Phil.Bird@med.monash.edu.au.

entry of the granule serine proteinase granzyme B (graB) into the target cell, which then activates caspases, cleaves a variety of other proteins, and rapidly translocates to nuclei inducing DNA fragmentation (reviewed in reference 59). CLs do not commit fratricide or undergo autolysis as they sequentially engage and destroy target cells (19, 33, 38). This implies that their apoptotic machinery is precisely regulated. We have shown that PI-9 is a very efficient graB inhibitor produced by CLs (57), endothelial cells, and epithelial cells (11a). Cells expressing intracellular PI-9 resist apoptosis induced by graB and perforin but do not resist Fas-mediated apoptosis, since PI-9 does not efficiently inhibit caspases (3, 6). We have therefore proposed that the role of PI-9 is to protect CLs against autolysis directed by ectopic or misdirected graB and to protect bystander cells from graB released by activated CLs (6, 8). Importantly, the inability of PI-9 to inhibit caspases allows CLs to be deleted via death receptor-mediated apoptosis at the conclusion of the immune response and permits a response to stress-mediated apoptotic signals.

PI-9 is present in the CL cytoplasm outside the granules containing graB, which is consistent with a role in inactivating mislocalized graB (57). Since graB introduced into the cytoplasm of a cell rapidly translocates to the nucleus and binds to an intranuclear component (31, 52, 61, 62), it is likely that efficient protection of a CL by PI-9 requires its presence in the nucleus. Here we show that PI-9 is present in the nuclei of CLs, endothelial cells, and epithelial cells, that nuclear import occurs in the absence of a classical NLS, and that related ov-serpins exhibit a similar nucleocytoplasmic distribution. Although it is small enough to diffuse into the nucleus, uptake of PI-9 is an active process that depends on cytosolic factors but not ATP. Export of PI-9 from the nucleus occurs through a leptomycin B (LMB)-sensitive pathway. We conclude that nucleocytoplasmic distribution is a common feature of intracellular ov-serpins consistent with their predicted cytoprotective functions and appears to involve an unconventional nuclear import pathway as well as a nuclear export pathway requiring the export receptor Crm1p (exportin).

MATERIALS AND METHODS

Plasmids. Plasmids used for expression of various proteins in COS-1 cells included pCMV/PI-9 (6) and pEUK/PAI-2 (50). A plasmid encoding PI-6 was constructed by subcloning the cDNA into the *Eco*RI site of pCMV2 (2). A plasmid encoding PI-8 was made by removing an internal *Eco*RI site in the PI-8 cDNA by site-directed mutagenesis and cloning the modified PI-8 cDNA into pSVTf (55). A monocyte neutrophil elastase inhibitor (MNEI) expression plasmid was constructed by removing the cDNA from pGEM-T/EI (41) using *Sac*II (ends removed using T4 DNA polymerase) and *Pst*I. This was cloned into pSVTf cut with *Sma*I and *Pst*I. The plasmid pEGFP/PI-9 encodes a fusion protein comprising the human codon-enhanced green fluorescent protein (GFP) fused to the N terminus of PI-9. It was constructed by isolating a PI-9 cDNA on a 1-kb *Bam*HI fragment from a yeast two-hybrid bait plasmid, pGTB/PI-9 (A. Calderone and P. Bird, unpublished data), and ligating it to *Bgl*II-digested pEGFP-c2 (Clontech). A similar fusion between neomycin 3′ phosphotransferase (neo) and PI-9 was also constructed. The neo gene was obtained by PCR amplification using pZeroBlunt (Invitrogen) as a template, the oligonucleotide primers 5′-GGGCTAGCCGCATGAATTGAACAAGATGGATTGCAC-3′ and 5′-CGCTCACCCGGGGAAGAACTCGTCAAGAAGCC-3′ (the latter introduces a *Sma*I site at the 3′ end), and Vent DNA polymerase (New England Biolabs) for 35 cycles of 95°C for 60 s, 50°C for 60 s, and 72°C for 60 s. The resulting 1-kb product was cloned into pZeroBlunt (Invitrogen) and then released and purified as a *Sma*I-*Eco*RI fragment. This was subcloned into pSVTf also digested with *Sma*I and *Eco*RI to generate pSVTf/neo. The plasmid pEGFP/PI-9 was digested with *Eag*I and treated with T4 DNA polymerase. It was then cut with *Sal*I, and the resulting 1.4-kb *Eag*I-*Sal*I fragment was ligated to pSVTf/neo digested with *Sma*I and *Sal*I to generate pSVTf/neoPI-9. A plasmid encoding a GFP-CrmA fusion protein was constructed by digesting the plasmid pGEM7zf/CrmA (gift of D. Pickup, Duke University Medical Center, Durham, N.C.) with *Nco*I (ends filled in using T4 DNA polymerase) and *Apa*I. The resulting fragment was cloned into pEGFP-c2 cut with *Eco*RI (ends filled with T4 DNA polymerase) and *Apa*I. The plasmid pEGFP/PAI-2 was constructed by removing the plasminogen activator inhibitor 2 (PAI-2) cDNA from pSHT/PAI-2 (50) by *Bam*HI (ends filled in using T4 DNA polymerase) and *Eco*RI digestion and cloning it into pEGFP-c2 cut with *Sac*I (ends removed using T4 DNA polymerase) and *Eco*RI. The plasmids pEGFP/PI-8 and pEGFP/MNEI were constructed by removing the appropriate cDNA from pSHT/PI-8 or pSHT/MNEI (unpublished data) using *Bam*HI and *Spe*I and cloning into pEGFP-c3 cut with *Bgl*II and *Xba*I. The plasmid pEGP/PI-6 was constructed by removing the PI-6 cDNA from the yeast two-hybrid bait vector pGTBK7/PI-6 (unpublished data) using *Eco*RI and *Sal*I and cloning it into pEGFP-c2 cut with *Eco*RI and *Sal*I.

Cells and transfections. Activated primary CLs were prepared from human peripheral blood as previously described (6). YT is a human NK leukemia cell line (68) and was maintained in RPMI 1640 containing 10% heat-inactivated fetal bovine serum, 50 U of penicillin/ml, 50 μg of streptomycin/ml, 2 mM glutamine, 0.1 mM β-mercaptoethanol, and 1 mM sodium pyruvate. The placental choriocarcinoma cell line BeWo was obtained from the American Type Culture Collection and was maintained in Ham's F12 containing 10% heat-inactivated fetal bovine serum, 50 U of penicillin/ml, 50 μg of streptomycin/ml, 2 mM glutamine. Human umbilical vein endothelial cells (HUVEC) were isolated and maintained as described (58). COS-1 cells were maintained in Dulbecco's modified Eagle's medium (DMEM) containing 10% fetal bovine serum, antibiotics, and 2 mM glutamine. Cells of the rat hepatoma tissue culture line (HTC; a derivative of Morris hepatoma 7288C) used for the in vitro transport studies were cultured in DMEM supplemented with 10% fetal bovine serum as described previously (26, 29, 30). COS-1 cells were transiently transfected by the dextran-chloroquine method (12).

Antibodies. Rabbit antibodies to recombinant PI-9 and recombinant PI-6 have been described earlier (50, 57). A rabbit polyclonal antiserum to PI-8 was raised in a similar fashion and affinity purified on immobilized recombinant PI-8. Rabbit antibodies raised to native MNEI, CrmA, and lactate dehydrogenase (LDH) were provided by E. Remold O'Donnell (Harvard University, Boston, Mass.), D. Pickup (Duke University Medical Center), and J. Wilson (Michigan State University, East Lansing, Mich.), respectively. A rat monoclonal antibody against human Apaf-1 (23) was a gift of D. Huang (Walter and Eliza Hall Institute, Melbourne, Australia). Mouse monoclonal antibodies to cytochrome *c* and PAI-2 were purchased from Research Diagnostics Inc. (clone 7H8.2C12; Flanders, N.J.) and American Diagnostica Inc. (Greenwich, Conn.), respectively. Anti-GFP monoclonal antibody was purchased from Boehringer Mannheim. The nuclear protein B23 was detected using a mouse monoclonal antibody (40). Rabbit pan-cytokeratin antibodies were purchased from DAKO.

Cell fractionation. Methods for the digitonin-based fractionation of YT, BeWo, and transfected COS-1 cells were based on previously published methods (23, 63, 65). A range of digitonin concentrations was tested in each experiment, and the results shown are those from cells treated with the lowest concentration that efficiently extracted the cytosolic marker protein (either LDH or Apaf-1) such that little or none was apparent in the subsequent nuclear fraction. Monolayers were removed from dishes by trypsinization and washed twice with ice-cold medium containing fetal calf serum and then washed once with ice-cold phosphate-buffered saline (PBS). Cells were counted and resuspended at 10^6/ml in HMKE buffer (20 mM HEPES [pH 7.2], 10 mM KCl, 5 mM $MgCl_2$, 1 mM EDTA, 250 mM sucrose). One-milliliter aliquots were pelleted at approximately 200 × *g* and resuspended in HMKE buffer containing protease inhibitors (1 mM phenylmethylsulfonyl fluoride, 1 μg of aprotinin/ml, 1 μg of pepstatin/ml, 1 μg of leupeptin/ml) and 50 to 200 μg of digitonin/ml (Sigma; 50-mg/ml stock in dimethyl sulfoxide). Cells were left on ice for 10 min and then centrifuged at 500 × *g* to separate cytosol from membranes, organelles, and cytoskeleton. The supernatant (cytosol fraction C) was carefully removed, and the pellet was washed in HMKE buffer. To extract proteins from membranes and organelles, the pellet was solubilized in extraction buffer containing 0.1 M Tris HCl (pH 9), 0.1 M NaCl, 5 mM KCl, 1 mM $CaCl_2$, 0.5 mM $MgCl_2$, 0.5% Nonidet P-40, and protease inhibitors for 20 min on ice. Samples were transferred to a 1.5-ml microcentrifuge tube and centrifuged at 15,000 × *g*, the supernatant was carefully removed (fraction N), and a solution containing 20 mM Tris HCl (pH 6.8) and 2% sodium dodecyl sulfate (SDS) was added to the pellet to solubilize cytoskeletal proteins. The resulting lysate was collected and passed through a 26G needle until no longer viscous (fraction R).

The protein content of fraction C was determined, and typically 10 μg of protein was used for immunoblotting. The detergent in fractions N and R precluded direct protein estimation. To analyze and compare protein complement and distribution in the fractions, all were made up to the same final volume so that a sample taken from one fraction and compared to an equal volume from another represents the same number of starting cells. In each experiment, equal volumes of fractions C, N, and R were reduced and subjected to electrophoresis on SDS–10% polyacrylamide gels. Fractionation of COS cells producing CrmA was performed according to the methods of Schikendanz et al. (49).

Rabbit antisera (PI-6, PI-9, and MNEI) were used at 1:2,000 to 1:5,000 dilutions for immunoblotting, and the B23 monoclonal antibody was used at a dilution of 1:4,000. The CrmA and PI-8 antisera were used at dilutions of 1:100. The Apaf-1, cytochrome *c*, PAI-2, LDH, and GFP antibodies were used at dilutions of 1:1,000. Immunoblots were developed with an enhanced chemiluminescence detection kit (DuPont).

Indirect immunofluorescence microscopy and in situ cell extractions. Cell monolayers grown on 12-well microscope slides were washed in PBS containing 0.1 mM $CaCl_2$ and 1.0 mM $MgCl_2$ (PBS+), fixed in 3.7% formaldehyde in PBS+ for 20 min, quenched with 20 mM ammonium chloride, and permeabilized by incubation in 0.5% Triton X-100 in PBS+ for 5 min. Alternatively, monolayers were fixed and permeabilized in 50% acetone–50% methanol for 2 min at room temperature. Glass slides used for nonadherent cells were first treated with poly-L-lysine (0.1 mg/ml) for 15 min at room temperature. Antigens were detected by incubation of the cells for 30 min with the appropriate dilution of primary antibody (typically 1:1,000 for PI-6 and PI-9 antisera, 1:50 for Apaf-1 antibodies, and 1:200 for all others). After being washed with PBS+ the cells were incubated with 1:200 dilutions of fluorescein isothiocyanate (FITC)- or rhodamine isothiocyanate-conjugated secondary antibodies. After 30 min cells were washed in PBS+ and, in some experiments, were stained with propidium iodide (1-μg/ml concentration in PBS) for 5 min at room temperature. Cells were washed, mounted in phenlyenediamine-buffered glycerol, and examined using either epifluorescence microscopy or confocal laser scanning microscopy (CLSM). In some indicated instances CLSM using 2-photon excitation was employed.

For in situ extractions, 10^4 BeWo cells per well were grown on 12-well microscope slides. Untreated cells were fixed and permeabilized as described above. Cells were stained with rabbit anti-PI-9 (1:1,000 dilution), rabbit anti-cytokeratin (1:200), and anti-Apaf-1 (1:50) followed by a 1:200 dilution of the appropriate secondary antibody conjugated to FITC. To remove proteins from the cytoplasm, cells were placed on ice, washed twice with ice-cold HMKE buffer, and then exposed to digitonin (25, 50, or 75 μg/ml) in 20 μl of HMKE buffer containing protease inhibitors for 10 min. At this point cells were either fixed for staining as above (digitonin treated) or washed with HMKE buffer and then incubated in 20 μl of extraction buffer for 10 min to remove detergent-soluble and salt-extractable (including most nuclear) proteins. The remaining monolayers were washed very gently and then fixed with formaldehyde and stained as above to visualize detergent-insoluble proteins.

Nuclear transport. Analysis of nuclear import kinetics at the single-cell level in vitro using mechanically perforated HTC cells in conjunction with CLSM (MRC-600; Bio-Rad) was performed as described previously (10, 16, 29). NLS-dependent nuclear protein import can be reconstituted in this system through the exogenous addition of cytosolic extract (untreated reticulocyte lysate [Promega]), an ATP regenerating system (0.125 mg of creatine kinase/ml, 30 mM creatine-phosphate, 2 mM ATP), and transport substrate. In some experiments 0.025% 3-[(3-cholamidopropyl)-dimethylammonio]-1-propanesulfonate (CHAPS) was used to permeabilize the nuclear envelope; under these conditions nuclear accumulation can only occur through binding to intranuclear components such as lamins or chromatin (16, 17). Image analysis of CLSM files was performed using the MacIntosh NIH Image 1.60 public domain software. Each point shown in Results (Table 1 and Fig. 5) represents the average of 6 to 10 separate measurements (the standard error of the mean [SEM] was <10.2% of the value of the mean) for each of nuclear (Fn) and cytoplasmic (Fc) fluorescence, respectively, with autofluorescence subtracted. Data were fitted for the function $Fn/c(t) = Fn/c_{max} \times (1 - e^{-kt})$, where Fn/c is the ratio of nuclear to cytoplasmic fluorescence intensity, *t* is time in minutes, Fn/c_{max} is the maximal level of nuclear accumulation, and *k* is the first-order rate constant (10, 16, 29). Recombinant PI-9 was produced in a yeast expression system and purified as described previously (57) and was conjugated to FITC using standard procedures (22). The T-ag–CcN–β-Gal fusion protein used as a control for nuclear import studies contains T-ag amino acids 111 to 135, including the NLS, fused N terminal to β-galactosidase amino acids 9 to 1,023 (29, 46). It was expressed in *Escherichia coli*, purified by affinity chromatography, and labeled with 5-iodoacetamidofluorescein as described previously (29, 46).

Estimation of the proportion of nuclear PI-9. Estimation of the nuclear and cytoplasmic volume for BeWo cells, YT cells, and HUVECs was performed using conventional as well as 2-photon CLSM (Bio-Rad) and standard cell measurement procedures. The percent nuclear PI-9 was calculated by multiplying the percent nuclear volume (>11 separate estimations) by the Fn/c for each cell type.

Treatment of cells with LMB. COS-1 cells were transfected with pCMV/PI-9 or RevMAPKK-GFP (24). Cells grown on 12-well microscope slides were exposed to 4 ng of LMB/ml in complete medium for 0, 3, and 6 h and then fixed with formaldehyde and permeabilized as described above. RevMAPKK/GFP in transfected cells was followed by GFP fluorescence, whereas pCMV/PI-9-transfected cells were stained with rabbit anti-PI-9 diluted 1:500 and then with FITC-conjugated anti-rabbit immunoglobulins. Samples were mounted in Permafluor

TABLE 1. In vitro nuclear import kinetics of PI-9 compared to those of control molecules

Molecule	Import conditions	Nuclear import parameter[a]		
		Fn/c_{max}	$t_{1/2}$ (min)	*n*
PI-9	+ ATP, + cytosol	2.26 ± 0.08	1.68 ± 0.52	2
	− ATP, + cytosol	2.46 ± 0.33	1.28 ± 0.41	3
	+ ATP, − cytosol	0.80 ± 0.04	ND[b]	2
	− ATP, − cytosol	1.12 ± 0.10	ND	2
	− ATP, + cytosol, + CHAPS	1.16 ± 0.01	ND	1
	− ATP, − cytosol, + CHAPS	0.96 ± 0.03	ND	1
T-ag-CcN-β-Gal	+ ATP, + cytosol	5.51 ± 0.21	12.4 ± 2.0	2
	− ATP, + cytosol	0.82 ± 0.13	ND	2
	+ ATP, − cytosol	1.10 ± 0.04	ND	2
	− ATP, + cytosol, + CHAPS	1.15 ± 0.15	ND	2
Dextran (70 kDa)	+ ATP, + cytosol	0.16 ± 0.03	ND	3
	− ATP, + cytosol	0.19 ± 0.02	ND	1
	− ATP, − cytosol	0.27 ± 0.06	ND	2
	− ATP, + cytosol, + CHAPS	0.98 ± 0.06	ND	2
	− ATP, − cytosol, + CHAPS	0.89 ± 0.09	ND	1
Dextran (20 kDa)	+ ATP, + cytosol	0.87 ± 0.04	ND	3

[a] Raw data were fitted for the function $Fn/c(t) = Fn/c_{max} \times (1 - e^{-kt})$, where *t* is time in minutes (10, 16, 26, 29, 30). Results represent the mean ± SEM; where *n* = 1, the standard error was determined from the curve fit.
[b] ND, not able to be determined due to low nuclear accumulation.

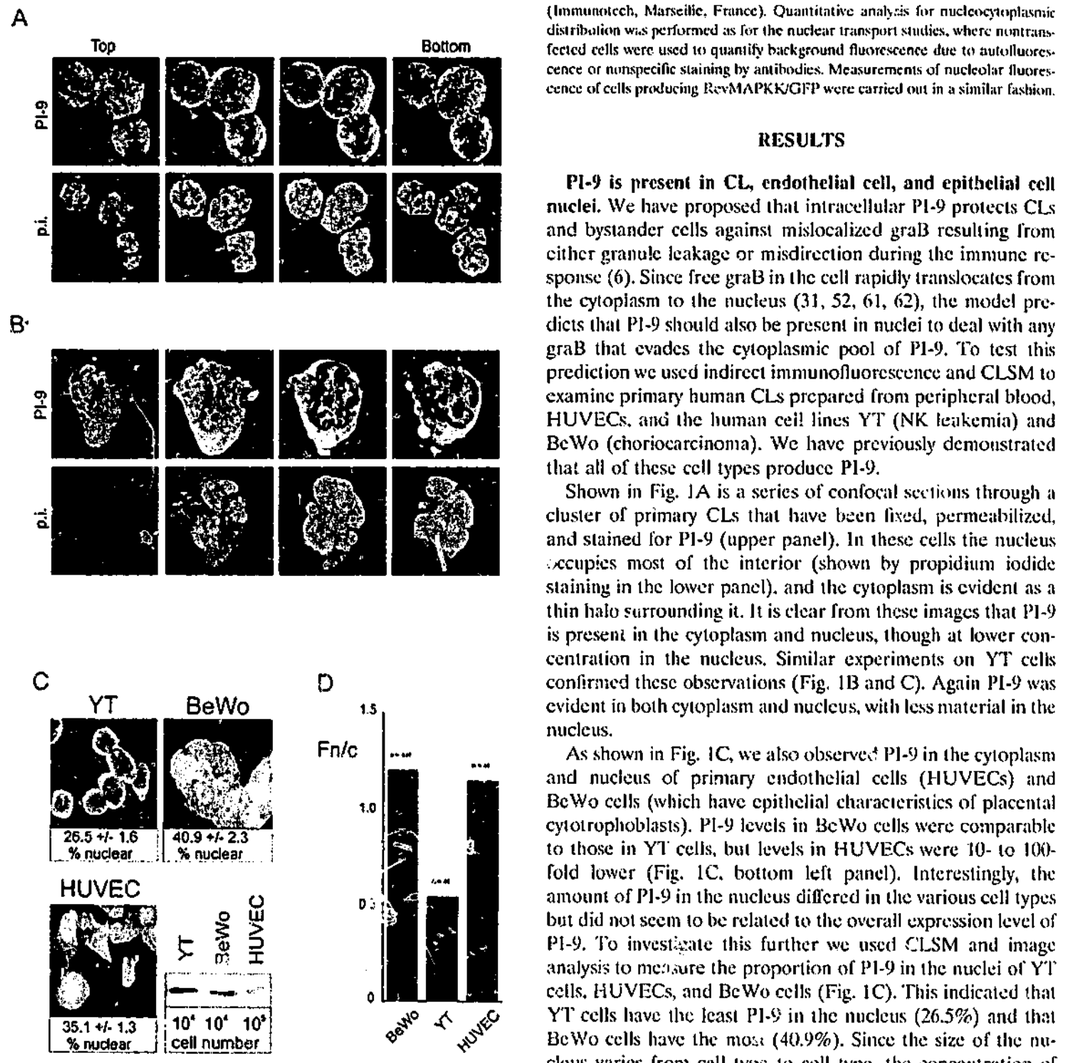

FIG. 1. Nucleocytoplasmic distribution of PI-9. (A) Human primary CLs. Interleukin-2-activated CLs were prepared from peripheral blood. Cells on glass slides were fixed and permeabilized with acetone-methanol and were incubated with rabbit antiserum against PI-9 and then incubated with FITC-conjugated anti-rabbit immunoglobulin and propidium iodide (p.i.). A series of CLSM sections through a cluster of cells shows PI-9 in both the nucleus and cytoplasm. (B) YT cells. Cells were fixed and stained as above. Shown is a series of CLSM sections of a single YT cell demonstrating PI-9 in the cytoplasm and nucleus. (C) Relative expression level and proportion of PI-9 in the nuclei of BeWo cells, YT cells, and HUVECs. Estimations of the nuclear and cytoplasmic volumes were performed using conventional and 2-photon CLSM and standard cell measurement procedures. The percent nuclear PI-9 was calculated by multiplying the percent nuclear volume by the ratio of nuclear to cytoplasmic fluorescence intensity (Fn/c). For comparison of PI-9 levels, 10^6 cells were lysed directly in SDS sample buffer, separated by SDS-polyacrylamide gel electrophoresis, and immunoblotted using PI-9 antibodies. Ten times more HUVEC than BeWo or YT lysate was run on the gel. (D) Concentration of PI-9 in the cytoplasm and nuclei of YT cells, BeWo cells, and HUVECs as measured by relative fluorescence intensity under CLSM. Results shown for the Fn/c ratio represent the mean ± SEM, with n being the number of cells analyzed.

(Immunotech, Marseille, France). Quantitative analysis for nucleocytoplasmic distribution was performed as for the nuclear transport studies, where nontransfected cells were used to quantify background fluorescence due to autofluorescence or nonspecific staining by antibodies. Measurements of nucleolar fluorescence of cells producing RevMAPKK/GFP were carried out in a similar fashion.

RESULTS

PI-9 is present in CL, endothelial cell, and epithelial cell nuclei. We have proposed that intracellular PI-9 protects CLs and bystander cells against mislocalized graB resulting from either granule leakage or misdirection during the immune response (6). Since free graB in the cell rapidly translocates from the cytoplasm to the nucleus (31, 52, 61, 62), the model predicts that PI-9 should also be present in nuclei to deal with any graB that evades the cytoplasmic pool of PI-9. To test this prediction we used indirect immunofluorescence and CLSM to examine primary human CLs prepared from peripheral blood, HUVECs, and the human cell lines YT (NK leukemia) and BeWo (choriocarcinoma). We have previously demonstrated that all of these cell types produce PI-9.

Shown in Fig. 1A is a series of confocal sections through a cluster of primary CLs that have been fixed, permeabilized, and stained for PI-9 (upper panel). In these cells the nucleus occupies most of the interior (shown by propidium iodide staining in the lower panel), and the cytoplasm is evident as a thin halo surrounding it. It is clear from these images that PI-9 is present in the cytoplasm and nucleus, though at lower concentration in the nucleus. Similar experiments on YT cells confirmed these observations (Fig. 1B and C). Again PI-9 was evident in both cytoplasm and nucleus, with less material in the nucleus.

As shown in Fig. 1C, we also observed PI-9 in the cytoplasm and nucleus of primary endothelial cells (HUVECs) and BeWo cells (which have epithelial characteristics of placental cytotrophoblasts). PI-9 levels in BeWo cells were comparable to those in YT cells, but levels in HUVECs were 10- to 100-fold lower (Fig. 1C, bottom left panel). Interestingly, the amount of PI-9 in the nucleus differed in the various cell types but did not seem to be related to the overall expression level of PI-9. To investigate this further we used CLSM and image analysis to measure the proportion of PI-9 in the nuclei of YT cells, HUVECs, and BeWo cells (Fig. 1C). This indicated that YT cells have the least PI-9 in the nucleus (26.5%) and that BeWo cells have the most (40.9%). Since the size of the nucleus varies from cell type to cell type, the concentration of PI-9 in the nucleus compared to the concentration in the cytoplasm may also vary. To investigate this we used image analysis to derive a value for the nuclear-to-cytoplasmic ratio (Fn/c) of PI-9 in the three cell types. As shown in Fig. 1D, YT cells have about twice the concentration of PI-9 in the cytoplasm as the nucleus, whereas HUVECs and BeWo cells have an equal concentration of PI-9 in the cytoplasm and nucleus.

To confirm that PI-9 is present in the nuclei of these cells we

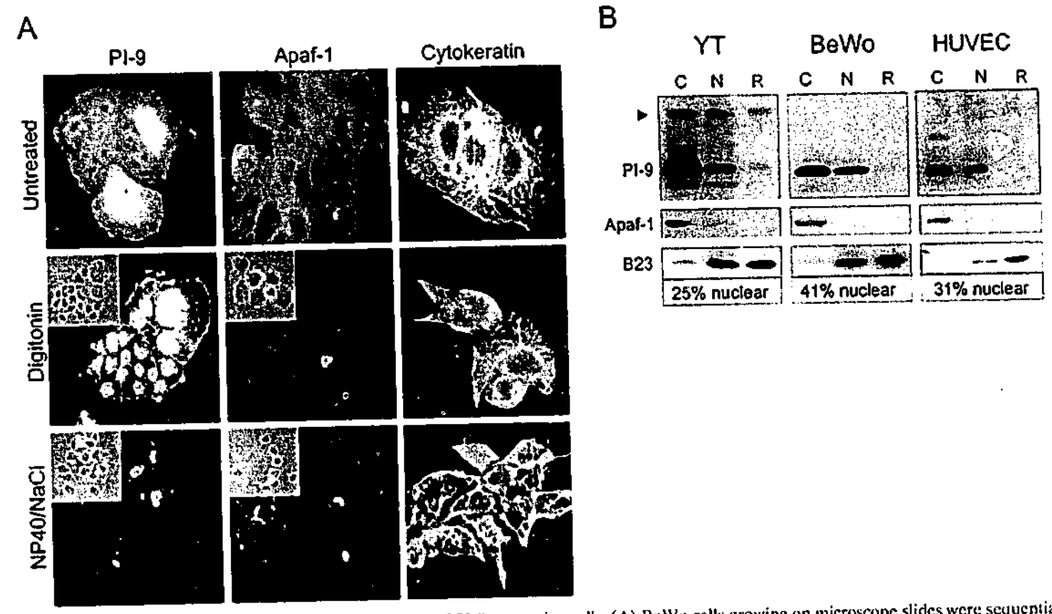

FIG. 2. In situ extraction and subcellular fractionation of PI-9 expressing cells. (A) BeWo cells growing on microscope slides were sequentially extracted with digitonin-containing and high salt-detergent-containing buffers. After each treatment, cells were fixed and permeabilized with acetone-methanol and incubated with antibodies against PI-9, Apaf-1, or cytokeratins. After being stained with FITC-conjugated anti-rabbit immunoglobulins, the cells were examined by phase-contrast (inset panels) and fluorescence microscopy. (B) YT cells, BeWo cells, and HUVECs were harvested and sequentially treated with digitonin, high salt-detergent, and SDS to generate cytosolic (C), nuclear (N), and remnant (R) fractions. Equal amounts of each fraction were separated by SDS–10% polyacrylamide gel electrophoresis and analyzed by immunoblotting with PI-9, Apaf-1, or B23 antibodies. The percentage of PI-9 in the nuclear fraction was estimated by densitometry. The PI-9–graB complex is indicated with an arrow.

carried out two digitonin-based fractionation procedures. One involved sequential extraction of protein from cells in situ with changes in protein content followed at the single-cell level using indirect immunofluorescence microscopy, and the other entailed fractionation of larger numbers of cells with analysis of the fractions by immunoblotting. Digitonin is extensively used in in vitro nuclear import studies to separate nuclei with intact envelopes and functional pore complexes from cytosolic components because it selectively permeabilizes the plasma membrane, leaving the nuclear membrane intact (23, 63, 65). Following digitonin treatment and washing to remove cytosolic protein, nuclei can be lysed in a high-salt buffer containing detergent to release nuclear proteins. Any remaining insoluble material contains mostly cytoskeletal and some nuclear or nucleolar protein that can be solubilized in SDS. In both procedures we expected to extract cytosolic, nuclear, and cytoskeletal protein sequentially. To verify this we followed the release of the cytosolic protein Apaf-1 (23), the nuclear or nucleolar protein B23 (40), and cytoskeletal cytokeratins.

As shown in Fig 2A, in situ extractions demonstrated PI-9 in the nuclei of BeWo cells. Untreated cells showed PI-9 in the cytoplasm and nucleus (upper left panel). Apaf-1 in the cytoplasm (upper center panel), and cytokeratin throughout the cell (upper right panel). Treatment of cells with digitonin completely removed Apaf-1 from the cytoplasm (middle center panel) but did not fully release PI-9 from cells, as the protein is clearly still evident in nuclei (middle left panel). Cytokeratin was not removed by digitonin treatment (right middle panel). Subsequent extraction with high salt and detergent completely removed PI-9 from nuclei (lower left panel) but did not remove cytokeratin from the cells (lower right panel), indicating that PI-9 is not associated with the cytoskeleton. In situ extraction experiments on HUVECs and YT cells yielded similar results (data not shown).

Immunoblotting analysis of digitonin-treated HUVECs, YT cells, and BeWo cells separated into cytoplasmic (C), nuclear (N), and remnant (R) fractions confirmed the results of the single-cell extraction procedure (Fig. 2B). PI-9 was evident in both the cytoplasmic and nuclear fractions of all the cell types and was not associated with cytoskeletal material. Densitometry was used to estimate the amount of nuclear PI-9 in these cells (Fig. 2B), and the resulting values were in very good agreement with the results of the confocal analysis (Fig. 1C).

The higher-molecular-weight species seen in both the cytosolic and nuclear fractions of YT cells represents PI-9 complexed with graB. Complex formation is a postlysis phenomenon, as graB is released from granules by detergents and rapidly equilibrates between the cytosol and nucleus via an unknown mechanism (61). We have shown previously that if cells are broken mechanically and intact granules are separated

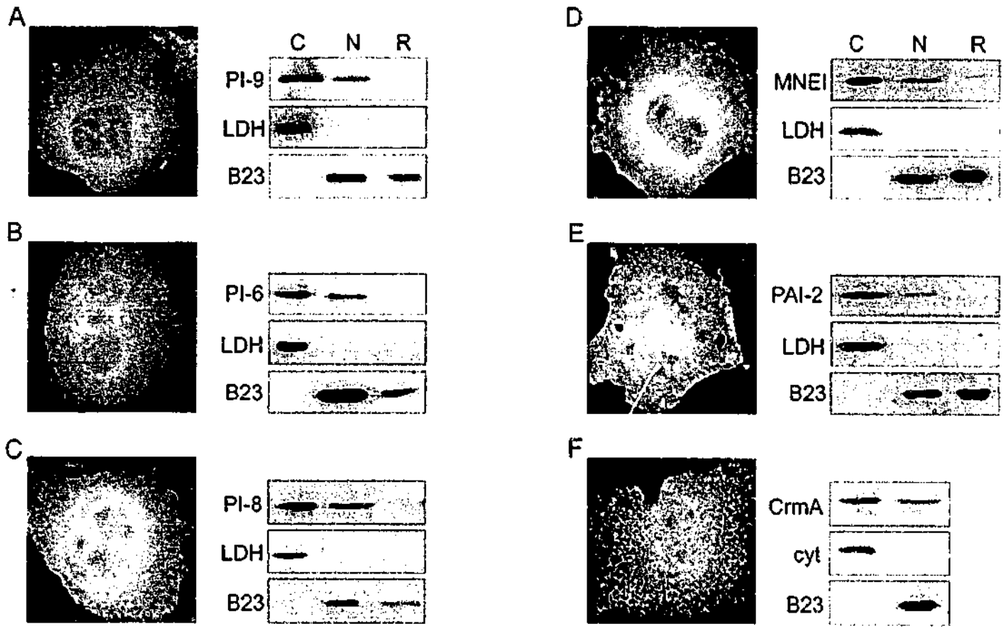

FIG. 3. Nucleocytoplasmic distribution of PI-9-related ov-serpins. COS-1 cells transiently transfected with appropriate expression vectors were grown either on glass slides for examination by indirect immunofluorescence or in dishes for cytosolic and nuclear fractionation experiments. Cells expressing either PI-9 (A), PI-6 (B), PI-8 (C), MNEI (D), PAI-2 (E), or CrmA (F) were fixed and stained with appropriate primary antibodies and then with FITC-conjugated secondary antibodies. In each case the images clearly show the serpin in the cytoplasm and nucleus. The distribution of protein within cytosolic (C), nuclear (N), or remnant (R) fractions in each transfected line was determined by immunoblotting. Also shown are the LDH and B23 controls for each experiment. CrmA-transfected cells were fractionated according to previously published methods (49), and cytochrome *c* (cyt) was used to monitor release of cytoplasmic protein.

from the soluble components, little or no complex is detected in the cytosol (57). Furthermore, if whole cells are lysed rapidly in SDS sample buffer, no complexes are observed (data not shown).

Taken together, the above results clearly show that PI-9 has a nucleocytoplasmic distribution in accordance with our cytoprotective model and that the proportion of PI-9 in the nucleus is not related to the expression level. To see if the nuclear localization of PI-9 requires a pathway or factors peculiar to HUVECs, YT cells, or BeWo cells, we also examined a number of other human cell lines of lymphoid or epithelial origin (SKW6, MCF7, HeLa) that are normally PI-9 negative but have been stably transfected with PI-9 cDNAs. In every case PI-9 was present in both the cell cytoplasm and nucleus (data not shown). We also expressed PI-9 in transiently transfected COS-1 cells (Fig. 3A). Fractionation experiments and epifluorescence microscopy of cells stained with rabbit anti-PI-9 antibodies showed PI-9 in both the cytoplasm and nucleus in these cells (Fig. 3A), and the concentration of nuclear PI-9 in transfected COS cells was similar to that of YT cells (F_n/c, ~0.5; see Fig. 6B). Thus, nuclear localization of PI-9 is unlikely to require cell type-specific machinery.

Related ov-serpins also exhibit a nucleocytoplasmic distribution. PI-9 belongs to the ov-serpin family that comprises intracellular proteins very similar in structure and size. Two ov-serpins (MENT and bomapin) possess conventional nuclear import signals located in a region of the molecule known as the interhelical loop (13, 21). PI-9 lacks this loop and has no identifiable NLS, implying that its uptake into the nucleus occurs via a different mechanism. To determine if this type of nuclear accumulation is unique to PI-9, we transiently transfected COS-1 cells with expression vectors encoding other ov-serpins lacking the interhelical loop and an identifiable NLS (PI-6, PI-8, MNEI) with an ov-serpin containing the loop but no obvious import signal (PAI-2) and with the viral intracellular serpin, CrmA. Cells were either fractionated for analysis by immunoblotting or plated on glass slides and prepared for examination by indirect immunofluorescence microscopy (Fig. 3). In every case, expression in the nucleus was detected by both methods, although the cytoplasmic-to-nuclear ratio varied from protein to protein. With the exception of PAI-2 (Fig. 3E), there was generally good correlation between the proportion of protein observed in the nuclei by microscopy and the amount evident by subcellular fractionation. For PAI-2 there appeared to be more material in the nucleus by microscopy than was indicated by analysis of fractions. The reason for the discrepancy is unknown but may reflect postlysis modification in the nuclear fractions of the epitope for the PAI-2 monoclonal antibody so that the protein is no longer recognized efficiently. This explanation is supported by the experiments on

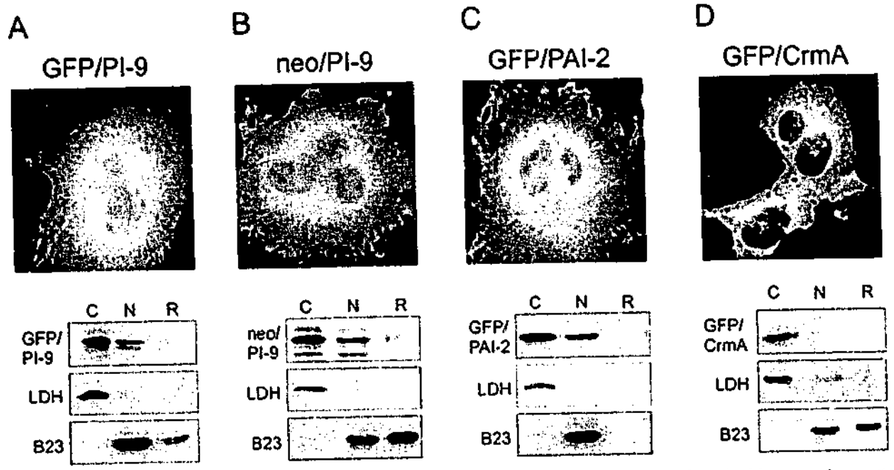

FIG. 4. PI-9 is imported into the nucleus through a facilitated mechanism. COS-1 cells were transfected with expression vectors encoding GFP–PI-9 (A), neo–PI-9 (B), GFP–PAI-2 (C), or GFP-CrmA (D), examined by indirect immunofluorescence microscopy, or fractionated into cytosolic and nuclear components. Cells were fixed and permeabilized using acetone-methanol and then incubated with primary antibodies (GFP-CrmA and GFP–PAI-2 were monitored using a monoclonal antibody against GFP) and the appropriate FITC-conjugated secondary antibodies. The distribution of protein within cytosolic (C), nuclear (N), or remnant (R) fractions in each transfected line was determined by immunoblotting with the same primary antibodies. Also shown are the LDH and B23 controls for each experiment.

the GFP–PAI-2 fusion protein (Fig. 4D) in which a different monoclonal antibody was used (anti-GFP) and no such discrepancy between the two methods was evident.

Finally, examination of primary human monocytes and mesothelial cells, which endogenously produce PAI-2, PI-6, and MNEI (51 and unpublished results), showed nucleocytoplasmic distributions of the three proteins (data not shown). Taken together, these results indicate that nucleocytoplasmic localization is a common feature of ov-serpins.

Nuclear accumulation of PI-9 is an active process. Proteins up to 40 to 60 kDa can pass freely through the nuclear pore complex. However, even very small proteins with specific nuclear functions carry NLSs, ensuring efficient nuclear targeting. Examination of the amino acid sequence of PI-9 and related serpins failed to reveal known classical, bipartite, or hnRNP A1 M9-like import signals (39). The lack of an identifiable NLS together with its relatively small size (42 kDa) suggested that PI-9 enters the nucleus by passive diffusion. To test this we generated a chimeric protein (GFP–PI-9) consisting of GFP (27 kDa) fused to the N terminus of PI-9. If PI-9 diffuses into the nucleus and does not require a dedicated NLS, the 69-kDa fusion protein should be excluded from the nucleus because it is too large to move through the pores.

By microscopy the fusion protein produced in transfected COS-1 cells was evident in both cytoplasm and nuclei (Fig. 4A). Fractionation experiments showed the 69-kDa fusion protein in the cytoplasm and nucleus, and densitometry indicated that the same proportion of GFP–PI-9 as PI-9 is found in nuclear fractions (approximately 20 to 30%). Pulse-chase experiments of metabolically labeled cells over 5 h showed that the fusion protein is stable and that no degradation into smaller (potentially diffusible) fragments occurred (data not shown).

To rule out the generation of a cryptic NLS during the construction of GFP–PI-9, we made a similar fusion (neo–PI-9) between the 28-kDa aminoglycoside 3′-phosphotransferase (neo) protein and PI-9. Like GFP, neo is small enough to passively enter the nucleus, but the chimeric protein should be too large to do so. Fractionation experiments and microscopy revealed that neo–PI-9 also enters the nucleus (Fig. 4B). Taken together these results suggest that although PI-9 is under the nominal nuclear pore cutoff, it enters the nucleus in a facilitated process.

To determine whether facilitated nuclear import is unique to PI-9, we also constructed similar fusion proteins consisting of GFP linked to PAI-2, PI-6, MNEI, PI-8, or CrmA. As judged by microscopy and fractionation of transfected COS cells, the GFP–PAI-2 fusion protein accumulated in the nucleus as efficiently as PAI-2 alone (Fig. 4C). By contrast, the GFP-CrmA fusion protein was essentially excluded from the nucleus (Fig. 4D), indicating that CrmA is not actively imported and that CrmA observed in the nucleus results from diffusion only (see Fig. 3F). Fusions between GFP and PI-6, MNEI, or PI-8 showed distributions similar to those of the parent proteins (data not shown). These results demonstrate that PI-9 and related ov-serpins can be imported into nuclei via a facilitated mechanism that does not depend on a classical NLS.

Nuclear uptake of PI-9 requires cytosolic factors but not ATP. Nuclear accumulation of PI-9 was also examined in vitro. As shown in Fig. 5, the nuclear import properties of FITC-labeled recombinant PI-9 were compared to those of control molecules at the single-cell level in mechanically perforated HTC cells (29). Addition of exogenous cytosol and an ATP-generating system to the HTC cells is sufficient to reconstitute nuclear transport, as shown by the uptake of the well-characterized chimeric protein (T-ag–CcN–β-Gal) which comprises a

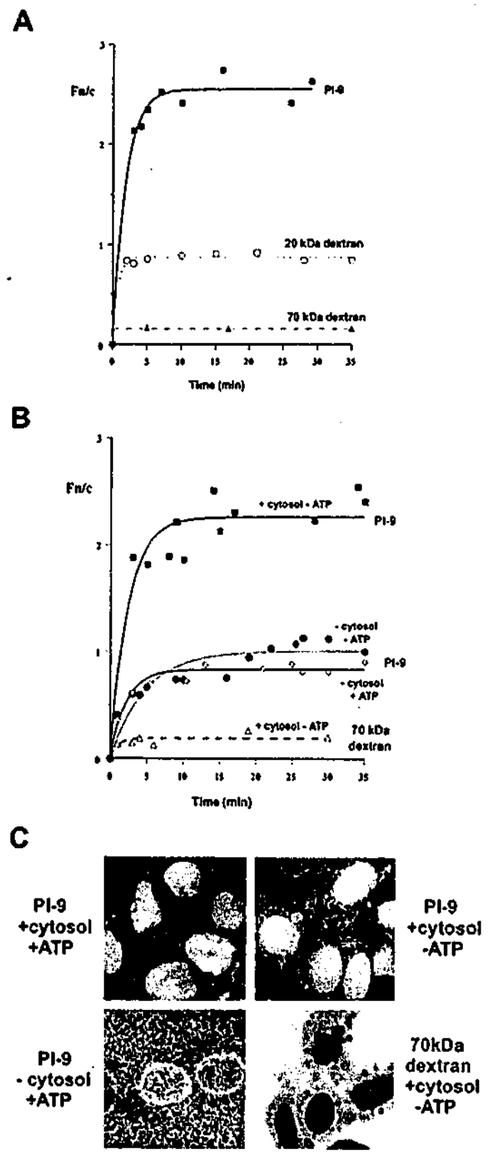

FIG. 5. Nuclear import kinetics of PI-9 in vitro. Uptake of FITC-conjugated PI-9 and dextran was examined in mechanically perforated HTC cells at room temperature in the presence (A) or absence (B) of exogenous cytosol and/or an ATP regenerating system as indicated. (C) CLSM images of nuclei 20 min after the addition of the indicated components. Fn/c is the ratio of nuclear to cytoplasmic fluorescence. Table 1 shows pooled data.

conventional NLS derived from T-Ag fused to the N terminus of *E. coli* β-galactosidase (46). This protein accumulated in the nucleus to levels over fivefold greater than those in the cytoplasm, with half-maximal accumulation achieved within 12 min (Table 1). By contrast, 70-kDa dextran was excluded from the nucleus (Fn/c_{max} of about 0.2), while 20-kDa dextran equilibrated between nuclear and cytoplasmic compartments but did not accumulate in the nucleus (Fn/c_{max} of about 1). In this system, nuclear accumulation of PI-9 in HTC cell nuclei was observed, occurring to a maximum of 2.5 times that of the cytoplasmic levels, with transport half maximal within 2 min (Table 1 and Fig. 5A).

Conventional signal-mediated nuclear protein import in vitro is dependent on energy in the form of ATP and exogenous cytosol (20), the latter containing the NLS-recognizing importin heterodimer, the monomeric guanine nucleotide-binding protein Ran, and other interacting proteins essential for nuclear accumulation (20). The conventional NLS-containing fusion protein T-ag–CcN–β-Gal requires both ATP and cytosol for nuclear accumulation (see Table 1 and reference 17). By contrast, nuclear import of PI-9 required cytosol but not ATP (Fig. 5B and Table 1).

The detergent CHAPS can be used to perforate the nuclear envelope to enable molecules to diffuse freely between cytoplasm and nucleoplasm (16, 17). For example, 70-kDa dextran is no longer excluded from nuclei after CHAPS treatment (Table 1). In the presence of CHAPS, nuclear accumulation can occur only through binding to nuclear components (16, 17). As demonstrated by T-ag–CcN–β-gal (Table 1), most proteins containing classical nuclear import signals do not exhibit nuclear accumulation in the presence of CHAPS; instead they equilibrate between the nuclear and cytoplasmic compartments. Likewise, in the presence of CHAPS PI-9 did not accumulate in the nucleus in either the absence or presence of cytosol (Table 1) and is thus clearly unable to bind to nuclear components and/or accumulate in the nucleus under these conditions. This contrasts with graB, which accumulates in nuclei in the presence of CHAPS by binding a nuclear component (28). In summary, PI-9 appears to accumulate in the nucleus through a novel nuclear import pathway which requires cytosolic factors, does not require ATP, and does not involve intranuclear binding.

Export of PI-9 from the nucleus occurs via a LMB-sensitive pathway. PI-9 is detectable in both the nucleus and the cytoplasm of the cell. Since PI-9 is able to localize strongly in the nucleus via a facilitated mechanism, it is likely that active export of PI-9 from the nucleus to the cytoplasm occurs in order to maintain the correct nucleocytoplasmic distribution. Most proteins exported from the nucleus travel on a pathway that can be blocked by the compound LMB (20). We therefore tested the ability of LMB to inhibit the export of PI-9, as indicated by increased nuclear accumulation of PI-9 in LMB-treated cells. As a control for LMB activity we obtained a plasmid encoding a mutant form of nucleolar human immunodeficiency virus (HIV) Rev linked to GFP (RevMAPKK/GFP) (24). This fusion protein also carries a strong, heterologous nuclear export signal (NES) from mitogen-activated protein kinase kinase. Under normal conditions, in the absence of LMB the vast majority of this protein is present in the cytoplasm, since the rate of nuclear export directed by this NES is far greater than that of nuclear import (24). However, in the presence of LMB nuclear export is prevented and there is a dramatic shift from predominantly cytoplasmic to predominantly nuclear compartmentalization of RevMAPKK/GFP,

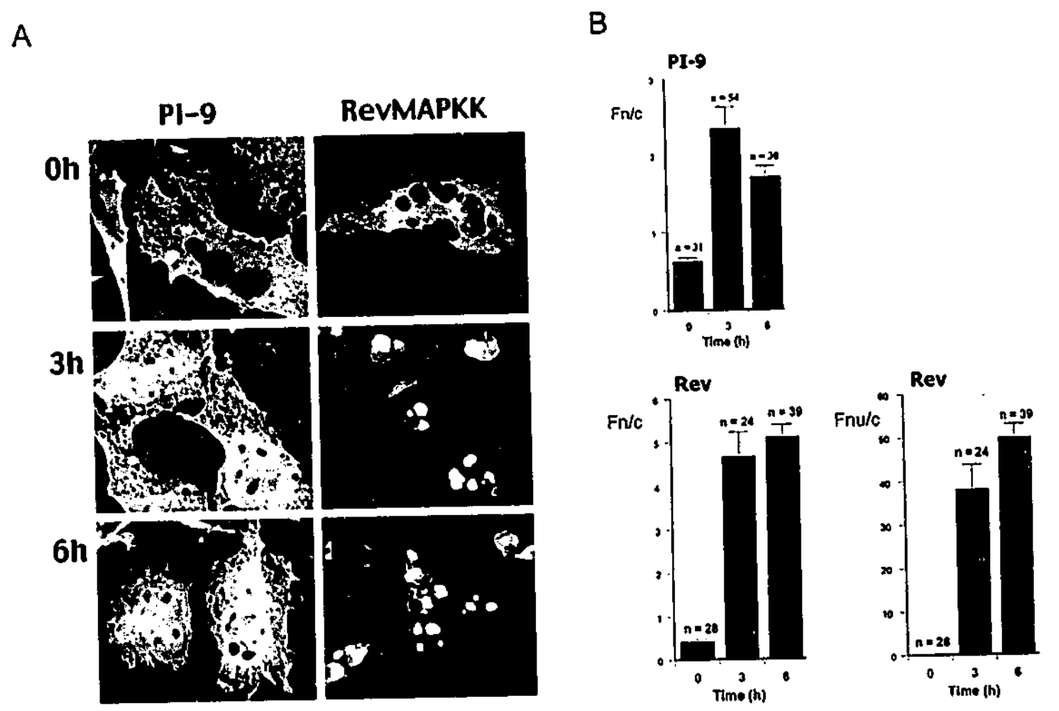

FIG. 6. Nuclear export of PI-9 is blocked by LMB. COS-1 cells transfected with the expression vectors encoding PI-9 or RevMAPKK/GFP were exposed to 4 ng of LMB/ml for the indicated times. Cells were prepared for visualization (A) and quantitation (B) of nuclear/cytoplasmic ratios (Fn/c) or nucleolar/cytoplasmic ratios (Fnu/c by CLSM as described in Materials and Methods). Results are the mean ± SEM, with *n* being the number of cells analyzed.

with most accumulation in the nucleoli, as expected for Rev (43).

COS-1 cells expressing PI-9 or RevMAPKK/GFP were exposed to LMB for 0, 3, or 6 h and then were examined by indirect immunofluorescence using CLSM to measure the ratio of fluorescence intensities in the cytosol and nucleus at the single-cell level (Fig. 6). As expected, RevMAPKK/GFP rapidly accumulated in the nucleolus, peaking at 3 h with a concentration 40- to 50-fold higher in the nucleolus than in the cytoplasm. Some RevMAPKK/GFP accumulated in the nucleus outside the nucleolus, and this concentration was fivefold higher than that in the cytoplasm. Nuclear accumulation of PI-9 was also observed, peaking at 3 h with two to three times the concentration in the nucleus than that in the cytoplasm. This represented a significant shift from untreated cells, which show about twice the concentration of PI-9 in the cytoplasm as that in the nucleus. These results clearly show that PI-9 is actively exported from the nucleus through a mechanism dependent on Crm1p (exportin).

DISCUSSION

The ov-serpins are an emerging subgroup of the serpin superfamily distinguished by their largely intracellular localization. Indeed, most of the new serpins recently identified through whole-genome analysis of *Caenorhabditis elegans* and *Drosophila melanogaster* have the characteristics of intracellular proteins (67 and A. Lesk, P. Bird, and J. Whisstock, unpublished results). Although 1 of the 12 human ov-serpins (bomapin) is imported into the nucleus via a classical NLS (13), we show here for the first time that PI-9 and at least four related human ov-serpins (PAI-2, MNEI, PI-6, and PI-8) enter nuclei without possessing obvious classical nuclear import signals. On the basis of the behavior of GFP fusion proteins, it is clear that import of these serpins depends almost entirely on a facilitated (active) pathway. This contrasts with the viral intracellular serpin CrmA, which has functional similarities to PI-9 but apparently enters the nucleus entirely by diffusion. On the basis of our results, it is reasonable to suggest that other ov-serpins—and perhaps unrelated intracellular serpins—will exhibit similar subcellular localization.

A nucleocytoplasmic distribution pattern is consistent with the proposed cytoprotective roles of several of these serpins. For example, it is thought that PI-9 protects cytotoxic and bystander cells against misdirected graB, which is known to translocate efficiently from the cytoplasm to the nucleus of cytotoxic and target cells and to degrade cytoplasmic and nuclear substrates (60). Obviously, the presence of PI-9 in both the cytoplasm and nucleus of a cell would provide efficient

protection against graB-mediated damage. Likewise, PI-6 and MNEI inhibit the monocyte and granulocyte granule proteinases, elastase, cathepsin G, and proteinase 3, and may also protect cells against protease-directed autolysis (51, 56). These proteinases are all small enough to enter nuclei by diffusion, so that if introduced into the host cell cytoplasm they have the potential to threaten viability in a manner similar to that of misdirected graB in cytotoxic cells. Indeed, cathepsin G can activate caspase 7 via cleavage at a noncanonical site (69) and cleaves the nuclear protein brm (5a), suggesting it is proapoptotic if released into the interior of the cell. The presence of PI-6 and MNEI in the nucleus as well as the cytoplasm therefore offers the cell an additional level of protection against misdirected granule proteinases. A similar protective role can be invoked for two other ov-serpins, SCCA-1 and SCCA-2, that were not investigated in this study. These proteins interact with lysosomal and mast cell proteinases, respectively (47, 48). Given that loss of lysosomal membrane integrity and the release of contents into the cytoplasm are known to occur under stress (11) and that lysosomal proteinases are also small enough to diffuse into the nucleus, it is possible that the SCCAs will also exhibit a nucleocytoplasmic distribution.

The role of PAI-2 in cells is probably different from that of other ov-serpins, although still cytoprotective in scope. PAI-2 protects cells against tumor necrosis factor alpha-mediated apoptosis (15) and virus infection (4). Protection against virus infection occurs through PAI-2-mediated induction of autocrine alpha and beta interferon, and it has been suggested that PAI-2 acts on a transcription factor pathway (4). Although the intracellular targets of PAI-2 are unknown, the presence of PAI-2 in the nucleus is certainly consistent with a direct or indirect impact on the transcription of cytoprotective factors.

An interesting question not addressed in our study is whether the nucleocytoplasmic distribution of PI-9 and other intracellular ov-serpins is regulated, in that levels of nuclear import or export alter in response to specific signals. Clearly different cell types show different proportions of nuclear PI-9 (compare HUVECs, YT cells, and BeWo cells), and this is not related to the expression level of PI-9, ruling out saturation of the nuclear import machinery. While different cells may possess different levels of key mediators of PI-9 import or export, an alternative possibility is that the nucleocytoplasmic distribution of PI-9 is actively regulated. There are several specific mechanisms by which nuclear transport can be regulated, perhaps the best known being cytoplasmic retention, in which a nuclear-targeted protein is held in the cytoplasm by binding either to an anchored structure or to a partner that sequesters its NLS (25). Signal-mediated phosphorylation or proteolysis then releases the protein by disrupting binding or revealing its NLS, allowing import to occur. It remains to be seen if the nucleocytoplasmic distribution of PI-9 and related ov-serpins alters in response to cell activation, differentiation, stress, or other stimuli and whether they have intracellular binding partners.

The structure of the nuclear pore and the main players in the import machinery are reasonably well understood (for reviews, see references 1 and 20). Import of proteins carrying a classical NLS involves the formation of a complex between the cargo, importin-α (adapter), and importin-β. In a process requiring energy, a G protein (Ran), Ran-binding proteins, guanine nucleotide exchange factors, and GTPase activators the complex docks at the nuclear pore, is translocated through it, and then dissociates within the nucleoplasm. Several lines of evidence suggest that alternative import routes and components are used by proteins lacking classical import signals. For example, importin-β family members can mediate the import of ribosomal proteins independently of importin-α, and other Ran-binding proteins have also been implicated in adapter-free transport. In this study we have shown that PI-9 accumulates in the nucleus via an atypical import pathway that requires cytosolic factors but not ATP, which may also hold true for other ov-serpins. Although it lacks an apparent classical NLS, PI-9 is imported via a facilitated process, as indicated by its ability to mediate uptake of large fusion proteins. Preliminary evidence suggests that PI-9 does indeed possess an NLS, but it is conformational, comprising a number of noncontiguous residues (unpublished results). Like many nuclear proteins, PI-9 is exported from the nucleus via an LMB-sensitive pathway, strongly implying that it possesses an NES and that the nuclear export receptor Crm1p (exportin) is involved.

MAPKK	^{26}D	L	Q	K	K	L	E	E	L	E	L	D	E	Q	Q				
Rev	^{73}L	Q	L	P	P	L	W	E	L	T	L	D	C	N	E				
Gle I	^{346}E	S	A	L	P	L	G	K	L	T	L	Y	L	I	L				
Rch1	^{201}G	A	V	D	P	L	P	L	L	A	L	L	A	V	P				
PI-9	^{221}Y	A	R	K	E	L	S	L	L	V	L	L	P	D	D				
PI-9	^{34}S	I	S	S	A	L	A	M	V	L	L	G	A	K	G				

FIG. 7. Potential Leu-rich NESs in PI-9. Shown are two sequences on PI-9 with similarity to known NESs on Rev (18), Gle1 (36), Rch1 (9), and mitogen-activated protein kinase kinase (MAPKK) (24). Conserved residues of the NES are boxed.

What is the import pathway followed by PI-9? Proteins bearing a classical NLS bind to importin-α, and translocation requires ATP in vitro (1, 20). Since PI-9 lacks a classical NLS, it may not bind importin-α. This is supported by preliminary experiments using established assays in which PI-9 failed to bind to mouse importin-α2 in either the presence or absence of importin-β (unpublished results). However, this conclusion should be qualified by noting that importin-α now appears to be a member of a larger family of proteins with similar functions and that there is some diversity in the sequence of signals recognized by importin-α (reviewed in references 1 and 55). Hence, the formal possibility that the PI-9 NLS binds a different importin-α family member cannot be excluded, but it is more likely that PI-9 is imported in a process that does not require importin-α. Perhaps it binds an importin-β family member directly, as is the case for import of ribosomal proteins and certain transcription factors (20, 42, 55).

PI-9 nuclear import is clearly distinguishable from conventional import on the basis of its ATP independence in vitro. This nonconventional mechanism is probably not unique or restricted to particular cell types, because nuclear import of PI-9 and related ov-serpins occurs in epithelial, lymphoid, and fibroblast lines. PI-9 does not accumulate in the nucleus in the presence of CHAPS, so its lower energy requirement for translocation is not due to retention or anchorage in the nucleus, as

is the case for the unconventional import of nucleoplasmin, granzymes A and B, and HIV Vpr and Tat (16, 28, 32, 52, 64). Further distinctions between the nonconventional import pathways utilized by the latter proteins and that utilized by PI-9 are that import of HIV Vpr does not require cytosolic factors, such as Ran or importins (32), while the import of Tat requires ATP hydrolysis but not cytosolic factors (16).

PI-9 apparently exits the nucleus via a conventional process. Its sensitivity to LMB indicates that egress depends on the factor Crm1p (exportin), which conventionally recognizes Leu-rich NESs (reviewed in reference 20). Studies on a number of exported proteins have led to the definition of a consensus NES, which comprises $LeuXxx_{(1-3)}LeuXxx_{(2-3)}LeuXxxLeu$, but not all sequences conforming to the consensus are functional, and avid interaction with Crm1p can occur in the absence of a consensus sequence (20, 24). As shown in Fig. 7, PI-9 has at least two sequences matching the consensus NES motif. However, the large number of available serpin crystal structures (66) and the overall sequence similarity between serpins have allowed us to build a model of PI-9 with a high degree of certainty based on the crystal structure of the related serpin, antithrombin (J. Whisstock and P. Bird, unpublished results). This clearly shows that both sequences are buried within the body of the molecule and would not be available for a protein-protein interaction unless PI-9 is unfolded. As there is no evidence at present that nuclear export requires unfolding of the passenger protein, this burying of a potential NES may explain why some sequences that match the consensus motif are not functional. We suggest that export of PI-9 either involves a linear NES that does not resemble the proposed consensus sequence or involves a conformational rather than linear NES. Alternatively, PI-9 may lack an NES altogether but can exit the nucleus by binding to a protein that possesses a classical NES.

ACKNOWLEDGMENTS

We thank B. Henderson (Westmead Hospital, Sydney, Australia) for advice and the RevMAPKK/GFP plasmid, A. Calderone for construction of the GFP–PAI-2 plasmid, and J. Whisstock (Monash University) for molecular modeling. We also thank D. Huang (Walter and Eliza Hall Institute) for Apaf-1 antibodies, E. Remold-O'Donnell (Center for Blood Research, Boston, Mass.) for MNEI antibodies, J. Wilson and J. Wang (Michigan State University) for LDH antiserum, and D. Pickup (Duke University Medical Center) for the CrmA cDNA and antiserum.

This work was supported by the National Health and Medical Research Council of Australia.

REFERENCES

1. **Adam, S. A.** 1999. Transport pathways of macromolecules between the nucleus and the cytoplasm. Curr. Opin. Cell Biol. **11**:402–406.
2. **Andersson, S., D. L. Davis, H. Dahlback, H. Jornvall, and D. W. Russell.** 1989. Cloning, structure, and expression of the mitochondrial cytochrome P-450 sterol 26-hydroxylase, bile acid biosynthetic enzyme. J. Biol. Chem. **264**:8222–8229.
3. **Annand, R. R., J. R. Dahlen, C. A. Sprecher, P. de Dreu, D. C. Foster, J. A. Mankovich, R. V. Talanian, W. Kisiel, and D. A. Giegel.** 1999. Caspase-1(interleukin-1b-converting enzyme) is inhibited by the human serpin analogue proteinase inhibitor 9. Biochem. J. **342**:655–665.
4. **Antalis, T. M., M. La Linn, K. Bunnag, L. Mateo, J. Gardner, J. L. Dickinson, K. Buttigieg, and A. Suhrbier.** 1998. The serine proteinase inhibitor (serpin) plasminogen activator inhibitor type 2 protects against viral cytopathic effects by constitutive interferon alpha/beta priming. J. Exp. Med. **187**:1799–1811.
5. **Belin, D.** 1993. Biology and facultative secretion of plasminogen activator inhibitor-2. Thrombo Haemostasis **70**:144–147.
5a. **Biggs, J. R., J. Yang, U. Gullberg, C. Muchardt, M. Yaniv, and A. S. Kraft.** 2001. The human brm protein is cleaved during apoptosis: the role of cathepsin-G. Proc. Natl. Acad. Sci. USA **98**:3814–3819.
6. **Bird, C. H., V. R. Sutton, J. Sun, C. E. Hirst, A. Novak, J. A. Trapani, and P. I. Bird.** 1998. Selective regulation of apoptosis: the cytotoxic lymphocyte serpin proteinase inhibitor 9 protects against granzyme B-mediated apoptosis without perturbing the Fas cell death pathway. Mol. Cell. Biol. **18**:6387–6398.
7. **Bird, P. I.** 1998. Serpins and regulation of cell death. Results Probl. Cell Differ. **24**:63–89.
8. **Bird, P. I.** 1999. Regulation of pro-apoptotic leukocyte granule serine proteinases by intracellular serpins. Immunol. Cell. Biol. **77**:47–57.
9. **Boche, J., and E. Fanning.** 1997. Nucleocytoplasmic recycling of the nuclear localization signal receptor alpha subunit in vivo is dependent on a nuclear export signal, energy and RCC1. J. Cell Biol. **139**:313–325.
10. **Briggs, L. J., D. Stein, J. Goltz, V. C. Corrigan, A. Efthymiadis, S. Hubner, and D. A. Jans.** 1998. The cAMP-dependent protein kinase site (Ser312) enhances dorsal nuclear import through facilitating nuclear localization sequence/importin interaction. J. Biol. Chem. **273**:22745–22752.
11. **Brunk, U. T., H. Dalen, K. Roberg, and H. B. Hellquist.** 1997. Photo-oxidative disruption of lysosomal membranes causes apoptosis of cultured human fibroblasts. Free Radic. Biol. Med. **23**:616–626.
11a. **Buzza, M. S., C. E. Hirst, C. H. Bird, P. Hosking, J. McKendrick, and P. I. Bird.** The granzyme B inhibitor, PI-9, is present in endothelial and mesothelial cells, suggesting it protects bystander cells during immune responses. Cell Immunol., in press.
12. **Chu, M., C. H. Bird, M. S. Teasdale, and P. I. Bird.** 1998. Turnover of thrombomodulin at the cell surface occurs at a similar rate to receptors that are not actively internalized. Thromb. Haemostasis **80**:119–127.
13. **Chuang, T. L., and R. R. Schleef.** 1999. Identification of a nuclear targeting domain in the insertion between helices C and D in protease inhibitor-10. J. Biol. Chem. **274**:11194–11198.
14. **Coughlin, P., J. Sun, L. Cerruti, H. H. Salem, and P. Bird.** 1993. Cloning and molecular characterization of a human intracellular proteinase inhibitor. Proc. Natl. Acad. Sci. USA **90**:9417–9421.
15. **Dickinson, J. L., E. J. Bates, A. Ferrante, and T. M. Antalis.** 1995. Plasminogen activator inhibitor 2 inhibits tumor necrosis factor alpha-induced apoptosis. Evidence for an alternate biological function. J. Biol. Chem. **270**:27894–27904.
16. **Efthymiadis, A., L. J. Briggs, and D. A. Jans.** 1998. The HIV-1 Tat nuclear localization sequence confers novel nuclear import properties. J. Biol. Chem. **273**:1623–1628.
17. **Efthymiadis, A., H. Shao, S. Hubner, and D. A. Jans.** 1997. Kinetic characterization of the human retinoblastoma protein bipartite nuclear localization sequence (NLS) in vivo and in vitro. A comparison with the SV40 large T-antigen NLS. J. Biol. Chem. **272**:22134–22139.
18. **Fischer, U., J. Huber, W. C. Boelens, I. W. Mattaj, and R. Luhrmann.** 1995. The HIV-1 Rev activation domain is a nuclear export signal that accesses an export pathway used by specific cellular RNAs. Cell **82**:475–483.
19. **Golstein, P.** 1974. Sensitivity of cytotoxic T cells to T-cell mediated cytotoxicity. Nature **252**:81–83.
20. **Gorlich, D., and U. Kutay.** 1999. Transport between the cell nucleus and the cytoplasm. Annu. Rev. Cell. Dev. Biol. **15**:607–660.
21. **Grigoryev, S. A., J. Bednar, and C. L. Woodcock.** 1999. MENT, a heterochromatin protein that mediates higher order chromatin folding, is a new serpin family member. J. Biol. Chem. **274**:5626–5636.
22. **Harlow, E., and D. Lane.** 1988. Antibodies. A laboratory manual. Cold Spring Harbor Laboratory, Cold Spring Harbor, N.Y.
23. **Hausmann, G., L. A. O'Reilly, R. van Driel, J. G. Beaumont, A. Strasser, J. A. Adams, and D. C. S. Huang.** 2000. Pro-apoptotic apoptosis protease-activating factor 1 (Apaf-1) has a cytoplasmic localization distinct from Bcl-2 or Bcl-xL. J. Cell Biol. **149**:623–633.
24. **Henderson, B. R., and A. Eleftheriou.** 2000. A comparison of the activity, sequence specificity, and CRM1-dependence of different nuclear export signals. Exp. Cell Res. **256**:213–224.
25. **Hood, J. K., and P. A. Silver.** 1999. In or out? Regulating nuclear transport. Curr. Opin. Cell Biol. **11**:241–247.
26. **Hubner, S., C. Y. Xiao, and D. A. Jans.** 1997. The protein kinase CK2 site (Ser111/112) enhances recognition of the simian virus 40 large T-antigen nuclear localization sequence by importin. J. Biol. Chem. **272**:17191–17195.
27. **Huntington, J. A., R. A. Read, and R. W. Carrell.** 2000. Structure of a serpin-protease complex shows inhibition by deformation. Nature **407**:923–926.
28. **Jans, D. A., L. J. Briggs, P. Jans, C. J. Froelich, G. Parasivam, S. Kumar, V. R. Sutton, and J. A. Trapani.** 1998. Nuclear targeting of the serine proteinase granzyme A (fragmentin-1). J. Cell Sci. **111**:2645–2654.
29. **Jans, D. A., M. J. Ackermann, J. R. Bischoff, D. H. Beach, and R. Peters.** 1991. p34cdc2-mediated phosphorylation at T124 inhibits nuclear import of SV-40 T antigen proteins. J. Cell Biol. **115**:1203–1212.
30. **Jans, D. A., and P. Jans.** 1994. Negative charge at the casein kinase II site flanking the nuclear localization signal of the SV40 large T-antigen is mech-

anistically important for enhanced nuclear transport. Oncogene 9:2961–2968.
31. **Jans, D. A., P. Jans, L. J. Briggs, V. Sutton, and J. A. Trapani.** 1996. Nuclear transport of granzyme B (fragmentin 2). J. Biol. Chem. 271:30781–30789.
32. **Jenkins, Y., M. McEntee, K. Weis, and W. C. Greene.** 1998. Characterization of HIV-1 Vpr nuclear import: analysis of signals and pathways. J. Cell Biol. 143:875–885.
33. **Kranz, D. M., and H. N. Eisen.** 1987. Resistance of cytotoxic lymphocytes to lysis by a clone of cytotoxic T lymphocytes. Proc. Natl. Acad. Sci. USA 84:3375–3379.
34. **Madison, E. L., and P. Bird.** 1992. A vector, pSHT, for the expression and secretion of protein domains in mammalian cells. Gene 121:179–180.
35. **Miyata, T., M. Nangaku, D. Suzuki, R. Inagi, K. Uragami, H. Sakai, K. Okubo, and K. Kurokawa.** 1998. A mesangium-predominant gene, megsin, is a new serpin upregulated in IgA nephropathy. J. Clin. Investig. 120:828–836.
36. **Murphy, R., and S. R. Wente.** 1996. An RNA-export mediator with an essential nuclear export signal. Nature 383:357–360.
37. **Nagata, S.** 1997. Apoptosis by death factor. Cell 88:355–365.
38. **Nagler-Anderson, C., C. R. Verret, A. A. Firmenich, M. Berne, and H. N. Eisen.** 1988. Resistance of primary CD8+ cytotoxic T lymphocytes to lysis by cytotoxic granules from cloned T cell lines. J. Immunol. 141:3299–3305.
39. **Nigg, E. A.** 1997. Nucleocytoplasmic transport: signals, mechanisms and regulation. Nature 386:779–787.
40. **Ochs, R., M. Lischwe, P. O'Leary, and H. Busch.** 1983. Localization of nucleolar phosphoproteins B23 and C23 during mitosis. Exp. Cell Res. 46:139–149.
41. **Ooms, L., J. Nicholl, P. Bird, and G. R. Sutherland.** 1995. Localization of the human monocyte/neutrophil elastase inhibitor gene to chromosome 6p25. Chromosome Res. 3:447.
42. **Pemberton, L. F., J. S. Rosenblum, and G. Blobel.** 1999. Nuclear import of the TATa-binding protein: mediation by the karyopherin Kap114p and a possible mechanism for intranuclear targeting. J. Cell Biol. 145:1407–1417.
43. **Perkins, A., A. W. Cochrane, S. M. Ruben, and C. A. Rosen.** 1989. Structural and functional characterization of the human immunodeficiency virus rev protein. J. Acquir. Immune Defic. Syndr. 2:256–263.
44. **Potempa, J., E. Korzus, and J. Travis.** 1994. The serpin superfamily of proteinase inhibitors: structure, function and regulation. J. Biol. Chem. 269: 15957–15960.
45. **Remold-O'Donnell, E.** 1993. The ovalbumin family of serpin proteins. FEBS Lett. 315:105–108.
46. **Rihs, H. P., and R. Peters.** 1989. Nuclear transport kinetics depend on phosphorylation-site-containing sequences flanking the karyophilic signal of the simian virus 40 T-antigen. EMBO J. 8:1479–1484.
47. **Schick, C., Y. Kamachi, A. J. Bartuski, S. Cataltepe, N. M. Schechter, P. A. Pemberton, and G. A. Silverman.** 1997. Squamous cell carcinoma antigen 2 is a novel serpin that inhibits the chymotrypsin-like proteinases cathepsin G and mast cell chymase. J. Biol. Chem. 272:1849–1855.
48. **Schick, C., P. A. Pemberton, G.-P. Shi, Y. Kamachi, S. Cataltepe, A. J. Bartuski, E. R. Gornstein, D. Bromme, H. A. Chapman, and G. A. Silverman.** 1998. Cross-class inhibition of the cysteine proteinases cathepsins K, L, and S by the serpin squamous cell carcinoma antigen 1: a kinetic analysis. Biochemistry 37:5258–5266.
49. **Schikendanz, J., K. H. Scheidtmann, and G. Walter.** 1986. Kinetics of nuclear transport and oligomerization of simian virus 40 large T antigen. Virology 148:47–57.
50. **Scott, F. L., P. B. Coughlin, C. Bird, L. Cerruti, J. A. Hayman, and P. Bird.** 1996. Proteinase inhibitor 6 cannot be secreted, which suggests it is a new type of cellular serpin. J. Biol. Chem. 271:1605–1612.
51. **Scott, F. L., C. E. Hirst, J. Sun, S. P. Bottomley, C. H. Bird, and P. I. Bird.** 1999. The intracellular serpin proteinase inhibitor 6 (PI-6) is expressed in monocytes and granulocytes and is a potent inhibitor of the azurophilic granule proteinase, cathepsin G. Blood 93:2089–2097.
52. **Shi, L., S. Mai, S. Israels, K. A. Browne, J. A. Trapani, and A. H. Greenberg.** 1997. Granzyme B (GraB) autonomously crosses the cell membrane and perforin initiates apoptosis and GraB nuclear localization. J. Exp. Med. 185:855–866.
53. **Smyth, M. J., and J. A. Trapani.** 1995. Granzymes: exogenous proteinases that induce target cell apoptosis. Immunol. Today 16:202–206.
54. **Stein, P. E., and R. W. Carrell.** 1995. What do dysfunctional serpins tell us about molecular mobility and disease. Struct. Biol. 2:96–113.
55. **Stochaj, U., and K. L. Rother.** 1999. Nucleocytoplasmic trafficking of proteins: with or without Ran? Bioessays 21:579–589.
56. **Sugimori, T., J. Conley, J. R. Hoidal, and E. Remold-O'Donnell.** 1995. Inhibitory properties of recombinant monocyte/neutrophil elastase inhibitor. Am. J. Respir. Cell Mol. Biol. 13:314–322.
57. **Sun, J., C. H. Bird, V. Sutton, L. McDonald, P. B. Coughlin, T. A. De Jong, J. A. Trapani, and P. I. Bird.** 1996. A cytosolic granzyme B inhibitor related to the viral apoptotic regulator cytokine response modifier A is present in cytotoxic lymphocytes. J. Biol. Chem. 271:27802–27809.
58. **Teasdale, M. S., C. H. Bird, and P. Bird.** 1994. Internalization of the anticoagulant thrombomodulin is constitutive and does not require a signal in the cytoplasmic domain. Immunol. Cell Biol. 72:480–488.
59. **Trapani, J. A.** 1998. Dual mechanisms of apoptosis induction by cytotoxic lymphocytes. Int. Rev. Cytol. 182:111–192.
60. **Trapani, J. A., and P. I. Bird.** 2000. Granzymes: mediation of pro-apoptotic and nonapoptotic functions of cytolytic lymphocytes and regulation by endogenous and circulating inhibitors, p. 179–196. *In* M. V. Sitkovsky and P. A. Henkart (ed.), Cytotoxic cells: basic mechanisms and medical applications. Lippincott, Williams & Wilkins, Philadelphia, Pa.
61. **Trapani, J. A., K. A. Browne, M. J. Smyth, and D. A. Jans.** 1996. Localization of granzyme B in the nucleus. J. Biol. Chem. 271:4127–4133.
62. **Trapani, J. A., M. J. Smyth, V. A. Apostolidis, M. Dawson, and K. Browne.** 1994. Granule serine proteinases are normal nuclear constituents of natural killer cells. J. Biol. Chem. 269:18359–18365.
63. **Tsay, Y.-G., N. Y. Lin, P. G. Voss, R. J. Patterson, and J. L. Wang.** 1999. Export of galactin-3 from nuclei of digitonin-permeabilized mouse 3T3 fibroblasts. Exp. Cell Res. 252:250–261.
64. **Vancurova, I., W. Lou, T. M. Paine, and P. L. Paine.** 1993. Nucleoplasmin uptake by facilitated transport and intranuclear binding. Eur. J. Cell Biol. 62:22–33.
65. **Vyakarnam, A., A. J. Lenneman, K. M. Lakkides, R. J. Patterson, and J. L. Wang.** 1998. A comparative nuclear localization study of galectin-1 with other splicing components. Exp. Cell Res. 242:419–428.
66. **Whisstock, J., R. Skinner, and A. M. Lesk.** 1998. An atlas of serpin conformations. Trends Biochem. Sci. 23:63–67.
67. **Whisstock, J. C., J. A. Irving, S. P. Bottomley, R. N. Pike, and A. M. Lesk.** 1999. Serpins in the Caenorhabditis elegans genome. Proteins 36:31–41.
68. **Yodoi, J., K. Teshigawara, T. Nikaido, K. Fukui, T. Noma, T. Honjo, M. Takigawa, M. Sasaki, N. Minato, M. Tsudo, et al.** 1985. TCGF (IL 2)-receptor inducing factor(s). I. Regulation of IL 2 receptor on a natural killer-like cell line (YT cells). J. Immunol. 134:1623–1630.
69. **Zhou, Q., and G. S. Salvesen.** 1997. Activation of pro-caspase-7 by serine proteases includes a non-canonical specificity. Biochem. J. 324:361–364.
70. **Zhou, Q., S. Snipas, K. Orth, M. Muzio, V. Dixit, and G. Salvesen.** 1997. Target protease specificity of the viral serpin CrmA. J. Biol. Chem. 272: 7797–7800.
71. **Zou, Z., A. Anisowicz, M. J. C. Hendrix, A. Thor, M. Neveu, S. Sheng, K. Rafidi, E. Seftor, and R. Sager.** 1994. Maspin, a serpin with tumor-suppressing activity in human mammary epithelial cells. Science 263:526–529.

Bibliography

Abts H. F., Welss T., Mirmohammadsadegh W., Kohrer K., Michel G. and Ruzicka T. (1999). Cloning and characterization of hurpin (proteinase inhibitor 13): A new skin-specific, UV-repressible serine proteinase inhibitor of the ovalbumin serpin family. *J Mol Biol* **293**: 29-39.

Adams J. M. and Cory S. (1998). The Bcl-2 protein family: arbiters of cell survival. *Science* **281**: 1322-1326

Adams J. M. and Cory S. (2001). Life-or-death decisions by the Bcl-2 protein family. *Trends Biochem Sci* **26**: 61-66.

Ahmad M., Srinivasula S. M., Wang L., Talanian R. V., Litwack G., Fernandes-Alnemri T. and Alnemri E. S. (1997). CRADD, a novel human apoptotic adaptor molecule for caspase-2, and FasL/tumor necrosis factor receptor-interacting protein RIP. *Cancer Res* **57**: 615-619.

Alimonti J. B., Shi L., Baijal P. K. and Greenberg A. H. (2001). Granzyme B induces BID-mediated cytochrome c release and mitochondrial permeability transition. *J Biol Chem* **276**: 6974-6982.

Almeida J., Bueno C., Alguero M. C., Sanchez M. L., de Santiago M., Escribano L., Diaz-Agustin B., Vaquero J. M., Laso F. J., San Miguel J. F. and Orfao A. (2001). Comparative analysis of the morphological, cytochemical, immunophenotypical, and functional characteristics of normal human peripheral blood lineage$^-$/CD16$^+$/HLA$^-$DR$^+$/CD14$^{-/lo}$ cells, CD14$^+$ monocytes, and CD16$^-$ dendritic cells. *Clin Immunol* **100**: 325-338.

Anderson P., Nagler-Anderson C., O'Brien C., Levine H., Watkins S., Slayter H. S., Blue M. L. and Schlossman S. F. (1990). A monoclonal antibody reactive with a 15-kDa cytoplasmic granule- associated protein defines a subpopulation of CD8+ T lymphocytes. *J Immunol* **144**: 574-582.

Andersson M., Gunne H., Agerberth B., Boman A., Bergman T., Sillard R., Jornvall H., Mutt V., Olsson B., Wigzell H. and et al. (1995). NK-lysin, a novel effector peptide of cytotoxic T and NK cells. Structure and cDNA cloning of the porcine form, induction by interleukin 2, antibacterial and antitumour activity. *Embo J* **14**: 1615-1625.

Andrade F., Roy S., Nicholson D., Thornberry N., Rosen A. and Casciola-Rosen L. (1998). Granzyme B directly and efficiently cleaves several downstream caspase substrates: implications for CTL-induced apoptosis. *Immunity* **8**: 451-460.

Andrin C., Pinkoski M. J., Burns K., Atkinson E. A., Krahenbuhl O., Hudig D., Fraser S. A., Winkler U., Tschopp J., Opas M., Bleackley R. C. and Michalak M. (1998). Interaction between a Ca2+-binding protein calreticulin and perforin, a component of the cytotoxic T-cell granules. *Biochemistry* **37**: 10386-10394.

Annand R. R., Dahlen J. R., Sprecher C. A., De Dreu P., Foster D. C., Mankovich J. A., Talanian R. V., Kisiel W. and Giegel D. A. (1999). Caspase-1 (interleukin-1beta-converting enzyme) is inhibited by the human serpin analogue proteinase inhibitor 9. *Biochem J* **342 Pt 3**: 655-665.

Antia R., Schlegel R. A. and Williamson P. (1992). Binding of perforin to membranes is sensitive to lipid spacing and not headgroup. *Immunol Lett* **32**: 153-157.

Apostolidis V. A., Browne K. A., Smyth M. J. and Trapani J. A. (1995). The peptide loop consisting of amino acids 139-157 of human granzyme B (fragmentin 2) contains an immunodominant epitope recognized by the mouse. *Mol Immunol* **32**: 909-917.

Ardavin C., Martinez del Hoyo G., Martin P., Anjuere F., Arias C. F., Marin A. R., Ruiz S., Parrillas V. and Hernandez H. (2001). Origin and differentiation of dendritic cells. *Trends Immunol* **22**: 691-700.

Ashany D., Savir A., Bhardwaj N. and Elkon K. B. (1999). Dendritic cells are resistant to apoptosis through the Fas (CD95/APO-1) pathway. *J Immunol* **163**: 5303-5311.

Ashton-Rickardt P. G. and Opferman J. T. (1999). Memory T lymphocytes. *Cell Mol Life Sci* **56**: 69-77.

Askew Y. S., Pak S. C., Luke C. J., Askew D. J., Cataltepe S., Mills D. R., Kato H., Lehoczky J., Dewar K., Birren B. and Silverman G. A. (2001). SERPINB12 is a novel member of the human ov-serpin family that is widely expressed and inhibits trypsin-like serine proteinases. *J Biol Chem* **276**: 49320-49330.

Astedt B., Wallen P. and Aasted B. (1979). Occurrence of both urokinase and tissue plasminogen activator in human seminal plasma. *Thromb Res* **16**: 463-472.

Athayde N., Romero R., Gomez R., Maymon E., Pacora P., Mazor M., Yoon B. H., Fortunato S., Menon R., Ghezzi F. and Edwin S. S. (1999). Matrix metalloproteinases-9 in preterm and term human parturition. *J Matern Fetal Med* **8**: 213-219.

Atkinson E. A., Barry M., Darmon A. J., Shostak I., Turner P. C., Moyer R. W. and Bleackley R. C. (1998). Cytotoxic T lymphocyte-assisted suicide. Caspase 3 activation is primarily the result of the direct action of granzyme B. *J Biol Chem* **273**: 21261-21266.

Babe L. M., Yoast S., Dreyer M. and Schmidt B. F. (1998). Heterologous expression of human granzyme K in Bacillus subtilis and characterization of its hydrolytic activity in vitro. *Biotechnol Appl Biochem* **27**: 117-124.

Baker E., Sayers T. J., Sutherland G. R. and Smyth M. J. (1994a). The genes encoding NK cell granule serine proteases, human tryptase-2 (TRYP2) and human granzyme A (HFSP), both map to chromosome 5q11-q12 and define a new locus for cytotoxic lymphocyte granule tryptases. *Immunogenetics* **40**: 235-237

Baker E., Sayers T. J., Sutherland G. R. and Smyth M. J. (1994b). The genes encoding NK cell granule serine proteases, human tryptase-2 (TRYP2) and human granzyme A (HFSP), both map to chromosome 5q11-q12 and define a new locus for cytotoxic lymphocyte granule tryptases. *Immunogenetics* **40**: 235-237.

Baranov V., Nagaeva O., Hammarstrom S. and Mincheva-Nilsson L. (2000). Lipids are a constitutive component of cytolytic granules. *Histochem Cell Biol* **114**: 167-171.

Barry M., Heibein J. A., Pinkoski M. J., Lee S. F., Moyer R. W., Green D. R. and Bleackley R. C. (2000). Granzyme B short-circuits the need for caspase 8 activity during granule-mediated cytotoxic T-lymphocyte killing by directly cleaving Bid. *Mol Cell Biol* **20**: 3781-3794.

Bartuski A. J., Kamachi Y., Schick C., Overhauser J. and Silverman G. A. (1997). Cytoplasmic antiproteinase 2 (PI8) and bomapin (PI10) map to the serpin cluster at 18q21.3. *Genomics* **43**: 321-328.

Beidler D. R., Tewari M., Friesen P. D., Poirier G. and Dixit V. M. (1995). The baculovirus p35 protein inhibits Fas- and tumor necrosis factor-induced apoptosis. *J Biol Chem* **270**: 16526-16528.

Bennett S. R., Carbone F. R., Karamalis F., Flavell R. A., Miller J. F. and Heath W. R. (1998). Help for cytotoxic-T-cell responses is mediated by CD40 signalling. *Nature* **393**: 478-480.

Beresford P. J., Xia Z., Greenberg A. H. and Lieberman J. (1999). Granzyme A loading induces rapid cytolysis and a novel form of DNA damage independently of caspase activation. *Immunity* **10**: 585-594.

Beresford P. J., Zhang D., Oh D. Y., Fan Z., Greer E. L., Russo M. L., Jaju M. and Lieberman J. (2001). Granzyme A activates an endoplasmic reticulum-associated caspase- independent nuclease to induce single-stranded DNA nicks. *J Biol Chem* **276**: 43285-43293.

Berthou C., Marolleau J. P., Lafaurie C., Soulie A., Dal Cortivo L., Bourge J. F., Benbunan M. and Sasportes M. (1995). Granzyme B and perforin lytic proteins are expressed in $CD34^+$ peripheral blood progenitor cells mobilized by chemotherapy and granulocyte colony-stimulating factor. *Blood* **86**: 3500-3506.

Bhardwaj N., Bender A., Gonzalez N., Bui L. K., Garrett M. C. and Steinman R. M. (1994). Influenza virus-infected dendritic cells stimulate strong proliferative and cytolytic responses from human CD8+ T cells. *J Clin Invest* **94**: 797-807.

Biggs J. R., Yang J., Gullberg U., Muchardt C., Yaniv M. and Kraft A. S. (2001). The human brm protein is cleaved during apoptosis: the role of cathepsin G. *Proc Natl Acad Sci U S A* **98**: 3814-3819.

Bird C. H., Sutton V. R., Sun J., Hirst C. E., Novak A., Kumar S., Trapani J. A. and Bird P. I. (1998). Selective regulation of apoptosis: the cytotoxic lymphocyte serpin proteinase inhibitor 9 protects against granzyme B-mediated apoptosis without perturbing the Fas cell death pathway. *Mol Cell Biol* **18**: 6387-6398.

Bird C. H., Blink E. J., Hirst C. E., Buzza M. S., Steele P. M., Sun J., Jans D. A. and Bird P. I. (2001). Nucleocytoplasmic distribution of the ovalbumin serpin PI-9 requires a nonconventional nuclear import pathway and the export factor Crm1. *Mol Cell Biol* **21**: 5396-5407.

Bird P. I., Gething M. J. and Sambrook J. (1987). Translocation in yeast and mammalian cells: not all signal sequences are functionally equivalent. *J Cell Biol* **105**: 2905-2914.

Bird P. I. (1999). Regulation of pro-apoptotic leucocyte granule serine proteinases by intracellular serpins. *Immunol Cell Biol* **77**: 47-57.

Bjorck P., Banchereau J. and Flores-Romo L. (1997). CD40 ligation counteracts Fas-induced apoptosis of human dendritic cells. *Int Immunol* **9**: 365-372.

Bjork I., Nordling K. and Olson S. T. (1993). Immunologic evidence for insertion of the reactive-bond loop of antithrombin into the A beta-sheet of the inhibitor during trapping of target proteinases. *Biochemistry* **32**: 6501-6505.

Bladergroen B. A., Strik M. C., Bovenschen N., van Berkum O., Scheffer G. L., Meijer C. J., Hack C. E. and Kummer J. A. (2001). The granzyme B inhibitor, protease inhibitor 9, is mainly expressed by dendritic cells and at immune-privileged sites. *J Immunol* **166**: 3218-3225.

Bladergroen B. A., Meijer C. J., ten Berge R. L., Hack C. E., Muris J. J., Dukers D. F., Chott A., Kazama Y., Oudejans J. J., van Berkum O. and Kummer J. A. (2002). Expression of the granzyme B inhibitor, protease inhibitor 9, by tumor cells in patients with non-Hogdkin and Hodgkin lymphoma: a novel protective mechanism for tumor cells to circumvent the immune system? *Blood* **99**: 232-237.

Blakely A., Gorman K., Ostergaard H., Svoboda K., Liu C. C., Young J. D. and Clark W. R. (1987). Resistance of cloned cytotoxic T lymphocytes to cell-mediated cytotoxicity. *J Exp Med* **166**: 1070-1083.

Bochan M. R., Goebel W. S. and Brahmi Z. (1995). Stably transfected antisense granzyme B and perforin constructs inhibit human granule-mediated lytic ability. *Cell Immunol* **164**: 234-239.

Boise L. H., Minn A. J., Noel P. J., June C. H., Accavitti M. A., Lindsten T. and Thompson C. B. (1995). CD28 costimulation can promote T cell survival by enhancing the expression of Bcl-XL. *Immunity* **3**: 87-98.

Bolme P., Henter J. I., Winiarski J., Elinder G., Ljungman P., Lonnerholm G. and Ringden O. (1995). Allogeneic bone marrow transplantation for hemophagocytic lymphohistiocytosis in Sweden. *Bone Marrow Transplant* **15**: 331-335.

Bossi G. and Griffiths G. M. (1999). Degranulation plays an essential part in regulating cell surface expression of Fas ligand in T cells and natural killer cells. *Nat Med* **5**: 90-96.

Braulke T., Gartung C., Hasilik A. and von Figura K. (1987). Is movement of mannose 6-phosphate-specific receptor triggered by binding of lysosomal enzymes? *J Cell Biol* **104**: 1735-1742.

Bromley S. K., Burack W. R., Johnson K. G., Somersalo K., Sims T. N., Sumen C., Davis M. M., Shaw A. S., Allen P. M. and Dustin M. L. (2001). The immunological synapse. *Annu Rev Immunol* **19**: 375-396.

Brooks A. G., Boyington J. C. and Sun P. D. (2000). Natural killer cell recognition of HLA class I molecules. *Rev Immunogenet* **2**: 433-448.

Broome H. E., Dargan C. M., Krajewski S. and Reed J. C. (1995). Expression of Bcl-2, Bcl-x, and Bax after T cell activation and IL-2 withdrawal. *J Immunol* **155**: 2311-2317.

Browne K. A., Blink E., Sutton V. R., Froelich C. J., Jans D. A. and Trapani J. A. (1999). Cytosolic delivery of granzyme B by bacterial toxins: evidence that endosomal disruption, in addition to transmembrane pore formation, is an important function of perforin. *Mol Cell Biol* **19**: 8604-8615.

Brunk U. T., Dalen H., Roberg K. and Hellquist H. B. (1997). Photo-oxidative disruption of lysosomal membranes causes apoptosis of cultured human fibroblasts. *Free Radic Biol Med* **23**: 616-626.

Brunk U. T., Neuzil J. and Eaton J. W. (2001). Lysosomal involvement in apoptosis. *Redox Rep* **6**: 91-97.

Bump N. J., Hackett M., Hugunin M., Seshagiri S., Brady K., Chen P., Ferenz C., Franklin S., Ghayur T., Li P. and et al. (1995). Inhibition of ICE family proteases by baculovirus antiapoptotic protein p35. *Science* **269**: 1885-1888.

Burkhardt J. K., Hester S., Lapham C. K. and Argon Y. (1990). The lytic granules of natural killer cells are dual-function organelles combining secretory and pre-lysosomal compartments. *J Cell Biol* **111**: 2327-2340.

Burns K., Helgason C. D., Bleackley R. C. and Michalak M. (1992). Calreticulin in T-lymphocytes. Identification of calreticulin in T- lymphocytes and demonstration that activation of T cells correlates with increased levels of calreticulin mRNA and protein. *J Biol Chem* **267**: 19039-19042.

Burrows J. A., Willis L. K. and Perlmutter D. H. (2000). Chemical chaperones mediate increased secretion of mutant alpha 1- antitrypsin (alpha 1-AT) Z: A potential pharmacological strategy for prevention of liver injury and emphysema in alpha 1-AT deficiency. *Proc Natl Acad Sci U S A* **97**: 1796-1801.

Buzza M. S., Hirst C. E., Bird C. H., Hosking P., McKendrick J. and Bird P. I. (2001). The granzyme B inhibitor, PI-9, is present in endothelial and mesothelial cells, suggesting that it protects bystander cells during immune responses. *Cell Immunol* **210**: 21-29.

Campbell E. J., Silverman E. K. and Campbell M. A. (1989). Elastase and cathepsin G of human monocytes. Quantification of cellular content, release in response to stimuli, and heterogeneity in elastase- mediated proteolytic activity. *J Immunol* **143**: 2961-2968

Caputo A., Fahey D., Lloyd C., Vozab R., McCairns E. and Rowe P. B. (1988). Structure and differential mechanisms of regulation of expression of a serine esterase gene in activated human T lymphocytes. *J Biol Chem* **263**: 6363-6369.

Carney D. F., Hammer C. H. and Shin M. L. (1986). Elimination of terminal complement complexes in the plasma membrane of nucleated cells: influence of extracellular Ca2+ and association with cellular Ca2+. *J Immunol* **137**: 263-270.

Carrell R. W., Whisstock J. and Lomas D. A. (1994). Conformational changes in serpins and the mechanism of alpha 1- antitrypsin deficiency. *Am J Respir Crit Care Med* **150**: S171-S175.

Carrell R. W. and Lomas D. A. (1997). Conformational disease. *Lancet* **350**: 134-138.

Casciola-Rosen L., Andrade F., Ulanet D., Wong W. B. and Rosen A. (1999). Cleavage by granzyme B is strongly predictive of autoantigen status: implications for initiation of autoimmunity. *J Exp Med* **190**: 815-826.

Cataltepe S., Gornstein E. R., Schick C., Kamachi Y., Chatson K., Fries J., Silverman G. A. and Upton M. P. (2000). Co-expression of the squamous cell carcinoma antigens 1 and 2 in normal adult human tissues and squamous cell carcinomas. *J Histochem Cytochem* **48**: 113-122.

Cella M., Jarrossay D., Facchetti F., Alebardi O., Nakajima H., Lanzavecchia A. and Colonna M. (1999). Plasmacytoid monocytes migrate to inflamed lymph nodes and produce large amounts of type I interferon. *Nat Med* **5**: 919-923.

Cella M., Facchetti F., Lanzavecchia A. and Colonna M. (2000). Plasmacytoid dendritic cells activated by influenza virus and CD40L drive a potent Th1 polarization. *Nat Immunol* **1**: 305-310.

Chai J., Shiozaki E., Srinivasula S. M., Wu Q., Dataa P., Alnemri E. S. and Shi Y. (2001). Structural basis of caspase-7 inhibition by XIAP. *Cell* **104**: 769-780.

Chinnaiyan A. M., O'Rourke K., Tewari M. and Dixit V. M. (1995). FADD, a novel death domain-containing protein, interacts with the death domain of Fas and initiates apoptosis. *Cell* **81**: 505-512.

Chinnaiyan A. M., Hanna W. L., Orth K., Duan H., Poirier G. G., Froelich C. J. and Dixit V. M. (1996). Cytotoxic T-cell-derived granzyme B activates the apoptotic protease ICE-LAP3. *Curr Biol* **6**: 897-899.

Chomczynski P. and Sacchi N. (1987). Single-step method of RNA isolation by acid guanidinium thiocyanate-phenol-chloroform extraction. *Anal Biochem* **162**: 156-159.

Chow M. K., Devlin G. L. and Bottomley S. P. (2001). Osmolytes as modulators of conformational changes in serpins. *Biol Chem* **382**: 1593-1599.

Chung S. S., Zhu L. J., Mo M. Y., Silvestrini B., Lee W. M. and Cheng C. Y. (1998). Evidence for cross-talk between Sertoli and germ cells using selected cathepsins as markers. *J Androl* **19**: 686-703.

Clem R. J., Fechheimer M. and Miller L. K. (1991). Prevention of apoptosis by a baculovirus gene during infection of insect cells. *Science* **254**: 1388-1390.

Clement M. V., Haddad P., Soulie A., Benvenuti C., Lichtenheld M. G., Podack E. R., Sigaux N. and Sasportes M. (1991). Perforin and granzyme B as markers for acute rejection in heart transplantation. *Int Immunol* **3**: 1175-1181.

Cohen S. B., Crawley J. B., Kahan M. C., Feldmann M. and Foxwell B. M. (1997). Interleukin-10 rescues T cells from apoptotic cell death: association with an upregulation of Bcl-2. *Immunology* **92**: 1-5.

Collins S. J. (1987). The HL-60 promyelocytic leukemia cell line: proliferation, differentiation, and cellular oncogene expression. *Blood* **70**: 1233-1244.

Cooley J., Takayama T. K., Shapiro S. D., Schechter N. M. and Remold-O'Donnell E. (2002). The serpin MNEI inhibits elastase-like and chymotrypsin-like serine proteases through efficient reactions at two active sites. *Biochemistry* **40**: 15762-15770.

Coughlin P., Nicholl J., Sun J., Salem H., Bird P. I. and Sutherland G. R. (1995). Chromosomal mapping of the human proteinase inhibitor 6 (PI6) gene to 6p25 by fluorescence in situ hybridization. *Genomics* **26**: 431-433.

Coughlin P. B., Sun J., Cerruti L., Salem H. H. and Bird P. I. (1993). Cloning and molecular characterization of a human intracellular serine proteinase inhibitor. *Proc Natl Acad Sci U S A* **90**: 9417-9421.

Criado M., Lindstrom J. M., Anderson C. G. and Dennert G. (1985). Cytotoxic granules from killer cells: specificity of granules and insertion of channels of defined size into target membranes. *J Immunol* **135**: 4245-4251.

Crook N. E., Clem R. J. and Miller L. K. (1993). An apoptosis-inhibiting baculovirus gene with a zinc finger-like motif. *J Virol* **67**: 2168-2174.

Dahlen J. R., Foster D. C. and Kisiel W. (1997). Human proteinase inhibitor 9 (PI9) is a potent inhibitor of subtilisin A. *Biochem Biophys Res Commun* **238**: 329-333.

Dahlen J. R., Foster D. C. and Kisiel W. (1998a). The inhibitory specificity of human proteinase inhibitor 8 is expanded through the use of multiple reactive site residues. *Biochem Biophys Res Commun* **244**: 172-177.

Dahlen J. R., Jean F., Thomas G., Foster D. C. and Kisiel W. (1998b). Inhibition of soluble recombinant furin by human proteinase inhibitor 8. *J Biol Chem* **273**: 1851-1854.

Dahlen J. R., Foster D. C. and Kisiel W. (1999). Inhibition of neutrophil elastase by recombinant human proteinase inhibitor 9. *Biochim Biophys Acta* **1451**: 233-241.

Darmon A. J., Nicholson D. W. and Bleackley R. C. (1995). Activation of the apoptotic protease CPP32 by cytotoxic T-cell-derived granzyme B. *Nature* **377**: 446-448.

Darmon A. J., Ley T. J., Nicholson D. W. and Bleackley R. C. (1996). Cleavage of CPP32 by granzyme B represents a critical role for granzyme B in the induction of target cell DNA fragmentation. *J Biol Chem* **271**: 21709-21712.

Davis J. E., Sutton V. R., Smyth M. J. and Trapani J. A. (2000). Dependence of granzyme B-mediated cell death on a pathway regulated by Bcl-2 or its viral homolog, BHRF1. *Cell Death Differ* 7: 973-983.

Davis R. L., Shrimpton A. E., Holohan P. D., Bradshaw C., Feiglin D., Collins G. H., Sonderegger P., Kinter J., Becker L. M., Lacbawan F., Krasnewich D., Muenke M., Lawrence D. A., Yerby M. S., Shaw C. M., Gooptu B., Elliott P. R., Finch J. T., Carrell R. W. and Lomas D. A. (1999). Familial dementia caused by polymerization of mutant neuroserpin. *Nature* **401**: 376-379.

Delon J. (2000). The immunological synapse. *Curr Biol* **10**: R214.

Deng W. P. and Nickoloff J. A. (1992). Site-directed mutagenesis of virtually any plasmid by eliminating a unique site. *Anal Biochem* **200**: 81-88.

Desagher S., Osen-Sand A., Montessuit S., Magnenat E., Vilbois F., Hochmann A., Journot L., Antonsson B. and Martinou J. C. (2001). Phosphorylation of bid by casein kinases I and II regulates its cleavage by caspase 8. *Mol Cell* **8**: 601-611.

Deveraux Q. L., Takahashi R., Salvesen G. S. and Reed J. C. (1997). X-linked IAP is a direct inhibitor of cell-death proteases. *Nature* **388**: 300-304.

Deveraux Q. L., Roy N., Stennicke H. R., Van Arsdale T., Zhou Q., Srinivasula S. M., Alnemri E. S., Salvesen G. S. and Reed J. C. (1998). IAPs block apoptotic events induced by caspase-8 and cytochrome c by direct inhibition of distinct caspases. *Embo J* **17**: 2215-2223.

Deveraux Q. L., Leo E., Stennicke H. R., Welsh K., Salvesen G. S. and Reed J. C. (1999). Cleavage of human inhibitor of apoptosis protein XIAP results in fragments with distinct specificities for caspases. *Embo J* **18**: 5242-5251.

Devlin G. L., Parfrey H., Tew D. J., Lomas D. A. and Bottomley S. P. (2001). Prevention of polymerization of M and Z alpha1-Antitrypsin (alpha1-AT) with trimethylamine N-oxide. Implications for the treatment of alpha1- at deficiency. *Am J Respir Cell Mol Biol* **24**: 727-732.

Dickinson J. L., Bates E. J., Ferrante A. and Antalis T. M. (1995). Plasminogen activator inhibitor type 2 inhibits tumor necrosis factor alpha-induced apoptosis. Evidence for an alternate biological function. *J Biol Chem* **270**: 27894-27904.

Dickinson J. L., Norris B. J., Jensen P. H. and Antalis T. M. (1998). The C-D interhelical domain of the serpin plasminogen activator inhibitor-type 2 is required for protection from TNFα induced apoptosis. *Cell Death Differ* **5**: 163-171.

Doolittle R. F. (1983). Angiotensinogen is related to the antitrypsin-antithrombin-ovalbumin family. *Science* **222**: 417-419.

Du C., Fang M., Li Y., Li L. and Wang X. (2000). Smac, a mitochondrial protein that promotes cytochrome c-dependent caspase activation by eliminating IAP inhibition. *Cell* **102**: 33-42.

Duan H., Orth K., Chinnaiyan A. M., Poirier G. G., Froelich C. J., He W. W. and Dixit V. M. (1996). ICE-LAP6, a novel member of the ICE/Ced-3 gene family, is activated by the cytotoxic T cell protease granzyme B. *J Biol Chem* **271**: 16720-16724.

Duan H. and Dixit V. M. (1997). RAIDD is a new 'death' adaptor molecule. *Nature* **385**: 86-89.

Dufourcq-Lagelouse R., Jabado N., Le Deist F., Stephan J. L., Souillet G., Bruin M., Vilmer E., Schneider M., Janka G., Fischer A. and de Saint Basile G. (1999). Linkage of familial hemophagocytic lymphohistiocytosis to 10q21-22 and evidence for heterogeneity. *Am J Hum Genet* **64**: 172-179.

Dunstone M. A., Dai W., Whisstock J. C., Rossjohn J., Pike R. N., Feil S. C., Le Bonniec B. F., Parker M. W. and Bottomley S. P. (2000). Cleaved antitrypsin polymers at atomic resolution. *Protein Sci* **9**: 417-420.

Dupuis M., Schaerer E., Krause K. H. and Tschopp J. (1993). The calcium-binding protein calreticulin is a major constituent of lytic granules in cytolytic T lymphocytes. *J Exp Med* **177**: 1-7.

Earnshaw W. C., Martins L. M. and Kaufmann S. H. (1999). Mammalian caspases: structure, activation, substrates, and functions during apoptosis. *Annu Rev Biochem* **68**: 383-424.

Ebnet K., Hausmann M., Lehmann-Grube F., Mullbacher A., Kopf M., Lamers M. and Simon M. M. (1995a). Granzyme A-deficient mice retain potent cell-mediated cytotoxicity. *Embo J* **14**: 4230-4239.

Ebnet K., Levelt C. N., Tran T. T., Eichmann K. and Simon M. M. (1995b). Transcription of granzyme A and B genes is differentially regulated during lymphoid ontogeny. *J Exp Med* **181**: 755-763.

Edwards K. M., Kam C. M., Powers J. C. and Trapani J. A. (1999). The human cytotoxic T cell granule serine protease granzyme H has chymotrypsin-like (chymase) activity and is taken up into cytoplasmic vesicles reminiscent of granzyme B-containing endosomes. *J Biol Chem* **274**: 30468-30473.

Ekert P. G., Silke J., Hawkins C. J., Verhagen A. M. and Vaux D. L. (2001). DIABLO promotes apoptosis by removing MIHA/XIAP from processed caspase 9. *J Cell Biol* **152**: 483-490.

Elliott P. R., Pei X. Y., Dafforn T. R. and Lomas D. A. (2000). Topography of a 2.0 A structure of alpha1-antitrypsin reveals targets for rational drug design to prevent conformational disease. *Protein Sci* **9**: 1274-1281.

Ellis H. M. and Horvitz H. R. (1986). Genetic control of programmed cell death in the nematode C. elegans. *Cell* **44**: 817-829.

Enari M., Sakahira H., Yokoyama H., Okawa K., Iwamatsu A. and Nagata S. (1998). A caspase-activated DNase that degrades DNA during apoptosis, and its inhibitor ICAD. *Nature* **391**: 43-50.

Engh R. A., Wright H. T. and Huber R. (1990). Modeling the intact form of the alpha 1-proteinase inhibitor. *Protein Eng* **3**: 469-477.

Evans E., Cooley J. and Remold-O'Donnell E. (1995). Characterization and cromosomal localization of ELANH2, the gene encoding human monocyte/neutrophil elastase inhibitor. *Genomics* **28**: 235-240.

Eyre H. J., Sun J., Sutherland G. R. and Bird P. I. (1996). Chromosomal mapping of the gene (PI9) encoding the intracellular serpin proteinase inhibitor 9 to 6p25 by fuorescence in situ hybridization. *Genomics* **37**: 406-408.

Faucheu C., Diu A., Chan A., Blanchet A., Miossec C., Herve F., Collard-Dutilleul V., Gu Y., Aldape R. and Lippke J. (1995). A novel human protease similar to the interleukin-1 beta converting enzyme induces apoptosis in transfected cells. *EMBO J.* **14**: 1914-1922.

Fernandes-Alnemri T., Armstrong R. C., Krebs J., Srinivasula S. M., Wang L., Bullrich F., Fritz L. C., Trapani J. A., Tomaselli K. J., Litwack G. and Alnemri E. S. (1996). In vitro activation of CPP32 and Mch3 by Mch4, a novel human apoptotic cysteine protease containing two FADD-like domains. *Proc Natl Acad Sci U S A* **93**: 7464-7469.

Fitton H. L., Pike R. N., Carrell R. W. and Chang W. S. (1997). Mechanisms of antithrombin polymerisation and heparin activation probed by the insertion of synthetic reactive loop peptides. *Biol Chem* **378**: 1059-1063.

Fraser S. A., Karimi R., Michalak M. and Hudig D. (2000). Perforin lytic activity is controlled by calreticulin. *J Immunol* **164**: 4150-4155.

Fritz I. B., Tung P. S. and Ailenberg M. (1993). Proteases and Antiproteases in the Seminiferous Tubule. The Sertoli Cell. L. D. Russell and M. D. Griswold. Clearwater, Cache River Press: 217-236.

Froelich C. J., Zhang X., Turbov J., Hudig D., Winkler U. and Hanna W. L. (1993). Human granzyme B degrades aggrecan proteoglycan in matrix synthesized by chondrocytes. *J Immunol* **151**: 7161-7171.

Froelich C. J., Hanna W. L., Poirier G. G., Duriez P. J., D'Amours D., Salvesen G. S., Alnemri E. S., Earnshaw W. C. and Shah G. M. (1996a). Granzyme B/perforin-mediated apoptosis of jurkat cells results in cleavage of poly(ADP-ribose) polymerase to the 89-kDa apoptotic fragment and less abundant 64-kDa fragment. *Biochem Biophys Res Comm* **227**: 658-665.

Froelich C. J., Orth K., Turbov J., Seth P., Gottlieb R., Babior B., Shah G. M., Bleackley R. C., Dixit V. M. and Hanna W. (1996b). New paradigm for lymphocyte granule-mediated cytotoxicity. Target cells bind and internalize granzyme B, but an endosomolytic agent is necessary for cytosolic delivery and subsequent apoptosis. *J Biol Chem* **271**: 29073-29079.

Fruth U., Prester M., Golecki J. R., Hengartner H., Simon H. G., Kramer M. D. and Simon M. M. (1987). The T cell-specific serine proteinase TSP-1 is associated with cytoplasmic granules of cytolytic T lymphocytes. *Eur J Immunol* **17**: 613-621.

Gahring L., Carlson N. G., Meyer E. L. and Rogers S. W. (2001). Granzyme B proteolysis of a neuronal glutamate receptor generates an autoantigen and is modulated by glycosylation. *J Immunol* **166**: 1433-1438.

Galvin J. P., Spaeny-Dekking L. H., Wang B., Seth P., Hack C. E. and Froelich C. J. (1999). Apoptosis induced by granzyme B-glycosaminoglycan complexes: implications for granule-mediated apoptosis in vivo. *J Immunol* **162**: 5345-5350.

Gan H., Newman G. W. and Remold H. G. (1995). Plasminogen activator inhibitor type 2 prevents programmed cell death of human macrophages infected with Mycobacterium avium, serovar 4. *J Immunol* **155**: 1304-1315.

Geiger B., Rosen D. and Berke G. (1982). Spatial relationships of microtubule-organizing centers and the contact area of cytotoxic T lymphocytes and target cells. *J Cell Biol* **95**: 137-143.

Geisberg M. and Dupont B. (1992). Cytolytic effector function is present in resting peripheral T lymphocytes. *Int Immunol* **4**: 1273-1281.

Gershenfeld H. K., Hershberger R. J., Shows T. B. and Weissman I. L. (1988). Cloning and chromosomal assignment of a human cDNA encoding a T cell- and natural killer cell-specific trypsin-like serine protease. *Proc Natl Acad Sci U S A* **85**: 1184-1188.

Geuze H. J., Slot J. W., Strous G. J., Hasilik A. and Von Figura K. (1984). Ultrastructural localization of the mannose 6-phosphate receptor in rat liver. *J Cell Biol* **98**: 2047-2054.

Geuze H. J., Slot J. W., Strous G. J., Hasilik A. and von Figura K. (1985). Possible pathways for lysosomal enzyme delivery. *J Cell Biol* **101**: 2253-2262.

Gluzman Y. (1981). SV-40-transformed simian cells support the replication of early SV40 mutants. *Cell* **23**: 175-182.

Grage-Griebenow E., Zawatzky R., Kahlert H., Brade L., Flad H. and Ernst M. (2001). Identification of a novel dendritic cell-like subset of $CD64^+$ / $CD16^+$ blood monocytes. *Eur J Immunol* **31**: 48-56.

Gray D. and Matzinger P. (1991). T cell memory is short-lived in the absence of antigen. *J Exp Med* **174**: 969-974.

Griffith T. S., Chin W. A., Jackson G. C., Lynch D. H. and Kubin M. Z. (1998). Intracellular regulation of TRAIL-induced apoptosis in human melanoma cells. *J Immunol* **161**: 2833-2840.

Griffiths G., Matteoni R., Back R. and Hoflack B. (1990). Characterization of the cation-independent mannose 6-phosphate receptor- enriched prelysosomal compartment in NRK cells. *J Cell Sci* **95**: 441-461.

Griffiths G. M. and Isaaz S. (1993). Granzymes A and B are targeted to the lytic granules of lymphocytes by the mannose-6-phosphate receptor. *J Cell Biol* **120**: 885-896.

Gross A., McDonnell J. M. and Korsmeyer S. J. (1999a). BCL-2 family members and the mitochondria in apoptosis. *Genes Dev* **13**: 1899-1911.

Gross A., Yin X. M., Wang K., Wei M. C., Jockel J., Milliman C., Erdjument-Bromage H., Tempst P. and Korsmeyer S. J. (1999b). Caspase cleaved BID targets mitochondria and is required for cytochrome c release, while BCL-XL prevents this release but not tumor necrosis factor-R1/Fas death. *J Biol Chem* **274**: 1156-1163.

Grouard G., de Bouteiller O., Banchereau J. and Liu Y. J. (1995). Human follicular dendritic cells enhance cytokine-dependent growth and differentiation of CD40-activated B cells. *J Immunol* **155**: 3345-3352.

Grouard G., Durand I., Filgueira L., Banchereau J. and Liu Y. J. (1996). Dendritic cells capable of stimulating T cells in germinal centres. *Nature* **384**: 364-367.

Gu Y., Sarnecki C., Fleming M. A., Lippke J. A., Bleackley R. C. and Su M. S. (1996). Processing and activation of CMH-1 by granzyme B. *J Biol Chem* **271**: 10816-10820.

Gunnarsson M., Lecander I. and Abrahamsson P. A. (1999). Factors of the plasminogen activator system in human testis, as demonstrated by in-situ hybridization and immunohistochemistry. *Mol Hum Reprod* **5**: 934-940.

Haddad P., Jenne D., Tschopp J., Clement M. V., Mathieu-Mahul D. and Sasportes M. (1991). Structure and evolutionary origin of the human granzyme H gene. *Int Immunol* **3**: 57-66.

Hameed A., Lowrey D. M., Lichtenheld M. and Podack E. R. (1988). Characterization of three serine esterases isolated from human IL-2 activated killer cells. *J Immunol* **141**: 3142-3147.

Hameed A., Truong L. D., Price V., Kruhenbuhl O. and Tschopp J. (1991). Immunohistochemical localization of granzyme B antigen in cytotoxic cells in human tissues. *Am J Pathol* **138**: 1069-1075.

Hansen M. H., Nielsen H. and Ditzel H. J. (2001). The tumor-infiltrating B cell response in medullary breast cancer is oligoclonal and directed against the autoantigen actin exposed on the surface of apoptotic cancer cells. *Proc Natl Acad Sci U S A* **98**: 12659-12664.

Harris J. L., Peterson E. P., Hudig D., Thornberry N. A. and Craik C. S. (1998). Definition and redesign of the extended substrate specificity of granzyme B. *J Biol Chem* **273**: 27364-27373.

Harvey N. L., Trapani J. A., Fernandes-Alnemri T., Litwack G., Alnemri E. S. and Kumar S. (1996). Processing of the Nedd2 precursor by ICE-like proteases and granzyme B. *Genes Cells* **1**: 673-685.

Hayes M. P., Berrebi G. A. and Henkart P. A. (1989). Induction of target cell DNA release by the cytotoxic T lymphocyte granule protease granzyme A. *J Exp Med* **170**: 933-946.

Heibein J. A., Barry M., Motyka B. and Bleackley R. C. (1999). Granzyme B-induced loss of mitochondrial inner membrane potential ($\Delta\Psi_m$) and cytochrome *c* release are caspase independent. *J Immunol* **163**: 4683-4693.

Heibein J. A., Goping I. S., Barry M., Pinkoski M. J., Shore G. C., Green D. R. and Bleackley R. C. (2000). Granzyme B-mediated cytochrome c release is regulated by the Bcl-2 family members Bid and Bax. *J Exp Med* **192**: 1391-1402.

Held W., MacDonald R. and Mueller C. (1990). Expression of genes encoding cytotoxic cell-associated serine proteases in thymocytes. *Inter Immunol* **2**: 57-62.

Hengartner M. O., Ellis R. E. and Horvitz H. R. (1992). Caenorhabditis elegans gene ced-9 protects cells from programmed cell death. *Nature* **356**: 494-499.

Henkart P., Henkart M., Millard P., Frederikse P., Bluestone J., Blumenthal R., Yue C. and Reynolds C. (1985). The role of cytoplasmic granules in cytotoxicity by large granular lymphocytes and cytotoxic T lymphocytes. *Adv Exp Med Biol* **184**: 121-138.

Henkart P. A., Millard P. J., Reynolds C. W. and Henkart M. P. (1984). Cytolytic activity of purified cytoplasmic granules from cytotoxic rat large granular lymphocyte tumors. *J Exp Med* **160**: 75-93.

Henkart P. A., Berrebi G. A., Takayama H., Munger W. E. and Sitkovsky M. V. (1987). Biochemical and functional properties of serine esterases in acidic cytoplasmic granules of cytotoxic T lymphocytes. *J Immunol* **139**: 2398-2405.

Henter J. I. and Elinder G. (1995). Haemophagocytic lymphohistiocytosis: an inherited primary form and a reactive secondary form. *Br J Haematol* **91**: 774-775.

Hermans I. F., Ritchie D. S., Yang J., Roberts J. M. and Ronchese F. (2000). CD8+ T cell-dependent elimination of dendritic cells in vivo limits the induction of antitumor immunity. *J Immunol* **164**: 3095-3101.

Heusel J. W., Wesselschmidt R. L., Shresta S., Russell J. H. and Ley T. J. (1994). Cytotoxic lymphocytes require granzyme B for the rapid induction of DNA fragmentation and apoptosis in allogeneic target cells. *Cell* **76**: 977-987.

Hildeman D. A., Mitchell T., Teague T. K., Henson P., Day B. J., Kappler J. and Marrack P. C. (1999). Reactive oxygen species regulate activation-induced T cell apoptosis. *Immunity* **10**: 735-744.

Hindmarsh E. J., Staykova M. A., Willenborg D. O. and Parish C. R. (2001). Cell surface expression of the 300 kDa mannose-6-phosphate receptor by activated T lymphocytes. *Immunol Cell Biol* **79**: 436-443.

Hirayoshi K., Kudo H., Takechi H., Nakai A., Iwamatsu A., Yamada K. M. and Nagata K. (1991). HSP47: a tissue-specific, transformation-sensitive, collagen-binding heat shock protein of chicken embryo fibroblasts. *Mol Cell Biol* **11**: 4036-4044.

Hirst C. E., Buzza M. S., Sutton V. R., Trapani J. A., Loveland K. L. and Bird P. I. (2001). Perforin-independent expression of granzyme B and proteinase inhibitor 9 in human testis and placenta suggests a role for granzyme B-mediated proteolysis in reproduction. *Mol Hum Reprod* **7**: 1133-1142.

Hooper J. D., Nicol D. L., Dickinson J. L., Eyre H. J., Scarman A. L., Normyle J. F., Stuttgen M. A., Douglas M. L., Loveland K. A., Sutherland G. R. and Antalis T. M. (1999). Testisin, a new human serine proteinase expressed by premeiotic testicular germ cells and lost in testicular germ cell tumors. *Cancer Res* **59**: 3199-3205.

Hopkins P. C., Chang W. S., Wardell M. R. and Stone S. R. (1997). Inhibitory mechanism of serpins. Mobility of the C-terminal region of the reactive-site loop. *J Biol Chem* **272**: 3905-3909.

Hsu H., Xiong J. and Goeddel D. V. (1995). The TNF receptor 1-associated protein TRADD signals cell death and NF- kappa B activation. *Cell* **81**: 495-504.

Hu S., Vincenz C., Ni J., Gentz R. and Dixit V. M. (1997). I-FLICE, a novel inhibitor of tumor necrosis factor receptor-1- and CD- 95-induced apoptosis. *J Biol Chem* **272**: 17255-17257.

Hu Z. Y., Liu Y. X., Liu K., Byrne S., Ny T., Feng Q. and Ockleford C. D. (1999). Expression of tissue type and urokinase type plasminogen activators as well as plasminogen activator inhibitor type-1 and type-2 in human and rhesus monkey placenta. *J Anat* **194**: 183-195.

Huang Y., Park Y. C., Rich R. L., Segal D., Myszka D. G. and Wu H. (2001). Structural basis of caspase inhibition by XIAP: differential roles of the linker versus the BIR domain. *Cell* **104**: 781-790.

Huntington J. A., Olson S. T., Fan B. and Gettins P. G. (1996). Mechanism of heparin activation of antithrombin. Evidence for reactive center loop preinsertion with expulsion upon heparin binding. *Biochemistry* **35**: 8495-8503.

Huntington J. A., Pannu N. S., Hazes B., Read R. J., Lomas D. A. and Carrell R. W. (1999). A 2.6 A structure of a serpin polymer and implications for conformational disease. *J Mol Biol* **293**: 449-455.

Huntington J. A., Read R. J. and Carrell R. W. (2000). Structure of a serpin-protease complex shows inhibition by deformation. *Nature* **407**: 923-926.

Irmler M., Hertig S., MacDonald H. R., Sadoul R., Becherer J. D., Proudfoot A., Solari R. and Tschopp J. (1995). Granzyme A is an interleukin 1 beta-converting enzyme. *J Exp Med* **181**: 1917-1922.

Irmler M., Thome M., Hahne M., Schneider P., Hofmann K., Steiner V., Bodmer J. L., Schroter M., Burns K., Mattmann C., Rimoldi D., French L. E. and Tschopp J. (1997). Inhibition of death receptor signals by cellular FLIP. *Nature* **388**: 190-195.

Irving J. A., Pike R. N., Lesk A. M. and Whisstock J. C. (2000). Phylogeny of the serpin superfamily: implications of patterns of amino acid conservation for structure and function. *Genome Res* **10**: 1845-1864.

Isaaz S., Baetz K., Olsen K., Podack E. and Griffiths G. M. (1995). Serial killing by cytotoxic T lymphocytes: T cell receptor triggers degranulation, re-filling of the lytic granules and secretion of lytic proteins via a non-granule pathway. *Eur J Immunol* **25**: 1071-1079.

Ito T., Inaba M., Inaba K., Toki J., Sogo S., Iguchi T., Adachi Y., Yamaguchi K., Amakawa R., Valladeau J., Saeland S., Fukuhara S. and Ikehara S. (1999). A $CD1a^+/CD11c^+$ subset of human blood dendritic cells is a direct precursor of Langerhans cells. *J Immunol* **163**: 1409-1419.

James E. L., Whisstock J. C., Gore M. G. and Bottomley S. P. (1999). Probing the unfolding pathway of alpha1-antitrypsin. *J Biol Chem* **274**: 9482-9488.

Jans D. A., Jans P., Briggs L. J., Sutton V. and Trapani J. A. (1996). Nuclear transport of granzyme B (fragmentin-2). Dependence of perforin in vivo and cytosolic factors in vitro. *J Biol Chem* **271**: 30781-30789.

Jans D. A., Sutton V. R., Jans P., Froelich C. J. and Trapani J. A. (1999). BCL-2 blocks perforin-induced nuclear translocation of granzymes concomitant with protection against the nuclear events of apoptosis. *J Biol Chem* **274**: 3953-3961.

Janssen O., Sanzenbacher R. and Kabelitz D. (2000). Regulation of activation-induced cell death of mature T-lymphocyte populations. *Cell Tissue Res* **301**: 85-99.

Jiang S. B., Ojcius D. M., Persechini P. M. and Young J. D. (1990a). Resistance of cytolytic lymphocytes to perforin-mediated killing. Inhibition of perforin binding activity by surface membrane proteins. *J Immunol* **144**: 998-1003.

Jiang S. B., Ojcius D. M. and Young J. D. (1990b). Perforin binding to cells and lipid membranes determined by a simple competition assay. *J Immunol Methods* **126**: 29-37.

Jin L., Abrahams J. P., Skinner R., Petitou M., Pike R. N. and Carrell R. W. (1997). The anticoagulant activation of antithrombin by heparin. *Proc Natl Acad Sci U S A* **94**: 14683-14688.

Joza N., Susin S. A., Daugas E., Stanford W. L., Cho S. K., Li C. Y., Sasaki T., Elia A. J., Cheng H. Y., Ravagnan L., Ferri K. F., Zamzami N., Wakeham A., Hakem R., Yoshida H., Kong Y. Y., Mak T. W., Zuniga-Pflucker J. C., Kroemer G. and Penninger J. M. (2001). Essential role of the mitochondrial apoptosis-inducing factor in programmed cell death. *Nature* **410**: 549-554.

Junqueira L.C., Carneiro J., Kelley R.O. Basic Histology. 8th edition. London : Prentice-Hall International, 1995.

Kadowaki N., Antonenko S., Lau J. Y. and Liu Y. J. (2000). Natural interferon alpha/beta-producing cells link innate and adaptive immunity. *J Exp Med* **192**: 219-226.

Kaiserman D., Knaggs S., Scarff K. L., Gillard A., Mirza G., Cadman M., McKeone R., Denny P., Cooley J., Benarafa C., Remold-O'Donnell E., Ragoussis J. and Bird P. I. (2002). Comparison of human chromosome 6p25 with murine chromosome 13 reveals a greatly expanded ov-serpin gene repertoire in the mouse. *Genomics* **in press**.

Kam C. M., Hudig D. and Powers J. C. (2000). Granzymes (lymphocyte serine proteases): characterization with natural and synthetic substrates and inhibitors. *Biochim Biophys Acta* **1477**: 307-323.

Kamada M. M., Michon J., Ritz J., Holldack J., Serafin W. E., Austen K. F., MacDermott R. P. and Stevens R. L. (1989). Identification of carboxypeptidase and tryptic esterase activities that are complexed to proteoglycans in the secretory granules of human cloned natural killer cells. *J Immunol* **142**: 609-615.

Kanamori H., Krieg S., Mao C., Di Pippo V. A., Wang S., Zajchowski D. A. and Shapiro D. J. (2000). Proteinase inhibitor 9, an inhibitor of granzyme B-mediated apoptosis, is a primary estrogen-inducible gene in human liver cells. *J Biol Chem* **275**: 5867-5873.

Kataoka T., Schroter M., Hahne M., Schneider P., Irmler M., Thome M., Froelich C. J. and Tschopp J. (1998). FLIP prevents apoptosis induced by death receptors but not by perforin/granzyme B, chemotherapeutic drugs, and gamma irradiation. *J Immunol* **161**: 3936-3942.

Kato H. and Torigoe T. (1977). Radioimmunoassay for tumor antigen of human cervical squamous cell carcinoma. *Cancer* **40**: 1621-1628.

Kato H., Miyauchi F., Morioka H., Fujino T. and Torigoe T. (1979). Tumor antigen of human cervical squamous cell carcinoma: correlation of circulating levels with disease progress. *Cancer* **43**: 585-590.

Kerr J. F., Wyllie A. H. and Currie A. R. (1972). Apoptosis: a basic biological phenomenon with wide-ranging implications in tissue kinetics. *Br J Cancer* **26**: 239-257.

Kirchhoff S., Muller W. W., Krueger A., Schmitz I. and Krammer P. H. (2000). TCR-mediated up-regulation of c-FLIPshort correlates with resistance toward CD95-mediated apoptosis by blocking death-inducing signaling complex activity. *J Immunol* **165**: 6293-6300.

Klein J. L., Selvakumar A., Trapani J. A. and Dupont B. (1990). Characterization of a novel, human cytotoxic lymphocyte-specific serine protease cDNA clone (CSP-C). *Tissue Antigens* **35**: 220-228.

Kohno N., Yamagata K., Yamada S., Kashiwabara S., Sakai Y. and Baba T. (1998). Two novel testicular serine proteases, TESP1 and TESP2, are present in the mouse sperm acrosome. *Biochem Biophys Res Commun* **245**: 658-665.

Komiyama T., Ray C. A., Pickup D. J., Howard A. D., Thornberry N. A., Peterson E. P. and Salvesen G. S. (1994). Inhibition of interleukin-1 beta converting enzyme by the cowpox virus serpin crmA. An example of cross-class inhibition. *J Biol Chem* **269**: 19331-19337.

Krahenbuhl O., Rey C., Jenne D., Lanzavecchia A., Groscurth P., Carrel S. and Tschopp J. (1988). Characterization of granzymes A and B isolated from granules of cloned human cytotoxic T lymphocytes. *J Immunol* **141**: 3471-3477.

Kranz D. M. and Eisen H. N. (1987). Resistance of cytotoxic T lymphocytes to lysis by a clone of cytotoxic T lymphocytes. *Proc Natl Acad Sci U S A* **84**: 3375-3379.

Krieg S. A., Krieg A. J. and Shapiro D. J. (2001). A Unique Downstream Estrogen Responsive Unit Mediates Estrogen Induction of Proteinase Inhibitor-9, a Cellular Inhibitor of IL-1beta- Converting Enzyme (Caspase 1). *Mol Endocrinol* **15**: 1971-1982.

Kuida K., Lippke J. A., Ku G., Harding M. W., Livingston D. J., Su M. S. and Flavell R. A. (1995). Altered cytokine export and apoptosis in mice deficient in interleukin- 1 beta converting enzyme. *Science* **267**: 2000-2003.

Kumar S. and Baglioni C. (1991). Protection from tumor necrosis factor-mediated cytolysis by overexpression of plasminogen activator inhibitor type 2. *J Biol Chem* **266**: 20960-20964.

Kummer J. A., Kamp A. M., van Katwijk M., Brakenhoff J. P., Radosevic K., van Leeuwen A. M., Borst J., Verweij C. L. and Hack C. E. (1993). Production and characterization of monoclonal antibodies raised against recombinant human granzymes A and B and showing cross reactions with the natural proteins. *J Immunol Methods* **163**: 77-83.

Kummer J. A., Kamp A. M., Tadema T. M., Vos W., Meijer C. J. and Hack C. E. (1995). Localization and identification of granzymes A and B-expressing cells in normal human lymphoid tissue and peripheral blood. *Clin Exp Immunol* **100**: 164-172.

Kupfer A. and Dennert G. (1984). Reorientation of the microtubule-organizing center and the Golgi apparatus in cloned cytotoxic lymphocytes triggered by binding to lysable target cells. *J Immunol* **133**: 2762-2766.

Lacroix M., Smith F. E. and Fritz I. B. (1977). Secretion of plasminogen activator by Sertoli cell enriched cultures. *Mol Cell Endocrinol* **9**: 227-236.

Lampelo S., Lalu K. and Vanha-Perttula T. (1987). Biochemical studies on dipeptidyl peptidases I to IV of the human placenta. *Placenta* **8**: 389-398.

Lauw F. N., Simpson A. J., Hack C. E., Prins J. M., Wolbink A. M., van Deventer S. J., Chaowagul W., White N. J. and van Der Poll T. (2000). Soluble granzymes are released during human endotoxemia and in patients with severe infection due to gram-negative bacteria. *J Infect Dis* **182**: 206-213.

Lawrence D. A., Ginsburg D., Day D. E., Berkenpas M. B., Verhamme I. M., Kvassman J. O. and Shore J. D. (1995). Serpin-protease complexes are trapped as stable acyl-enzyme intermediates. *J Biol Chem* **270**: 25309-25312.

Le Gouill C., Parent J. L., Rola-Pleszczynski M. and Stankova J. (1994). Analysis of recombinant plasmids by a modified alkaline lysis method. *Anal Biochem* **219**: 164.

Legros-Maida S., Soulie A., Benvenuti C., Wargnier A., Vallee N., Berthou C., Guillet J., Sasportes M. and Sigaux N. (1994). Granzyme B and perforin can be used as predictive markers of acute rejection in heart transplantation. *Eur J Immunol* **24**: 229-233.

Li H., Zhu H., Xu C. J. and Yuan J. (1998). Cleavage of BID by caspase 8 mediates the mitochondrial damage in the Fas pathway of apoptosis. *Cell* **94**: 491-501.

Li P., Allen H., Banerjee S., Franklin S., Herzog L., Johnston C., McDowell J., Paskind M., Rodman L., Salfeld J. and et al. (1995). Mice deficient in IL-1 beta-converting enzyme are defective in production of mature IL-1 beta and resistant to endotoxic shock. *Cell* **80**: 401-411.

Li P., Nijhawan D., Budihardjo I., Srinivasula S. M., Ahmad M., Alnemri E. S. and Wang X. (1997). Cytochrome c and dATP-dependent formation of Apaf-1/caspase-9 complex initiates an apoptotic protease cascade. *Cell* **91**: 479-489.

Lin C. C., Meier M., Sorensen O., Sasi R., Tainaka T. and Bleackley R. C. (1990). Chromosome localization of two human serine protease genes to region 14q11.2----q12 by in situ hybridization. *Cytogenet Cell Genet* **53**: 169-171.

Liu C. C., Rafii S., Granelli-Piperno A., Trapani J. A. and Young J. D. (1989). Perforin and serine esterase gene expression in stimulated human T cells. Kinetics, mitogen requirements, and effects of cyclosporin A. *J Exp Med* **170**: 2105-2118.

Liu X., Zou H., Slaughter C. and Wang X. (1997). DFF, a heterodimeric protein that functions downstream of caspase-3 to trigger DNA fragmentation during apoptosis. *Cell* **89**: 175-184.

Liu X., Li P., Widlak P., Zou H., Luo X., Garrard W. T. and Wang X. (1998). The 40-kDa subunit of DNA fragmentation factor induces DNA fragmentation and chromatin condensation during apoptosis. *Proc Natl Acad Sci U S A* **95**: 8461-8466.

Loebermann H., Tokuoka R., Deisenhofer J. and Huber R. (1984). Human alpha 1-proteinase inhibitor. Crystal structure analysis of two crystal modifications, molecular model and preliminary analysis of the implications for function. *J Mol Biol* **177**: 531-557.

Lomas D. A. and Carrell R. W. (1993). A protein structural approach to the solution of biological problems: alpha 1-antitrypsin as a recent example. *Am J Physiol* **265**: L211-219.

Lomas D. A., Elliott P. R., Chang W. S., Wardell M. R. and Carrell R. W. (1995). Preparation and characterization of latent α_1-antitrypsin. *J Biol Chem* **270**: 5282-5288.

Loyer V., Fontaine P., Pion S., Hetu F., Roy D. C. and Perreault C. (1999). The in vivo fate of APCs displaying minor H antigen and/or MHC differences is regulated by CTLs specific for immunodominant class I- associated epitopes. *J Immunol* **163**: 6462-6467.

Luciani M. F., Brunet J. F., Suzan M., Denizot F. and Golstein P. (1986). Self-sparing of long-term in vitro-cloned or uncloned cytotoxic T lymphocytes. *J Exp Med* **164**: 962-967.

Ludewig B., Bonilla W. V., Dumrese T., Odermatt B., Zinkernagel R. M. and Hengartner H. (2001). Perforin-independent regulation of dendritic cell homeostasis by $CD8^+$ T cells in vivo: implications for adaptive immunotherapy. *Eur J Immunol* **31**: 1772-1779.

Luo X., Budihardjo I., Zou H., Slaughter C. and Wang X. (1998). Bid, a Bcl2 interacting protein, mediates cytochrome c release from mitochondria in response to activation of cell surface death receptors. *Cell* **94**: 481-490.

Lyons-Giordano B., Loskutoff D., Chen C. S., Lazarus G., Keeton M. and Jensen P. J. (1994). Expression of plasminogen activator inhibitor type 2 in normal and psoriatic epidermis. *Histochemistry* **101**: 105-112.

MacDonald G., Shi L., Vande Velde C., Lieberman J. and Greenberg A. H. (1999). Mitochondria-dependent and -independent regulation of Granzyme B- induced apoptosis. *J Exp Med* **189**: 131-144.

MacIvor D. M., Pham C. T. and Ley T. J. (1999). The 5' flanking region of the human granzyme H gene directs expression to T/natural killer cell progenitors and lymphokine-activated killer cells in transgenic mice. *Blood* **93**: 963-973.

Maestri N. E., Hauser E. R., Bartholomew D. and Brusilow S. W. (1991). Prospective treatment of urea cycle disorders. *J Pediatr* **119**: 923-928.

Mahadeva R., Dafforn T. R., Carrell R. W. and Lomas D. A. (2001). Six-mer peptide selectively anneals to a pathogenic serpin conformation and blocks polymerisation: Implications for the prevention of Z alpha-1 antitrypsin related cirrhosis. *J Biol Chem* **28**: 28.

Martin S. J., Amarante-Mendes G. P., Shi L., Chuang T.-H., Casiano C. A., O'Brien G. A., Fitzgerald P., Tan E. M., Bokoch G. M., Greenberg A. H. and Green D. R. (1996). The cytotoxic cell protease granzyme B initiates apoptosis in a cell-free system by proteolytic processing and activation of the ICE/CED-3 family protease, CPP32, via a novel two-step mechanism. *EMBO J* **15**: 2407-2416.

Martinou I., Fernandez P. A., Missotten M., White E., Allet B., Sadoul R. and Martinou J. C. (1995). Viral proteins E1B19K and p35 protect sympathetic neurons from cell death induced by NGF deprivation. *J Cell Biol* **128**: 201-208.

Masson D., Peters P. J., Geuze H. J., Borst J. and Tschopp J. (1990). Interaction of chondroitin sulfate with perforin and granzymes of cytolytic T-cells is dependent on pH. *Biochemistry* **29**: 11229-11235.

Mast A. E., Enghild J. J. and Salvesen G. (1992). Conformation of the reactive site loop of α_1-proteinase inhibitor probed by limited proteolysis. *Biochemistry* **31**: 2720-2728.

McGettrick A. F., Barnes R. C. and Worrall D. M. (2001). SCCA2 inhibits TNF-mediated apoptosis in transfected HeLa cells. The reactive centre loop sequence is essential for this function and TNF- induced cathepsin G is a candidate target. *Eur J Biochem* **268**: 5868-5875.

Medema J. P., Toes R. E., Scaffidi C., Zheng T. S., Flavell R. A., Melief C. J., Peter M. E., Offringa R. and Krammer P. H. (1997). Cleavage of FLICE (caspase-8) by granzyme B during cytotoxic T lymphocyte-induced apoptosis. *Eur J Immunol* **27**: 3492-3498.

Medema J. P., de Jong J., van Hall T., Melief C. J. and Offringa R. (1999). Immune escape of tumors in vivo by expression of cellular FLICE- inhibitory protein. *J Exp Med* **190**: 1033-1038.

Medema J. P., de Jong J., Peltenburg L. T., Verdegaal E. M., Gorter A., Bres S. A., Franken K. L., Hahne M., Albar J. P., Melief C. J. and Offringa R. (2001a). Blockade of the granzyme B/perforin pathway through overexpression of the serine protease inhibitor PI-9/SPI-6 constitutes a mechanism for immune escape by tumors. *Proc Natl Acad Sci U S A* **98**: 11515-11520.

Medema J. P., Schuurhuis D. H., Rea D., van Tongeren J., de Jong J., Bres S. A., Laban S., Toes R. E., Toebes M., Schumacher T. N., Bladergroen B. A., Ossendorp F., Kummer J. A., Melief C. J. and Offringa R. (2001b). Expression of the serpin serine protease inhibitor 6 protects dendritic cells from cytotoxic T lymphocyte-induced apoptosis. Differential modulation by T helper type 1 and type 2 cells. *J Exp Med* **194**: 657-668.

Medley Q. G., Kedersha N., O'Brien S., Tian Q., Schlossman S. F., Streuli M. and Anderson P. (1996). Characterization of GMP-17, a granule membrane protein that moves to the plasma membrane of natural killer cells following target cell recognition. *Proc Natl Acad Sci U S A* **93**: 685-689.

Meehan T., Loveland K. L., de Kretser D., Cory S. and Print C. G. (2001). Developmental regulation of the bcl-2 family during spermatogenesis: Insights into the sterility of bcl-w-/- male mice. *Cell Death Differ* **8**: 225-233.

Mescher M. F. (1995). Molecular interactions in the activation of effector and precursor cytotoxic T lymphocytes. *Immunol Rev* **146**: 177-210.

Metkar S. S., Wang B., Aguilar-Santelises M., Raja S. M., Uhlin-Hansen L., Podack E., Trapani J. A. and Froelich C. J. (2002). Cytotoxic cell granule-mediated apoptosis: A multimeric delivery system where perforin delivers granzyme B-serglycin complexes without plasma membrane permeabilization. *Immunity*: in press.

Miura M., Zhu H., Rotello R., Hartwieg E. A. and Yuan J. (1993). Induction of apoptosis in fibroblasts by IL-1 beta-converting enzyme, a mammalian homolog of the C. elegans cell death gene ced-3. *Cell* **75**: 653-660.

Monks C. R., Freiberg B. A., Kupfer H., Sciaky N. and Kupfer A. (1998). Three-dimensional segregation of supramolecular activation clusters in T cells. *Nature* **395**: 82-86.

Mottonen J., Strand A., Symersky J., Sweet R. M., Danley D. E., Geoghegan K. F., Gerard R. D. and Goldsmith E. J. (1992). Structural basis of latency in plasminogen activator inhibitor-1. *Nature* **355**: 270-273.

Motyka B., Korbutt G., Pinkoski M. J., Heibein J. A., Caputo A., Hobman M., Barry M., Shostak I., Sawchuk T., Holmes C. F., Gauldie J. and Bleackley R. C. (2000). Mannose 6-phosphate/insulin-like growth factor II receptor is a death receptor for granzyme B during cytotoxic T cell-induced apoptosis. *Cell* **103**: 491-500.

Mullbacher A., Ebnet K., Blanden R. V., Hla R. T., Stehle T., Museteanu C. and Simon M. M. (1996). Granzyme A is critical for recovery of mice from infection with the natural cytopathic viral pathogen, ectromelia. *Proc Natl Acad Sci U S A* **93**: 5783-5787.

Munday N. A., Vaillancourt J. P., Ali A., Casano F. J., Miller D. K., Molineaux S. M., Yamin T. T., Yu V. L. and Nicholson D. W. (1995). Molecular cloning and pro-apoptotic activity of ICErelII and ICErelIII, members of the ICE/CED-3 family of cysteine proteases. *J Biol Chem* **270**: 15870-15876.

Muzio M., Chinnaiyan A. M., Kischkel F. C., O'Rourke K., Shevchenko A., Ni J., Scaffidi C., Bretz J. D., Zhang M., Gentz R., Mann M., Krammer P. H., Peter M. E. and Dixit V. M. (1996). FLICE, a novel FADD-homologous ICE/CED-3-like protease, is recruited to the CD95 (Fas/APO-1) death--inducing signaling complex. *Cell* **85**: 817-827.

Muzio M., Salvesen G. S. and Dixit V. M. (1997). FLICE induced apoptosis in a cell-free system. Cleavage of caspase zymogens. *J Biol Chem* **272**: 2952-2956.

Nagaraju K., Cox A., Casciola-Rosen L. and Rosen A. (2001). Novel fragments of the Sjogren's syndrome autoantigens alpha-fodrin and type 3 muscarinic acetylcholine receptor generated during cytotoxic lymphocyte granule-induced cell death. *Arthritis Rheum* **44**: 2376-2386.

Nakashima T., Pak S. C., Silverman G. A., Spring P. M., Frederick M. J. and Clayman G. L. (2000). Genomic cloning, mapping, structure and promoter analysis of *HEADPIN*, a serpin which is down-regulated in head and neck cancer cells. *Biochim Biophys Acta* **1492**: 441-446

Nordling K. and Bjork I. (1996). Identification of an epitope in antithrombin appearing on insertion of the reactive-bond loop into the A beta-sheet. *Biochemistry* **35**: 10436-10440.

Oehen S., Waldner H., Kundig T. M., Hengartner H. and Zinkernagel R. M. (1992). Antivirally protective cytotoxic T cell memory to lymphocytic choriomeningitis virus is governed by persisting antigen. *J Exp Med* **176**: 1273-1281.

Oehen S. and Brduscha-Riem K. (1998). Differentiation of naive CTL to effector and memory CTL: correlation of effector function with phenotype and cell division. *J Immunol* **161**: 5338-5346.

Ohadi M., Lalloz M. R., Sham P., Zhao J., Dearlove A. M., Shiach C., Kinsey S., Rhodes M. and Layton D. M. (1999). Localization of a gene for familial hemophagocytic lymphohistiocytosis at chromosome 9q21.3-22 by homozygosity mapping. *Am J Hum Genet* **64**: 165-171.

Ojcius D. M., Jiang S. B., Persechini P. M., Storch J. and Young J. D. (1990). Resistance to the pore-forming protein of cytotoxic T cells: comparison of target cell membrane rigidity. *Mol Immunol* **27**: 839-845.

Ojcius D. M., Muller S., Hasselkus-Light C. S., Young J. D. and Jiang S. (1991). Plasma membrane-associated proteins with the ability to partially inhibit perforin-mediated lysis. *Immunol Lett* **28**: 101-108.

Olweus J., BitMansour A., Warnke R., Thompson P. A., Carballido J., Picker L. J. and Lund-Johansen F. (1997). Dendritic cell ontogeny: a human dendritic cell lineage of myeloid origin. *Proc Natl Acad Sci U S A* **94**: 12551-12556.

Ooms L., Nicholl J., Bird P. and Sutherland G. R. (1995). Localization of the human monocyte/neutrophil elastase inhibitor gene to chromosome 6p25. *Chromosome Res* **3**: 447.

Opferman J. T., Ober B. T. and Ashton-Rickardt P. G. (1999). Linear differentiation of cytotoxic effectors into memory T lymphocytes. *Science* **283**: 1745-1748.

Opferman J. T., Ober B. T., Narayanan R. and Ashton-Rickardt P. G. (2001). Suicide induced by cytolytic activity controls the differentiation of memory CD8(+) T lymphocytes. *Int Immunol* **13**: 411-419.

Orth K., Chinnaiyan A. M., Garg M., Froelich C. J. and Dixit V. M. (1996). The CED-3/ICE-like protease Mch2 is activated during apoptosis and cleaves the death substrate lamin A. *J Biol Chem* **271**: 16443-16446.

Owen M. C., Brennan S. O., Lewis J. H. and Carrell R. W. (1983). Mutation of the antitrypsin to antithrombin. α_1-antitrypsin Pittsburgh (358 Met leads to Arg), a fatal bleeding disorder. *N Engl J Med* **309**: 694-698.

Page L. J., Darmon A. J., Uellner R. and Griffiths G. M. (1998). L is for lytic granules: lysosomes that kill. *Biochim Biophys Acta* **1401**: 146-156.

Pasternack M. S., Bleier K. J. and McInerney T. N. (1991). Granzyme A binding to target cell proteins. Granzyme A binds to and cleaves nucleolin in vitro. *J Biol Chem* **266**: 14703-14708.

Pemberton P. A., Stein P. E., Pepys M. B., Potter J. M. and Carrell R. W. (1988). Hormone binding globulins undergo serpin conformational change in inflammation. *Nature* **336**: 257-258.

Pena S. V. and Krensky A. M. (1997). Granulysin, a new human cytolytic granule-associated protein with possible involvement in cell-mediated cytotoxicity. *Semin Immunol* **9**: 117-125.

Pera M. F., Blasco Lafita M. J. and Mills J. (1987). Cultured stem cells from human testicular teratomas: the nature of human embryonal carcinoma and its comparison with two types of yolk-sac carcinoma. *Int J Cancer* **40**: 334-343.

Pera M. F., Blasco Lafita M. J., Cooper S., Mason M., Mills J. and Monoghan P. (1988). Analysis of cell-differentiation lineage in human teratomas using new monclonal antibodies to cytostructutral antigens of embryonal carcinoma cells. *Differentiation* **39**: 139-149.

Pera M. F., Cooper S., Mills J. and Parrington J. M. (1989). Isolation and characterization of a multipotent clone of human embryonal carcinoma cells. *Differentiation* **42**: 10-23.

Peters P. J., Geuze H. J., Van der Donk H. A., Slot J. W., Griffith J. M., Stam N. J., Clevers H. C. and Borst J. (1989). Molecules relevant for T cell-target cell interaction are present in cytolytic granules of human T lymphocytes. *Eur J Immunol* **19**: 1469-1475.

Peters P. J., Borst J., Oorschot V., Fukuda M., Krahenbuhl O., Tschopp J., Slot J. W. and Geuze H. J. (1991). Cytotoxic T lymphocyte granules are secretory lysosomes, containing both perforin and granzymes. *J Exp Med* **173**: 1099-1109.

Pham C. T., MacIvor D. M., Hug B. A., Heusel J. W. and Ley T. J. (1996). Long-range disruption of gene expression by a selectable marker cassette. *Proc Natl Acad Sci U S A* **93**: 13090-13095.

Pham C. T. and Ley T. J. (1999). Dipeptidyl peptidase I is required for the processing and activation of granzymes A and B in vivo. *Proc Natl Acad Sci U S A* **96**: 8627-8632.

Picard V., Marque P. E., Paolucci F., Aiach M. and Le Bonniec B. F. (1999). Topology of the stable serpin-protease complexes revealed by an autoantibody that fails to react with the monomeric conformers of antithrombin. *J Biol Chem* **274**: 4586-4593.

Pinkoski M. J., Winkler U., Hudig D. and Bleackley R. C. (1996). Binding of granzyme B in the nucleus of target cells. Recognition of an 80-kilodalton protein. *J Biol Chem* **271**: 10225-10229.

Pinkoski M. J., Hobman M., Heibein J. A., Tomaselli K., Li F., Seth P., Froelich C. J. and Bleackley R. C. (1998). Entry and trafficking of granzyme B in target cells during granzyme B- perforin-mediated apoptosis. *Blood* **92**: 1044-1054.

Pinkoski M. J., Heibein J. A., Barry M. and Bleackley R. C. (2000). Nuclear translocation of granzyme B in target cell apoptosis. *Cell Death Differ* **7**: 17-24.

Pinkoski M. J., Waterhouse N. J., Heibein J. A., Wolf B. B., Kuwana T., Goldstein J. C., Newmeyer D. D., Bleackley R. C. and Green D. R. (2001). Granzyme B-mediated apoptosis proceeds predominantly through a Bcl-2- inhibitable mitochondrial pathway. *J Biol Chem* **276**: 12060-12067.

Podack E. R., Lowrey D. M., Lichtenheld M. and Hameed A. (1988). Function of granule perforin and esterases in T cell-mediated reactions. Components required for delivery of molecules to target cells. *Ann N Y Acad Sci* **532**: 292-302.

Podack E. R. (1992). Perforin: structure, function, and regulation. *Curr Top Microbiol Immunol* **178**: 175-184.

Poe M., Bennett C. D., Biddison W. E., Blake J. T., Norton G. P., Rodkey J. A., Sigal N. H., Turner R. V., Wu J. K. and Zweerink H. J. (1988). Human cytotoxic lymphocyte tryptase. Its purification from granules and the characterization of inhibitor and substrate specificity. *J Biol Chem* **263**: 13215-13222.

Poe M., Blake J. T., Boulton D. A., Gammon M., Sigal N. H., Wu J. K. and Zweerink H. J. (1991). Human cytotoxic lymphocyte granzyme B. Its purification from granules and the characterization of substrate and inhibitor specificity. *J Biol Chem* **266**: 98-103.

Poorafshar M. and Hellman L. (1999). Cloning and structural analysis of leydin, a novel human serine protease expressed by the Leydig cells of the testis. *Eur J Biochem* **261**: 244-250.

Potempa J., Korzus E. and Travis J. (1994). The serpin superfamily of proteinase inhibitors: structure, function, and regulation. *J Biol Chem* **269**: 15957-15960.

Print C. G. and Loveland K. L. (2000). Germ cell suicide: new insights into apoptosis during spermatogenesis. *Bioessays* **22**: 423-430

Puthalakath H., Huang D. C., O'Reilly L. A., King S. M. and Strasser A. (1999). The proapoptotic activity of the Bcl-2 family member Bim is regulated by interaction with the dynein motor complex. *Mol Cell* **3**: 287-296.

Quan L. T., Caputo A., Bleackley R. C., Pickup D. J. and Salvesen G. S. (1995). Granzyme B is inhibited by the cowpox virus serpin cytokine response modifier A. *J Biol Chem* **270**: 10377-10379.

Quan L. T., Tewari M., O'Rourke K., Dixit V., Snipas S. J., Poirier G. G., Ray C., Pickup D. J. and Salvesen G. S. (1996). Proteolytic activation of the cell death protease Yama/CPP32 by granzyme B. *Proc Natl Acad Sci U S A* **93**: 1972-1976.

Rabizadeh S., LaCount D. J., Friesen P. D. and Bredesen D. E. (1993). Expression of the baculovirus p35 gene inhibits mammalian neural cell death. *J Neurochem* **61**: 2318-2321.

Rao N. V., Rao G. V. and Hoidal J. R. (1997). Human dipeptidyl-peptidase I. Gene characterization, localization, and expression. *J Biol Chem* **272**: 10260-10265.

Ray C. A., Black R. A., Kronheim S. R., Greenstreet T. A., Sleath P. R., Salvesen G. S. and Pickup D. J. (1992). Viral inhibition of inflammation: cowpox virus encodes an inhibitor of the interleukin-1 beta converting enzyme. *Cell* **69**: 597-604.

Remold-O'Donnell E., Nixon J. C. and Rose R. M. (1989). Elastase inhibitor: Characterization of the human elastase inhibitor molecule associated with monocytes, macrophages, and neutrophils. *J Exp Med* **169**: 1071-1086.

Remold-O'Donnell E. (1993). The ovalbumin family of serpin proteins. *FEBS Letters* **315**: 105-108.

Riedl S. J., Renatus M., Schwarzenbacher R., Zhou Q., Sun C., Fesik S. W., Liddington R. C. and Salvesen G. S. (2001). Structural basis for the inhibition of caspase-3 by XIAP. *Cell* **104**: 791-800.

Riewald M. and Schleef R. R. (1995). Molecular cloning of bomapin (protease inhibitor 10), a novel human serpin that is expressed specifically in the bone marrow. *J Biol Chem* **270**: 26754-26757.

Riewald M. and Schleef R. R. (1996). Human cytoplasmic antiproteinase neutralizes rapidly and efficiently chymotrypsin and trypsin-like proteases utilizing distinct reactive site residues. *J Biol Chem* **271**: 14526-14532.

Riewald M., Chuang T., Neubauer A., Riess H. and Schleef R. R. (1998). Expression of bomapin, a novel human serpin, in normal/malignant hematopoiesis and in the monocytic cell lines THP-1 and AML-193. *Blood* **91**: 1256-1262.

Riley S. C., Leask R., Denison F. C., Wisely K., Calder A. A. and Howe D. C. (1999). Secretion of tissue inhibitors of matrix metalloproteinases by human fetal membranes, decidua and placenta at parturition. *J Endocrinol* **162**: 351-359.

Ronday H. K., van der Laan W. H., Tak P. P., de Roos J. A., Bank R. A., TeKoppele J. M., Froelich C. J., Hack C. E., Hogendoorn P. C., Breedveld F. C. and Verheijen J. H. (2001). Human granzyme B mediates cartilage proteoglycan degradation and is expressed at the invasive front of the synovium in rheumatoid arthritis. *Rheumatology* **40**: 55-61.

Rothstein T. L., Mage M., Jones G. and McHugh L. L. (1978). Cytotoxic T lymphocyte sequential killing of immobilized allogeneic tumor target cells measured by time-lapse microcinematography. *J Immunol* **121**: 1652-1656.

Roy N., Deveraux Q. L., Takahashi R., Salvesen G. S. and Reed J. C. (1997). The c-IAP-1 and c-IAP-2 proteins are direct inhibitors of specific caspases. *Embo J* **16**: 6914-6925.

Sakahira H., Enari M. and Nagata S. (1998). Cleavage of CAD inhibitor in CAD activation and DNA degradation during apoptosis. *Nature* **391**: 96-99.

Salamonsen L. A. (1999). Role of proteases in implantation. *Rev Reprod* **4**: 11-22.

Sanchez-Torres C., Garcia-Romo G. S., Cornejo-Cortes M. A., Rivas-Carvalho A. and Sanchez-Schmitz G. (2001). $CD16^+$and $CD16^-$ human blood monocyte subsets differentiate in vitro to dendritic cells with different abilities to stimulate $CD4^+$ T cells. *Int Immunol* **13**: 1571-1581.

Sanderson C. J. (1976). The mechanism of T cell mediated cytotoxicity. II. Morphological studies of cell death by time-lapse microcinematography. *Proc R Soc Lond B Biol Sci* **192**: 241-255.

Sauer B. (1998). Inducible gene targeting in mice using the Cre/lox system. *Methods* **14**: 381-392.

Saunders D. N., Buttigieg K. M., Gould A., McPhun V. and Baker M. S. (1998). Immunological detection of conformational neoepitopes associated with the serpin activity of plasminogen activator inhibitor type-2. *J Biol Chem* **273**: 10965-10971.

Sayers T. J., Wiltrout T. A., Sowder R., Munger W. L., Smyth M. J. and Henderson L. E. (1992). Purification of a factor from the granules of a rat natural killer cell line (RNK) that reduces tumor cell growth and changes tumor morphology. Molecular identity with a granule serine protease (RNKP-1). *J Immunol* **148**: 292-300.

Sayers T. J., Lloyd A. R., McVicar D. W., O'Connor M. D., Kelly J. M., Carter C. R., Wiltrout T. A., Wiltrout R. H. and Smyth M. J. (1996). Cloning and expression of a second human natural killer cell granule tryptase, HNK-Tryp-2/granzyme 3. *J Leukoc Biol* **59**: 763-768.

Sayers T. J., Brooks A. D., Ward J. M., Hoshino T., Bere W. E., Wiegand G. W., Kelley J. M. and Smyth M. J. (2001). The restricted expression of granzyme M in human lymphocytes. *J Immunol* **166**: 765-771.

Schechter I. and Berger A. (1967). On the size of the active site in proteases I Papain. *Biochem Biophys Res Commun* **27**: 157-162.

Schick C., Kamachi Y., Bartuski A. J., Cataltepe S., Schechter N. M., Pemberton P. A. and Silverman G. A. (1997). Squamous cell carcinoma antigen 2 is a novel serpin that inhibits the chymotrypsin-like proteinases cathepsin G and mast cell chymase. *J Biol Chem* **272**: 1849-1855.

Schleef R. R. and Chuang T. L. (2000). Protease inhibitor 10 inhibits tumor necrosis factor alpha -induced cell death. Evidence for the formation of intracellular high M(r) protease inhibitor 10-containing complexes. *J Biol Chem* **275**: 26385-26389.

Schmitz I., Kirchhoff S. and Krammer P. H. (2000). Regulation of death receptor-mediated apoptosis pathways. *Int J Biochem Cell Biol* **32**: 1123-1136.

Schneider S. S., Schick C., Fish K. E., Miller E., Pena J. C., Treter S. D., Hui S. M. and Silverman G. A. (1995). A serine proteinase inhibitor locus at 18q21.3 contains a tandem duplication of the human squamous cell carcinoma antigen gene. *Proc Natl Acad Sci U S A* **92**: 3147-3151.

Schoenberger S. P., Toes R. E., van der Voort E. I., Offringa R. and Melief C. J. (1998). T-cell help for cytotoxic T lymphocytes is mediated by CD40-CD40L interactions. *Nature* **393**: 480-483.

Schreuder H. A., de Boer B., Dijkema R., Mulders J., Theunissen H. J. M., Grootenhuis P. D. J. and Hol W. G. J. (1994). The intact and cleaved human antithrombin III complex as a model for serpin-proteinase interactions. *Nat Struct Biol* **1**: 48-54.

Scott F. L., Coughlin P. B., Bird C., Cerruti L., Hayman J. A. and Bird P. (1996). Proteinase inhibitor 6 cannot be secreted, which suggests it is a new type of cellular serpin. *J Biol Chem* **271**: 1605-1612.

Scott F. L., Eyre H. J., Ooms L., Sun J., Bird P. I. and Sutherland G. R. (1997). Proteinase inhibitor 8 Map position 18q21.3. *Chromosome Res* **5**: 279.

Scott F. L., Paddle-Ledinek J. E., Cerruti L., Coughlin P. B., Salem H. H. and Bird P. I. (1998). Proteinase inhibitor 6 (PI-6) expression in human skin: induction of PI-6 and a PI-6/proteinase complex during keratinocyte differentiation. *Exp Cell Res* **245**: 263-271.

Scott F. L., Eyre H. J., Lioumi M., Ragoussis J., Irving J. A., Sutherland G. R. and Bird P. I. (1999a). Human ovalbumin serpin evolution: Phylogenetic analysis, gene organization, and identification of new *PI8*-related genes suggest that two interchromosomal and several intrachromosomal duplications generated the gene clusters at 18q21.3-q23 and 6p25. *Genomics* **62**: 490-499.

Scott F. L., Hirst C. E., Sun J., Bird C. H., Bottomley S. P. and Bird P. I. (1999b). The intracellular serpin proteinase inhibitor 6 is expressed in monocytes and granulocytes and is a potent inhibitor of the azurophilic granule protease, cathepsin G. *Blood* **93**: 2089-2097.

Shapiro S. D., Campbell E. J., Welgus H. G. and Senior R. M. (1991). Elastin degradation by mononuclear phagocytes. *Ann N Y Acad Sci* **624**: 69-80.

Sharif-Askari E., Alam A., Rheaume E., Beresford P. J., Scotto C., Sharma K., Lee D., DeWolf W. E., Nuttall M. E., Lieberman J. and Sekaly R. P. (2001). Direct cleavage of the human DNA fragmentation factor-45 by granzyme B induces caspase-activated DNase release and DNA fragmentation. *Embo J* **20**: 3101-3113.

Shi L., Kam C. M., Powers J. C., Aebersold R. and Greenberg A. H. (1992). Purification of three cytotoxic lymphocyte granule serine proteases that induce apoptosis through distinct substrate and target cell interactions. *J Exp Med* **176**: 1521-1529.

Shi L., Chen G., MacDonald G., Bergeron L., Li H., Miura M., Rotello R. J., Miller D. K., Li P., Seshadri T., Yuan J. and Greenberg A. H. (1996). Activation of an interleukin 1 converting enzyme-dependent apoptosis pathway by granzyme B. *Proc Natl Acad Sci U S A* **93**: 11002-11007.

Shi L., Mai S., Israels S., Browne K., Trapani J. A. and Greenberg A. H. (1997). Granzyme B (GraB) autonomously crosses the cell membrane and perforin initiates apoptosis and GraB nuclear localization. *J Exp Med* **185**: 855-866.

Shi Y. (2001). A structural view of mitochondria-mediated apoptosis. *Nat Struct Biol* **8**: 394-401.

Shiner M., Eran M., Freier S., Faber J. and Branski D. (1998). Are intraepithelial lymphocytes in celiac mucosa responsible for inducing programmed cell death (apoptosis) in enterocytes? Histochemical demonstration of perforins in cytoplasmic granules of intraepithelial lymphocytes. *J Pediatr Gastroenterol Nutr* **27**: 393-396.

Shiver J. W., Su L. and Henkart P. A. (1992). Cytotoxicity with target DNA breakdown by rat basophilic leukemia cells expressing both cytolysin and granzyme A. *Cell* **71**: 315-322.

Siegal F. P., Kadowaki N., Shodell M., Fitzgerald-Bocarsly P. A., Shah K., Ho S., Antonenko S. and Liu Y. J. (1999). The nature of the principal type 1 interferon-producing cells in human blood. *Science* **284**: 1835-1837.

Silverman G. A., Bird P. I., Carrell R. W., Church F. C., Coughlin P. B., Gettins P. G., Irving J. A., Lomas D. A., Luke C. J., Moyer R. W., Pemberton P. A., Remold-O'Donnell E., Salvesen G. S., Travis J. and Whisstock J. C. (2001). The serpins are an expanding superfamily of structurally similar but functionally diverse proteins. Evolution, mechanism of inhibition, novel functions, and a revised nomenclature. *J Biol Chem* **276**: 33293-33296.

Sivasothy P., Dafforn T. R., Gettins P. G. and Lomas D. A. (2000). Pathogenic alpha 1-antitrypsin polymers are formed by reactive loop- beta-sheet A linkage. *J Biol Chem* **275**: 33663-33668.

Skinner M. and Marbrook J. (1987). The most efficient cytotoxic T lymphocytes are the least susceptible to lysis. *J Immunol* **139**: 985-987.

Skinner R., Abrahams J. P., Whisstock J. C., Lesk A. M., Carrell R. W. and Wardell M. R. (1997). The 2.6 A structure of antithrombin indicates a conformational change at the heparin binding site. *J Mol Biol* **266**: 601-609.

Skinner R., Chang W. S., Jin L., Pei X., Huntington J. A., Abrahams J. P., Carrell R. W. and Lomas D. A. (1998). Implications for function and therapy of a 2.9 A structure of binary-complexed antithrombin. *J Mol Biol* **283**: 9-14.

Skriver K., Wikoff W. R., Patston P. A., Tausk F., Schapira M., Kaplan A. P. and Bock S. C. (1991). Substrate properties of C1 inhibitor Ma (alanine 434----glutamic acid). Genetic and structural evidence suggesting that the P12-region contains critical determinants of serine protease inhibitor/substrate status. *J Biol Chem* **266**: 9216-9221.

Smokovitis A., Kokolis N., Taitzoglou I. and Rekkas C. (1992). Plasminogen activator: the identification of an additional proteinase at the outer acrosomal membrane of human and boar spermatozoa. *Int J Fertil* **37**: 308-314.

Smyth M. J., Browne K. A., Kinnear B. F., Trapani J. A. and Warren H. S. (1995a). Distinct granzyme expression in human CD3- CD56+ large granular- and CD3- CD56+ small high density-lymphocytes displaying non-MHC-restricted cytolytic activity. *J Leukoc Biol* **57**: 88-93.

Smyth M. J., O'Connor M. D., Kelly J. M., Ganesvaran P., Thia K. Y. and Trapani J. A. (1995b). Expression of recombinant human Met-ase-1: a NK cell-specific granzyme. *Biochem Biophys Res Commun* **217**: 675-683.

Smyth M. J., O'Connor M. D., Trapani J. A., Kershaw M. H. and Brinkworth R. I. (1996). A novel substrate-binding pocket interaction restricts the specificity of the human NK cell-specific serine protease, Met-ase-1. *J Immunol* **156**: 4174-4181.

Smyth M. J., Kelly J. M., Sutton V. R., Davis J. E., Browne K. A., Sayers T. J. and Trapani J. A. (2001). Unlocking the secrets of cytotoxic granule proteins. *J Leukoc Biol* **70**: 18-29.

Sower L. E., Froelich C. J., Allegretto N., Rose P. M., Hanna W. D. and Klimpel G. R. (1996a). Extracellular activities of human granzyme A. Monocyte activation by granzyme A versus alpha-thrombin. *J Immunol* **156**: 2585-2590.

Sower L. E., Klimpel G. R., Hanna W. and Froelich C. J. (1996b). Extracellular activities of human granzymes. I. Granzyme A induces IL6 and IL8 production in fibroblast and epithelial cell lines. *Cell Immunol* **171**: 159-163.

Spaeny-Dekking E. H., Hanna W. L., Wolbink A. M., Wever P. C., Kummer A. J., Swaak A. J., Middeldorp J. M., Huisman H. G., Froelich C. J. and Hack C. E. (1998). Extracellular granzymes A and B in humans: detection of native species during CTL responses in vitro and in vivo. *J Immunol* **160**: 3610-3616.

Spaeny-Dekking E. H., Kamp A. M., Froelich C. J. and Hack C. E. (2000). Extracellular granzyme A, complexed to proteoglycans, is protected against inactivation by protease inhibitors. *Blood* **95**: 1465-1472.

Spaner D., Raju K., Radvanyi L., Lin Y. and Miller R. G. (1998). A role for perforin in activation-induced cell death. *J Immunol* **160**: 2655-2664.

Sprecher C. A., Morgenstern K. A., Mathewes S., Dahlen J. R., Schrader S. K., Foster D. C. and Kisiel W. (1995). Molecular cloning, expression, and partial characterization of two novel members of the ovalbumin family of serine proteinase inhibitors. *J Biol Chem* **270**: 29854-29861.

Spring P., Nakashima T., Frederick M., Henderson Y. and Clayman G. (1999). Identification and cloning of headpin, a novel differentially expressed serpin that maps to chromosome 18q. *Biochem Biophys Res Commun* **264**: 299-304.

Srinivasula S. M., Ahmad M., Fernandes-Alnemri T., Litwack G. and Alnemri E. S. (1996a). Molecular ordering of the Fas-apoptotic pathway: the Fas/APO-1 protease Mch5 is a CrmA-inhibitable protease that activates multiple Ced-3/ICE- like cysteine proteases. *Proc Natl Acad Sci U S A* **93**: 14486-14491.

Srinivasula S. M., Fernandes-Alnemri T., Zangrilli J., Robertson N., Armstrong R. C., Wang L., Trapani J. A., Tomaselli K. J., Litwack G. and Alnemri E. S. (1996b). The Ced-3/interleukin 1beta converting enzyme-like homolog Mch6 and the lamin-cleaving enzyme Mch2alpha are substrates for the apoptotic mediator CPP32. *J Biol Chem* **271**: 27099-27106.

Srinivasula S. M., Hegde R., Saleh A., Datta P., Shiozaki E., Chai J., Lee R. A., Robbins P. D., Fernandes-Alnemri T., Shi Y. and Alnemri E. S. (2001). A conserved XIAP-interaction motif in caspase-9 and Smac/DIABLO regulates caspase activity and apoptosis. *Nature* **410**: 112-116.

Stein P. E., Leslie A. G. W., Finch J. T., Turnell W. G., McLaughlin P. J. and Carrell R. W. (1990). Crystal structure of ovalbumin as a model for the reactive centre of serpins. *Nature* **347**: 99-102.

Stein P. E. and Chothia C. (1991). Serpin tertiary structure transformation. *J Mol Biol* **221**: 615-621.

Stein P. E. and Carrell R. W. (1995). What do dysfunctional serpins tell us about molecular mobility and disease? *Nat Struct Biol* **2**: 96-113.

Steiner D. F. (1998). The proprotein convertases. *Curr Opin Chem Biol* **2**: 31-39.

Stennicke H. R., Jurgensmeier J. M., Shin H., Deveraux Q., Wolf B. B., Yang X., Zhou Q., Ellerby H. M., Ellerby L. M., Bredesen D., Green D. R., Reed J. C., Froelich C. J. and Salvesen G. S. (1998). Pro-caspase-3 is a major physiologic target of caspase-8. *J Biol Chem* **273**: 27084-27090.

Stennicke H. R. and Salvesen G. S. (1999). Catalytic properties of the caspases. *Cell Death Differ* **6**: 1054-1059.

Stennicke H. R., Ryan C. A. and Salvesen G. S. (2002). Reprieval from execution: The molecular basis of caspase inhibition. *Trends Biochem Sci* (in press).

Stepp S. E., Dufourcq-Lagelouse R., Le Deist F., Bhawan S., Certain S., Mathew P. A., Henter J. I., Bennett M., Fischer A., de Saint Basile G. and Kumar V. (1999). Perforin gene defects in familial hemophagocytic lymphohistiocytosis. *Science* **286**: 1957-1959.

Stinchcombe J. C., Bossi G., Booth S. and Griffiths G. M. (2001). The Immunological Synapse of CTL Contains a Secretory Domain and Membrane Bridges. *Immunity* **15**: 751-761.

Stinchcombe J. C. and Griffiths G. M. (2001). Normal and abnormal secretion by haemopoietic cells. *Immunology* **103**: 10-16.

Stratikos E. and Gettins P. G. (1999). Formation of the covalent serpin-proteinase complex involves translocation of the proteinase by more than 70 A and full insertion of the reactive center loop into beta-sheet A. *Proc Natl Acad Sci U S A* **96**: 4808-4813.

Su B., Bochan M. R., Hanna W. L., Froelich C. J. and Brahmi Z. (1994). Human granzyme B is essential for DNA fragmentation of susceptible target cells. *Eur J Immunol* **24**: 2073-2080.

Sugimori T., Cooley J., Hoidal J. R. and Remold-O'Donnell E. (1995). Inhibitory properties of recombinant monocyte/neutrophil elastase inhibitor. *Am J Respir Cell Mol Biol* **13**: 314-322.

Suidan H. S., Bouvier J., Schaerer E., Stone S. R., Monard D. and Tschopp J. (1994). Granzyme A released upon stimulation of cytotoxic T lymphocytes activates the thrombin receptor on neuronal cells and astrocytes. *Proc Natl Acad Sci U S A* **91**: 8112-8116.

Suidan H. S., Clemetson K. J., Brown-Luedi M., Niclou S. P., Clemetson J. M., Tschopp J. and Monard D. (1996). The serine protease granzyme A does not induce platelet aggregation but inhibits responses triggered by thrombin. *Biochem J* **315**: 939-945.

Suminami Y., Nagashima S., Vujanovic N. L., Hirabayashi K., Kato H. and Whiteside T. L. (2000). Inhibition of apoptosis in human tumour cells by the tumour-associated serpin, SCC antigen-1. *Br J Cancer* **82**: 981-989.

Summers K. L., Hoch B. D., McKenzie J. L. and Hart D. N. J. (2001). Phenotypic characterization of five dendritic cell subsets in human tonsils. *Am J Pathol* **159**: 285-295.

Sun J., Coughlin P., Salem H. H. and Bird P. (1995). Production and characterization of recombinant human proteinase inhibitor 6 expressed in Pichia pastoris. *Biochim Biophys Acta* **1252**: 28-34.

Sun J., Bird C. H., Sutton V., McDonald L., Coughlin P. B., De Jong T. A., Trapani J. A. and Bird P. I. (1996). A cytosolic granzyme B inhibitor related to the viral apoptotic regulator cytokine response modifier A is present in cytotoxic lymphocytes. *J Biol Chem* **271**: 27802-27809.

Sun J., Ooms L., Bird C. H., Sutton V. R., Trapani J. A. and Bird P. I. (1997). A new family of 10 murine ovalbumin serpins includes two homologs of proteinase inhibitor 8 and two homologs of the granzyme B inhibitor (proteinase inhibitor 9). *J Biol Chem* **272**: 15434-15441.

Sun J., Stephens R., Mirza G., Kanai H., Ragoussis J. and Bird P. I. (1998). A serpin gene cluster on human chromosome 6p25 contains PI6, PI9 and ELANH2 which have a common structure almost identical to the 18q21 ovalbumin serpin genes. *Cytogenet Cell Genet* **82**: 273-277.

Sun J., Bird C. H., Buzza M. S., McKee K. E., Whisstock J. C. and Bird P. I. (1999). Expression and purification of recombinant human granzyme B from Pichia pastoris. *Biochem Biophys Res Commun* **261**: 251-255.

Sun J., Whisstock J. C., Harriott P., Walker B., Novak A., Thompson P. E., Smith A. I. and Bird P. I. (2001). Importance of the P4' residue in human granzyme B inhibitors and substrates revealed by scanning mutagenesis of the PI-9 reactive center loop. *J Biol Chem* **276**: 15177-15184.

Susin S. A., Zamzami N., Castedo M., Hirsch T., Marchetti P., Macho A., Daugas E., Geuskens M. and Kroemer G. (1996). Bcl-2 inhibits the mitochondrial release of an apoptogenic protease. *J Exp Med* **184**: 1331-1341.

Susin S. A., Lorenzo H. K., Zamzami N., Marzo I., Snow B. E., Brothers G. M., Mangion J., Jacotot E., Costantini P., Loeffler M., Larochette N., Goodlett D. R., Aebersold R., Siderovski D. P., Penninger J. M. and Kroemer G. (1999). Molecular characterization of mitochondrial apoptosis-inducing factor. *Nature* **397**: 441-446.

Susskind B., Shornick M. D., Iannotti M. R., Duffy B., Mehrotra P. T., Siegel J. P. and Mohanakumar T. (1996). Cytolytic effector mechanisms of human CD4+ cytotoxic T lymphocytes. *Hum Immunol* **45**: 64-75.

Suthanthiran M. and Strom T. B. (1998). Mechanisms and management of acute renal allograft rejection. *Surg Clin North Am* **78**: 77-94.

Sutton V. R., Davis J. E., Cancilla M., Johnstone R. W., Ruefli A. A., Sedelies K., Browne K. A. and Trapani J. A. (2000). Initiation of apoptosis by granzyme B requires direct cleavage of Bid, but not direct granzyme B-mediated caspase activation. *J Exp Med* **192**: 1403-1414.

Tak P. P., Spaeny-Dekking L., Kraan M. C., Breedveld F. C., Froelich C. J. and Hack C. E. (1999). The levels of soluble granzyme A and B are elevated in plasma and synovial fluid of patients with rheumatoid arthritis (RA). *Clin Exp Immunol* **116**: 366-370.

Takai Y., Masuko T. and Takeuchi H. (1997). Lipid structure of cytotoxic granules in living human killer T lymphocytes studied by Raman microspectroscopy. *Biochim Biophys Acta* **1335**: 199-208.

Talanian R. V., Yang X. H., Turbov J., Seth P., Ghayur T., Casiano C. A., Orth K. and Froelich C. J. (1997). Granule-mediated killing: Pathways for granzyme B-initiated apoptosis. *J Exp Med* **186**: 1323-1331.

Thomas D. A., Du C., Xu M., Wang X. and Ley T. J. (2000). DFF45/ICAD can be directly processed by granzyme B during the induction of apoptosis. *Immunity* **12**: 621-632.

Thomas D. A., Scorrano L., Putcha G. V., Korsmeyer S. J. and Ley T. J. (2001). Granzyme B can cause mitochondrial depolarization and cell death in the absence of BID, BAX, and BAK. *Proc Natl Acad Sci U S A* **98**: 14985-14990.

Thome M., Schneider P., Hofmann K., Fickenscher H., Meinl E., Neipel F., Mattmann C., Burns K., Bodmer J. L., Schroter M., Scaffidi C., Krammer P. H., Peter M. E. and Tschopp J. (1997). Viral FLICE-inhibitory proteins (FLIPs) prevent apoptosis induced by death receptors. *Nature* **386**: 517-521.

Thornberry N. A., Rano T. A., Peterson E. P., Rasper D. M., Timkey T., Garcia-Calvo M., Houtzager V. M., Nordstrom P. A., Roy S., Vaillancourt J. P., Chapman K. T. and Nicholson D. W. (1997). A combinatorial approach defines specificities of members of the caspase family and granzyme B. *J Biol Chem* **272**: 17907-17911.

Thornberry N. A., Chapman K. T. and Nicholson D. W. (2000). Determination of caspase specificities using a peptide combinatorial library. *Methods Enzymol* **322**: 100-110.

Trapani J. A., Klein J. L., White P. C. and Dupont B. (1988). Molecular cloning of an inducible serine esterase gene from human cytotoxic lymphocytes. *Proc Natl Acad Sci U S A* **85**: 6924-6928.

Trapani J. A., Browne K. A., Dawson M. and Smyth M. J. (1993). Immunopurification of functional Asp-ase (natural killer cell granzyme B) using a monoclonal antibody. *Biochem Biophys Res Commun* **195**: 910-920.

Trapani J. A., Smyth M. J., Apostolidis V. A., Dawson M. and Browne K. A. (1994). Granule serine proteases are normal nuclear constituents of natural killer cells. *J Biol Chem* **269**: 18359-18365.

Trapani J. A., Jans D. A., Jans P. J., Smyth M. J., Browne K. A. and Sutton V. R. (1998a). Efficient nuclear targeting of granzyme B and the nuclear consequences of apoptosis induced by granzyme B and perforin are caspase-dependent, but cell death is caspase-independent. *J Biol Chem* **273**: 27934-27938.

Trapani J. A., Jans P., Smyth M. J., Froelich C. J., Williams E. A., Sutton V. R. and Jans D. A. (1998b). Perforin-dependent nuclear entry of granzyme B precedes apoptosis, and is not a consequence of nuclear membrane dysfunction. *Cell Death Differ* **5**: 488-496.

Trapani J. A. and Jans D. A. (1999). Lymphocyte-mediated cytolysis: dual apoptotic mechanisms with overlapping cytoplasmic and nuclear signalling pathways. *Results Probl Cell Differ* **23**: 78-102.

Travis J. and Salvesen G. S. (1983). Human plasma proteinase inhibitors. *Annu Rev Biochem* **52**: 655-709.

Tremblay G. M., Wolbink A. M., Cormier Y. and Hack C. E. (2000). Granzyme activity in the inflamed lung is not controlled by endogenous serine proteinase inhibitors. *J Immunol* **165**: 3966-3969.

Trevani A. S., Andonegui G., Giordano M., Nociari M., Fontan P., Dran G. and Geffner J. R. (1996). Neutrophil apoptosis induced by proteolytic enzymes. *Lab Invest* **74**: 711-721.

Tsatas D., Baker M. S., Moses E. K. and Rice G. E. (1998). Gene expression of plasminogen activation cascade components in human term gestational tissues with labour onset. *Mol Hum Reprod* **4**: 101-106.

Uellner R., Zvelebil M. J., Hopkins J., Jones J., MacDougall L. K., Morgan B. P., Podack E., Waterfield M. D. and Griffiths G. M. (1997). Perforin is activated by a proteolytic cleavage during biosynthesis which reveals a phospholipid-binding C2 domain. *Embo J* **16**: 7287-7296.

van Boeckel C. A., Grootenhuis P. D. and Visser A. (1994). A mechanism for heparin-induced potentiation of antithrombin III. *Nat Struct Biol* **1**: 423-425.

Van de Craen M., Van den Brande I., Declercq W., Irmler M., Beyaert R., Tschopp J., Fiers W. and Vandenabeele P. (1997). Cleavage of caspase family members by granzyme B: a comparative study in vitro. *Eur J Immunol* **27**: 1296-1299.

Vandenabeele S., Hochrein H., Mavaddat N., Winkel K. and Shortman K. (2001). Human thymus contains 2 distinct dendritic cell populations. *Blood* **97**: 1733-1741.

Venkatachalam K. V., Huang W., LaRocco M. and Palzkill T. (1994). Characterization of TEM-1 beta-lactamase mutants from positions 238 to 241 with increased catalytic efficiency for ceftazidime. *J Biol Chem* **269**: 23444-23450.

Verhagen A. M., Ekert P. G., Pakusch M., Silke J., Connolly L. M., Reid G. E., Moritz R. L., Simpson R. J. and Vaux D. L. (2000). Identification of DIABLO, a mammalian protein that promotes apoptosis by binding to and antagonizing IAP proteins. *Cell* **102**: 43-53.

Verma S., Zhao L. J. and Chinnadurai G. (2001). Phosphorylation of the pro-apoptotic protein BIK: mapping of phosphorylation sites and effect on apoptosis. *J Biol Chem* **276**: 4671-4676.

Verret C. R., Firmenich A. A., Kranz D. M. and Eisen H. N. (1987). Resistance of cytotoxic T lymphocytes to the lytic effects of their toxic granules. *J Exp Med* **166**: 1536-1547.

Vincenz C. and Dixit V. M. (1997). Fas-associated death domain protein interleukin-1beta-converting enzyme 2 (FLICE2), an ICE/Ced-3 homologue, is proximally involved in CD95- and p55-mediated death signaling. *J Biol Chem* **272**: 6578-6583.

Wang S., Miura M., Jung Y., Zhu H., Gagliardini V., Shi L., Greenberg A. H. and Yuan J. (1996). Identification and characterization of Ich-3, a member of the interleukin-1beta converting enzyme (ICE)/Ced-3 family and an upstream regulator of ICE. *J Biol Chem* **271**: 20580-20587.

Wano Y., Uchiyama T., Fukui K., Uchino H. and Yodoi J. (1984). Characterization of human interleukin 2 receptor (Tac antigen) in normal and leukemic T cells: co-expression of normal and aberrant receptors on Hut-102 cells. *J Immunol* **132**: 3005-3010.

Warren H. S. and Kinnear B. F. (1999). Quantitative analysis of the effect of CD16 ligation on human NK cell proliferation. *J Immunol* **162**: 735-742.

Warren H. S. and Skipsey L. J. (1991). Phenotypic analysis of a resting subpopulation of human peripheral blood NK cells: the FcR gamma III (CD16) molecule and NK cell differentiation. *Immunology* **72**: 150-157.

Wei A., Rubin H., Cooperman B. S. and Christianson D. W. (1994). Crystal structure of an uncleaved serpin reveals the conformation of an inhibitory loop. *Nature Struct Biol* **1**: 251-258.

Wei M. C., Lindsten T., Mootha V. K., Weiler S., Gross A., Ashiya M., Thompson C. B. and Korsmeyer S. J. (2000). tBID, a membrane-targeted death ligand, oligomerizes BAK to release cytochrome c. *Genes Dev* **14**: 2060-2071.

Wei M. C., Zong W. X., Cheng E. H., Lindsten T., Panoutsakopoulou V., Ross A. J., Roth K. A., MacGregor G. R., Thompson C. B. and Korsmeyer S. J. (2001). Proapoptotic BAX and BAK: a requisite gateway to mitochondrial dysfunction and death. *Science* **292**: 727-730.

Wever P. C., Van Der Vliet H. J., Spaeny L. H., Wolbink A. M., Van Diepen F. N., Froelich C. J., Hack C. E. and ten Berge I. J. (1998). The CD8+ granzyme B+ T-cell subset in peripheral blood from healthy individuals contains activated and apoptosis-prone cells. *Immunology* **93**: 383-389.

Whisstock J., Skinner R. and Lesk A. M. (1998). An atlas of serpin conformations. *Trends Biochem Sci* **23**: 63-67.

Whisstock J. C., Skinner R., Carrell R. W. and Lesk A. M. (2000). Conformational changes in serpins: I. The native and cleaved conformations of alpha(1)-antitrypsin. *J Mol Biol* **296**: 685-699.

Whitehead R. H. and Little J. H. (1973). Tissue culture studies on human malignant melanoma. Pigment Cell I. Mechanisms in Pigmentation. V. J. McGovern and P. Russell. Basel, Karger: 382.

Wilczynska M., Fa M., Ohlsson P. I. and Ny T. (1995). The inhibition mechanism of serpins. Evidence that the mobile reactive center loop is cleaved in the native protease-inhibitor complex. *J Biol Chem* **270**: 29652-29655.

Wilharm E., Parry M. A., Friebel R., Tschesche H., Matschiner G., Sommerhoff C. P. and Jenne D. E. (1999). Generation of catalytically active granzyme K from Escherichia coli inclusion bodies and identification of efficient granzyme K inhibitors in human plasma. *J Biol Chem* **274**: 27331-27337.

Willems F., Amraoui Z., Vanderheyde N., Verhasselt V., Aksoy E., Scaffidi C., Peter M. E., Krammer P. H. and Goldman M. (2000). Expression of c-FLIP(L) and resistance to CD95-mediated apoptosis of monocyte-derived dendritic cells: inhibition by bisindolylmaleimide. *Blood* **95**: 3478-3482.

Willingham M. C., Pastan I. H. and Sahagian G. G. (1983). Ultrastructural immunocytochemical localization of the phosphomannosyl receptor in Chinese hamster ovary (CHO) cells. *J Histochem Cytochem* **31**: 1-11.

Wolf B. B., Schuler M., Echeverri F. and Green D. R. (1999). Caspase-3 is the primary activator of apoptotic DNA fragmentation via DNA fragmentation factor-45/inhibitor of caspase-activated DNase inactivation. *J Biol Chem* **274**: 30651-30656.

Wong B. R., Josien R., Lee S. Y., Sauter B., Li H. L., Steinman R. M. and Choi Y. (1997). TRANCE (tumor necrosis factor [TNF]-related activation-induced cytokine), a new TNF family member predominantly expressed in T cells, is a dendritic cell-specific survival factor. *J Exp Med* **186**: 2075-2080.

Xue D. and Horvitz H. R. (1995). Inhibition of the Caenorhabditis elegans cell-death protease CED-3 by a CED-3 cleavage site in baculovirus p35 protein. *Nature* **377**: 248-251.

Yang J. J., Kettritz R., Falk R. J., Jennette J. C. and Gaido M. L. (1996). Apoptosis of endothelial cells induced by the neutrophil serine proteases proteinase 3 and elastase. *Am J Pathol* **149**: 1617-1626.

Yang X., Stennicke H. R., Wang B., Green D. R., Janicke R. U., Srinivasan A., Seth P., Salvesen G. S. and Froelich C. J. (1998). Granzyme B mimics apical caspases. Description of a unified pathway for trans-activation of executioner caspase-3 and -7. *J Biol Chem* **273**: 34278-34283.

Yannelli J. R., Sullivan J. A., Mandell G. L. and Engelhard V. H. (1986). Reorientation and fusion of cytotoxic T lymphocyte granules after interaction with target cells as determined by high resolution cinemicrography. *J Immunol* **136**: 377-382.

Yasukawa M., Ohminami H., Arai J., Kasahara Y., Ishida Y. and Fujita S. (2000). Granule exocytosis, and not the fas/fas ligand system, is the main pathway of cytotoxicity mediated by alloantigen-specific CD4(+) as well as CD8(+) cytotoxic T lymphocytes in humans. *Blood* **95**: 2352-2355.

Ye R. D., Ahern S. M., Le Beau M. M., Lebo R. V. and Sadler J. E. (1989). Structure of the gene for human plasminogen activator inhibitor-2. The nearest mammalian homologue of chicken ovalbumin. *J Biol Chem* **264**: 5495-5502.

Yeh W. C., Itie A., Elia A. J., Ng M., Shu H. B., Wakeham A., Mirtsos C., Suzuki N., Bonnard M., Goeddel D. V. and Mak T. W. (2000). Requirement for Casper (c-FLIP) in regulation of death receptor-induced apoptosis and embryonic development. *Immunity* **12**: 633-642.

Young J. D., Cohn Z. A. and Podack E. R. (1986a). The ninth component of complement and the pore-forming protein (perforin 1) from cytotoxic T cells: structural, immunological, and functional similarities. *Science* **233**: 184-190.

Young J. D., Hengartner H., Podack E. R. and Cohn Z. A. (1986b). Purification and characterization of a cytolytic pore-forming protein from granules of cloned lymphocytes with natural killer activity. *Cell* **44**: 849-859.

Young J. L., Sukhova G. K., Foster D., Kisiel W., Libby P. and Schonbeck U. (2000). The serpin proteinase inhibitor 9 is an endogenous inhibitor of interleukin 1beta-converting enzyme (caspase-1) activity in human vascular smooth muscle cells. *J Exp Med* **191**: 1535-1544.

Young J. W. and Steinman R. M. (1990). Dendritic cells stimulate primary human cytolytic lymphocyte responses in the absence of CD4+ helper T cells. *J Exp Med* **171**: 1315-1332.

Zalman L. S., Brothers M. A. and Muller-Eberhard H. J. (1985). A C9 related channel forming protein in the cytoplasmic granules of human large granular lymphocytes. *Biosci Rep* **5**: 1093-1100.

Zanovello P., Cerundolo V., Bronte V., Giunta M., Panozzo M., Biasi G. and Collavo D. (1989). Resistance of lymphokine-activated T lymphocytes to cell-mediated cytotoxicity. *Cell Immunol* **122**: 450-460.

Zapata J. M., Takahashi R., Salvesen G. S. and Reed J. C. (1998). Granzyme release and caspase activation in activated human T-lymphocytes. *J Biol Chem* **273**: 6916-6920.

Zeng W., Silverman G. A. and Remold-O'Donnell E. (1998). Structure and sequence of human *M/NEI* (monocyte/neutrophil elastase inhibitor), an ov-serpin family gene. *Gene* **213**: 179-187.

Zha J., Harada H., Yang E., Jockel J. and Korsmeyer S. J. (1996). Serine phosphorylation of death agonist BAD in response to survival factor results in binding to 14-3-3 not BCL-X(L). *Cell* **87**: 619-628.

Zha J., Weiler S., Oh K. J., Wei M. C. and Korsmeyer S. J. (2000). Posttranslational N-myristoylation of BID as a molecular switch for targeting mitochondria and apoptosis. *Science* **290**: 1761-1765.

Zhang D., Beresford P. J., Greenberg A. H. and Lieberman J. (2001a). Granzymes A and B directly cleave lamins and disrupt the nuclear lamina during granule-mediated cytolysis. *Proc Natl Acad Sci U S A* **98**: 5746-5751.

Zhang D., Pasternack M. S., Beresford P. J., Wagner L., Greenberg A. H. and Lieberman J. (2001b). Induction of rapid histone degradation by the cytotoxic T lymphocyte protease Granzyme A. *J Biol Chem* **276**: 3683-3690.

Zhang M., Volpert O., Shi Y. H. and Bouck N. (2000). Maspin is an angiogenesis inhibitor. *Nature Med* **6**: 196-199.

Zhou Q. and Salvesen G. S. (1997). Activation of pro-caspase-7 by serine proteases includes a non- canonical specificity. *Biochem J* **324**: 361-364.

Zhou Q., Snipas S., Orth K., Muzio M., Dixit V. M. and Salvesen G. S. (1997). Target protease specificity of the viral serpin CrmA. Analysis of five caspases. *J Biol Chem* **272**: 7797-7800.

Zou H., Henzel W. J., Liu X., Lutschg A. and Wang X. (1997). Apaf-1, a human protein homologous to C. elegans CED-4, participates in cytochrome c-dependent activation of caspase-3. *Cell* **90**: 405-413.

Zou Z., Anisowicz A., Hendrix M. J. C., Thor A., Neveu M., Sheng S., Rafidi K., Seftor E. and Sager R. (1994). Maspin, a serpin with tumor-suppressing activity in human mammary epithelial cells. *Science.* **263**: 526-529.

Zunino S. J., Bleackley R. C., Martinez J. and Hudig D. (1990). RNKP-1, a novel natural killer-associated serine protease gene cloned from RNK-16 cytotoxic lymphocytes. *J Immunol* **144**: 2001-2009.